Delineation of functional roles of parasite-specific inserts in the malarial S-adenosylmethionine decarboxylase / ornithine decarboxylase

By

Marni Williams
25026519

Submitted in partial fulfilment of the requirements for the degree MSc. Biochemistry in the Faculty of Natural and Agricultural Science

Department of Biochemistry
University of Pretoria
Pretoria
South Africa

February 2008

I declare that the thesis/dissertation, which I hereby submit for the degree MSc. Biochemistry at the University of Pretoria, is my own work and has not previously been submitted by me for a degree at this or any other tertiary institution.

SIGNATURE: ……..

DATE: …….

Acknowledgements

- Prof A.I. Louw, University of Pretoria, South Africa (Promoter)
- Dr L. Birkholtz, University of Pretoria, South Africa (Co-promoter)
- Prof R.D. Walter, Dr C. Wrenger, Dr I.B. Müller, M. Eschbach, B. Bergmann, Bernhard Nocht Institute for Tropical Medicine, Hamburg, Germany (Collaborative research visit in 2006)
- Dr P.F.G. Sims, Manchester Interdisciplinary Biocentre, Manchester, United Kingdom (Mass spectrometric analysis)
- Dr M. Rautenbach, University of Stellenbosch, South Africa (Design of synthetic peptides)
- G.A. Wells, University of Pretoria, South Africa (Secondary structure predictions)
- National Research Foundation (Grand holder's bursary)
- Family and friends

Contents

List of Figures

List of Tables

List of Abbreviations

ACC	Acetyl-CoA carboxylase
ACT	Artemisinin-based combination therapy
ADA	Adenosine deaminase
AdoDATO	S-adenosyl-1,8-diamino-3-thio-octane
AdoMet	S-adenosylmethionine
AdoMetDC	S-adenosylmethionine decarboxylase
AdoMetDC/ODC	S-adenosylmethionine decarboxylase/ornithine decarboxylase
AHT	Anhydrotetracycline
AMA-1	Apical membrane antigen 1
AMP	Adenosine 5'-monophosphate
APA	3-Aminooxy-1-aminopropane
AZ	Antizyme
bp	Base pair
BSA	Bovine serum albumin
bZIP	Basic-leucine-zipper
CCMB	Calcium-manganese based
CPM	Counts per minute
CSP	Circumsporozoite protein
DDT	bis (4-chlorophenyl)-1,1,1-trichloroethane
DFMO	α-Difluoromethylornithine
DHFR	Dihydrofolate reductase
DHFS	Dihydrofolate synthase
DHNA	Dihydroneopterin aldolase
DHPS	Dihydropteroate synthase
DHS	Deoxyhypusine synthase
DMSO	Dimethyl sulfoxide
DOHH	Deoxyhypusine hydroxylase
DNA	Deoxyribonucleic acid
dNTP	Deoxyribonucleotide 5'-triphosphate
DTT	Dithiothreitol
EDTA	Ethylenediamine tetraaceticacid
eIF5A	Eukaryotic translation initiation factor 5A
ENR	Enoyl-ACP-reductase
FMP-1	Falciparum merozoite protein 1
FP	Fowl pox
FPGS	Folylpolyglutamate synthase
FPLC	Fast protein liquid chromatography
Glc6PD/6PGL	Glucose-6-phosphate dehydrogenase/6-phosphoglucolactonase
GluK	Glutamate-5-kinase
Glu-PRed	Glutamylphosphate reductase
GLURP	Glutamine-rich protein
GluS	Glutamate synthase
GMP	Guanosine 5'-monophosphate
GpA	Glycophorin A
GTP	Guanosine 5'-triphosphate
GTPCH	Guanosine 5'-triphosphate cyclohydrolase I

HABA	4-Hydroxy azobenzene-2-carboxylic acid
HBsAg	Hepatitis B surface antigen
HCA	Hydrophobic cluster analysis
HDM2	Human double minute 2
HGXPRT	Hypoxanthine-guanine-xanthine phosphoribosyl transferase
HIV/AIDS	Human immunodeficiency virus/acquired immunodeficiency syndrome
HPLC	High performance liquid chromatography
Hrs	Hours
HSP	Heat shock protein
HSS	Homospermidine synthase
IMP	Inosine 5'-monophosphate
kb	Kilobase
kDa	Kilodalton
LB	Luria Bertani
LCRs	Low-complexity regions
LSA-1	Liver stage antigen 1
4MCHA	*trans*-4-methylcyclohexylamine
MDM2	Mouse double minute 2
ME-TRAP	Multi-epitope thrombospondin-related adhesive protein
MMV	Medicines for Malaria Venture
MS	Mass spectrometry
MSP	Merozoite surface protein
MTA	5'-Methylthioadenosine
MTI	5'-Methylthioinosine
MVA	Modified vaccinia virus Ankara
MVI	Malaria Vaccine Initiative
MW	Molecular weight
NaCl	Sodium chloride
NADH	Nicotinamide adenine dinucleotide
nt	nucleotide
OAc	Acetate
OAT	Ornithine aminotransferase
ODC	Ornithine decarboxylase
pABA	*p*-aminobenzoic acid
PAGE	Polyacrylamide gel electrophoresis
PAO	Polyamine oxidase
PBS	Phosphate buffered saline
PCR	Polymerase chain reaction
PCRed	1-Pyrroline-5-carboxylate reductase
PdxK	Pyridoxal kinase
PfEMP1	*Plasmodium falciparum* erythrocyte membrane protein 1
Pfs	*P. falciparum* surface antigens
PNP	Purine nucleoside phosphorylase
PLP	Pyridoxal-5'-phosphate
PMSF	Phenylmethylsulfonyl fluoride
PPPK	Hydroxymethyldihydropterin pyrophosphokinase
QCM	QuickChange™ site-directed mutagenesis

RBC	Red blood cell
RBM	Roll Back Malaria
RE	Restriction enzyme
rPfHinge-ODC	Recombinant *P. falciparum* ODC plus 144 amino acids of the hinge region
rPfODC	Recombinant *P. falciparum* ODC
RNA	Ribonucleic acid
rpm	Revolutions per minute
SA	Specific activity
SDS	Sodium dodecylsulphate
SDS-PAGE	Sodium dodecylsulphate polyacrylamide gel electrophoresis
SEC	Size-exclusion chromatography
SERCA	Sarcoplasmic-endoplasmic reticulum calcium adenosine triphosphatase
SHMT	Serine hydroxymethyltransferase
SNAP25	Synaptosome-associated protein 25
SNARE	Soluble *N*-ethylmaleimide-sensitive factor attachment protein receptors
SpdSyn	Spermidine synthase
SpmSyn	Spermine synthase
SSAT	Spermidine/spermine-N^1-acetyltransferase
TAE	Tris-acetate ethylenediamine tetraaceticacid
TEMED	N,N,N,N -Tetramethyl-Ethylenediamine
Tm	Melting temperature
TRAP	Thrombospondin-related adhesive protein
Tris-HCl	Trishydroxy (methyl-amino) methane/hydrochloric acid
TS	Thymidylate synthase
U	Units
UNICEF	United Nations Children's Fund
UV	Ultra Violet
WHO	World Health Organisation

Summary

The polyamines putrescine, spermidine and spermine play essential roles in the proliferation and differentiation of most eukaryotic cells. Inhibition of the polyamine pathway is known to have antitumour and antiparasitic effects and α-difluoromethylornithine (DFMO), a polyamine biosynthesis inhibitor, is clinically used in the treatment of African sleeping sickness caused by *Trypanosoma brucei gambiense*. Ornithine decarboxylase (ODC) and S-adenosylmethionine decarboxylase (AdoMetDC) are the rate-limiting enzymes in polyamine metabolism. Usually, these enzymes are individually regulated, however, in the malaria parasite, *Plasmodium falciparum*, these enzymes are part of a unique bifunctional PfAdoMetDC/ODC protein. In addition, compared to homologous proteins, this malarial protein contains six unique parasite-specific inserted regions, which can be targeted with novel drugs.

A modified restriction enzyme-mediated inverse PCR method was developed to delete the largest parasite-specific insert (411 bp) from the large *PfAdoMetDC/ODC* gene (4257 bp). The method was compared to existing deletion mutagenesis PCR protocols and was shown to be the most effective method (80% mutagenesis efficiency) as opposed to the 40% positively mutated clones obtained with the overlapping primer method in deleting a >100 bp region. The independent removal of all three the PfAdoMetDC domain parasite-specific inserts and subsequent activity analysis thereof showed that these inserts are essential for the catalytic activities of both the decarboxylase domains. *Plasmodia* conserved secondary structures within these inserts were identified and were also shown to be very important for domain activities, possibly through protein-protein interactions across and within the domains of the bifunctional complex for the efficient regulation of intracellular polyamine levels.

The N-terminally located O1 insert in the PfODC domain is a highly conserved and structurally distinct insert, which is essential for both domain activities. Previous studies showed that the deletion of this insert prevents dimerisation of the PfODC monomers and as a result influences association of PfODC with the PfAdoMetDC domain to form the bifunctional ~330 kDa complex. In addition, immobilisation of the insert via the mutagenesis of flanking Gly residues and the disruption of a single conserved α-helix within the insert severely affected both PfODC and PfAdoMetDC activities. It was thus hypothesised that the helix is involved in protein-protein interactions and the dimerisation of the PfODC domain. Size-exclusion chromatography of the monofunctional PfODC and bifunctional PfAdoMetDC/ODC proteins with disrupted helices resulted in the elution of only the monomeric (~85 kDa) and heterodimeric PfAdoMetDC/ODC (~160 kDa) proteins,

respectively. The mono- and bifunctional wild type and immobile proteins eluted as both dimeric PfODC (~170 kDa) and heterotetrameric (~330 kDa) fractions as a result of intact protein-protein interactions. These results were subsequently exploited in the design and application of a parasite-specific, mechanistically novel, inhibitory peptide specific for this non-homologous insert in the bifunctional protein. A 1000x molar excess of a synthetic peptide, complementary to the α-helix within the O1 insert but opposite in charge, resulted in a ~40% inhibition of the PfODC enzyme. This study thus provides a proof-of-principle for the use of an inhibitory peptide targeting a parasite-specific insert in the dimerisation interface of a uniquely bifunctional malarial protein.

Chapter 1: Literature review

1.1 Malaria

Malaria in Africa kills a vast number of children every year. By the time you have read the next paragraph, two children will have died: in Africa, a child dies from malaria every 30 seconds, which translates to a massive 2880 children per day (Finkel, 2007).

Malaria, together with HIV/AIDS and tuberculosis, is one of the world's most vital public health challenges compromising development in poverty-stricken countries and accounting for up to an overwhelming 2.7 million deaths per annum (Gardner *et al.*, 2002). More than 3 billion people (~40%) reside in areas of the world where malaria is prevalent. As such, the disease is largely responsible for the poor economic growth of these areas, which further contributes to more cases of malaria (Figure 1.1) (Korenromp *et al.*, 2005). Malaria is a complicated disease and its spread may be attributable to a variety of factors such as ecological and socio-economic conditions, displacement of large population groups, agricultural malpractices causing an increase in vector breeding, parasite resistance to antimalarial drugs and vector resistance to insecticides. In 1998, The World Health Organisation (WHO) established a global partnership called Roll Back Malaria (RBM) in an attempt to halve the world's malaria frequency by 2010 (http://www.rbm.who.int). Apart from RBM, a number of promising antimalarial drug and vaccine discovery projects have also been launched. This includes the Medicines for Malaria Venture (MMV) funded by a number of organisations including The Bill and Melinda Gates Foundation, for the development of novel antimalarials. The latter has also contributed more than 300 million US dollars to the Malaria Vaccine Initiative (MVI).

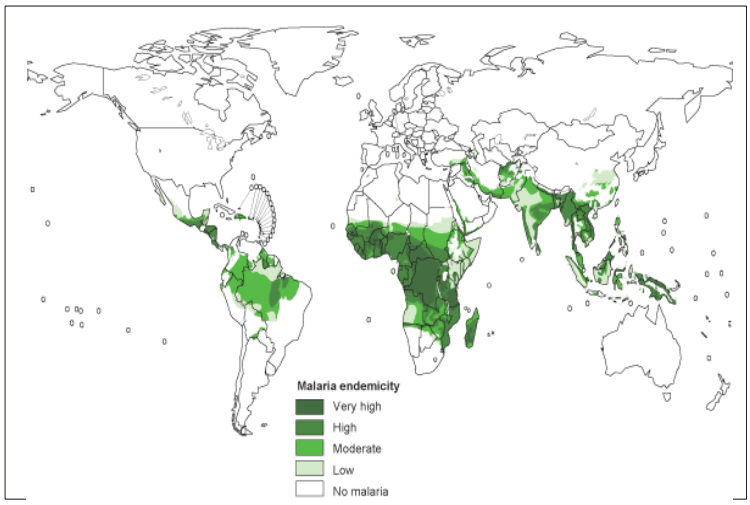

Figure 1.1: The worldwide distribution of malaria.
(http://www.rbm.who.int).

1.2 The *P. falciparum* life cycle

Malaria is caused by an infection from the intracellular Apicomplexan parasites of the *Plasmodium* genus. The genus consists of unicellular, eukaryotic protozoan parasites with a number of different species affecting humans including *P. falciparum* (the most severe form), *P. malariae, P. vivax* and *P. ovale* (Hoffman *et al.*, 2002). The parasites of the Apicomplexan phylum have complex life cycles and are all characterised by the presence of a special apical complex that is involved in host-cell invasion and which includes the microneme, dense granules and rhoptries (Figure 1.2) (Cowman and Crabb, 2006).

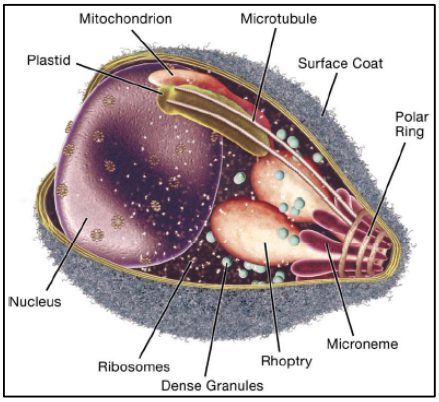

Figure 1.2: The *P. falciparum* merozoite showing the apical complex and other major cellular organelles and structures.
Taken from (Cowman and Crabb, 2006).

P. falciparum parasites invade host cells in order to acquire a rich source of nutrients. At the same time, these cells protect the parasites from host immune responses. The parasites are transmitted by the female *Anopheles gambiae* and *A. funestus* (Southern Africa) mosquitoes, which serve as vectors for the sexual reproduction of the parasites while the mammalian host provides the parasites with a niche for asexual development. The mosquitoes inject a sporozoite form of the parasites into the subcutaneous layer of the host skin during a blood meal. The sporozoites rapidly move to the liver where they infect the hepatocytes and differentiate into thousands of merozoites. These are subsequently released into the bloodstream where they invade erythrocytes. This invasion characterises the onset of the intra-erythrocytic asexual blood stage of the parasitic life cycle. The parasite cycles through ring, trophozoite and schizont stages and in so doing produce between 16 and 32 daughter merozoites per erythrocyte egression. This is accompanied by the characteristic bursts of fever and anaemia associated with the disease. The daughter merozoites repeat the asexual cycle by invading free erythrocytes (Figure 1.3 a). Some intra-erythrocytic stages, however, develop into male or female gametocytes that are ingested by the mosquito during its next blood meal. These develop into male and female gametes inside the mosquito's gut where they fuse to form diploid zygotes. The zygotes differentiate into ookinetes that subsequently

cross the midgut and develop into oocysts from which sporozoites are released. These sporozoites are stored in the salivary glands and are once again injected into the human host by the mosquito to repeat the parasitic life cycle, and thus increasing the number of malaria infectious cases (Figure 1.3 b) (Wirth, 2002).

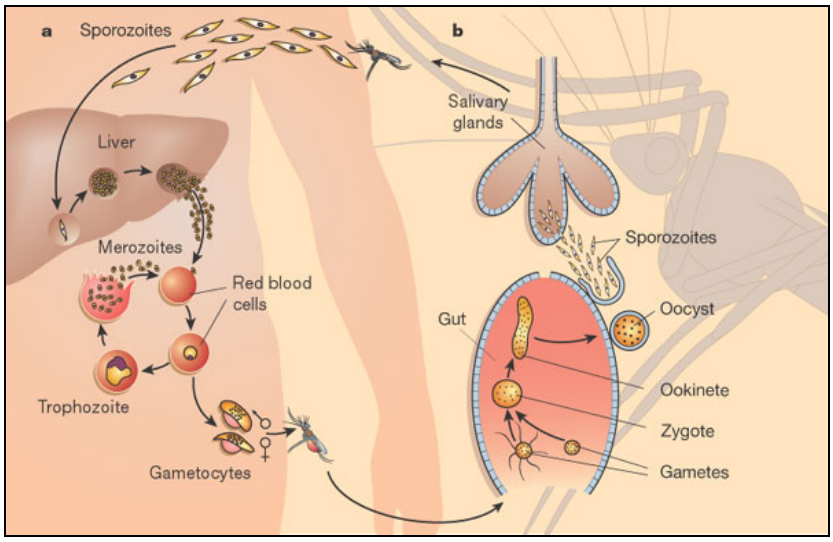

Figure 1.3: The life cycle of the *P. falciparum* parasite.
(a) The asexual stage of the *P. falciparum* life cycle within the human host, (b) the sexual stage within the mosquito host (Wirth, 2002).

1.3 Treating malaria

The development of a highly efficient, novel drug against any disease is in itself a challenging process but the development of an antimalarial is an exceptionally daunting task. The areas where malaria is prevalent at epidemic proportions are mostly devoid of trained physicians and health workers who possess the skills necessary for the early diagnosis of the disease as well as its efficient treatment. Novel antimalarials must be orally bioavailable, as the diseased individuals will most probably not have access to facilities such as hospitals and clinics. The treatment time period must also be less than a week to reduce the risks associated with the development of parasite resistance to the drugs, which may also be reduced with the use of combination-based therapy. Finally, the drugs must be cheap and have a relatively extended shelf life (Nwaka and Hudson, 2006).

1.3.1 Vector control

Alternative strategies to reduce the prevalence of malaria include the use of insecticide-treated bed nets and reduction of the vector population with insecticide spraying. Kingsley Holgate is a South African adventurer who took it upon himself to help fight Africa's largest killer. His epic yearlong journey, called the African Rainbow Expedition, started in 2005 and

was set off by Land Rover from Zululand in South Africa and continued along the African east coast to the Kenya-Somali border. Along the way, the expedition team visited remote villages to hand out insecticide-treated bed nets with the “One net, one life” motto in mind. A total of 10 000 nets were distributed, which is but a drop in the ocean, but the example set by this remarkable man was hoped to inspire others to reach out and help fight this devastating disease (http://www.kingsleyholgate.co.za). Since then, a partnership between Kingsley and the Nando’s fast food group has been established to continue the fight against malaria (Figure 1.4). With the support of Nando’s, the initiative aims to distribute thousands of insecticide-treated bed nets and malaria prevention information leaflets throughout Africa (http://www.nandos.co.za/Diary/AboutDiary.html).

ONE NET • ONE LIFE
MALARIA PREVENTION

Nando's life

Figure 1.4: Kingsley Holgate and his One net, one life anti-malaria compaign supported by Nando’s.
(http://www.kingsleyholgate.co.za/e_arainbow.html).

As far as indoor insecticide spraying is concerned, bis(4-chlorophenyl)-1,1,1-trichloroethane (better known as DDT) remains the most powerful and successful pesticide to date and is responsible for the eradication of malaria from the United States and Europe. In South Africa, the discontinued use of DDT in the 1990s resulted in the worst malaria epidemic the country has experienced since the introduction of indoor spraying in the 1950s (Figure 1.5). The reintroduction of DDT in 2000 resulted in an overall decrease in the number of malaria cases of approximately 50% in 2002 (Maharaj *et al.*, 2005). DDT is not only effective against malaria vectors but is equally potent at alleviating various other arthropod-borne diseases such as yellow fever, African sleeping sickness, dengue fever and typhus. However, DDT was also extensively used in agriculture where enormous quantities were aerially sprayed onto crops to curb pests. This widespread and uncontrolled use of DDT raised concerns in the 1960s amongst environmentalists who described possible catastrophic consequences for both the environment and humans leading to the ban of DDT use in the 1980s (Weissmann, 2006). Little scientific evidence, however, exists to support these concerns and no toxic effects caused by DDT in humans have been noted when used in low concentrations as required for the control of malaria vectors inside houses (Rogan and Chen, 2005). Since then, the efforts of several public health officials and malaria experts have resulted in the

restricted use of DDT in Africa for malaria vector control only and not in agriculture (Dugger, 2006).

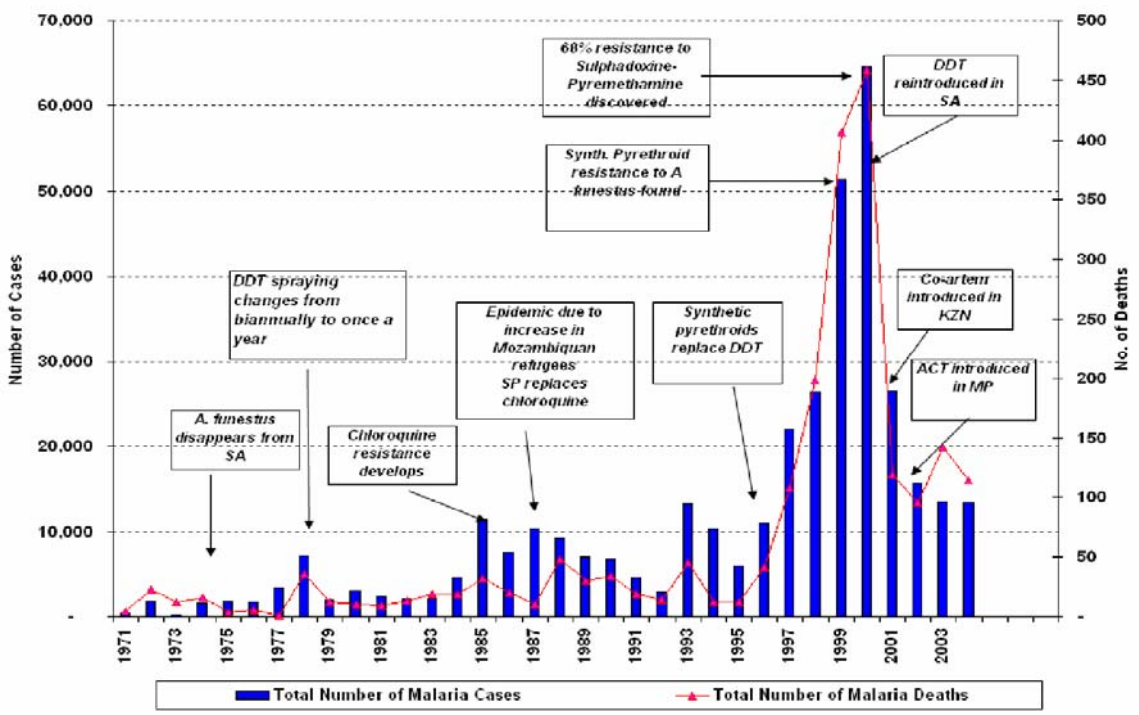

Figure 1.5: Annual recorded malaria cases and deaths in South Africa (1971-2004).
Taken from a report compiled by (Thiel, 2005).

Malaria parasite transmission can additionally be prevented by the treatment of parasite vectors with a drug that blocks the sexual development of the parasites within the mosquito. Coleman tested the effect of 8-aminoquinolines on the sexual development of *P. berghei* and *P. falciparum* parasites in *A. stephensi* mosquitoes. The drug-fed mosquitoes produced fewer oocysts than the control-fed group, and in addition, the sporozoites that did manage to develop from the oocysts could not enter the salivary glands of the mosquito, and therefore prevented the parasites from being transmitted back to the mice (Coleman *et al.*, 1994). The antifolate drugs proguanil and pyrimethamine have also been shown to be sporontocidal. These drugs caused a reduction in oocysts in sensitive strains and pyrimethamine was also reported to directly damage ookinetes (Bray *et al.*, 1959). Gillet *et al*. showed that α-difluoromethylornithine (DFMO), a polyamine pathway inhibitor interferes with *P. berghei* sporozoite development in *A. stephensi* mosquitoes. Only one mouse out of 16 exposed to DFMO-treated mosquitoes contracted malaria. DFMO thus exerts its most deleterious effects on the stages where active cell division is taking place, namely the exo-erythrocytic schizogonous and sporogonous stages (Gillet *et al.*, 1983).

1.3.2 Vaccine development

The development of a safe and effective vaccine against infection represents an alternative method for treating parasitic diseases. Despite extensive efforts, not a single vaccine against any of the human parasitic diseases is currently available. Some malaria experts, however, remain adamant that vaccination may be the most valuable strategy for reducing mortality associated with malaria (Miller and Hoffman, 1998). People living in malaria endemic areas develop low levels of protective immunity against *P. falciparum* infection after five years of age but this immunity is never complete and seems to be specific for the parasite strain residing in a specific area. Protective immunity is therefore lost once the host moves into an area where a different strain resides and also once the host is no longer chronically infected (Bull and Marsh, 2002).

The complex life cycle of the malaria parasite, which allows it to co-exist with the host's immune response, is largely responsible for the absence of a successful vaccine (Todryk and Hill, 2007). Current vaccine development strategies focus on different protein antigens that are expressed during the different stages of the life cycle, namely the pre-erythrocytic (sporozoite and schizont-infected hepatic cells), the asexual intra-erythrocytic (merozoite-infected erythrocytes) and sexual exo-erythrocytic (gametocyte) stages (Figure 1.6) (Todryk and Hill, 2007). An ideal vaccine against malarial infection should therefore induce immune responses against every stage of the life cycle. Such a multistage, multivalent and multi-immune response vaccine presents the best strategy for a successful vaccine in the treatment of malaria (Doolan and Hoffman, 1997).

Antibodies directed against antigens on the surface of extracellular sporozoites (e.g. circumsporozoite protein, CSP) would result in the neutralisation of sporozoite infectivity in the bloodstream. Preliminary studies of the RTS,S/AS02 malaria vaccine (GlaxoSmithKline Biologicals) in African infants showed that the vaccine is safe, well-tolerated and reduces parasite infection and clinical illness due to malaria. The vaccine consists of two polypeptides; RTS corresponds to CSP amino acids 207-395 of *P. falciparum* 3D7 fused to the N-terminus of the hepatitis B surface antigen (HBsAg) and S consists of 226 amino acids of HBsAg (Stoute, 2007). A Phase II trail conducted in Mozambique reported that the vaccine is 65% effective against new infections over a three-month follow-up period after infants received three doses of the vaccine and reduced clinical malaria episodes by 35% over a six-month follow-up period starting after the first dose (Aponte *et al.*, 2007).

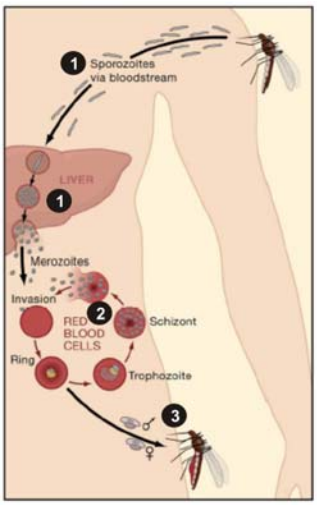

	Stage	Main target	Antigen	Vaccine
1	Pre-erythrocytic	Sporozoites	CSP	RTS,S/AS02A
		Hepatocytes	ME-TRAP	FP9/MVA, ME-TRAP
			LSA-1	LSA-1-AS02
			CSP	AdHu35
2	Asexual intra-erythrocytic	Merozoites	$MSP\text{-}1_{42}$	FMP-1-AS02
			AMA-1	AMA-1-AS02
			GLURP/MSP-3	GMZ2
			$AMA\text{-}1/MSP\text{-}1_{19}$	PfCp2.9
3	Sexual exo-erythrocytic	Gametocytes	Pfs25	-
			Pfs28	-
			Pfs48/45	-
			Pfs230	-

Figure 1.6: Selected malaria vaccines targeting different antigens in specific stages of the parasite life cycle.
(1) Pre-erythrocytic stage vaccines prevent host parasitic infection and disease development, (2) asexual erythrocytic stage vaccines block the multiplication of daughter merozoites, and (3) sexual stage vaccines prevent parasite transmission (Todryk and Hill, 2007). Abbreviations: CSP, circumsporozoite protein; ME-TRAP, multi-epitope thrombospondin-related adhesive protein; LSA-1, liver stage antigen 1; MSP, merozoite surface protein; AMA-1, apical membrane antigen 1; GLURP, glutamine-rich protein; Pfs, *P. falciparum* surface antigens; FP, fowl pox; MVA, modified vaccinia virus Ankara; AdHu35, human adenovirus serotype 35; FMP-1, Falciparum merozoite protein-1; PfCp2.9, *P. falciparum* chimeric protein 2.

Pre-erythrocytic stage vaccines focus on expressed parasite proteins on the sporozoite-infected hepatocyte surface, which elicit $CD8^+$ and $CD4^+$ T-cell responses resulting in reduced liver-stage malaria infection. These proteins include CSP, thrombospondin-related adhesive protein (TRAP), liver stage antigen 1 (LSA-1) and merozoite stage protein 1 (MSP-1). The FP9/MVA, ME-TRAP vaccine (University of Oxford), containing the T-cell-inducing vaccine vector (fowl pox strain FP9), followed by boosting with a second antigen-encoding vector modified vaccinia virus Ankara (MVA), which delivers TRAP, is fused to several liver-stage antigen T-cell epitopes (ME-TRAP). This prime-boost regimen with the concomitant delivery of the malaria antigens serves to extend the T-cell response against the infected hepatocytes (Gilbert *et al.*, 2006).

Extracellular merozoites released from the hepatocytes can be neutralised by antibodies directed against several surface antigens (MSP, apical membrane antigen 1 and glutamate-rich protein). Vaccines in this group that are currently undergoing clinical trials include the 42 kDa C-terminal $MSP\text{-}1_{42}$ vaccine as well as an apical membrane antigen 1 (AMA-1) vaccine consisting of the AMA-1 ectodomain. Both antigens are reconstituted in AS02A (Walter Reed Army Institute of Research) (Polhemus *et al.*, 2007).

In erythrocytic stage vaccines, antibodies raised to antigens on the erythrocyte plasma membrane (e.g. *P. falciparum* erythrocyte membrane protein 1, PfEMP1) would result in the

destruction of the infected erythrocyte or prevent the cytoadherence of these infected cells (Doolan and Hoffman, 1997). Blood-stage vaccines, however, are limited by the polymorphic character of the antigens, which creates diversity that restricts the efficacy of the vaccine representative of a particular genotype (Anders and Saul, 2000).

Finally, neutralising antibodies to pre-fertilization (e.g. Pfs48/45 and Pfs230) or post-fertilization (Pfs25 and Pfs28) gametocyte surface antigens could ensure that any remaining infection will not be transmitted back to the mosquito vector (Doolan and Hoffman, 1997).

1.3.3 Current antimalarials

Various drugs have been developed and used in the fight against malaria. As with the vaccines, antimalarials target different stages of the parasite life cycle within the human host and specifically interfere with processes that are essential to parasite survival. Eradication of malaria with the use of antimalarials is, however, continuously compromised by the increased prevalence of parasite resistance to the small amount of available commercial drugs. Figure 1.7 shows the different stages of the parasite life cycle and drugs that specifically target these stages of parasite development.

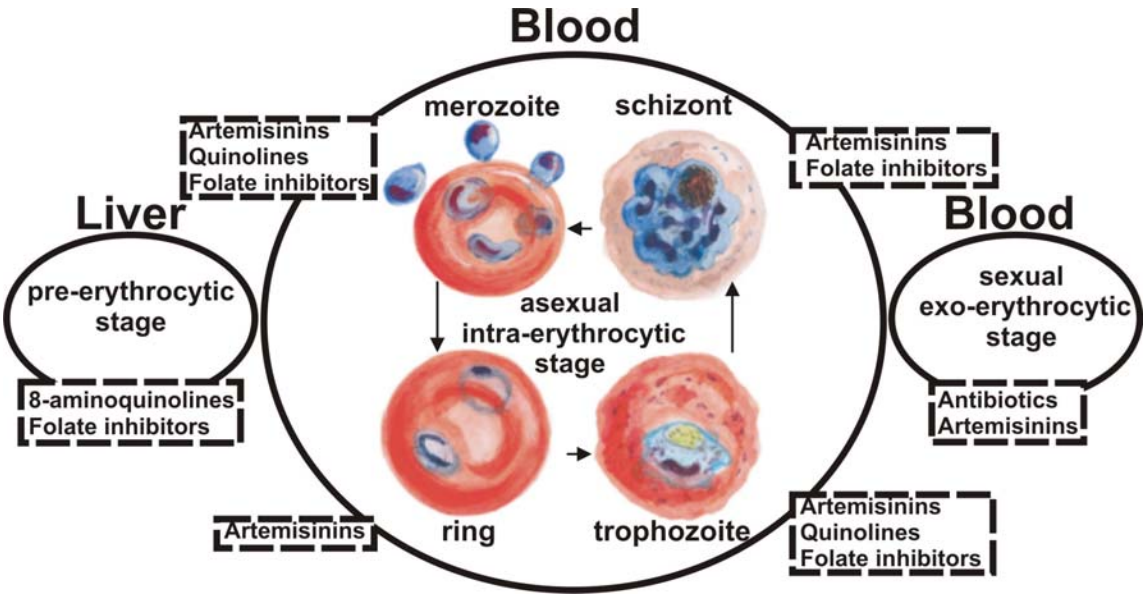

Figure 1.7: A schematic diagram of the parasite life cycle within the human host showing the targets of different antimalarials during the developmental stages.
The pre-erythrocytic, asexual intra-erythrocytic and sexual exo-erythrocytic stages are shown. The different intra-erythrocytic phases of malaria parasite development are also given. Finally, drugs that have been used at each stage are shown in the dashed boxes (Chauhan and Srivastava, 2001; Olliaro, 2001; Korenromp *et al.*, 2005).

A list of some antimalarials is given in Table 1.1. The proposed mechanisms of action of these different drug classes are also listed.

Table 1.1: Different antimalarial drug classes together with their mechanisms of action Compiled from (Chauhan and Srivastava, 2001; Olliaro, 2001; Korenromp *et al.*, 2005).

Stage	Drug class	Drug compounds	Mechanism of action
Pre-erythrocytic	Aminoquinolines	Primaquine (also gametocytocidal)	Unknown
	Hydroxynaphthoquinone	Atovaquone (also sporontocidal)	Interferes with cytochrome electron transport
Asexual intra-erythrocytic	Aminoquinolines	Chloroquine (also gametocytocidal)	Inhibits haem detoxification
		Quinine (also gametocytocidal)	Inhibits haem detoxification
	Sulfonamides	Sulfadoxine	Inhibits DHPS
	Sulfones	Dapsone	Inhibits DHPS
	Amidines	Proguanil (active as cycloguanil, also active against pre-erythrocytic forms and sporontocidal)	Inhibits DHFR
	Pyrimidines	Pyrimethamine (also sporontocidal and interferes with sexual reproduction)	Inhibits DHFR (used in combination with sulfadoxine or dapsone)
	4-Methanolquinoline	Mefloquine	Inhibits haem detoxification
	Sesquiterpene lactone	Artemisinin and derivatives (also gametocytocidal)	Inhibits calcium adenosine triphosphatase
Exo-erythrocytic	Antibiotics	Tetracycline (also active against intra-erythrocytic forms)	Inhibitors of aminoacyl-tRNA binding during protein synthesis
		Doxycycline (also active against intra-erythrocytic forms)	Inhibitors of aminoacyl-tRNA binding during protein synthesis

1.3.3.1 Quinolines

The bark of the *Cinchona* tree has been used for centuries to treat fever associated with malarial infection from which the active ingredient is quinine. It remained the antimalarial of choice until the 1940s, when other antimalarials such as its chloroquine derivative replaced quinine. Quinine, however, is still used today to treat clinical malaria and not as a prophylaxis due to its side effects and poor tolerability. Chloroquine is a 4-aminoquinoline derivative of quinine and for many years it was the main antimalarial drug used in the treatment of malaria until parasite resistance developed in the 1950s. It remains the most popular antimalarial developed to date due to its safety, low cost and efficacy. (Bjorkman and Phillips-Howard, 1990; Yeh and Altman, 2006). Today, the widespread resistance to the drug has rendered its use as a therapeutic agent useless, even though it still shows some efficacy in the treatment of the other human malaria parasites (Korenromp *et al.*, 2005).

Despite more than three decades of research, the exact molecular mechanism of chloroquine action remains a controversial topic. It is believed that the weak-base drug accumulates in the acidic food vacuole of the parasite where it prevents haem detoxification

(Bray *et al.*, 2005). Chloroquine resistance in malaria parasites has been attributed to reduced concentrations of the drug in the food vacuole possibly due to drug efflux, pH modification in the vacuole, the role of a Na^+/H^+ exchanger and transporters (Foley and Tilley, 1998; Bray *et al.*, 2005). In *P. falciparum*, two genes have been implicated in resistance, namely *Pfmdr1* and *Pfcrt*, which encodes Pgh1 and PfCRT, respectively. Both these proteins are localised to the food vacuole membrane. Mutations in these genes could lead to small increases in the food vacuole pH thus reducing the amount of chloroquine that can accumulate, rendering the drug ineffective (Spiller *et al.*, 2002). Alternatively, PfCRT may increase the efflux of chloroquine by directly interacting with the drug (Cooper *et al.*, 2007). Resistance is associated with several mutations in the PfCRT protein, while the loss of a Lys residue at position 76 has been shown as the critical mutation rendering the *P. falciparum* parasites resistant to the drug. This residue is located within the first transmembrane segment of PfCRT and may therefore play an important role in the properties of the channel or transporter (Cooper *et al.*, 2005). Mutations in the *Pfmdr1* gene is associated with resistance to mefloquine, quinine and halofantrine (Reed *et al.*, 2000).

A number of related aminoquinolines have since been developed and applied, including:

- Amodiaquine: effective against chloroquine-resistant strains, possible cross-resistance with chloroquine, safety limitation (Korenromp *et al.*, 2005; Bathurst and Hentschel, 2006)
- Atovaquone: usually used in combination with proguanil (Malarone®), resistance reported in 1996, cost limitation (Korenromp *et al.*, 2005; Bathurst and Hentschel, 2006)
- Lumefantrine: usually coformulated with artemether (Co-Artem™) and is highly effective against multi-drug resistant *P. falciparum* (Korenromp *et al.*, 2005)
- Halofantrine (Halfan): resistance reported in 1992, cost and safety limitations (Bathurst and Hentschel, 2006)
- Mefloquine (Lariam®): resistance reported in 1982, cost and safety limitations (Bathurst and Hentschel, 2006)
- Primaquine: used for its gametocytocidal effect (*P. falciparum*) and its efficacy against intra-hepatic forms of all types of malaria, no resistance, safety limitations (Chauhan and Srivastava, 2001; Bathurst and Hentschel, 2006)

1.3.3.2 Antifolates

The antifolates are some of the most widely used antimalarials. However, their role in malaria prevention is hampered by the rapid emergence of resistance once the parasites are placed under drug pressure. The direct effect of folate biosynthesis inhibition is a reduction in the synthesis of the amino acids serine and methionine as well as in pyrimidines, which leads to

decreased synthesis of DNA. The antifolate drugs target the intra-erythrocytic stages as well as the gametocytes of *P. falciparum* (Olliaro, 2001).

The antifolates can generally be divided into two classes; the type-1 antifolates mimic the *p*-aminobenzoic acid (pABA) substrate of dihydropteroate synthase (DHPS) and include the sulfonamides (sulfadoxine) and sulfones (dapsone), while the type-2 antifolates (pyrimethamine and proguanil) inhibit dihydrofolate reductase (DHFR) (Olliaro, 2001). Interestingly both of these classes of target proteins are arranged on separate bifunctional enzymes (hydroxymethyldihydropterin pyrophosphokinase/dihydropteroate synthase or PPPK/DHPS and dihydrofolate reductase/thymidylate synthase or DHFR/TS) (Ivanetich and Santi, 1990). In addition, malaria parasites are capable of *in vivo* folate salvage from the extracellular environment as well as synthesising folate derivatives from simple precursors. The mechanism of exogenous folate uptake by a carrier-mediated process has important implications in increasing the sensitivity of the antifolate inhibitors and is being investigated as a novel drug target (Wang *et al.*, 2007).

Pyrimethamine is a diaminopyrimidine and is mostly used in combination with sulfadoxine (Fansidar™) or dapsone leading to the simultaneous inhibition of DHFR and DHPS. Pyrimethamine crosses the blood-brain barrier as well as the placenta. Resistance to sulfadoxine-pyrimethamine combination therapy, however, emerged rapidly due to the appearance of point mutations in the active sites of the target enzymes resulting in reduced drug binding capacity (Cowman and Lew, 1990; Plowe *et al.*, 1997).

1.3.3.3 Artemisinins

Artemisinin is a sesquiterpene lactone extracted from the leaves of *Artemisia annua*. It is a potent, fast acting blood schizontocide that shows efficacy against all *Plasmodium* species. Its efficacy is especially broad and shows activity against all the asexual stages of the parasites including the gametocytes (Figure 1.7) (Korenromp *et al.*, 2005). The latter makes this class of antimalarials especially important as they reduce the transmission potential through its gametocytocidal activity.

Originally the mechanism of action of artemisinin was thought to be mediated by the peroxide ring of the drug, which is cleaved and activated by ferrous iron in the heme stores into toxic free radicals that can subsequently damage intracellular targets via alkylation (Meshnick *et al.*, 1991). Recently, however, this theory was challenged by evidence that artemisinin exerts its inhibitory effects on the malarial sarcoplasmic-endoplasmic reticulum calcium ATPase (SERCA) resulting in an alteration of intracellular calcium levels (Eckstein-Ludwig *et al.*,

2003). The exact mechanism of action, however, remains elusive and different studies have produced contradicting results [reviewed in (Krishna *et al.*, 2004)].

Several derivatives of artemisinin have been developed since artemisinin itself is poorly absorbed and include dihydroartemisinin, artesunate (sodium salt of the hemisuccinate ester of artemisinin), artemether (methyl ether of dihydroartemisinin) and artemether (ethyl ether of artemisinin) (Korenromp *et al.*, 2005). Currently, the WHO recommends artemisinin-based combination therapy (ACT) as the first-line treatment against malaria infections where resistance to other antimalarials is prevalent. One of the obvious disadvantages of using ACT for malaria case-management in Africa is the increased cost involved in combining therapies. Even so, several reasons exist for combining antimalarials with an artemisinin derivative, namely: 1) an increase in the efficacy of the antimalarials; 2) a decrease in the treatment time period; and 3) a reduced risk of resistant parasites arising through mutation (Kremsner and Krishna, 2004).

Several ACTs that have been developed and may have entered clinical trails are listed below (Gelb, 2007):

- Pyramax: artesunate and the 4-aminoquinoline pyronaridine
- Co-Artem™: artemether and lumefantrine
- Artekin™: dihydroartemisinin and the quinoline-based drug piperaquine
- Lapdap™: artesunate, chlorproguanil and dapsone
- ASAQ: artesunate and amodiaquine

There are several reasons why the appearance of parasite resistance to artemisinin was originally thought to be unlikely or at least delayed: 1) parasites are not exposed to the drug for prolonged periods due to the short half-life of the drug; 2) artemisinin is gametocytocidal, which reduces the transmission potential and spread of the parasite; and 3) the frequent use of artemisinin combined with other antimalarials (ACT) was specifically introduced to delay the onset of resistance (Meshnick, 2002). Evidence for *in vitro* resistance to an artemisinin derivative, however, appeared in field isolates from French Guiana in 2005. The increased artemether IC_{50}s were ascribed to the presence of a mutation in the SERCA *PfATPase6* gene and was attributed to inappropriate drug use that exerted selection pressures, favouring the emergence of parasites with an artemether-resistant *in vitro* profile. Even though reduced *in vitro* drug susceptibility is not tantamount to diminished therapeutic effectiveness, it could lead to complete resistance and thus called for the rapid deployment of drug combinations (Jambou *et al.*, 2005). Lapdap™, a combination of chlorproguanil (targets DHFR), dapsone (targets DHPS) and the artemisinin derivative artesunate, was introduced in 2003 as malaria

therapeutic to replace sulfadoxine-pyrimethamine treatment in Africa (Edwards and Biagini, 2006). No resistance has been detected to date (Bathurst and Hentschel, 2006).

1.3.3.4 Antibiotics

Several antibiotics such as tetracycline, doxycycline and minocycline are active against the exo-erythrocytic as well as the asexual blood stages of the *P. falciparum* parasite. The tetracyclins are antibiotics that were originally derived from *Streptomyces* species, but are usually synthetically prepared. They interfere with aminoacyl-tRNA binding and therefore inhibit protein synthesis in the parasite's apicoplast or mitochondrion (Korenromp *et al.*, 2005). This is due to the presence of genomes in the mitochondrion and apicoplast that encode prokaryote-like ribosomal RNAs, tRNAs and various proteins (Wilson *et al.*, 1996). Doxycycline is a synthetic tetracycline derivative with a longer half-life than tetracycline. A disadvantage of these type of antibiotics as antimalarials is the development of photosensitivity during treatment, which is an obvious drawback for tourists entering malaria areas (Korenromp *et al.*, 2005).

1.3.4 Novel antimalarial targets

Despite the availability of various antimalarials and attempts aimed at preventing parasite infection with the use of suitable vaccines, high malaria mortality continues to persist in endemic areas while the deadline of the RBM endeavour is rapidly approaching. The identification of novel drug targets that can possibly reduce the prevalence of malaria without inducing rapid resistance thus remains imperative and a major challenge for researchers in the field of infectious diseases. A good starting point for the identification of drug targets is to pinpoint differences between host and parasite essential metabolic pathways that are more easily identified once the parasite physiology and host-parasite relationships are better understood. The presence or absence of specific essential pathway enzymes and special features thereof can subsequently be identified and investigated for possible chemotherapeutic intervention strategies.

1.3.4.1 Type II fatty acid biosynthesis

The Apicomplexan plastid, or apicoplast, originated from an endosymbiotic cyanobacterium, which once lived within the host, and the original acquisition of the plastid presumably provided the host with various anabolic products. In addition, several biosynthetic pathways similar to those in plant and algal chloroplasts have been characterised in apicoplasts, including a malaria specific type II fatty acid synthesis pathway. This pathway has major differences compared to the type I fatty acid synthesis pathway found in humans and thus allows for good drug target discovery opportunities (Ralph *et al.*, 2001).

It has been suggested that fatty acids are synthesised for the formation of the parasitophorous vacuole during erythrocyte invasion of the *P. falciparum* parasites and is thus essential for successful infection of the host cells (McFadden and Roos, 1999). Acetyl-CoA carboxylase (ACC) catalyses the first committed step of the *de novo* fatty acid synthesis pathway and provides the sole source of malonyl-CoA (Gornicki, 2003). This rate-limiting enzyme is targeted by the arloxyphenoxyproprionate class of Gram-negative herbicides (Golz *et al.*, 1994). Current research is focussing on the interaction between the herbicides and ACC for the development of more potent ACC inhibitors. Enoyl-ACP-reductase (FabI) catalyses and controls the rate of the final step of fatty acid elongation and is inhibited *in vitro* and *in vivo* by the broad spectrum antibiotic and antifungal, triclosan (Surolia and Surolia, 2001). Despite the *in vivo* efficacy of triclosan, it is too early to apply it in the field since pharmacokinetic and toxicological evaluations remain absent. The molecular mechanism of the inhibitors are known and the 3-dimensional structure of FabI has also been solved, which provides a basis for further rational design of novel inhibitors against type II fatty acid biosynthesis in *P. falciparum* (Gornicki, 2003).

1.3.4.2 DNA topoisomerases

DNA topoisomerases are complex enzymes that control the topological state of DNA and include the type I (transiently cleaves and then reseals one DNA strand) and type II (cleaves and reseals both DNA strands) topoisomerases. The type II topoisomerase, or DNA gyrase, also catalyses DNA supercoiling (Chauhan and Srivastava, 2001).

Recently, the presence of topoisomerases in the protozoan-infected erythrocytes has been observed, which encouraged studies on these enzymes as possible antimalarial targets. Camptothecin has been shown to kill parasites through its inhibitory effects on topoisomerase I (Bodley *et al.*, 1998) while specific antisense oligonucleotides to topoisomerase II decreases the growth of the parasites in culture (Noonpakdee *et al.*, 2003). The future challenge of drug discovery with the DNA topoisomerases as targets is the structural determination of these proteins. This will aid the design of chemical entities, which can ascertain the actual worth of targeting these sites in malaria chemotherapy.

1.3.4.3 Polyamine biosynthesis

Several studies have investigated the importance of polyamines and their involvement in various processes within the cell. In most organisms, the polyamine pathway has been fully elucidated and a decade of research has resulted in major advances in our understanding of polyamine biosynthesis in the malaria-causing parasite. Wang and Assaraf have respectively shown that interruption of polyamine biosynthesis hampers the development of disease-causing *Trypanosoma brucei gambiense* and *P. falciparum* parasites (Assaraf *et al.*, 1984;

Wang, 1995). Further studies have identified unique parasite-specific properties in the *P. falciparum* polyamine pathway, which present possible targets for chemotherapeutic intervention (Müller *et al.*, 2000; Wrenger *et al.*, 2001; Birkholtz *et al.*, 2004). A sensible approach is thus the biochemical characterisation (both structural and functional) of the pathway's constituent enzymes for rational drug development strategies (Birkholtz *et al.*, 2004). The polyamine biosynthesis pathway as drug target in *P. falciparum* will thus be the main focus of this study.

1.4 Polyamines

The physiologically important polyamines putrescine, spermidine and spermine are found in all living organisms except the Methano- and Halobacteriales (Hamana and Matsuzaki, 1992). The widespread presence of these polyamines signifies its considerable contribution to the survival of living eukaryotic and prokaryotic cells. They have been implicated in many growth processes such as cell differentiation and proliferation (Cohen, 1971; Bachrach, 1973; Tabor and Tabor, 1976; Heby, 1981), which is reflected by the general abundance of polyamines and increased activity of its biosynthetic enzymes during stages of rapid growth (Assaraf *et al.*, 1984; Russell, 1985). Polyamine levels are thus closely regulated as their depletion may lead to growth arrest and aberrant embryonic development (Johnson, 1994) while their accumulation may result in apoptosis (Poulin *et al.*, 1995; Tobias and Kahana, 1995; Xie *et al.*, 1997). The intracellular polyamine levels are maintained at optimal levels by tight regulation of its synthesis, degradation as well as their uptake and secretion from and into the extracellular compartment. The importance of the naturally occurring polyamines as well as their regulation by various biosynthetic and catabolic enzymes has led to the identification of various enzymes in the polyamine pathway as drug targets for the treatment of cancer and parasitic diseases.

The positive charges residing on the amine groups of the polyamines at physiological pH are responsible for the specialised functions of these ubiquitous organic cations. Polyamines are, simply put, low molecular weight (MW), long-chain aliphatic carbon compounds derived from amino acids with multiple amine groups (Figure 1.8) (Whaun and Brown, 1983). The positive charges allow for electrostatic interactions with anionic molecules such as nucleic acids, proteins and lipids (Tabor, 1962).

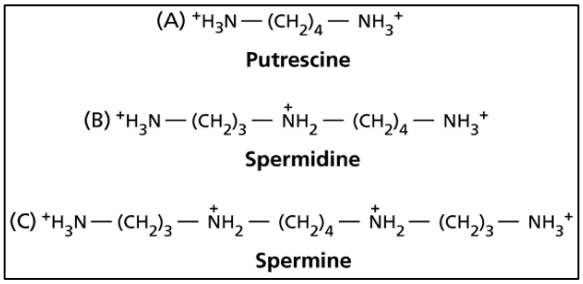

Figure 1.8: Structures of the positively charged polyamines: the divalent putrescine, trivalent spermidine and tetravalent spermine.

Electrostatic associations between polyamines and DNA result in the stabilisation of these molecules, which often promotes DNA bending. This subsequently facilitates the binding of gene regulatory elements and thus indirectly influences transcription (Tabor, 1962; Feuerstein *et al.*, 1986; Feuerstein *et al.*, 1989; Kerppola, 1998). Polyamines additionally influence transcription by modifying chromatin structure via the stimulation of histone acetyltransferase (Hobbs *et al.*, 2002). One of the most unique post-translational protein modifications is the spermidine-dependent hypusinilation of eukaryotic translation initiation factor, eIF5A. The function of eIF5A is not entirely understood but it appears to be essential for cell proliferation as its depletion arrests yeast cells in the G1 stage of the cell cycle (Kang and Hershey, 1994). Cells maintain optimal levels of polyamines as they play paradoxical roles in the prevention as well as in the stimulation of cell death. Increased levels of polyamines protect cells by steering them into the proliferative pathway and away from cell death (Thomas and Thomas, 2001). However, the accumulation of excess intracellular putrescine triggers apoptosis possibly due to an imbalance in intracellular positive and negative charges and the decreased formation of modified eIF5A (Tome *et al.*, 1997; Xie *et al.*, 1997).

1.4.1 Polyamine metabolism in *P. falciparum*

Polyamines are essential components in all living cells where they execute multiple functions, such as cell proliferation and macromolecular synthesis. Interference with the biosynthesis of these polycationic molecules has been applied in the search for antitumour drugs [for review see (Seiler, 2003)]. Inhibitors to almost all of the biosynthetic enzymes have been successfully designed and tested for application in antitumour therapeutic intervention (Marton and Pegg, 1995). Although success in finding antitumour drugs that target the polyamine pathway has been limited, it does suggest that these kinds of drugs may be useful against rapidly proliferating parasites. The parasite's pathway is distinctly different from that of the human's, which means that interference with the parasite's polyamine biosynthetic pathway could have more severe consequences on the parasite than its mammalian host (Figure 1.9) (Müller *et al.*, 2001). Obvious differences between the main polyamine

biosynthetic enzymes in the two organisms may provide possible drug target development opportunities for the treatment of parasitic infectious diseases.

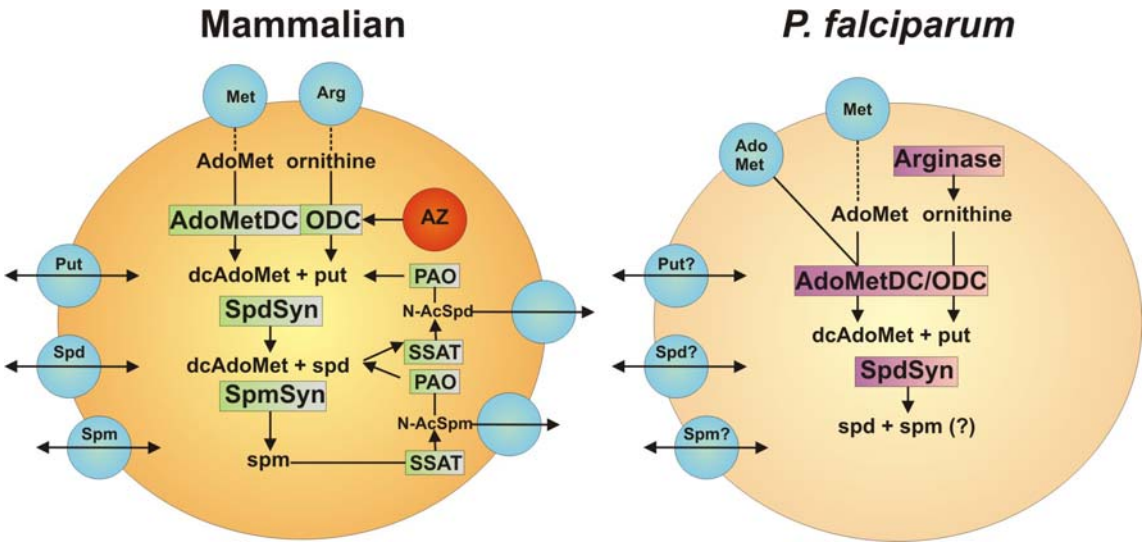

Figure 1.9: Outlines of the polyamine metabolic pathways in the mammalian cell and the *P. falciparum* parasite.
Transporters are shown as blue circles. Intermediates and reaction products are written in plain text while the enzymes producing these are given in green (mammalian cell) and purple (parasite) boxes. Abbreviations: AdoMetDC, S-adenosylmethionine decarboxylase; ODC, ornithine decarboxylase; dcAdoMet, decarboxylated S-adenosylmethionine; put, putrescine; SpdSyn, spermidine synthase; SpmSyn, spermine synthase; spd, spermidine; spm, spermine; SSAT, spermidine/spermine-N^1-acetyltransferase; PAO, polyamine oxidase; N-AcSpd and N–AcSpm, N^1-acetylated spermidine and spermine; AZ, antizyme; Met, methionine; AdoMet, S-adenosylmethionine; Arg, arginine.

Polyamines are synthesised via the decarboxylation of ornithine to putrescine by the enzyme ornithine decarboxylase (ODC*).* The diamine putrescine then acts as the precursor of spermidine and spermine. Another decarboxylation enzyme, S-adenosylmethionine decarboxylase (AdoMetDC), synthesises decarboxylated S-adenosylmethionine (dcAdoMet), which serves as a donor of propylamine moieties for the synthesis of spermidine and spermine. These last two reactions are catalysed by spermidine synthase (SpdSyn) and spermine synthase (SpmSyn), respectively (Müller *et al.*, 2000). SpmSyn has, however, not been identified in *P. falciparum* although PfSpdSyn is capable of synthesising low levels of spermine (Haider *et al.*, 2005).

A more detailed diagram of the *P. falciparum* pathway for polyamine biosynthesis and its side reactions is given in Figure 1.10.

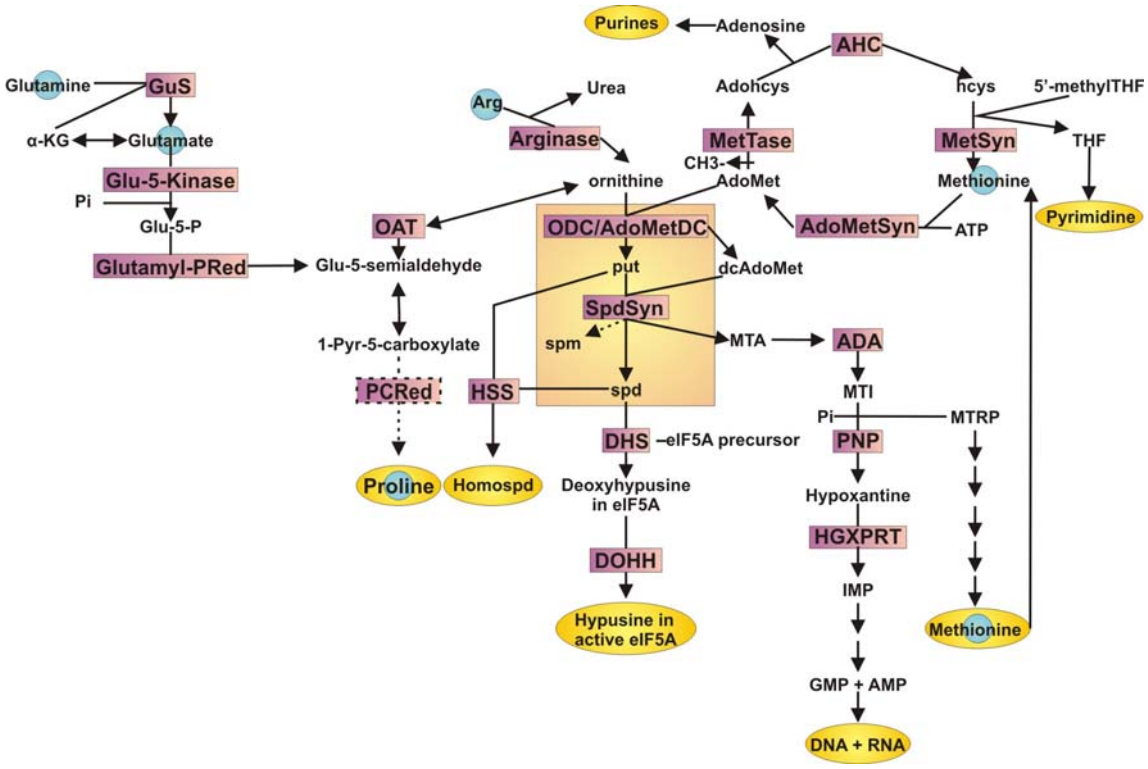

Figure 1.10: The polyamine biosynthesis pathway in *P. falciparum*.
The polyamine biosynthesis pathway is given in the central orange block. Substrates and products for which transporters have been characterised are shown as blue circles. Yellow circles represent products of some of the side reactions of the polyamine pathway. Abbreviations: ODC/AdoMetDC, ornithine decarboxylase/S-adenosylmethionine decarboxylase; put, putrescine; SpdSyn, spermidine synthase; spm, spermine; spd, spermidine; AdoMet, S-adenosylmethionine; MetTase, methionine transferase; CH3-, methyl group; Adohcys, S-adenosylhomocysteine; AHC, adenosylhomocysteinase; hcys, homocysteine; 5'-methylTHF, 5'-methyltetrahydrofolate; THF, tetrahydrofolate; MetSyn, methionine synthase; AdoMetSyn, S-adenosylmethionine synthetase; dcAdoMet, decarboxylated S-adenosylmethionine; MTA, 5'-deoxy-5'-(methylthio) adenosine; ADA, adenosine deaminase; MTI, 5'-methylthioinosine; Pi, inorganic phosphate; PNP, purine nucleoside phosphorylase; HGXPRT, hypoxantine-guanine-xanthine-phosphoribosyl transferase; IMP, inosine 5'-monophosphate; GMP, guanosine 5'-monophosphate; AMP, adenosine 5'-monophosphate; ATP, adenosine 5'-triphosphate; MTRP, 5'-deoxy-5'-(methylthio) ribose-1-phosphate; Arg, arginine; OAT, ornithine aminotransferase; Glu-5-semialdehyde, glutamate-5-semialdehyde; 1-Pyr-5-carboxylate, 1-pyrroline-5-carboxylase; PCRed, 1-Pyr-5-carboxylase reductase; Glutamyl-PRed, glutamylphosphate reductase; Glu-5-P, glutamate-5-phosphate; α-KG, α-ketoglutarate; GluS, glutamate synthase; HSS, homospermidine synthase; Homospd, homospermidine; eIF5A, eukaryotic initiation factor 5A; DHS, deoxyhypusine synthase; DOHH, deoxyhypusine hydroxylase.

1.4.2 Polyamine transporters

The presence of a specific polyamine transport system in malarial parasite-infected erythrocytes remains a controversial subject. Transport systems have, however, been suggested to exist based on three specific observations. It is a well-studied observation that parasites induce numerous biochemical, structural and functional changes in infected erythrocytes resulting in the membrane becoming more permeable to various solutes via new permeability pathways (Ginsberg, 1990; Deitsch and Wellems, 1996). Evidence also suggests that the replenishment of intracellular polyamine pools in parasites treated with

polyamine biosynthesis enzyme inhibitors is due to an influx of polyamines across the membrane (Seiler *et al.*, 1996; Singh *et al.*, 1997). Finally, the exogenous addition of putrescine rescues DFMO-treated *P. falciparum* cultures, which suggests that the parasites are able to internalise and metabolise putrescine for growth and macromolecular synthesis. This last observation might explain why *in vitro* DFMO treatment has a mere cytostatic effect on parasites as reduced intracellular polyamine pools are replenished with exogenous polyamines (Assaraf *et al.*, 1984; Assaraf *et al.*, 1987).

To date, the only polyamine transporter that has been characterised in *Plasmodia* is the *P. knowlesi*-induced putrescine-specific transporter (Singh *et al.*, 1997). Haider *et al*. used *trans*-4-methylcyclohexylamine (4MCHA) to inhibit PfSpdSyn. The addition of spermidine did not result in the resumption of parasite growth, which indicates inefficient uptake of spermidine by the infected erythrocytes and an apparent absence of a spermidine-specific transporter in *P. falciparum*-infected erythrocytes (Haider *et al.*, 2005). The direct targets of this inhibitor are, however, unknown and it is possible that additional sites may be effected in *P. falciparum* (Haider *et al.*, 2005). However, PfAdoMetDC inhibition could not be rescued by the addition of putrescine or spermidine in *P. falciparum* parasites (Das Gupta *et al.*, 2005). The effects of ODC inhibitors were, on the other hand, completely abolished by putrescine supplementation, suggesting the presence of a putrescine transporter system (Das Gupta *et al.*, 2005), which is true for both *P. falciparum* and *P. berghei* parasites (Hollingdale *et al.*, 1985; Assaraf *et al.*, 1987).

In the process of drug discovery it is empirical to take note of strategies that parasites employ to counteract the depletion of a specific essential compound. The most effective drug will be one that interferes with the biosynthesis of a specific essential compound, such as putrescine, and at the same time obstructs its uptake into the *P. falciparum*-infected erythrocyte as a competitive inhibitor of a putrescine-specific transporter.

1.4.3 Polyamine levels during malarial infection

Human erythrocytes only contain trace amounts of polyamines and lack the enzymes necessary for active polyamine biosynthesis (Das Gupta *et al.*, 2005). *P. falciparum* invasion of these erythrocytes leads to rapid proliferation within the host cells and this rapid growth and differentiation of the parasites coincide with high intracellular concentrations of putrescine, spermidine and spermine in the parasites (Assaraf *et al.*, 1984). Spermidine is the major polyamine during all stages of growth (Figure 1.11) (Das Gupta *et al.*, 2005).

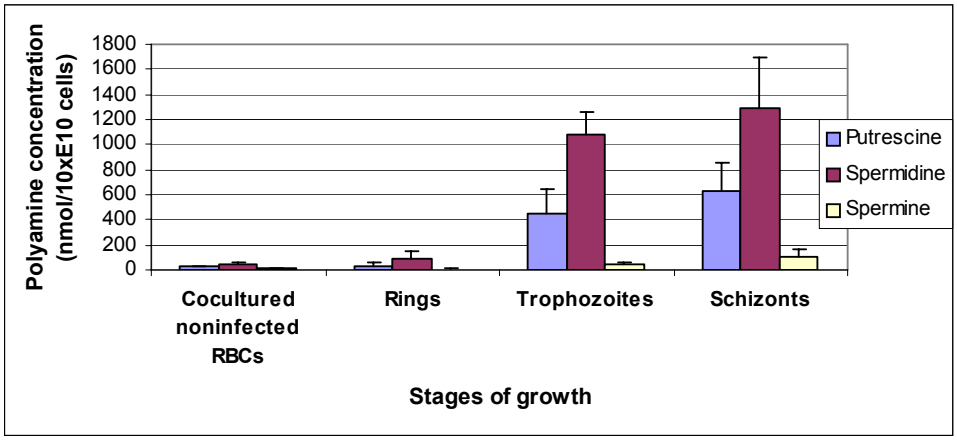

Figure 1.11: Stage-specific polyamine content of *P. falciparum*-infected erythrocytes. Adapted from (Das Gupta *et al.*, 2005).

Polyamines are significantly increased during the trophozoite and schizont stages of parasitic growth compared to that of the normal uninfected erythrocytes. The difference in polyamine levels between the various stages is most pronounced when putrescine and spermidine are compared. Spermine levels are only slightly elevated in the parasitized cells (Figure 1.11). These increases in polyamine content are proportional to the parasitaemia, the activities of the polyamine biosynthetic enzymes, and also the biosynthesis of proteins and nucleic acids (Assaraf *et al.*, 1984; Das Gupta *et al.*, 2005).

1.4.4 Polyamine biosynthetic enzymes as drug targets

The importance of polyamines in parasitic growth suggests that the inhibition of the polyamine pathway will interfere with the proliferation of the parasites (Assaraf *et al.*, 1984). This inhibition can be approached by three general routes: 1) with the application of active site-based inhibitors targeting the pathway's essential biosynthetic enzymes; 2) by interfering with polyamine transport; and 3) by using non-functional polyamine structural analogues to replace functional polyamines resulting in an altered intracellular polyamine homeostasis (Müller *et al.*, 2001). Biochemical studies on the polyamine pathway enzymes have highlighted important differences between the host and parasite enzymes such as size, substrate specificities and unique structural features. Differences between the mammalian and *P. falciparum* AdoMetDC and ODC enzymes are listed in Table 1.2.

Table 1.2: Mammalian ODC and AdoMetDC *versus P. falciparum* AdoMetDC/ODC
Compiled from (Krause *et al.*, 2000; Müller *et al.*, 2001; Wrenger *et al.*, 2001; Wells *et al.*, 2006).

Mammalian AdoMetDC, ODC	PfAdoMetDC/ODC
1. Separate monofunctional proteins	1. Arranged on bifunctional protein
2. Limited ODC inhibition by putrescine	2. PfODC more strongly feedback regulated by putrescine
3. AdoMetDC stimulated by putrescine	3. PfAdoMetDC not stimulated by putrescine
4. AdoMetDC inhibition by Tris	4. No PfAdoMetDC inhibition by Tris
5. Inserts absent	5. Presence of parasite-specific inserts
6. Half-lives between 15 and 35 min	6. Half-life of more than 2 hrs

The ability of substrate analogues to interfere with polyamine enzyme activity as well as their effects on parasite growth has been investigated. DFMO is a well-known enzyme-activated irreversible inhibitor of ODC and causes the alkylation of the enzyme's active site. Even though its effect on *P. falciparum* growth is only cytostatic, it has been successfully applied in the treatment of West African sleeping sickness caused by *T. brucei gambiense* (Assaraf *et al.*, 1984; Wang, 1995). The success rate in DFMO treatment of the latter infections may be attributed to several aspects: 1) rapid division of parasitic cells results in a higher polyamine requirement than in the host cells; 2) trypanosomes also use spermidine to produce trypanothione, which maintains the intracellular redox state (Fairlamb *et al.*, 1987); 3) the trypanosomal ODC is more stable and has a longer half-life than that of the host's (Phillips *et al.*, 1987); and 4) DFMO may be effectively transported into the trypanosomal parasites as the drug does not have to cross several membranes as is the case for the intracellular malaria parasites (Wrenger *et al.*, 2001).

The ODC inhibitor 3-aminooxy-1-aminopropane (APA) and its derivatives CGP52622A and CGP54169A as well as the AdoMetDC inhibitors CGP40215A and CGP48664A severely effect PfAdoMetDC/ODC activity and results in reduced intracellular polyamine concentrations (Das Gupta *et al.*, 2005). MDL73811 irreversibly inhibits PfAdoMetDC and is roughly a 1000-fold more effective than DFMO treatment (Wright *et al.*, 1990). Bitonti's group also showed that the bis(benzyl)-polyamine analogue, MDL27695, rapidly inhibits the *in vitro* growth of both chloroquine-sensitive and resistant *P. falciparum* strains, and if administered in combination with DFMO, cures malaria in *P. berghei*-infected mice (Bitonti *et al.*, 1989).

Treatment of *P. falciparum* with the potent PfSpdSyn inhibitor, dicyclohexylamine, completely arrests parasite growth of both chloroquine-sensitive and resistant strains (Kaiser *et al.*, 2001) and its derivative 4MCHA, results in up to 85% growth arrest within 48 hrs when used in micromolar quantities (Haider *et al.*, 2005).

Crystal structures and homology models of the polyamine metabolic enzymes are helpful to visualise the interaction between the inhibitor and the active site residues, providing a physical glimpse into a formerly unknown chemical space. These structures are particularly helpful in the identification and *in silico* testing of a specific set of lead chemical compounds, which would have been painstaking to test experimentally (Mehlin, 2005). Homology models provide an excellent alternative to obtaining structural information due to the challenges involved in expressing pure and sufficient amounts of *P. falciparum* proteins required for crystallisation studies. Homology models of three *P. falciparum* polyamine biosynthetic proteins have been solved and published, i.e. PfAdoMetDC (Wells *et al.*, 2006), PfODC (Birkholtz *et al.*, 2003) and PfSpdSyn (Burger *et al.*, 2007) [also crystallised, PDB entry 2HTE and (Dufe *et al.*, 2007)].

A structure for the PfAdoMetDC domain of the bifunctional PfAdoMetDC/ODC was produced by homology modeling, which revealed a number of novel properties. In comparison to the monofunctional human AdoMetDC, PfAdoMetDC undergoes more protein–protein interactions within the bifunctional arrangement. This more protein rich environment results in lower sequence identity to the template for those regions that are involved in these new interactions, which was found to correspond to the one face of PfAdoMetDC. The model showed that the replacement of a single residue within the active site of PfAdoMetDC is responsible for the lack of Tris inhibition. Basic or non-polar residues also replace certain residues and prevent any interaction with putrescine due to repulsion between these residues and the amine ends of putrescine. These differences in human and parasite active sites, as revealed with homology modeling, can be exploited in the design of potential parasite-specific inhibitors (Wells *et al.*, 2006).

A homology model has also been created for PfODC bound to DFMO, as well as the substrate analogues CGP52622A and CGP54169A. Possible interactions between these ligands and the PfODC active site residues were identified. The DFMO interacting site is conserved amongst different species, which explains its non-specific binding to ODC from different organisms. Both the substrate analogues interact with parasite-specific residues that are unique to PfODC explaining the competitive inhibition of PfODC without affecting the human counterpart. The model thus provides support for further studies aimed at exploring these compounds as possible antimalarial agents (Birkholtz *et al.*, 2003).

A PfSpdSyn homology model could also explain its effective inhibition with 4MCHA. This inhibitor was shown, with the help of molecular dynamics, to bind in the putrescine-binding cavity via its amine group while its hydrophobic region protrudes into an adjacent hydrophobic cavity. Information on inhibitor interactions obtained from the PfSpdSyn model is

useful for further research in the development of parasite-specific inhibitors based on structural information and different computational methods (Burger *et al.*, 2007). Recently, the crystal structure of PfSpdSyn in complex with dcAdoMet, 4MCHA and another inhibitor S-adenosyl-1,8-diamino-3-thio-octane (AdoDATO) became available. The structure with bound dcAdoMet showed that this substrate stabilises the active site gatekeeper as well as changes the active site conformation for the subsequent binding of the second substrate, putrescine. The mode of interactions with the inhibitors also revealed important binding sites that may be modified for the synthesis of future, more potent inhibitors (Dufe *et al.*, 2007).

Apart from the characteristics already mentioned here, there are unique properties of the rate-limiting bifunctional PfAdoMetDC/ODC that can be exploited during the design of antimalarial drugs as will be highlighted in the subsequent section.

1.4.4.1 The bifunctional PfAdoMetDC/ODC protein

The bifunctional PfAdoMetDC/ODC protein has a predicted molecular mass of ~330 kDa. The PfAdoMetDC domain is located at the N-terminus and consists of residues 1-529, the C-terminal PfODC domain consists of residues 805-1419 while the hinge region connecting these two domains spans residues 530-804 (Figure 1.12) (Müller *et al.*, 2000). PfAdoMetDC is post-translationally cleaved into two low (9 kDa) and two high (60 kDa) molecular weight subunits The PfAdoMetDC and PfODC domains combine to form an enzymatically active heterotetrameric complex, consisting of a PfODC homodimeric component and a heterotetrameric PfAdoMetDC component, two bifunctional heterodimers of 166 kDa each thus associate to form the active bifunctional heterotetrameric protein of ~330 kDa (Figure 1.12) (Müller *et al.*, 2000).

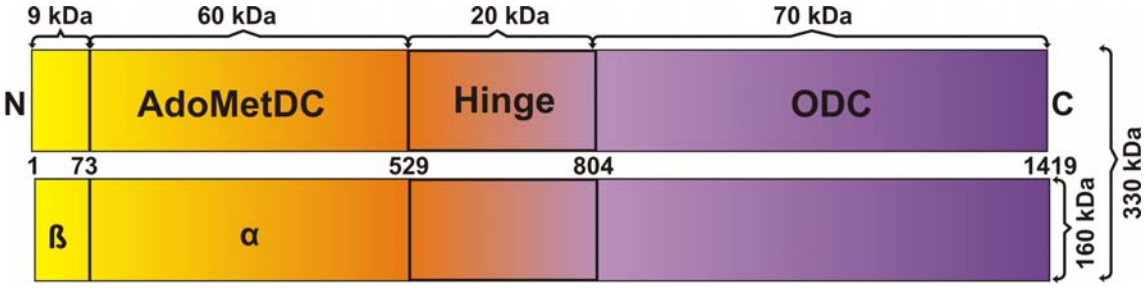

Figure 1.12: Schematic diagram of the bifunctional *P. falciparum* AdoMetDC/ODC protein. The N-terminal PfAdoMetDC domain consists of α and β chains and is connected to the C-terminal PfODC domain via a hinge region. The sizes of the individual domains, dimeric components and the heterotetrameric complex are also given (Müller *et al.*, 2000).

The individual domains participate in direct protein-protein interactions (Birkholtz *et al.*, 2004), while their active sites have been shown to function independently (Wrenger *et al.*, 2001). A possible explanation for the bifunctional arrangement could be that controlling the

abundance and activity of a single protein regulates polyamine biosynthesis (Müller *et al.*, 2001).

1.4.4.2 Ornithine decarboxylase

The vitamin B6-derived cofactor pyridoxal-5'-phosphate (PLP) is absolutely essential for the proper functioning of the ODC enzyme during the transimination of ornithine. Two active sites are formed at the interface of the homodimeric protein as a consequence of the dimerisation of the PfODC monomers and consist of residues that are donated by both of these. The homology model showed that the two PfODC monomers are arranged in a head-to-tail manner where the N-terminal of one monomer faces the C-terminal of the other and *vice versa* (Figure 1.13) (Birkholtz *et al.*, 2003).

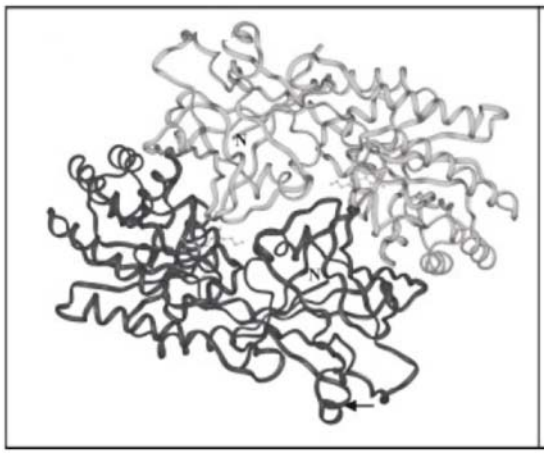

Figure 1.13: The head-to-tail organisation of the two monofunctional *P. falciparum* ODC monomers.
The two monomers are shown in different shades of grey and viewed from the bottom. Taken from (Birkholtz *et al.*, 2003).

The specific activity of PfODC for its substrate ornithine is 93.2 pmol/min/mg with a *K*m value of 42.4 µM (Müller *et al.*, 2000). The monofunctional homodimeric PfODC domain has a molecular mass of approximately 140 kDa (Birkholtz *et al.*, 2004). The expression and catalytic properties of two different recombinant constructs of PfODC have been investigated. The first construct is a recombinant PfODC protein (rPfODC) and the second one included 144 amino acids of the hinge region (rPfHinge-ODC). The *K*m value of rPfHinge-ODC for ornithine is approximately four times lower than that of rPfODC indicating that the hinge region is involved in substrate binding while the presence of the hinge region also increased the specific activity of the PfODC enzyme (Krause *et al.*, 2000).

The hinge region connecting the two domains of the bifunctional protein is involved in the folding of PfODC and causes a 10-fold increase in its specific activity. These results led to

further investigations of possible protein-protein interactions between the bifunctional domains (Krause *et al.*, 2000; Wrenger *et al.*, 2001). Domain-domain interactions have been reported to play a role in the Plasmodial bifunctional DHFR/TS where the catalytic activity of TS is dependent on its interaction with DHFR (Shallom *et al.*, 1999). These interactions are, however, not mirrored in PfAdoMetDC/ODC. The specific activities of the respective enzymes are not effected when the neighbouring enzyme is inhibited or when its substrate is omitted suggesting that the active sites of the two domain enzymes act independently (Wrenger *et al.*, 2001).

Several amino acids essential for catalytic activity (cofactor and DFMO binding) and dimerisation are conserved in the PfODC sequence even though the overall homology of PfAdoMetDC/ODC to the mammalian monofunctional counterparts is low (Müller *et al.*, 2000). Mammalian ODC is relatively unstable with a half-life of several minutes due to the action of antizyme and the presence of a C-terminal PEST region involved in the recruitment of the 26S proteasome (Russell, 1985; Hayashi and Murakami, 1995). ODC in *Crithidia fasciculata* (a non-pathogenic trypanosomatid) is also a metabolically unstable protein and is rapidly degraded in mammalian systems, whereas the closely related *Leishmania donovani* ODC is not. The degradation of *C. fasciculata* ODC in the mammalian systems was shown to be dependent on a functional 26S proteasome and, in contrast to the degradation of mammalian ODC, does not involve antizyme but instead appears to be associated with the poly-ubiquitination of the enzyme (Nasizadeh *et al.*, 2003; Persson *et al.*, 2003).

Closer inspection of the PfODC sequence also revealed a high abundance of Pro, Glu and Ser residues that may constitute a PEST sequence for degradative signalling. This, however, was thought not to be the case since PfODC has been shown to be relatively stable (Assaraf *et al.*, 1988). This theory is also supported by the differential host-parasite responses to the irreversible inhibitor, DFMO (Müller *et al.*, 2001).

Apart from the bifunctional nature of the PfAdoMetDC/ODC protein, PfODC also has another unique characteristic compared to the mammalian counterpart. This domain contains two parasite-specific inserts (namely O1 and O2) that have no homology to other proteins in other organisms (Birkholtz *et al.*, 2003) and are discussed in more detail in section 1.4.4.4.

1.4.4.3 S-adenosylmethionine decarboxylase

PfAdoMetDC activity is located on the N-terminus of the bifunctional PfAdoMetDC/ODC protein. This unique pyruvoyl-utilising decarboxylase has a *K*m value of 33.5 µM for its substrate AdoMet and a specific activity of 14.8 pmol/min/mg (Müller *et al.*, 2000). Experiments have shown that PfAdoMetDC lacks the regulatory mechanism proposed for

mammalian cells to relate putrescine abundance to spermidine synthesis as this enzyme is not stimulated by high levels of putrescine (Wrenger *et al.*, 2001; Wells *et al.*, 2006). The *P. falciparum* and eukaryotic AdoMetDC domains consist of an αββα-sandwich (Figure 1.14) (Wells *et al.*, 2006), which is formed from an autocatalytic cleavage event that produces the N-terminal β-chain (9 kDa) and the C-terminal α-chain (60 kDa). The dimerisation of PfAdoMetDC/ODC leads to the formation of the active site between the two β-sheets (Ekstrom *et al.*, 1999; Bennett *et al.*, 2002).

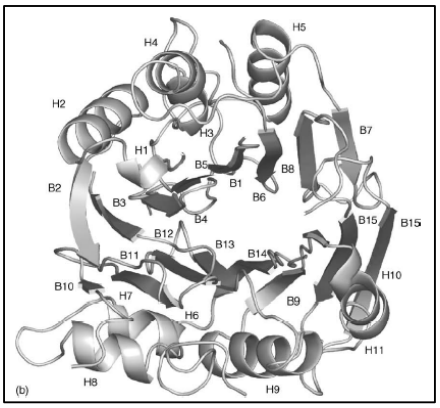

Figure 1.14: Diagram of the monofunctional *P. falciparum* AdoMetDC homology model showing the αββα structural arrangement.
Taken from (Wells *et al.*, 2006).

Unlike mammalian AdoMetDC, PfAdoMetDC is not inhibited by Tris, which may be due to four amino acid substitutions in the active site when compared to the mammalian counterpart. The lack of PfAdoMetDC stimulation with putrescine also seems to be due to the replacement of acidic residues with basic or non-polar residues (specifically Lys15 and Lys215) in the putrescine-binding site needed for the binding of the positive amine putrescine terminals. The positively charged PfAdoMetDC putrescine-binding pocket thus repels the positively charged putrescine molecules. The PfAdoMetDC domain also contains insertions that interrupt regions of homology to mammalian AdoMetDC (Wells *et al.*, 2006).

1.4.4.4 Parasite-specific inserts

An interesting feature of Plasmodial genomes, apart from the A+T richness, is the presence of rapidly diverging, species-specific, non-globular, possibly low-complexity containing regions that are either present in tandem repeats or sparsely distributed insertions, which are absent in orthologues. The insertions are mostly flexible, hydrophilic areas due to the presence of mainly Asn residues and therefore form loops that extrude from the protein core. The frequency of low-complexity regions (LCRs) in *P. falciparum* is particularly high and can be found in enzymes such as RNA polymerases (Bzik, 1991), glutamylcysteine synthetase (Lüersen *et al.*, 1998) and DNA topoisomerase (Cheesman *et al.*, 1994). The presence of

these regions in Plasmodial proteins raises questions about their origin and how they are maintained within the parasite genome (Pizzi and Frontali, 2000; Pizzi and Frontali, 2001). Compared to the size of the independent mammalian AdoMetDC and ODC enzymes, the PfAdoMetDC/ODC bifunctional protein size is much larger due to the presence of several parasite-specific inserts that interrupt sequence homology within both the domains (Birkholtz *et al.*, 2003; Birkholtz *et al.*, 2004; Wells *et al.*, 2006). The inserts range in size from 6 to 180 amino acids (Wells *et al.*, 2006). They have been shown to mediate physical interactions between the two domains by stabilising interdomain protein-protein interactions, thereby regulating the activity of both domains (Birkholtz *et al.*, 2004). The PfAdoMetDC domain contains inserts A1 (residues 57-63), A2 (residues 110-137) and A3 (residues 259-408) (Wells *et al.*, 2006). The hinge occupies residues 530-804 and is for all purposes also considered as an insert (Wells *et al.*, 2006), while the O1 (residues 1047-1085) and O2 (residues 1156-1302) inserts are present in the PfODC domain (Birkholtz *et al.*, 2003).

The O1 insert is particularly important for both the domain activities. Deletion of O1 reduces the PfAdoMetDC and PfODC activities by 77% and 94%, respectively (Birkholtz *et al.*, 2004). Furthermore when this 39 amino acid insert was deleted, the wild type PfAdoMetDC and the mutant PfODC domains failed to assemble into the heterotetrameric complex. The PfODC monomers also failed to dimerise, which could be due to a conformational change at the dimer interface upon deletion of the insert. The O1 insert is thus important for both inter- and intramolecular protein-protein interactions within the PfODC domain thereby facilitating bifunctional complex formation (Birkholtz *et al.*, 2004).

The O1 parasite-specific insert has considerable secondary structure. Original reports indicated the presence of four anti-parallel β-sheets but subsequent analysis improvements in the software now indicates the presence of a highly conserved α-helix. The insert appears to lie parallel to the protein core, looping out towards the C-terminus at the same side as the entrance to the active site (Birkholtz *et al.*, 2004). The insert is also flanked by mobile Gly residues (Gly1036-1038 and Gly1083) suggesting that insert O1 may be acting as a flexible gatekeeper for substrate entry into the active site pocket (Birkholtz *et al.*, 2004). Mutational analyses showed that the mobility of this insert is vital for the decarboxylase activities of both domains since the correct positioning of the α-helix may mediate physical contacts between the two domains (Roux, 2006). This may be communicated to the respective active sites via long-range interactions (Myers *et al.*, 2001). The smaller insert O1 is also better conserved between Plasmodial species (Birkholtz *et al.*, 2004).

The O2 insert forms no significant secondary structures and is more important for PfODC than for PfAdoMetDC activity since it is spatially removed from the N-terminus (Birkholtz *et*

al., 2004). However, this insert contains several (NND)x-repeats that could play an important role in the formation of the PfODC homodimer through the formation of a polar zipper (Perutz *et al.*, 1994; Birkholtz *et al.*, 2004; Roux, 2006). This is not unusual for a *P. falciparum* protein, as it has been shown that ~35% of these proteins contain amino acid repeats, with Asn being the most abundant (Singh *et al.*, 2004). However, deletion of this 23-residue region depleted the PfAdoMetDC activity by only 27% and the PfODC activity by 46% (Roux, 2006).

The 180 residue hinge region connects the PfAdoMetDC and PfODC regions (Müller *et al.*, 2000) and is involved in the conformational stability and the correct quaternary structure formation of the PfODC domain (Krause *et al.*, 2000). FPLC studies showed that the hinge stabilises the heterotetrameric bifunctional protein complex by mediating interdomain interactions between the two domains (Birkholtz *et al.*, 2004). Several secondary structures occur in this region, notably two α-helixes and a β-sheet (Roux, 2006). It is possible that the α-helices have an indirect effect on the catalytic activities of both enzyme domains due to contributions to interdomain interactions. Deletion of the β-sheet appeared to result in multiple conformations of the bifunctional enzyme, with variable catalytic activity, suggesting that this secondary structure is essential for the stabilisation of the entire protein (Roux, 2006).

Since the deletion mutagenesis studies done by Birkholtz *et al*. in 2004, the so-called A1 insert has been divided into inserts A2 and A3 when the homology model of PfAdoMetDC was solved (Birkholtz *et al.*, 2004; Wells *et al.*, 2006). This means that the activity depletion results of the A1 insert have been updated.

It is not yet known exactly how the domains of PfAdoMetDC/ODC interact and what specific residues play important roles in these interactions. The exact protein interaction areas need to be examined for their possible involvement in domain interactions and activities. In addition, the noteworthy effect that the deletion of the O1 parasite-specific insert has on the entire PfAdoMetDC/ODC protein indicates that this area may likely be important for protein-protein interactions involved in the dimerisation of PfODC. It is thus important to analyse the function of specific areas in this insert, which can then be used as a platform for the design and application of an interface interference peptide.

1.5 Research aims

This study aims to delineate functional areas within the PfAdoMetDC parasite-specific inserts as well as to determine the importance of the O1 insert to the bifunctional *P. falciparum* PfAdoMetDC/ODC. Three distinct studies were thus undertaken:

Chapter 2: An efficient method for the deletion of parasite-specific inserts in malarial genes. In this chapter, a novel inverse PCR method as particularly suitable for the deletion of large areas (>100 bp) in large malarial genes was investigated. The method successfully deleted the largest insert in the PfAdoMetDC domain.

Chapter 3: Delineation of structural features of the parasite-specific inserts in PfAdoMetDC. In this chapter, the roles of the parasite-specific inserts in the PfAdoMetDC domain as well as the secondary structures within these were investigated.

Chapter 4: Investigations of the conserved O1 parasite-specific insert. The role of the O1 parasite-specific insert in the dimerisation and activity of this domain was investigated. Specific synthetic peptides were subsequently designed and tested as possible inhibitors of protein activity via interference with protein-protein interactions.

Chapter 5: Concluding discussion

The results within this dissertation have been published and/or presented as follows:

Chapter 2: 1) Williams, M., A.I. Louw, L. Birkholtz (2007). "Deletion mutagenesis of large areas in *Plasmodium falciparum* genes: a comparative study." Malaria Journal **64**: 1-9

2) SASBMB XXth, University of Kwazulu-Natal, Pietermaritzburg, July 2006. Poster title: An improved method for the deletion of large areas in large genes. M. Williams, A.I. Louw, L. Birkholtz.

Chapter 3: 1) Molecular Cell Biology Group Symposium, University of Witwatersrand, Johannesburg, October 2006. Presentation title: Structure-function analysis of the O1 parasite-specific insert in the uniquely bifunctional S-adenosylmethionine decarboxylase/ornithine decarboxylase of *Plasmodium falciparum*. M. Williams, A.I. Louw, L. Birkholtz.

2) Manuscript in preparation: Delineation of structural features within the parasite-specific inserts involved in enzymatic activities of the bifunctional S-adenosylmethionine decarboxylase/ornithine decarboxylase of *Plasmodium falciparum*. Williams, M., S. Roux, G.A. Wells, L. Birkholtz, A.I. Louw.

Chapter 4: 1) Manuscript in preparation: A conserved parasite-specific insert influences the activities of the bifunctional S-adenosylmethionine decarboxylase/ornithine decarboxylase of *Plasmodium falciparum*. Williams, M., S. Roux, G.A. Wells, L. Birkholtz, A.I. Louw.

Chapter 2: An efficient method for the deletion of parasite-specific inserts in malarial genes

2.1 Introduction

Specialised organisms like *P. falciparum* have unique adaptations that include generally larger protein sizes compared to orthologues due to the bifunctional arrangement of proteins and the presence of parasite-specific inserts (Mehlin *et al.*, 2006). In general, these inserts are species-specific, rapidly diverging, non-globular regions containing low-complexity areas consisting of mainly Lys and Asn residues that form flexible prion-like domains extending from the protein core (Pizzi and Frontali, 2000; Pizzi and Frontali, 2001). Up to 90% of *P. falciparum* proteins contain at least one low-complexity region that may co-localise with parasite-specific inserts. These proteins are also up to 50% longer compared to their yeast counterparts (Gardner *et al.*, 2002; DePristo *et al.*, 2006). The exact evolutionary origin and functional advantages of these inserts remain elusive. It has, however, been proposed by Karlin *et al*. that these inserted regions are adaptive as they appear to promote protein-protein interactions and mRNA stability (Karlin *et al.*, 2002). For example, in *P. falciparum* it has been demonstrated that stabilisation of interdomain interactions of the bifunctional malarial drug target, DHFR/TS, is mediated via an essential parasite-specific insert (Shallom *et al.*, 1999; Yuvaniyama *et al.*, 2003). DHFR/TS also regulates its own translation by binding to cognate mRNA (Zhang and Rathod, 2002). Some parasite-specific inserts have been implicated in malaria pathogenesis due to an increase in the antigen diversity and resultant incomplete immune response of the human host to *P. falciparum* (Gardner *et al.*, 2002).

Due to the ever-increasing resistance of malarial parasites to commercially available drugs, it is of extreme importance to identify novel drug targets. The bifunctional *P. falciparum* AdoMetDC/ODC (PfAdoMetDC/ODC) regulates the synthesis of polyamines, essential molecules for DNA and RNA stabilisation (Assaraf *et al.*, 1987). In addition to its unique bifunctional nature, the protein contains six parasite-specific inserts of up to 180 residues (Müller *et al.*, 2000; Birkholtz *et al.*, 2004; Wells *et al.*, 2006). Previous analysis of the structure-activity relationships indicated that these inserts are important for activity of the respective decarboxylase domains and act as mediators of protein-protein interactions in the bifunctional protein complex (Birkholtz *et al.*, 2004).

Site-directed mutagenesis is an important technique used in studying protein structure-activity relationships. Non-PCR based deletion mutagenesis methods mostly use sequence-

specific exonuclease-based enzymatic procedures but has the disadvantage that a single-stranded template is required (Braman, 2002). Since the development of PCR, oligonucleotide-mediated site-directed deletion mutagenesis has become a technically straightforward and efficient endeavour [reviewed in (Ishii *et al.*, 1998; Braman, 2002)]. Widely used PCR-based mutagenesis methods include the QuickChange™ site-directed mutagenesis (QCM) and ExSite™ methods (Stratagene) that are effective for the deletions of areas of up to 12 bp (Figure 2.1 A and B, respectively) (Papworth *et al.*, 1996). Several modifications to the QCM have been reported to be successful for deletions in large genes. This includes a partial overlapping primer design method allowing seven bp deletions (Figure 2.1 C) (Zheng *et al.*, 2004) and inverse PCR methods with a maximal deletion of 102 bp (Figure 2.1 D) (Wang and Wilkinson, 2001). However, none of these methods have been reported to be consistent in removing areas >100 bp in genes (Makarova *et al.*, 2000).

In this study, a restriction enzyme (RE)-mediated inverse PCR is described that successfully removes large areas in abnormally large genes (gene size ~4300 bp). This method was specifically designed for use on large parasite-specific inserts of the large PfAdoMetDC/ODC protein. The deletion mutagenesis efficiency of this RE-mediated inverse PCR method was compared to the existing methods described above by deleting a 411 bp parasite-specific insert in the PfAdoMetDC domain of the bifunctional PfAdoMetDC/ODC protein. In addition, its application to delete an insert in another malarial gene was also investigated to validate the method.

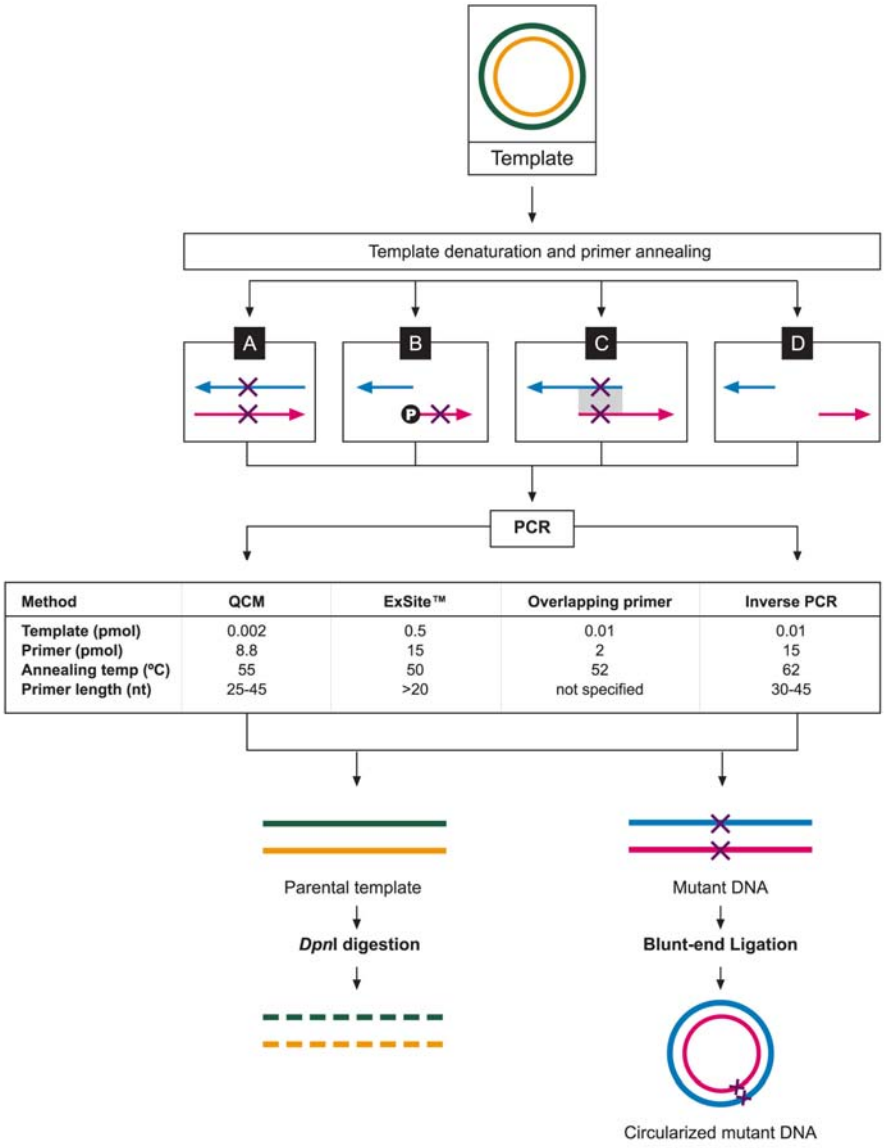

Method	QCM	ExSite™	Overlapping primer	Inverse PCR
Template (pmol)	0.002	0.5	0.01	0.01
Primer (pmol)	8.8	15	2	15
Annealing temp (°C)	55	50	52	62
Primer length (nt)	25-45	>20	not specified	30-45

Figure 2.1: Overview of four currently used deletion mutagenesis PCR methods.
(A) QuickChange™ site-directed mutagenesis method, (B) ExSite™ site-directed mutagenesis method, (C) Overlapping primer method, (D) Inverse PCR method. The template plasmid (green and yellow, top panel) is denatured during the first step of the PCR reaction to allow the primers containing the desired mutation to anneal to the specific target sites. In the QCM method the primers completely overlap and the mutations are incorporated into both of the primers (A). The ExSite primers do not overlap at all; instead only one of the primers contains the mutation. One or both of the primers must also be phosphorylated (B). Partial overlapping at the 3'-ends is characteristic of the overlapping primers. The mutation is present in both of the primers within the overlapping region (C). And finally, primers for the inverse PCR method do not overlap, but simply start at the opposite ends of the desired area to be deleted (D). The pink and blue arrows are the sense and antisense primers. Crosses on the primers represent the mutation sites and P is the single phosphorylated ExSite™ primer in (B). The primers are extended during which the desired mutations are incorporated and subsequently amplified. Two different linear PCR products are created during the PCR reactions, parental template and mutated DNA. The parental DNA is degraded by a *Dpn*I digestion step while the mutant DNA is circularised by blunt-end ligation. The newly formed mutant plasmids can subsequently be transformed into competent cells.

2.2 Methods

2.2.1 Deletion mutagenesis PCR

2.2.1.1 Cloning of genes into pASK-IBA3

All five methods described below (QCM, ExSite™, overlapping primer, inverse PCR and RE-mediated inverse PCR) used the *P. falciparum AdoMetDC/ODC* gene (gene size ~4300 bp) cloned into a pASK-IBA3 vector [vector size ~3100 bp (Institut für Bioanalytik, Germany)] as template (total template size ~7400 bp and called pA/Owt henceforth) (Müller *et al.*, 2000; Birkholtz *et al.*, 2004; Wells *et al.*, 2006). All methods were used to delete the 411 bp A3 insert in the PfAdoMetDC domain. The *P. falciparum* pyridoxal kinase (*PfPdxK*, gene size ~1500 bp) was also cloned into the same pASK-IBA3 vector (total template size ~4600 bp) (Wrenger *et al.*, 2005) to delete a 618 bp parasite-specific insert (A.O. Tastan Bishop, personal communication). The mutagenesis primers that were used in each of the deletion mutagenesis methods are listed in Table 2.1 below.

Table 2.1: Primers used for the various deletion mutagenesis protocols

Primer Pair	Primer	Length (bp)	Tm* (°C)	Primer Sequence (5' to 3')	Mutagenesis method
P1	A3consF	43	78	gctttatgatagtagtgatgctgataatt ataataaggaaagc	QuickChange™ site-directed method
	A3consR	43	78	gctttccttattataattatcagcatcact actatcataaagc	
P2	A3overF	49	79	gatagtagtgatgctgat↓aattataat aaggagagctttttatataatg	Overlapping primer method
	A3overR	55	80	gctttccttattataatt↓atcagcatca ctactatcataaagctttaaattatcc	
P3	A3reF	27	73(62)	CGCggatccaattataataaggaa agc	ExSite™, Inverse (Wang and Wilkinson, 2001) and RE-mediated inverse PCR methods
	A3reR	34	79(69)	CGCggatccatcagcatcactacta tcataaagc	
P4	PdxkF	34	78(67)	CGCggatccaatctaaattttctttgg gtatgtg	RE-mediated inverse PCR method
	PdxkR	38	79(67)	CGCggatcctttccttcttaattcaagt atatttttgg	

The *Bam*HI restriction sites for primer pairs P3 and P4 are underlined. Capital letters show the 5'-terminal overhangs of the P3 and P4 primer pairs The P3 primer pair was used with and without *Bam*HI restriction digestion for the RE-mediated inverse PCR and inverse PCR methods, respectively. * The Tm's were calculated according to the Stratagene formula: 81.5 + 0.41(%GC) - 675/N) or for primer pairs P3 and P4 with the Rychlik *et al*. formula: 69.3 + 0.41(%GC) - (650/N) (Rychlik *et al.*, 1990) as indicated in parentheses. ↓ indicates where the deletions were made with the overlapping primer method.

2.2.1.2 QuickChange™ site-directed mutagenesis (QCM)

According to the manufacturers' recommendations, a 50 µl reaction contained 10 ng template (0.002 pmol for the 7400 bp template used here), 125 ng of each of the primers (8.8 pmol

each of A3consF and R), 1 × *Pfu* reaction buffer, 200 µM of each dNTP and 2.5 U *Pfu* DNA polymerase (Fermentas, Canada). The temperature cycles were as follows: incubation at 95°C for 30 sec, followed by 30 cycles of 95°C for 30 sec, 55/60°C for 1 min, 68°C for 2 min/kb and a final extension at 68°C for 2 min/kb.

2.2.1.3 ExSite™ PCR-based site-directed mutagenesis

The PCR reaction with a final volume of 25 µl was set up as follows: 0.5 pmol template, 15 pmol of each primer (A3reF and R), 1 × *Pfu* reaction buffer, 200 µM of each dNTP and 2.5 U *Pfu* DNA polymerase (Fermentas, Canada). The temperature cycles were as follows: incubation at 94°C for 4 min, 50°C for 2 min, 68°C for 2 min/kb of template, followed by 18 cycles of 94°C for 1 min, 56°C for 2 min and 68°C for 1 min/kb, followed by a final incubation at 68°C for 5 min.

2.2.1.4 Overlapping primer method

A typical deletion mutagenesis reaction with a final volume of 50 µl, contained 50 ng template (0.01 pmol for the 7400 bp template), 2 pmol of each primer (A3overF and R), 1 × *Pfu* reaction buffer, 200 µM of each dNTP and 2 U of *Pfu* DNA polymerase (Fermentas, Canada). The cycling parameters were 94°C for 3 min, 16 cycles of 94°C for 1 min, 52°C for 1 min and 2 min/kb at 68°C with a final extension for 1 hr at 68°C (Zheng *et al.*, 2004).

2.2.1.5 Inverse PCR method

The PCR reaction set up followed the protocol as indicated by Wang *et al*. A typical deletion mutagenesis reaction with a 50 µl final volume contained 1 ng template (0.15 fmol for the 7400 bp template), 150 ng of both primers (15 pmol of A3reF and R), 1 × *Pfu* reaction buffer, 200 µM of each dNTP and 2.5 U *Pfu* DNA polymerase (Fermentas, Canada). The temperature cycles were as follows: 95°C for 3 min, 18 cycles of 95°C for 45 sec, 62°C for 1 min and 68°C for 2 min/kb, with a final extension at 68°C for 2 min/kb. The same reaction was also repeated with the addition of 5% dimethyl sulfoxide (DMSO) (Wang and Wilkinson, 2001).

2.2.1.6 RE-mediated inverse PCR method

For the RE-mediated inverse PCR method described here a typical deletion mutagenesis reaction with a 50 µl final volume contained 50 ng template (0.01 pmol for the 7400 bp template), 150 ng of both primers (15 pmol each of A3reF and R), 1 × *Pfu* reaction buffer, 200 µM of each dNTP and 2.5 U ExTaq DNA polymerase (TaKaRa Biomedicals, Japan). The temperature cycles were typically as follows: 95°C for 3 min, 18 cycles of 95°C for 45 sec, 56°C (Table 2.1) or 62°C for 1 min and 68°C for 2 min/kb, with a final extension at 68°C for 2 min/kb (Wang and Wilkinson, 2001). However, follow-up experiments have shown a 10^5

molar excess primer:template ratio to be optimal (where the best results were obtained with 0.15 fmol template and 15 pmol primer).

The effectiveness of this method in deleting a parasite-specific insert in another A+T rich *P. falciparum* gene was also tested. The reaction conditions and temperature cycles for the removal of the insert from *PfPdxK* were identical as given above.

All PCR reactions were performed in a GeneAmp 9700 thermocycler (PE Applied Biosystems, USA).

2.2.1.7 Analysis of mutagenesis products

PCR products were visualised with 1% w/v agarose (Whitehead Scientific, SA) electrophoresis in TAE (40 mM Tris-OAc and 1 mM EDTA, pH 8.0) containing ethidium bromide (1 µg/ml). The electrophoresis runs were performed in Minnie Submarine HE33 Gel units [Hoeffer Scientific systems, (Amersham Biosciences, UK)] at a speed of 8 V/cm. DNA bands were visualised at a wavelength of 312 nm on a Spectroline TC-312A UV transilluminator (Spectronics Corporation, Germany) and gel images were captured digitally with a 4.0 mega pixel Canon Powershot G2 camera using the IC Capture Software.

Correctly sized PCR products were subsequently treated with 10 U of *Dpn*I for 3 hrs at 37°C to remove parental templates. For the RE-mediated inverse PCR method, 10 U *Bam*HI (Fermentas, Canada) was additionally added to the *Dpn*I digestion in a dual compatibility buffer Tango™ (33 mM Tris-OAc, 10 mM Mg-OAc, 66 mM K-OAc, 0.1 mg/ml BSA, pH 7.9). Products were purified with the High-Pure PCR product purification kit (Roche Diagnostics, Germany) and ligated for 16 hrs with 3 U of T4 DNA Ligase (Promega, USA) at 22°C for blunt-end ligation and 4°C for sticky-end ligation (RE-mediated inverse PCR product). The resulting circular plasmids were transformed into electrocompetent DH5α cells (Gibco BRL, Life Technologies, USA).

2.2.1.8 Electroporation into DH5α cells

DH5α *E. coli* (Gibco BRL, Life Technologies) cells were inoculated in 10 ml Luria Bertani (LB) liquid medium (1% w/v tryptone, 0.5% w/v yeast extract, 1% w/v NaCl, pH 7.5) and grown overnight at 37°C with agitation. The overnight culture was diluted 1:100 in 500 ml preheated LB-medium. The inoculations were grown at 37°C with agitation (250 rpm) until the optical density at 600 nm reached 0.5. The cultures were placed on ice for 20 min. The following steps were performed on ice. The cells were harvested at 1000 x g for 10 min at 4°C. Pellets were resuspended in 10 ml cold dddH_2O with swirling motions. Ice-cold dddH_2O (240 ml) was added to the cell suspensions and gently mixed after which the cells were once again

collected at 1000 x g at 4°C for 10 min. The supernatants were then discarded and the pellets were resuspended in the remaining fluid. These wash steps were repeated once again. The pellets were resuspended in 10 ml 10% v/v sterile glycerol and transferred to sterile 50 ml centrifuge tubes. These were incubated on ice for 1 hr. The cells were pelleted at 1000 x g for 10 min at 4°C and the supernatants were immediately discarded. The pellets were resuspended in 1 ml 10% v/v glycerol, aliquoted into ice old Eppendorf tubes and immediately frozen at -70°C.

The plasmids were precipitated in the presence of 1 mg/ml tRNA and 0.3 M NaOAc (pH 5), followed by the addition of three volumes of absolute ethanol. The mixtures were centrifuged at maximum speed for 40 min at 4°C. Supernatants were discarded and the pellets were washed with 100 µl 70% ethanol and centrifuged for 10 min at the same speed. The pellets were dried *in vacuo* and subsequently dissolved in 5 µl dddH_2O.

The electrocompetent DH5α cells (100 µl) were thawed on ice to which the concentrated plasmids were added. These mixtures were placed into ice old electroporation cuvettes (Eppendorf, Germany) and immediately electroporated at 2000 V. Preheated LB-glucose (20 mM glucose in LB-medium) was immediately added to the shocked cells and incubated at 37°C for 30 min in a shaking incubator (250 rpm). Cells containing the transformed plasmids were plated onto LB-amp agar plates (1% agar w/v in LB-medium with 100 µg/ml ampicillin) and incubated overnight at 37°C (250 rpm).

2.2.1.9 Plasmid isolation

The plasmids from five clones for each of the three different mutagenesis methods that produced PCR products were isolated. Five colonies of each were inoculated overnight in 5 ml LB-amp (LB-medium with 50 µg/ml ampicillin) at 37°C in a shaking incubator set at 250 rpm. The cells were collected by centrifugation for 10 min at 13000 x g in a Heraeus Sepatech Medifuge. The High Pure Plasmid Isolation kit (Roche diagnostics, Germany) was used for plasmid isolation and the instructions were followed according to the manufacturer's protocol. Briefly, the pellets were suspended in 250 µl Suspension buffer (50 mM Tris-HCl, 10 mM EDTA, pH 8) followed by the addition of 250 µl Lysis buffer (0.2 M NaOH, 1% w/v SDS). The suspensions were incubated at room temperature for 5 min. A volume of 350 µl pre-cooled Binding buffer (4 M guanidine hydrochloride, 0.5 M KOAc, pH 4.2) was added to each suspension followed by an incubation period on ice for 5 min. The suspensions were centrifuged at 13 000 x g for 10 min after which the supernatants were transferred to separate filter-tubes and once again centrifuged for 1 min at the same speed. The filters were washed with Wash buffer II (20 mM NaCl, 2 mM Tris-HCl, pH 7.5) and the DNA was eluted in 100 µl Elution buffer (1 mM Tris-HCl, pH 8.5), after which the concentrations of the

purified plasmids were determined spectrophotometrically on a GeneQuantpro spectrophotometer (Amersham Biosciences, UK).

The concentrations were measured at a wavelength of 260 nm and the purities were analysed by their A260/280 ratio. A pure double-stranded plasmid should have a A260/280 ratio between 1.7 and 1.9 (Sambrook *et al.*, 1989).

2.2.1.10 Restriction enzyme mapping

Five clones for each of the three different mutagenesis methods that produced PCR products were analysed with *Hind*III restriction mapping. In the wild type pA/Owt plasmid, this enzyme should cut three times resulting in bands of ~3900, ~3100 and ~450 bp. However, in the ~400 bp deletion mutants, one of the sites is removed resulting in only two bands sized ~3900 and ~3100 bp. Application of the RE-mediated inverse PCR method on the deletion of ~600 bp from the *PfPdxK* gene also resulted in a PCR product. Five clones were analysed with *Eco*RI restriction mapping. The deletion removes an *Eco*RI site resulting in the linearisation of only the wild type non-mutated DNA (~4600 bp template).

2.2.1.11 Nucleotide sequencing

These same clones were thereafter analysed with nucleotide sequencing to confirm the mutagenesis results. The K215A1 (5'-gcttctacgtttgcattctgttcgg-3') sequencing primer was used as it binds 46 residues upstream of this area in *PfAdoMetDC/ODC*. Nucleotide sequencing of the *PfPdxK* mutants was not performed as mutagenesis could be confirmed by both the decrease in PCR product size (~4000 bp) and the removal of the *Eco*RI digestion site upon the deletion of the 618 bp parasite-specific insert.

The reactions were made up to a final volume of 20 µl and contained ~750 ng template, 5 pmol of the sequencing primer, 1 x Big Dye Sequencing buffer (400 mM Tris-HCl, 10 mM $MgCl_2$, pH 9.0) and 2 µl of Big Dye Ready Reaction mix version 3.1 (Applied Biosystems, USA). The sequencing cycles were performed in a GeneAmp 9700 thermocycler (PE Applied Biosystems, USA) with an initial denaturation step at 96°C for 1 min followed by 25 cycles of denaturation for 10 sec at 96°C, annealing at 50°C for 5 sec and extension at 60°C for 1 min. The labelled extension products were purified with ethanol precipitation. Briefly, the products were mixed with 2 µl of 3 M NaOAc (pH 4.6) and 50 µl ice-cold absolute ethanol. These were then centrifuged at 11 000 x g for 30 min at 4°C. The supernatants were discarded and the DNA washed with 250 µl 70% ethanol and subsequently collected by centrifugation for 10 min at the same speed. The pellets were dried *in vacuo* and stored at 4°C in the dark.

The products were analysed with an ABI PRISM 3100 capillary sequencer (PE Applied Biosystems). Sequences obtained were evaluated with the BioEdit version 5 (Hall, 1999).

2.3 Results and Discussion

2.3.1 Analysis of mutagenesis products

The wild type malarial *PfAdoMetDC/ODC* gene cloned into pASK-IBA3 was used as template for a comparative study of all the deletion mutagenesis methods described here (Figure 2.2 A and C, lane 1). Subsequent gel electrophoresis analysis of the PCR products obtained by the different methods showed that only the overlapping primer method, inverse PCR method and RE-mediated inverse PCR method yielded products ~7000 bp in size (Figure 2.2 B and C, lanes 2, 3, 4). However, no PCR products could be visualised for the QCM or ExSite™ methods.

The products obtained by the overlapping primer method, inverse PCR and RE-mediated inverse PCR method were further analysed for mutagenesis efficiency with *Hind*III restriction enzyme screening and occurrence of the expected ~3900 and ~3100 bp bands.

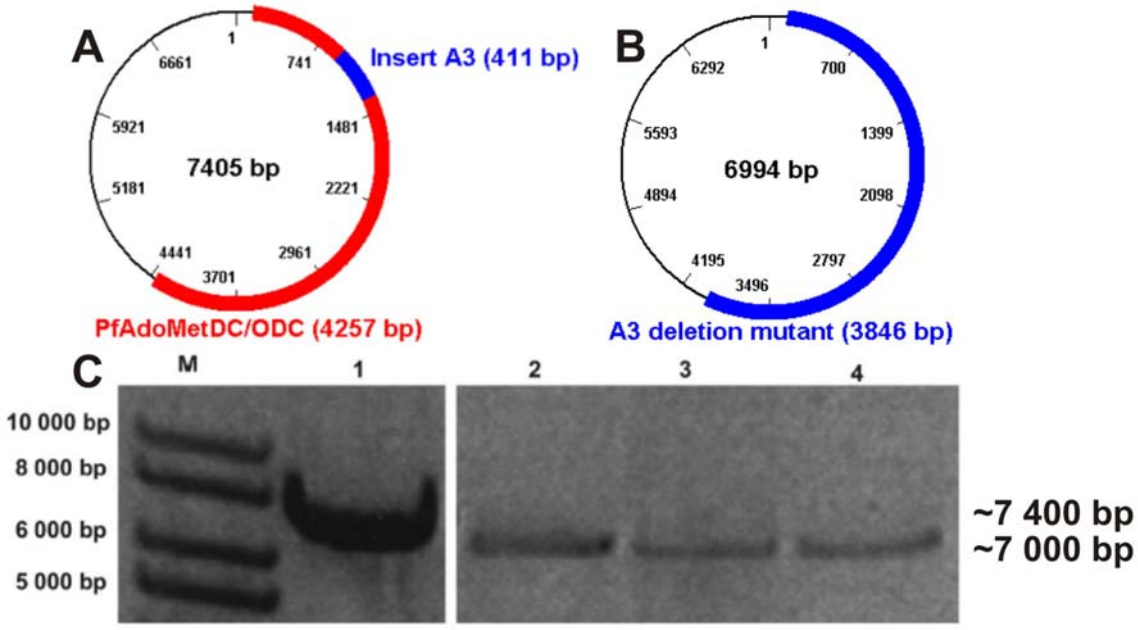

Figure 2.2: Agarose gel electrophoresis of the PCR products obtained with the various deletion mutagenesis PCR methods.
Schematic representations of the wild type (A) (gene size 4257 bp) and the 411 bp deletion mutant (B) (gene size 3846 bp) *PfAdoMetDC/ODC* genes inserted into a pASK-IBA3 vector (vector size ~3100 bp). (A) Wild type *PfAdoMetDC/ODC* is shown in red and the insert region in blue (B). The agarose electrophoresis gel of the deletion mutagenesis PCR products is given in (C) indicating the wild type PCR product (~7400 bp) and the deletion mutants (~7000 bp) produced by the different deletion mutagenesis methods. (M) 1 kb DNA marker, (1) A/Owt, (2) Overlapping primer, (3) Inverse and (4) RE-mediated inverse PCR products.

Two out of five clones obtained with the overlapping method were mutant and did not contain the 411 bp insert. No transformation-competent mutated genes were obtained for the inverse PCR method. The RE-mediated inverse PCR method described here resulted in four mutated out of five clones analysed. Nucleotide sequencing verified the 40% and 80% mutagenesis efficiencies obtained for the overlapping primer and RE-mediated inverse PCR methods, respectively (Table 2.2).

Table 2.2: Deletion mutagenesis efficiency results for the different protocols used

Primer pair	Mutagenesis method	PCR product size	RE mapping with *Hind*III	Deletion efficiency after nucleotide sequencing (%)
P1	QuickChange™ site-directed	No product	NA	0
P2	Overlapping primer	7000 bp	~3900 bp ~3100 bp	40
P3	ExSite™	No product	NA	0
	Inverse PCR	7000 bp	~3900 bp ~3100 bp	0
	RE-mediated inverse PCR	7000 bp	~3900 bp ~3100 bp	80

Five clones were analysed for each of the different PCR-based mutagenesis methods based on duplicate PCR products.

Figure 2.3 shows representative nucleotide sequences of the deletion products after the A3 insert was removed from *PfAdoMetDC/ODC* with the overlapping primer (A) and RE-mediated inverse PCR (B) methods. With the latter method, the *Bam*HI recognition sites of the forward and reverse primers are inserted in place of the deleted insert.

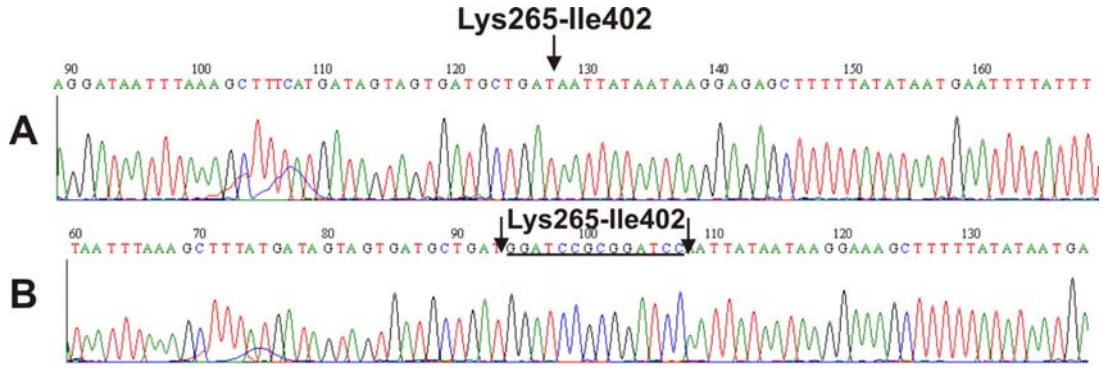

Figure 2.3: Nucleotide sequencing chromatograms of the largest insert deletion products (A/OΔA3) obtained with the overlapping primer and RE-mediated inverse PCR methods.
The arrow in (A) indicates the position where the overlapping primer method removed the A3 insert. The black bar in (B) shows the nucleotides corresponding to the *Bam*HI recognition sites that were inserted in place of the insert during the RE-mediated inverse PCR method.

The QuickChange™ site-directed mutagenesis method (QCM) requires that both of the mutagenic primers contain the desired mutation and anneal to the same sequence on

opposite strands of the plasmid. The method is limited to primers of 25 to 45 nt in length with melting temperatures approximately 10°C above the extension temperature of 68°C. The mutation should preferably be in the centre of the primer flanked by at least ten bases on either side. The GC content must also be at least 40%, and the primers must terminate in a G or a C base, which is challenging when working with the A+T rich genome of *P. falciparum*. The QCM method claims 80% efficiency for point mutagenesis but was unsuccessful in this deletion mutagenesis study (Table 2.2). This also explains previous inconsistent results produced in this laboratory by application of the QCM deletion mutagenesis method for the deletion of significantly sized areas in various other malaria genes (Birkholtz *et al.*, 2004).

The ExSite™ PCR-based site-directed mutagenesis method uses higher template concentrations and reduced PCR cycles to minimise potential second-site mutations. Primers for this method must be greater than 20 bases in length. The mismatched portions of the primers should be at or near the 5'-terminus of one or both of the primers with 15 or more of the matching sequence at the 3'-terminus. One or both of the primers must be 5'-phosphorylated. In order to make a specific mutation, the alteration must be included within the primers and their 5'-termini must meet but not overlap. Any bases between the 5'-termini will subsequently be deleted in the final product. The application of the ExSite™ method did not result in any product (Table 2.2).

Zheng and his co-workers modified the QCM protocol by using primers with partial overlaps at the 5'-termini to prevent self-extension [overlapping primer method, (Zheng *et al.*, 2004)]. This method was applied to vectors of up to 12 000 bp in length and yielded significantly improved PCR mutagenesis results. The modified primers were proposed to overcome the limitation of the melting temperature of primer design dictated by QCM. At least eight non-overlapping bases must be present on the 3'-termini of the primers, and the mutations may be as close as four nt away from the 5'-terminus. The primers must also terminate in a G or a C residue. The overlapping primer method was reported to delete up to seven bp (Zheng *et al.*, 2004) and had a 40% mutagenesis efficiency in deleting 411 bp from the ~7400 bp template in this study (Table 2.2).

Inverse PCR employs two inverted tail-to-tail primers to amplify an entire gene/vector except for the region that needs to be deleted. This method has been successful in deleting up to 102 bp in large plasmids (12 000 bp) (Wang and Wilkinson, 2001). According to Wang *et al*., for this method to be effective the primers must be similar in size, between 30 and 45 nt in length and have a melting temperature of at least 78°C with an applied annealing temperature of 68°C (Wang and Wilkinson, 2001). The number of PCR cycles must also be preferably less than 20. The application of this method produced the expected 7000 bp

deletion product as judged by gel electrophoresis only in the absence of DMSO (Figure 2.2 C, lane 3). However, the correct deletion product was not present in any of the five clones screened (Table 2.2). The primary causes for such background after PCR-based mutagenesis techniques could include the mis-priming and subsequent generation of incorrect, transformation-competent PCR products or the self-annealing of the 5'-overhanging CGC ends of the primers that could prevent subsequent blunt-ended ligation (Chiu *et al.*, 2004). The results presented here support other examples, which suggests that a maximum of only 12 bp can be removed with the inverse PCR method (Makarova *et al.*, 2000).

The inverse PCR method was subsequently modified to incorporate unique restriction enzyme sites at the 5'-ends of both the inverted tail-to-tail primers (RE-mediated inverse PCR, Figure 2.4). The primers of the RE-mediated inverse PCR method designed here included 5'-terminal overhangs (CGC in this instance) to improve the efficiency of the restriction digestions. This is followed by unique restriction enzyme sites that generate sticky-ends to improve the ligation efficiency (Sambrook *et al.*, 1989). This would additionally increase the number of deletion products by eliminating any primary product still containing the inserted region. The designed primers were not dependent on a similar length due to the requirement to terminate in one or more G or C bases at the 3'-end to increase the specificity of the PCR reaction. This feature is particularly important in the application of PCR on A+T rich *P. falciparum* genes. This method produced four out of five correct mutated products for a large area (411 bp) in a large gene (*PfAdoMetDC/ODC*, gene size 4257 bp) (Table 2.2).

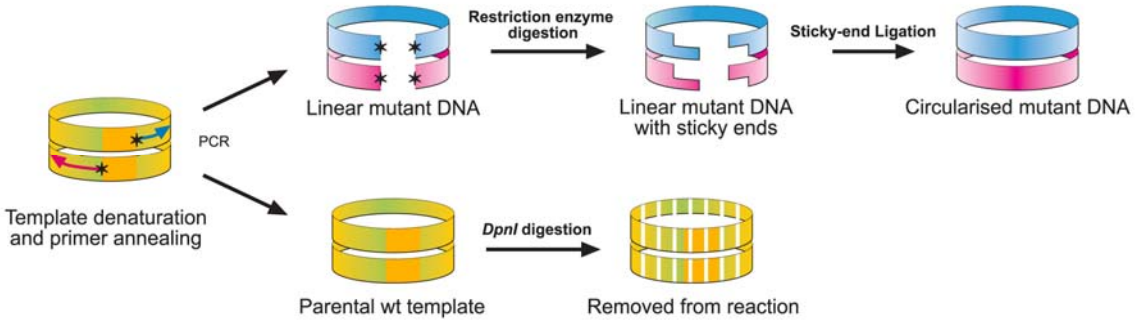

Figure 2.4: Schematic representation of the RE-mediated inverse PCR method.
The primers are designed in such a way that they contain unique restriction enzyme sites (represented by stars) and anneal to the opposite ends of the desired region to be deleted. The PCR reaction results in the synthesis of both parental, wild type template DNA (yellow and green in the bottom panel), which is subsequently removed during a *Dpn*I digestion step, as well as linear mutated DNA (pink and blue in the top panel). Digestion with the unique restriction enzyme creates linear DNA with sticky-ends, which improves the ligation efficiency and subsequent circularisation of the PCR product containing the deletion mutation.

In addition, the RE-mediated inverse PCR method was verified with a second *P. falciparum* gene as template to prove that this method is efficient in deleting large areas from smaller A+T rich genes.

2.3.2 Verification of the RE-mediated inverse PCR method

The subsequent application of the RE-mediated inverse PCR method on a second A+T rich malarial gene (*PfPdxK*, gene size 1536 bp) resulted in a PCR product that greatly differed in size compared to that of the wild type (Figure 2.5).

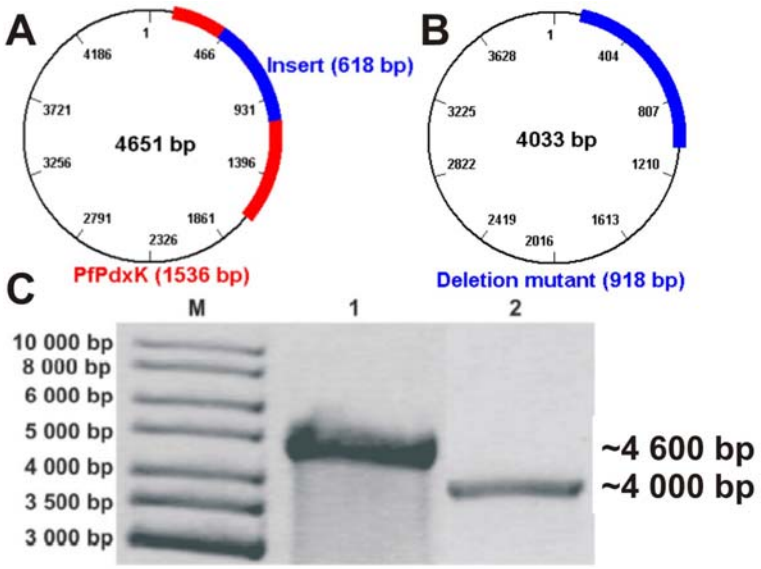

Figure 2.5: Agarose gel electrophoresis of the PfPdxK insert-deleted PCR product after RE-mediated inverse PCR.
Schematic representations of the wild type (A) (gene size 1536 bp) and the 618 bp deletion mutant (B) (gene size 918 bp) *PfPdxK* genes inserted into pASK-IBA3 vectors (vector size ~3100 bp). Wild type *PfPdxK* (A) is shown in red while the deletion mutant is in blue (B). The gel of the deletion mutagenesis PCR products is given in (C) showing the wild type product of ~4600 bp and the deletion mutant at ~4000 bp produced by the RE-mediated inverse PCR method. (M) 1 kb DNA marker, (1) wild type PfPdxK, (2) RE-mediated inverse PCR product.

Five clones were analysed with *Eco*RI restriction mapping. The deletion of the insert in *PfPdxK* removes an *Eco*RI site resulting in the linearisation of only the wild type plasmid (~4600 bp) (Figure 2.6).

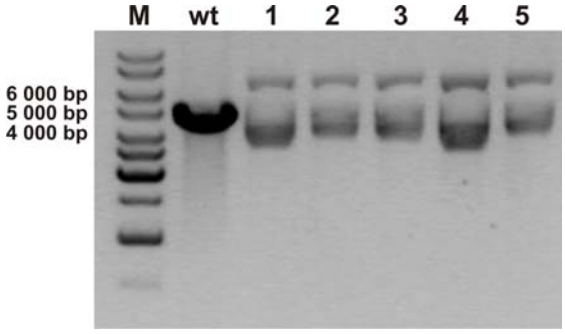

Figure 2.6: *Eco*RI restriction enzyme mapping of the wild type and insert-deleted PfPdxK plasmids obtained with the RE-mediated inverse PCR method.
The agarose electrophoresis gel of the restriction enzyme digested products shows the linear wild type *Eco*RI digested product ~4600 bp (wt) and the circular deletion mutant plasmids of ~4000 bp (Lanes 1 to 5). (M) 1 kb DNA marker.

Restriction enzyme mapping showed that the insert was deleted in all five of the plasmids that were analysed giving a 100% mutagenesis efficiency. The RE-mediated inverse PCR method is therefore highly efficient in deleting up to 618 bp (roughly one third of the entire gene) in a smaller malarial gene. The efficacy of this method may therefore be influenced by the template size, with smaller templates resulting in marginally higher efficacy. However, this is not dependent on the particular gene sequence.

The RE-mediated inverse PCR method is a straightforward method in which the primers do not require either 5'-phosphorylation or purification by polyacrylamide gel electrophoresis or HPLC as specified by the general inverse PCR protocol (Wang and Wilkinson, 2001). Large deletions can be made without increasing the length of the primers as the desired mutation is not incorporated into the primer sequence but is simply deleted by extending the plasmid during the PCR reaction. A further advantage of this method is that PCR temperature cycles of less than 20 are needed, which decreases the incidence of DNA polymerase error rates. The method was not dependent on the addition of 5% DMSO (results not shown) as is often needed by the inverse PCR method for the prevention of secondary structure formation in both primers and template. Additionally, there is no requirement for a high primer GC content as with the QCM method, which is useful with the A+T rich *P. falciparum* genes. Primer options for QCM and inverse PCR are furthermore limited by the requirement that the primer melting temperature must be >78°C, which was not the case in the RE-mediated inverse method. In the absence of unique restriction sites, alternative methods including DiSec/TriSec (Dietmaier *et al.*, 1993), which allows the generation of specified sticky-ends, may be used or a restriction-independent method like the overlapping primer method should suffice.

In this chapter, the inability in deleting a reasonably large (>100 bp) DNA region with existing oligonucleotide-based deletion mutagenesis methods led to the application of a highly

efficient RE-mediated inverse PCR method for the deletion of large areas in abnormally large *P. falciparum* genes. In the next chapter, the use of this method in the deletion of inserts in the PfAdoMetDC domain of PfAdoMetDC/ODC will be described.

Chapter 3: Delineation of the roles of structural features in the PfAdoMetDC parasite-specific inserts on bifunctional activity

3.1 Bifunctional enzymes in *P. falciparum*

Besides PfAdoMetDC/ODC, several other bifunctional genes have been described in *P. falciparum*. Bifunctional enzymes are particularly abundant in the folate biosynthesis pathway of the malarial parasite, i.e. PPPK/DHPS, dihydrofolate synthase/folylpolyglutamate synthase (DHFS/FPGS) and DHFR/TS (Nirmalan *et al.*, 2002).

The functional advantages of the bifunctional arrangement of Plasmodial proteins remain uncertain. It has been proposed that some of these proteins originated from gene-fusion [e.g. glucose-6-phosphate dehydrogenase/6-phosphoglucolactonase, *PfGlc6PD/6PGL* of *P. berghei* (Clarke *et al.*, 2001)] or gene-duplication events [e.g. guanylyl cyclase α and β (Carucci *et al.*, 2000)] resulting in acquired functionalities such as substrate channeling, coordinated regulation of both the abundance and activities of the proteins and intramolecular interactions. These evolutionary acquired characteristics may be important for the parasites during immune evasion. For example, the pentose phosphate pathway bifunctional enzyme Glc6PD/6PGL, is involved in protecting the parasites against oxidative stress during erythrocyte infection, while at the same time the efficiency of the pathway is improved by the bifunctional nature of the two enzymes as the product of the Glc6PD reaction is immediately available for hydrolysis by 6PGL (Clarke *et al.*, 2001). Another example where substrate channelling takes place is the direct transfer of dihydrofolate from TS to DHFR. Positive residues along the surface of the two enzymes' active sites form an electrostatic highway for the channelling of the negatively charged substrate (Knighton *et al.*, 1994). The advantages of a direct transfer include shorter transit times for pathway intermediates, no loss of intermediates by diffusion and the protection of labile solvents from the surrounding environment (Ovadi, 1991).

Substrate channelling, however, is not a functional advantage of PfAdoMetDC/ODC, as the reaction product synthesised by PfODC does not serve as the substrate for PfAdoMetDC and *vice versa*. Studies done by Wrenger *et al*. also showed that mutations in the active site of one domain or an inhibitor against it does not effect the activity of the neighbouring domain (Wrenger *et al.*, 2001). It has also been shown that specific regions within the two domains are involved in intramolecular interactions resulting in the correct folding and stabilisation of the bifunctional protein (Birkholtz *et al.*, 2004). A biological advantage of the bifunctional

arrangement of PfAdoMetDC/ODC in *P. falciparum* might thus be that the abundance and activity of the two proteins is regulated in a combined manner for the maintenance of optimum polyamine levels.

3.2 Parasite-specific inserts in PfAdoMetDC/ODC

Plasmodium proteins are unusually longer in size compared to their yeast orthologues, which is mostly due to the insertion or expansion of LCRs (Gardner *et al.*, 2002) present in nearly all of *P. falciparum* proteins (Pizzi and Frontali, 2001). LCRs in proteins characteristically consist of a limited set of amino acids, often contain repeats of one or more residues and do not adopt definite structures (Wootton, 1994). Similarly, parasite-specific inserts also exist as non-globular regions and often contain LCRs, consisting mainly of Lys and Asn residues. These are species-specific, rapidly diverging areas within proteins that form flexible domains extending from the protein core (Pizzi and Frontali, 2000; Pizzi and Frontali, 2001).

A number of theories exist regarding the evolution and function of LCRs in proteins. The prevalence of LCRs at antigenic loci has linked these areas to antigenic diversity for reduced effectiveness of the human immune response (Hughes, 2004). The parasite-specific inserts in PfAdoMetDC/ODC, however, do not show significant antigenicity suggesting a different role of these areas (Birkholtz, 2002). LCRs have alternatively been implied in mRNA stability (Xue and Forsdyke, 2003) and protein-protein interactions (Karlin *et al.*, 2002). A systematic study of LCRs by DePristo *et al.* led them to propose that the abundance and the amino acid composition of LCRs in *P. falciparum* is merely as a result of the A+T rich genome of the parasites and that these areas have not been evolutionary maintained for their functional and adaptive roles (DePristo *et al.*, 2006). Areas rich in positively charged Asn residues have been described as prion-domains, which mediate protein-protein interactions and contribute to either homo- or hetero-aggregation of polypeptides (Singh *et al.*, 2004). Polar residues (Asp and Glu) have also been predicted to mediate protein-protein interactions via modular polar zipper domains because of the capacity of their side chains to form hydrogen bonded networks (Perutz *et al.*, 1994; Michelitsch and Weissman, 2000). A highly probable explanation for the presence of parasite-specific inserts in PfAdoMetDC/ODC and the high abundance of charged residues therein might thus be the formation of intramolecular protein-protein interactions for the stabilisation of the heterotetrameric bifunctional complex.

The bifunctional PfAdoMetDC/ODC enzyme contains six Plasmodial conserved parasite-specific inserts, designated A1, A2, A3 (in the PfAdoMetDC domain), the hinge region, O1 and O2 (in the PfODC domain) (Müller *et al.*, 2000; Birkholtz *et al.*, 2004; Wells *et al.*, 2006). The roles that these insertions play in the activities of the proteins have previously been

investigated (Birkholtz *et al.*, 2004). Secondary structure prediction analysis of the parasite-specific inserts revealed several Plasmodial conserved structures within the inserts. The secondary structures in the hinge region and the PfODC inserts were investigated in a previous study (Roux, 2006). Figure 3.1 summarises the effects of various point mutations and deletions on domain activities within PfAdoMetDC/ODC.

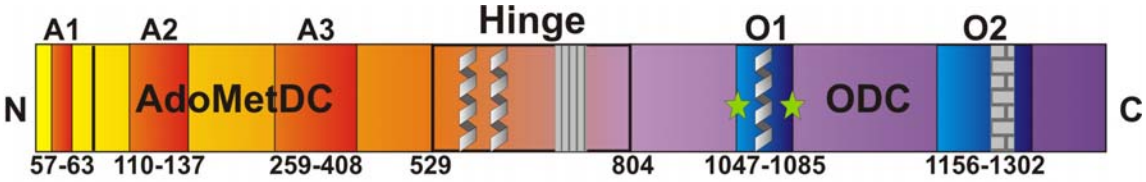

Mutation	% AdoMetDC activity	% ODC activity	Reference
Monofx AdoMetDC + hinge (1-660)	119	-	Wrenger *et al.*, 2001
Central hinge deletion (573-752)	67	50	Birkholtz *et al.*, 2004
1st helix breaker in hinge	87	66	Roux, 2006
2nd helix breaker in hinge	36	33	Roux, 2006
Beta sheet deletion in hinge (573-752)	89	127	Roux, 2006
Monofx ODC (805-1419)	-	3	Krause *et al.*, 2000
Monofx ODC + hinge (660-1419)	-	6	Krause *et al.*, 2000
Insert O1 deletion (1047-1085)	23	6	Birkholtz *et al.*, 2004
1st Gly to Ala displacement in O1	17	0	Roux, 2006
2nd Gly to Ala displacement in O1	33	3	Roux, 2006
Helix breaker in O1	6	0	Roux, 2006
Insert O2 deletion (1156-1302)	48	3	Birkholtz *et al.*, 2004
Conserved repeat deletion in O2	72	54	Roux, 2006
Deletion of inserts O1 and O2	30	3	Birkholtz *et al.*, 2004

Figure 3.1: The bifunctional *P. falciparum* AdoMetDC/ODC protein together with results of previous structure-function relationship studies.
Only the heterodimeric form of the bifunctional protein is shown. The N-and C-termini as well as the positions of the parasite-specific inserts are indicated (A1, A2, A3, hinge, O1, O2) (Birkholtz *et al.*, 2003; Birkholtz *et al.*, 2004; Wells *et al.*, 2006). Secondary structures within the parasite-specific inserts are also shown. The β-sheet is represented by a striped area while the repeat (NND)x region in insert O2 is shown as a bricked area. The activities are normalised as a percentage of the wild type PfAdoMetDC/ODC activity. Helices were disrupted with the insertion of Pro point mutations.

The functions of the unique parasite-specific inserts and the conserved structures within these are important in studies aimed at targeting these areas in PfAdoMetDC/ODC with possible chemo-preventative inhibitors.

3.3 Identification of secondary structures

Secondary structures are responsible for the local conformations of proteins and are also involved in the initiation of protein folding and its conformational stabilisation (Richardson, 1981). The formation of secondary structures are favoured by some amino acids and discouraged by others, and it is these structural propensities of residues that form the basis of a number of algorithms designed to predict secondary structures. More than three

decades ago, Chou and Fasman documented that amino acids have different propensities to initiate the folding of regular secondary structures such as α-helices and β-sheets (Chou and Fasman, 1974). They created a prediction model that assigns values to each residue and then a simple algorithm is applied to determine the most probable secondary structure that will form. The conformational parameters of each amino acid were calculated by the frequency of the given amino acid within a protein, its frequency within a given type of secondary structure, and the fraction of amino acids occurring in that particular type of structure. These parameters ultimately give an indication of the probability that an amino acid will be found in a helix, sheet or coil. Nucleation sites for the folding of a particular structure can thus be located and extended until a stretch of amino acids are encountered that are not suitably found in that type of structure or until a stretch is encountered that has a greater disposition for another type of secondary structure (Chou and Fasman, 1974). Since then, several models have been developed to predict secondary structure folding based on the primary sequence of amino acids in a polypeptide.

The Garnier method is very similar to the Chou-Fasman method but it additionally takes into account the immediate environment of the respective residue when predicting a probable structure (Sternberg, 1996).

3.3.1 Hydrophobic cluster analysis

In the “Hydrophobic core collapse” model, protein-folding cooperativity is due to the assembly of non-polar residues within a core. Subsequent development of hydrophobic clusters and cores results in the formation of secondary structures. This model is consistent with data showing a concurrent collapse of protein and some secondary structure formation in the early stages of protein folding (Chan *et al.*, 1995).

The established connection between hydrophobic interactions and consequent protein folding has led to the development of hydrophobic cluster analysis (HCA) as an efficient method to represent an amino acid sequence, 2-dimensionally, in the absence of a 3-dimensional structure. These hydrophobic clusters tend to fold into secondary structures and are thus useful to identify functional areas within a protein (Gaboriaud *et al.*, 1987). Indeed, hydrophobic amino acids dominate the internal core of a protein, whereas hydrophilic amino acids mostly occur on the protein surface to protect the core from the solvent. As a result, the hydrophobic amino acids tend to cluster into a stable and compact structure that is typical of a particular fold (Callebaut *et al.*, 1997).

HCA allows one to compare a protein sequence with unknown structure, such as that of the parasite-specific inserts, with a known structure from, for example, a related species, where the main chain folding of the latter protein provides a starting point for the structural modelling of the former protein (Gaboriaud *et al.*, 1987). This is because a marked difference in amino acid identity does not necessarily imply major differences in the overall 3-dimensional folding of the proteins (Argos, 1987).

In this study HCA, in addition to secondary structure prediction programmes, was thus applied to determine the overall structural content of the seemingly functionless parasite-specific inserts in the PfAdoMetDC domain of *P. falciparum* AdoMetDC/ODC. Structural delineation of the parasite-specific inserts provides important insights towards the rational design and development of specific inhibitory compounds targeting these areas.

3.3.2 The roles of secondary structures in protein-protein interactions and motif formation

Any specified residue within a protein may participate in various interactions, including those within a secondary structural element as well as those in long-range interactions a considerable distance away in the amino acid sequence (Kwok *et al.*, 2002). The identification of secondary structures represents the first step in describing the tertiary and super-secondary topologies of proteins such as barrels and bundles.

3.3.2.1 α-Helices and protein-protein interactions

Periodical secondary structures such as helices and sheets are the main components of homodimeric interfaces where 40% of the interface residues are helical ones (Guharoy and Chakrabarti, 2007). α-Helices also serve as important recognition regions for the binding and interaction of other proteins, DNA and RNA (Davis *et al.*, 2007). The majority of integral membrane proteins adopt α-helical transmembrane segments that may form well-packed bundles. These helical structures are stabilised within the membrane as the backbone amide-carbonyl hydrogen bonds are satisfied within the helix and are isolated from the non-polar environment of the surrounding lipid bilayer (White and Wimley, 1999).

Glycophorin A (GpA) is arguably the best-studied example showing the role that helices play in intramolecular protein-protein interactions and the dimerisation of protein monomers. GpA is an integral membrane sialoglycoprotein in the human erythrocyte that associates to form a dimer via side-by-side interactions between transmembrane α-helices. It was discovered early that the dimeric form of the protein cannot be separated into its monomeric forms with

sodium dodecylsulphate (SDS), which demonstrates the strength of this interaction mediated solely by the transmembrane region (Bormann *et al.*, 1989; Lemmon *et al.*, 1992).

Leucine zippers or coiled-coils are perhaps the simplest protein units that can be classified as small dimeric proteins (Wendt *et al.*, 1997). These consist of two peptides in a roughly α-helical conformation, wound around each other into a bundle of right-handed helices, coiled about one another to form a left-handed superhelix quaternary structure (Gromiha and Parry, 2004). The fundamental structure consists of a repeating seven-residue motif (*abcdefg*) where the *a* and *d* positions are characteristically occupied by non-polar residues comprising the hydrophobic core of the helix-helix interface, while residues at the peripheral positions *e* and *g* are mostly charged residues forming salt-bridges with each other and hydrophobic contacts with the core residues. The side chains of one helix protrude into the cavities formed by the side chains of the adjacent helix in a regular manner termed knobs-into-holes or leucine zipper packing. Leucine zippers in the basic-leucine-zipper (bZIP) family of transcription factors mediate the dimerisation of two basic protein domains to form a DNA-binding site, showing the involvement of helices in intra- and intermolecular protein-protein interactions, respectively. Leucine zippers can be homodimeric as in the yeast GCN4 transcription factor or heterodimeric as in the jun-fos type transcription factors (Wendt *et al.*, 1997).

Another example of helix involvement in intermolecular protein-protein interactions is the transmembrane domains of SNARE proteins. The mechanism of fusion between a vesicle to a target membrane protein (e.g. Ca^{2+}-mediated neurotransmitter release) is regulated by interactions via a set of proteins termed the soluble *N*-ethylmaleimide-sensitive factor (NSF) attachment protein receptors (SNARE) complex. This complex includes SNAP25 (synaptosome-associated protein) and transmembrane proteins that are located on the target membrane (t-SNARE) and the vesicle membrane (v-SNARE) (Ungar and Hughson, 2003). The fusion capability of this complex involves sequence-specific interactions between the v- and t-SNAREs via extremely stable coiled-coils holding the vesicle close to the target membrane for subsequent fusion. These interactions can only be broken by NSF-catalysed hydrolysis of ATP dissociating the complex or the introduction of an interference protein (Kroch and Fleming, 2006).

Proteins mostly perform their functions through their interactions with other molecules or with itself, and the identification of these inter- and intramolecular binding sites are important for functional annotation studies, the understanding of molecular recognition processes and rational drug target development and design strategies. It will thus prove useful to identify interacting areas within the parasite-specific inserts of PfAdoMetDC/ODC that can be

targeted with compounds to prevent these interactions from taking place and in such a manner influence protein activity.

3.3.2.2 β-Sheets, barrels and turns

β-Sheets are not common as binding sites in protein-protein interactions, which are mostly fulfilled by the helical secondary structures. Chakraborty *et al*., however, reported that a four-stranded β-sheet excised from the HIV gp120 protein, forms the binding site of the neutralising CD4-binding antibody namely 17b (Chakraborty *et al.*, 2005). Initially, it was also thought that α-helical transmembrane bundles formed all integral membrane proteins including transporters and ion channels. Now it is evident that transmembrane β-barrels are also involved in the formation of transbilayer porins, K^+ and related voltage-gated ion channels and epithelial Na^+ channels (Sansom and Kerr, 1995).

β-Barrel membrane proteins are found in the outer membranes of mitochondria, chloroplasts and Gram-negative bacteria and span the membranes as β-sheets. Alternating hydrophilic and hydrophobic residues facing the membrane environment and hydrophilic interior of the barrel, respectively, forms the entire transmembrane protein (Schneider *et al.*, 2007). β-Turns are also important motifs involved in the biological recognition of various proteins and peptides. They form regular recognition motifs for antibody-peptide complexes and peptide hormones, such as angiotensin II, gonadotrophin releasing hormone, somatostatin and many more. They are often evolutionary conserved and are believed in some cases to initiate protein folding (Tran *et al.*, 2005).

Following the identification of conserved secondary structures within PfAdoMetDC/ODC, disrupting an α-helix or deleting a β-sheet can give an indication of their possible involvement in protein-protein interactions and activity. The cyclic nature of Pro makes it an unique amino acid as its amide group lacks the hydrogen atom necessary for hydrogen bond stabilisation in regular secondary structures (Orzáez *et al.*, 2004). The replacement of a residue that has a high frequency in α-helices with a Pro residue can thus be employed to disrupt the folding event from taking place. For example, the replacement of an Ile residue, a strong helix-former, with a Pro residue, a helix breaker, within the 42-amino acid amyloid β-peptide, which is responsible for increased levels of oxidative stress in Alzheimer's disease, resulted in the disruption of a helix that caused a decrease in amyloid peptide aggregation, oxidative stress and neurotoxicity (Kanski *et al.*, 2002).

An important aspect to consider with regards to Pro residues is *cis-trans* isomerisation. The Pro hypothesis states that protein molecules, especially slow-folding ones, possess non-native isomers of peptide bonds between Pro and the next residue in a polypeptide chain

and that key steps in the refolding event are limited by the rate of slow reisomerisation of the incorrect Pro-peptide bonds. The enzyme responsible for the *cis*-in-equilibrium-*trans* isomerisation of Pro-peptide bonds is prolyl isomerase and its activity is dependent on the accessibility of the particular Pro bond in the refolding protein chain (Lang *et al.*, 1987). The introduction of a Pro residue may therefore result in general conformational changes instead of a desired conformational disruption in the region of the helix. This enzyme is present in *P. falciparum* (PDB entry: Pf08_0121).

Prior research has focussed on delineated areas of the parasite-specific inserts in the PfODC domain as well as the hinge region (Table 3.1). These studies showed that the bifunctional protein depends on the presence of these areas for their proper functioning and/or complex formation. The present study therefore focussed on the parasite-specific inserts within the PfAdoMetDC domain to determine their roles in bifunctional activity. The presence of *Plasmodia* conserved secondary structures within these was also identified, which could possibly be responsible for the activities and/or stabilisation of the bifunctional PfAdoMetDC/ODC complex via protein-protein interactions as in the examples given above.

3.4 Methods

3.4.1 Delineation of structural features within the PfAdoMetDC parasite-specific inserts

It was previously thought that low-complexity-containing parasite-specific inserts do not contain any significant structures and mostly form non-globular, surface exposed loops (Pizzi and Frontali, 2001). The application of secondary structure prediction algorithms in past and present studies on the parasite-specific inserts in PfAdoMetDC/ODC have, however, predicted the presence of several conserved α-helices and β-sheets in both the domains as well as the hinge region (Roux, 2006). Similarly, the DHFR/TS crystal structure was also shown to contain parasite-specific inserts with definite structures (Yuvaniyama *et al.*, 2003).

The structural alignment of the PfAdoMetDC domain was previously performed (Wells *et al.*, 2006). The AdoMetDC domains of *Plasmodium* spp. are highly divergent from other eukaryotic enzymes mostly due to the presence of *Plasmodium*-specific inserts, which is why a structure-based approach was followed in order to optimise the alignment. Initial studies suggested the presence of one large PfAdoMetDC insert (Müller *et al.*, 2000; Birkholtz *et al.*, 2004), but subsequent multiple alignments, however, identified three inserts within this domain i.e. A1, A2 and A3 (Wells *et al.*, 2006).

Manual adjustments were made during homology modeling of the PfAdoMetDC domain to prevent the disruption of secondary structures that involve areas of the insert and the main protein chain (Wells *et al.*, 2006). It is, however, still possible that the inserts themselves adopt defined secondary structures that may confer structural functionalities to these areas. The sequences of the parasite-specific inserts were thus investigated for the presence of such structural features. The A2 and A3 parasite-specific inserts sequences of three *Plasmodia* species (*P. falciparum*, *P. berghei* and *P. yoelii*) were subjected to numerous secondary structure prediction algorithms from different web servers listed in Figure 3.3 (G.A. Wells, personal communication). During the homology modeling of PfAdoMetDC, insert A1 was moved two residues downstream to occupy residues Lys57 to Glu63. This was done in order to prevent its involvement in the second β-strand of PfAdoMetDC and as such was thus not investigated for the presence of any secondary structures (Wells *et al.*, 2006).

In addition, hydrophobic cluster analysis diagrams of the A2 and A3 inserts were constructed by subjecting their insert amino acid sequences to the DrawHCA programme (Gaboriaud *et al.*, 1987). During HCA, the amino acid sequence is written on a classical α-helix with 3.6 amino acids per turn and smoothed on a cylinder (Figure 3.2 a). In such a representation, residues *i* and *i*+18 (after five helical turns) will have similar positions parallel to the axis of the cylinder (e.g. Figure 3.2 a, G246 and E264). An easier representation of the 3-dimensional helical structure is subsequently obtained when the cylinder is cut parallel to its axis and unrolled (Figure 3.2 b). The widely separated distribution of some amino acids upon unrolling (e.g. Figure 3.2 b, F253 and L254) are then corrected by duplicating the representation, which gives a better indication of each amino acid's immediate environment (Figure 3.2 c).

Sets of adjacent hydrophobic amino acids (Ile, Leu, Phe, Trp, Met, Tyr, Val) are finally encircled to create hydrophobic clusters. Particular amino acids are highlighted: a star for Pro, which confers the greatest constraint to the polypeptide chain; a diamond for Gly, which confers the largest freedom to the chain; and squares with a dot or not for Ser and Thr, respectively, as these two polar amino acids can mask their polarity, particularly within helices (Figure 3.2 d).

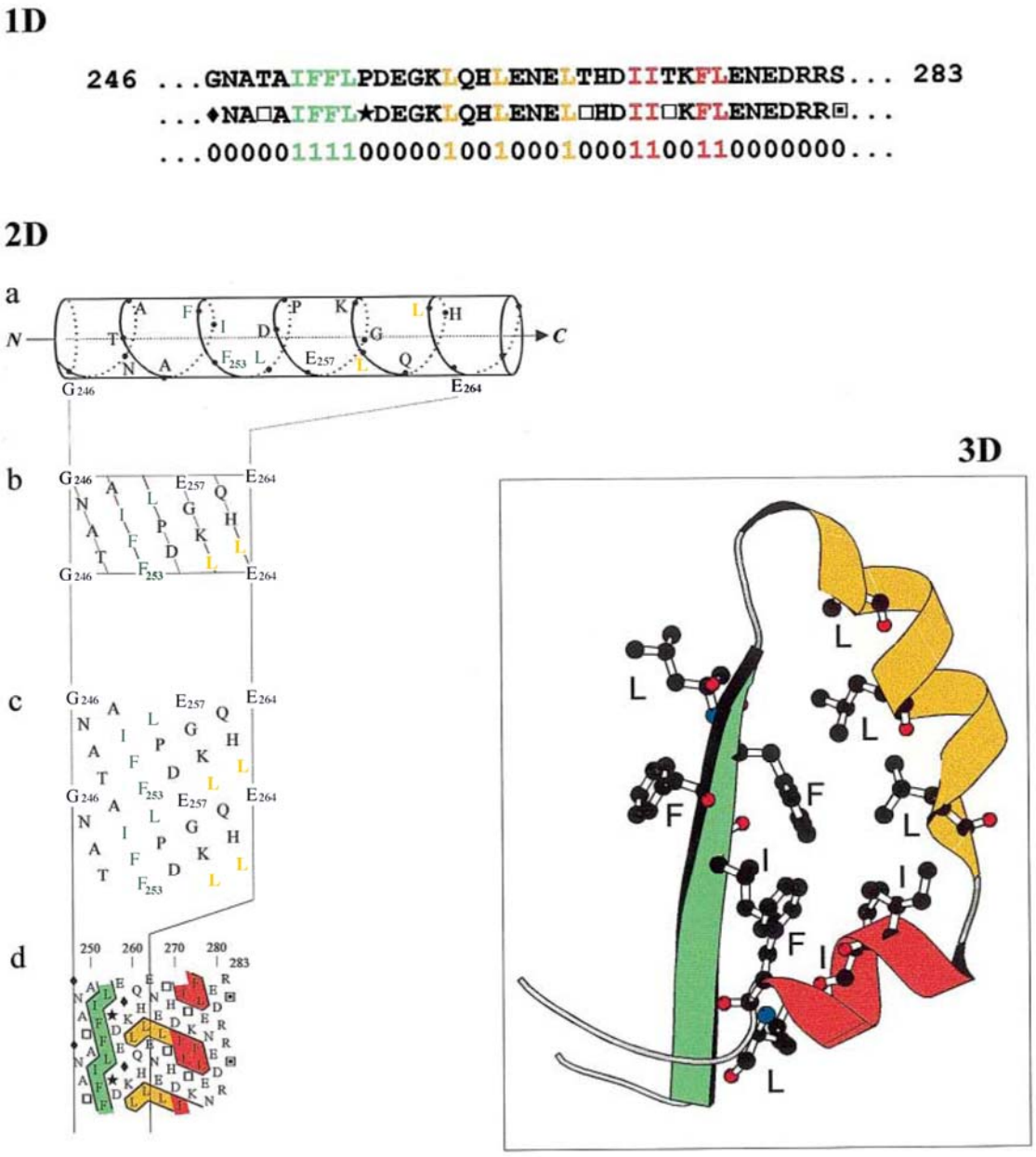

Figure 3.2: Hydrophobic cluster analysis: between sequence and structure.
The linear 1-dimensional sequence (1D) of a segment of human α_1-antitrypsin is shown with coloured hydrophobic amino acids (first line). The same sequence is represented using the HCA code for the Gly, Pro, Thr and Ser amino acids (second line). The direct translation into a numbered code where 1=hydrophobic and 0=hydrophilic is also represented (third line). The sequence is displayed on a cylinder (a), which is cut parallel to its axis and unrolled into a bi-dimensional diagram (b). In (c), this diagram is compacted and duplicated. Hydrophobic amino acids form clusters (d), which are illustrated by the corresponding 3-dimensional structure (3D). The vertical cluster (green) is associated with a β-strand whereas the horizontal one (yellow and orange) corresponds to α-helices. Sequence stretches separating clusters correspond to loops or hinges between domains. A hydrophobic cluster always starts and ends with a hydrophobic amino acid coded with a 1.

3.4.2 Nucleotide deletion of the PfAdoMetDC parasite-specific inserts and mutagenesis of delineated areas

3.4.2.1 Cloning of *PfAdoMetDC/ODC* into pASK-IBA3

The *P. falciparum AdoMetDC/ODC* gene (~4300 bp) was cloned into a pASK-IBA3 vector [~3100 bp, (Institut für Bioanalytik, Germany)] and used as template during the mutagenesis reactions (total template size ~7400 bp and called pA/Owt henceforth) (Müller *et al.*, 2000).

3.4.2.2 Mutagenesis PCR

The size of the A3 parasite-specific insert prompted an investigation into available deletion mutagenesis methods and led to the development of the RE-mediated inverse PCR method (Williams *et al.*, 2007). The applicability of the method was tested on and proven to be highly efficient when the largest A3 insert in the PfAdoMetDC domain was removed (Chapter 2). This section will therefore only include the deletion mutagenesis of the smaller A1 and A2 parasite-specific inserts.

The partial overlapping primer method by Zheng *et al*. was applied in the design of the primers for the deletion of the A1 (7 amino acids) and A2 (28 amino acids) inserts (Zheng *et al.*, 2004). The principles of this method are described in section 2.2.1.4. The primers for the deletion of the A1 (A1F and R) and A2 (A2F and R) are listed in Table 3.1 and mutagenesis PCR was performed as stipulated in section 2.2.1.4 to create the A/OΔA1 and A/OΔA2 mutations, respectively.

Table 3.1: The mutagenic primers and their properties for the deletion of the smaller parasite-specific inserts in PfAdoMetDC

Primer	Length (nt)	Tm* (°C)	Primer Sequence (5' to 3')
A1F	46	73	cggaaataagtgaggac^cgatgtcgtgtgtatttattgtcagagag
A1R	51	73	taaatacacacgacatcg^gtcctcacttatttccgatacaatactacaac
A2F	53	68	catatggataat^gaacatttcctttattgttttttacacatatgaattaccg
A2R	48	65	caataaaggaaatgttc^attatccatatgatatattaataaatcaacc

* The Tm's were calculated according to the Rychlik *et al*. formula:
69.3 + 0.41(%GC) – (650/N) where N is the number of nucleotides (Rychlik *et al.*, 1990). Blue letters indicate where the 5'-ends of the forward and reverse primers overlap. ^ Indicates where the deletions of the inserts are located.

For the disruption of the α-helix within insert A2 identified above, a specific residue conserved between the different secondary structure predictions and located in the centre of the specific area was disrupted through point mutation. The strong Ile helix-former at position 132 was replaced with a conformationally rigid Pro residue using the overlapping primer design method (Zheng *et al.*, 2004). In the case of the first β-sheet in insert A3, the conserved eight amino acid structure predicted (Val284 to Tyr291) by the secondary

structure algorithms was simply deleted with the RE-mediated inverse PCR method described in Chapter 2 (Williams *et al.*, 2007).

The mutagenesis primers for the disruption of the α-helix in A2 and the deletion of the β-sheet in A3 are given in Table 3.2. The A2aF and R primers were used to introduce a Pro as helix breaker at position 132 while the A3bF and R primers were used for the deletion of the β-sheet in insert A3. The A3b primers contain 5'-overhanging CGC ends followed by unique *Bam*HI RE sites.

Table 3.2: The mutagenic primers and their properties for the disruption of the secondary structures within the PfAdoMetDC parasite-specific inserts

Primer	Length (nt)	Tm* (°C)	Primer Sequence (5' to 3')
A2aF	25	56	cat aat **cca** gct gaa ttc ata aaa
A2aR	22	56	c agc **tgg** att atg gaa ttt ctc
A3bF	27	63	CGC ggatcc aag aat gaa agt aca ttg
A3bR	29	67	CGC ggatcc cat tcc tgt atc ttc ata tg

* The Tm's were calculated according to the Rychlik *et al*. formula:
69.3 + 0.41(%GC) – (650/N) where N is the number of nucleotides (Rychlik *et al.*, 1990). Blue letters indicate where the 5'-ends of the forward and reverse primers overlap. The nucleotides written in bold specify the Ile132Pro point mutation while the capital letters represent the 5'-overhanging ends followed by the *Bam*HI restriction enzyme sites (underlined) for the RE-mediated inverse PCR primers.

The pA/Owt plasmid was used as template during PCR mutagenesis for the disruption of the α-helix and deletion of the β-sheet to produce constructs A/OpA2a and A/OΔA3b, respectively, where "a" represents an α-helix and "b" a β-sheet. The mutagenesis reactions for the partial overlapping and RE-mediated inverse PCR methods were followed as described in sections 2.2.1.4 and 2.2.1.6, respectively.

3.4.2.3 Post-PCR manipulations

The PCR products were visualised with agarose electrophoresis gels as described in section 2.2.1.7 to ensure that PCR products of approximately 7400 bp (gene size ~4300 bp, vector size ~3100 bp) were obtained.

All the PCR products were subsequently treated with 10 U of *Dpn*I (Fermentas, Canada) for 3 hrs at 37°C. The same quantity of *Bam*HI (Fermentas, Canada) was additionally added to the *Dpn*I digestion reaction of the RE-mediated inverse PCR A/OΔA3b product in a dual compatibility buffer Tango™ (33 mM Tris-OAc, 10 mM Mg-OAc, 66 mM K-OAc, 0.1 mg/ml BSA, pH 7.9). The insert-deleted products were purified with the High-Pure PCR product purification kit (Roche Diagnostics, Germany) while the secondary structure AOpA2a and A/OΔA3b mutants were cleaned with the NucleoSpin® Extract II PCR cleanup kit (Macherey-

Nagel, Germany). The pure DNA samples were finally circularised for 16 hrs with 3 U of T4 DNA Ligase (Promega, USA) at 22°C (A/OΔA1, A/OΔA2 and A/OpA2a) and 4°C (A/OΔA3b) for blunt- and sticky-ended ligation, respectively. The mutant, circular DNA samples (pA/OΔA1, pA/OΔA2, pA/OpA2a and pA/OΔA3b) were subsequently electroporated into DH5α cells as described in section 2.2.1.8.

3.4.2.4 Plasmid isolation and nucleotide sequencing

The plasmids from five clones for each mutation were inoculated in 5 ml LB-amp (LB-medium with 50 µg/ml ampicillin) and allowed to grow overnight at 37°C and 250 rpm. Plasmids were subsequently isolated from the overnight cultures with the use of the High Pure Plasmid Isolation kit from Roche (section 2.2.1.9) and the peqGOLD Plasmid Miniprep Kit I (Biotechnologie, Germany), which is based on the rapid alkaline-SDS lysis method.

Verification of the insert deletions was performed with nucleotide sequencing as described in section 2.2.1.11. The SamRSf1 (5'-aatgaacggaatttttgaag-3') primer was used for the detection of the A/OΔA1 mutant and K215A2 (5'-ccgaacagaatccaaacgtagaag-3') was used to detect the A/OΔA2 insert deletion. The K215A2 primer was also used to detect the A/OpA2a mutation. A helix-disrupted mutant will contain Pro instead of Ile at position 132. The K215A1 (5'-gcttctacgtttgcattctgttcgg-3') sequencing primer was used for the verification of the β-sheet deletion within insert A3.

3.4.3 Recombinant protein expression and isolation of the mutated PfAdoMetDC/ODC proteins

The previously transformed DH5α cells containing the pASK-IBA3 vectors (Institut für Bioanalytik, Germany) with the wild type *PfAdoMetDC/ODC* gene (pA/Owt) and those lacking the three individual PfAdoMetDC parasite-specific inserts (pA/OΔA1, pA/OΔA2 and pA/OΔA3, created in Chapter 2) were grown overnight in 5 ml LB-amp (LB-medium with 50 µg/ml ampicillin) at 37°C with agitation at 250 rpm. The plasmids were isolated as described in section 2.2.1.9. The isolated wild type (pA/Owt) and mutant (pA/OΔA1, pA/OΔA2 and pA/OΔA3) plasmids were subsequently recombinantly expressed.

The plasmids were heat shock transformed into the AdoMetDC and ODC deficient EWH331 *E. coli* protein expression cells (Hafner *et al.*, 1979).

3.4.3.1 Heat shock transformation

Cells were grown overnight in 5 ml LB-medium at 30°C with moderate shaking. The culture was diluted 1:10 ml in 50 ml LB-glucose (20 mM glucose in LB-medium) and grown at 30°C

with moderate shaking until an OD550 of 0.3 was reached. The culture was then transferred into 50 ml centrifuge tubes and incubated on ice for 10 min after which the cells were collected by centrifugation at 1500 x g and 4°C for 15 min. The pellets were dissolved in 8.35 ml cold CCMB (80 mM $CaCl_2$, 20 mM $MnCl_2$, 10 mM $MgCl_2$, 10 mM KOAc, 10% v/v glycerol, pH 6.4) and incubated on ice for 20 min. These were centrifuged for 10 min as above. The pellets were finally resuspended in 2.1 ml CCMB, aliquoted into ice-cold Eppendorfs (100 µl) and stored at -70°C (Hanahan *et al.*, 1991).

The prepared heat shock competent EWH331 cells were thawed on ice to which 10 ng of the different plasmids were separately added, followed by incubation on ice for 30 min. The cells were heat shocked for 90 sec at 42°C and immediately transferred to ice for 2 min. A volume of 800 µl preheated LB-glucose (20 mM glucose in LB-medium) was added to each and incubated at 37°C for 30 min with agitation (Sambrook *et al.*, 1989). The transformed cells were subsequently plated on LB-amp agar plates (1% w/v agar in LB-medium with 100 µg/ml ampicillin) by two general routes to ensure that single colonies would be obtained. Volumes of 100 µl of each of the inoculations were plated. This would result in the growth of individual colonies if the transformation reactions were highly efficient while the growth of colonies from such a small volume would be scarce if only a few cells were successfully transformed. In the latter case, to ensure that transformed cells would be plated, the cells were firstly concentrated by a short centrifugation step. The pelleted cells were resuspended in the remaining LB-glucose and plated on the agar plates.

3.4.3.2 Protein expression induction and expression

Single colonies were picked from each plate and inoculated overnight in 10 ml LB-amp (LB-medium with 50 µg/ml ampicillin) in a shaking incubator at 37°C and 250 rpm. The overnight cultures were diluted 1:100 in 500 ml LB-amp and grown at 37°C with agitation until an optical density of 0.5 at 600 nm was reached. Protein expression of the constructs containing the wild type and insert-deleted mutants were induced with 200 ng/ml anhydrotetracycline [AHT, (Institut für Bioanalytik, Germany)] for the controlled expression from the *tet* promoter. The constitutive expression of the *tet* repressor keeps the promoter in a repressed state until the repression is chemically relieved by the addition of AHT. The system is thus highly regulated and expression leakage is kept to a minimum. The cultures were subsequently grown overnight at 22°C with shaking at 200 rpm to allow recombinant expression to take place. An additional feature of the pASK-IBA3 vectors is the presence of a C-terminal *Strep*-tag (NH_2-Trp-Ser-His-Pro-Gln-Phe-Glu-Lys-OH) that can be used for the isolation of the proteins on a *Strep*-Tactin affinity column (Institut für Bioanalytik).

3.4.3.3 Isolation of the *Strep*-tagged recombinant proteins

The cells were harvested by centrifugation at 1500 x g for 30 min at 4°C in a Beckman J-6 centrifuge (Beckman, USA). The pellets were dissolved in 1 ml ice-cold Wash Buffer (150 mM NaCl, 1mM EDTA, 100 mM Tris, pH 8). Approximately 0.1 mg/ml lysozyme (Roche Diagnostics, Germany) was added to each to degrade the cell membranes followed by 0.1 mM Phenylmethylsulfonyl fluoride [PMSF, (Roche Diagnostics)] as protease inhibitor. The suspensions were incubated on ice for 30 min after which PMSF was once again added. The cells were disrupted with the use of a Sonifier Cell Disruptor B-30 instrument (Instrulab, South Africa) with an attached flat microtip by pulsing the suspension for 10 cycles of 45 sec each with 1 min rest periods in between at an output control of 3. PMSF was added to each suspension to prevent the exposed proteins from being degraded by serine proteases. The suspensions were transferred into ice-cold 10 ml ultracentrifuge tubes, balanced to the second decimal, and ultracentrifuged at 4°C for 1 hr at 100 000 x g in a Beckman Avanti J-25 centrifuge with a fixed angle rotor (Beckman). The supernatants were transferred into ice-cold sterile 10 ml tubes.

The recombinant proteins were purified from the total soluble protein extracts with *Strep*-Tactin affinity chromatography (Institut für Bioanalytik, Germany). The *Strep*-tag fused to the recombinant proteins has a high affinity for the streptavidin in the matrix. Each protein extract was loaded into a Chromabond® 15 ml PP column (Macherey-Nagel, Germany) containing a 1 cm^3 bed volume of *Strep*-Tactin beads at 4°C and was allowed to run through three times. The beads were subsequently washed three times with 10 ml Wash Buffer each (150 mM NaCl, 1mM EDTA, 100 mM Tris, pH 8) and the bound protein was finally eluted five times from the streptavidin with the same 5 ml of Elution Buffer (150 mM, NaCl, 1mM EDTA, 2.5 mM desthiobiotin, 100 mM Tris, pH 8), and collected in four fractions on ice. The desthiobiotin in the Elution Buffer reversibly competes with binding to the streptavidin and thus releases the *Strep*-tag fused proteins. The beads were finally regenerated for future use with Regeneration Buffer [150 mM NaCl, 1mM EDTA, 1mM 4-hydroxy azobenzene-2-carboxylic acid [HABA, (Sigma-Aldrich, UK)], 100 mM Tris, pH 8]. HABA, in turn, displaces the desthiobiotin from the affinity beads such that it can be used for the next protein isolation experiment. The protein samples were kept at 4°C until further use.

3.4.3.4 Protein concentration determination

The concentrations of the isolated proteins were determined by means of the Bradford assay (Bradford, 1976). Binding of the dye to the basic and aromatic residues in the protein leads to an absorbency shift from 465 to 595 nm, which can be detected by a spectrophotometer. Bovine serum albumin [BSA, (Promega, USA)] was used as the standard protein to set up a standard curve from which the unknown protein's concentration could be determined. A 1

mg/ml stock BSA solution was used to prepare a standard dilution series consisting of the following concentrations in µg/ml: 200, 100, 50, 25, 12.5 and 6.25. A 96 well ELISA plate was used to which 150 µl of the Bradford dye (Pierce, USA) was added per 50 µl of each standard dilution and the isolated protein fractions in duplicate. The A595 was read with a Multiskan Ascent scanner (Thermo Labsystems, USA) and the trend line resulting from the standard curve of absorbency at 595 *versus* standard dilution was deemed reliable if the R^2 value was >95%.

3.4.3.5 SDS-PAGE analysis

The isolated proteins were separated with SDS-polyacrylamide gel electrophoresis (SDS-PAGE) (Laemmli, 1970). The gel was composed of a 7.5% separating (7.5% w/v acrylamide, 0.375 M Tris-HCl, pH 8.8, 0.1% w/v SDS) and 4% stacking gel (4% w/v acrylamide, 0.13 M Tris-HCl, pH 6.8, 0.1% w/v SDS). The samples were diluted 4:1 in sample buffer (0.06 M Tris-HCl, pH 6.8, 0.1% v/v glycerol, 2% w/v SDS, 0.05% v/v β-mercaptoethanol, 0.025% v/v bromophenol blue) and boiled for 5 min. Electrophoresis was carried out with SDS electrophoresis running buffer (0.25 M Tris-HCl, pH 8.3, 0.1% w/v SDS, 192 mM glycine) in a Biometra electrophoresis system (Biometra, Germany). A 10-200 kDa protein ladder (Fermentas, Canada) was loaded as a molecular size marker together with each prepared protein sample. The electrophoresis was run at 60 V until the front reached the separating gel after which the voltage was increased to 100 V.

The protein bands were visualised with silver staining, a highly sensitive method for the detection of low protein quantities on a gel. The gels were firstly fixed for 30 min with 30% v/v ethanol and 10% v/v acetic acid followed by gel sensitisation for 30 min with 30% v/v ethanol, 0.5 M NaOAc, 0.5% v/v glutaraldehyde and 0.2% w/v $Na_2S_2O_3$. The gels were subsequently washed three times for 10 min each with $dddH_2O$. Protein bands were silver stained for 30 min with 0.1% w/v $AgNO_3$ and 0.25% v/v formaldehyde and washed briefly with $dddH_2O$. Staining development was carried out in 2.5% w/v Na_2CO_3 and 0.01% v/v formaldehyde and terminated with 0.05 M EDTA [adapted from (Merril *et al.*, 1981)]. Densitometric analyses to determine the relative quantities of each band on the gels (Appendix A and B, Figures 1A and 1B) were obtained with a VersaDoc Imaging System Model 3000 (BioRad, USA) and the Quantity One™ Software programme.

3.4.3.6 MS analysis of the mutant PfAdoMetDC/ODC proteins

The pA/Owt, pA/OΔA2 and pA/OΔA3 vectors were recombinantly expressed and purified as described in section 3.4.3 and separated on a 7.5% SDS-PAGE (section 3.4.3.6). The proteins were visualised with colloidal Coomassie staining. This method of staining is based on the colloidal properties of Coomassie Brilliant Blue G-250 whereby a shift in the dye

occurs from the colloidal form to the molecular dispersed form upon the addition of methanol that enables the dye to disperse into the gel. The proteins are stained with very high sensitivity while background staining is kept at a minimum (Neuhoff *et al.*, 1988). A 0.1% w/v Coomassie Brilliant Blue G-250 solution (Sigma-Aldrich, UK) containing 10% w/v ammonium sulphate and 2% v/v phosphoric acid was prepared and subsequently diluted 4:1 with methanol. The diluted solution was used to stain the gel for at least 24 hrs after which it was briefly washed in 25% v/v methanol and 10% v/v acetic acid. The gel was destained with 25% v/v methanol for approximately 30 min. The stained gel was dried and the desired protein bands were cut from the gel and sent to Dr P.F.G. Sims (Manchester Interdisciplinary Biocentre, UK) for mass spectrometry (MS) analysis.

3.4.3.7 AdoMetDC and ODC activity assays

The various protein samples were tested for their PfAdoMetDC and PfODC activities in the bifunctional protein and compared to those of the wild type activities. These activities were determined by measuring the release of the ^{14}C-labelled reaction product, $^{14}CO_2$. PfAdoMetDC uses the substrate S-adenosyl-[carboxy-^{14}C]methionine [56.2 mCi/mmol, (Amersham Biosciences, UK)] while PfODC uses L-[1-^{14}C]ornithine [47.7 mCi/mmol, (Amersham Biosciences)] (Krause *et al.*, 2000; Müller *et al.*, 2000; Birkholtz *et al.*, 2004). The PfAdoMetDC and PfODC protein activity determination reaction setup is shown in Table 3.3.

Table 3.3: The AdoMetDC and ODC radioactivity assay reactions

Reagent	Final concentration	
	AdoMetDC	ODC
AdoMet	99 µM	-
Ornithine	-	90 µM
[^{14}C]AdoMet (10x dilution)	12.5 nCi (1 µM)	-
[1-^{14}C]ornithine	-	125 nCi (10 µM)
DTT	1 mM	1 mM
EDTA	1 mM	1 mM
PLP		40 µM
KH_2PO_4 (pH 7.5)	40 mM	-
Tris-HCl (pH 7.5)	-	40 mM
Enzyme	~5 µg	~5 µg
Total volume	**250 µl**	

Decarboxylase enzyme activity determination reactions were performed in 50 ml glass tubes in duplicate for each insert-deleted mutant protein together with its corresponding wild type PfAdoMetDC/ODC protein. The blank reactions contained H_2O. Whatman no.2 filter papers (Merck, Germany) were folded lengthwise and inserted into 2 ml open-ended inner tubes to which 40 µl hydroxide of hyamine (PE Applied Biosystems, USA) was added to trap the released $^{14}CO_2$ in the form of hyamine carbonate. The inner tubes were then placed inside the glass tubes and sealed with rubber stoppers. The reactions were allowed to take place at

37°C for 30 min in a shaking water bath and terminated by the precipitation of the proteins with the injection of 500 µl of 30% w/v trichloro-acetic acid. The acidic mixtures were neutralised with ~40 mM $NaHCO_3$ while the free $^{14}CO_2$ was diluted at the same time with the release of excess unlabeled CO_2. The tubes were once again incubated for 30 min at 37°C. The filter papers were separately transferred to 4 ml Pony-Vial H/I tubes (PE Applied Biosystems) to which 4 ml of Ultima Gold XR scintillation fluid (PE Applied Biosystems) was added. The radioactivity was counted with a Tri-Carb series 2800 TR liquid scintillation counter (PE Applied Biosystems). The results were analysed with the QuantaSmart™ Software programme and were calculated as the mean of three independent experiments carried out in duplicate and expressed as specific activity (SA) in nmol/min/mg. The results of the mutant specific activities are also expressed as a percentage of the wild type SA.

The specific activity is calculated as follows (the relative quantity of each protein was taken into account to calculate the amount of protein in the assay sample, Appendix A and B):

$$SA = \frac{\text{CPM x nmol substrate}}{\text{mg protein x min x total CPM}}$$

In order to account for the smaller size of the mutant proteins, the normalised activities to the full-length wild type proteins were calculated with the following formula:

$$\% \text{ Activity} = SA \times \frac{\text{MW mutant}}{\text{MW AdoMetDC/ODC}} \times 100$$

All of the above experiments were also repeated with the plasmids containing the disrupted secondary structures within the A2 and A3 parasite-specific inserts.

3.4.3.8 Statistical analysis

The significance of the results was calculated with a non-directional two-tailed t-Test assuming unequal variances. Results with *p* values smaller than 0.05 meant that there was a significant difference between the control and sample population.

3.5 Results and Discussion

3.5.1 The identification of structural features within the PfAdoMetDC inserts

Based on the results from secondary structure prediction programmes, a conserved nine amino acid α-helix was identified within insert A2, which contains six amino acids that show preference for helix formation (Figure 3.3, A2). Three possible secondary structures could be seen when insert A3 was investigated. The first β-sheet (residues 268-272) consists of five

residues of which four favour β-sheet formation. This structure was, however, not investigated due to its small size. The second, larger eight-residue sheet (residues 284-291) of which five amino acids have high propensities to form β-sheets was considered as a structure that may have an important function within the A3 insert. While the last sheet consisting of residues 387-392, of which only three show weak preference for β-sheet formation, was also not investigated (Figure 3.3, A3).

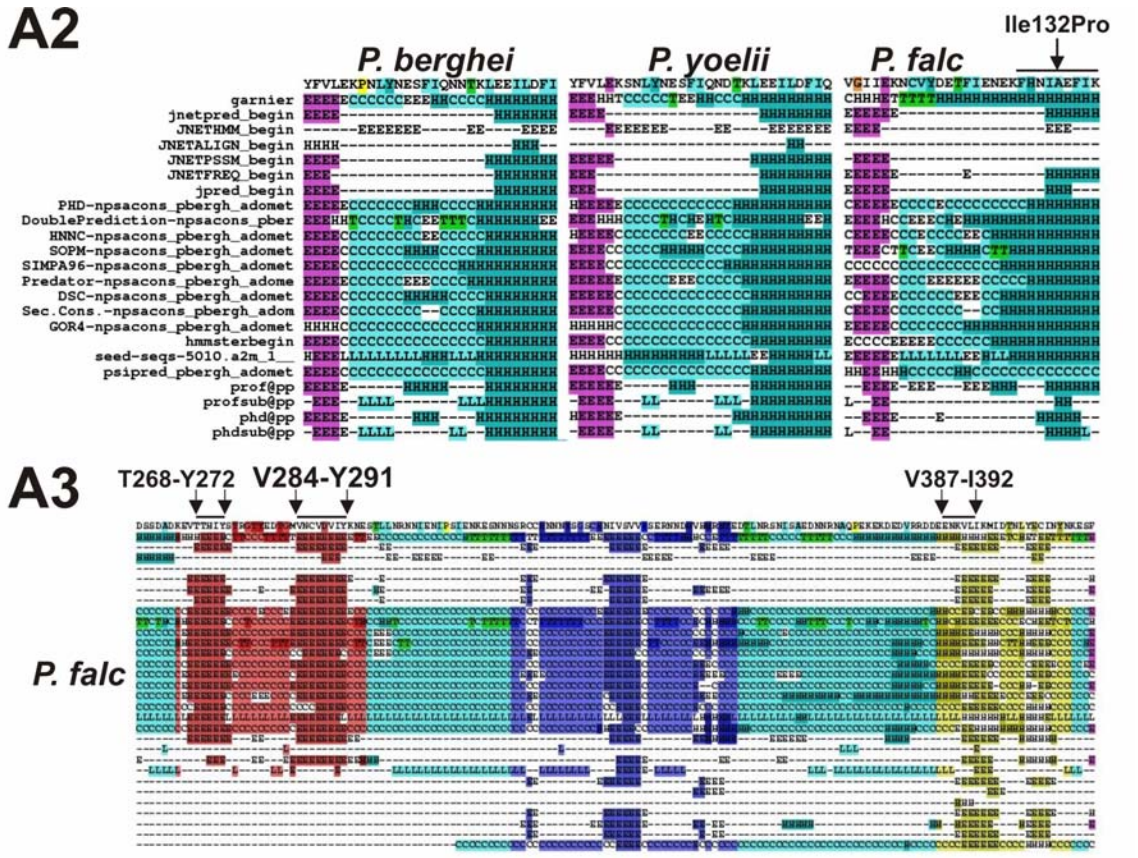

Figure 3.3: Secondary structure prediction results of the A2 and A3 insert sequences.
The legends on the left list the secondary structure prediction programmes that were used. The α-helix within A2 is indicated with a black bar. The arrow shows the position where a helix breaker (Ile132Pro) can be introduced during site-directed mutagenesis. β-sheets within insert A3 are indicated with black bars in the bottom panel. The arrows indicate the start and end positions of the areas. For simplicity, only the *P. falciparum* sequence is shown. Dashed lines are areas where secondary structures are absent and correspond to loops. Abbreviations: H, helix; C/L, coils; E, β-sheet; T, turns.

HCA diagrams of the A2 and A3 parasite-specific inserts confirmed the results obtained with the secondary structure prediction programmes above (Figure 3.3). Figure 3.4 gives the amino acid sequences of the inserts together with the two-state codes of these. The A2 insert contains one particular structure encoded by 10010011 (Figure 3.4, A2). This coding sequence represents a frequently encountered α-helix cluster consisting of eight amino acids, four of which are hydrophobic (Callebaut *et al.*, 1997). The cluster also starts and ends with hydrophilic residues and is separated from the previous cluster with four non-

hydrophobic residues. For insert A3, two specific clusters could be identified (Figure 3.4, A3). These structures most likely correspond to β-sheets as they are arranged in vertical-type clusters; they are also once again flanked with hydrophobic residues and are distinct as they are separated from adjacent structures with at least four hydrophilic residues (Callebaut *et al.*, 1997).

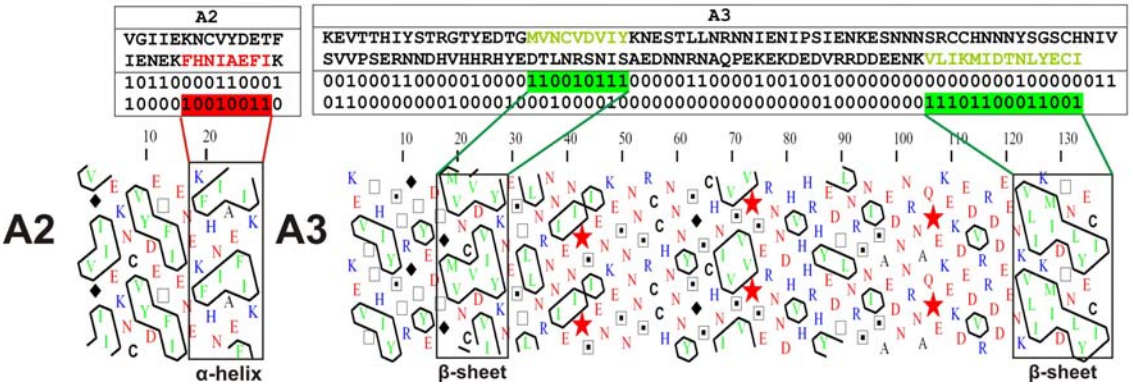

Figure 3.4: HCA plots for the A2 and A3 parasite-specific inserts in *P. falciparum* AdoMetDC/ODC.
The HCA plot of the A2 parasite-specific insert is given on the left while the plot for A3 is given on the right. The amino acid sequences and HCA codes of the two respective inserts are given above the plots. The strong and moderate hydrophobic amino acids (Val, Ile, Leu, Phe, Met, Trp, Tyr) are grouped together in clusters and shown in green, the basic amino acids (Lys, His, Arg) are shown in blue, while the acidic amino acids (Asp, Glu) are shown in red. Particular amino acids are highlighted: a star for Pro, a diamond for Gly and squares with a dot or not for Ser and Thr, respectively. The boxes indicate the secondary structures in the two plots: an α-helix in A2 (red) and two β-sheets in A3 (green) (Callebaut *et al.*, 1997).

Based on these results obtained with both secondary structure prediction programmes (Figure 3.3) and HCA (Figure 3.4), two structures were further investigated: the α-helix in A2 and the second β-sheet in insert A3. The third β-sheet in A3 is positioned close to the edge of the parasite-specific insert and its folding might therefore involve residues outside of the 137 residue insert. In addition, this β-sheet in insert A3 predicted with HCA was also identified with secondary structure prediction programmes above but these showed that the cluster is interspersed with several α-helix preference residues and was thus not further investigated.

3.5.2 Deletion of the parasite-specific inserts in PfAdoMetDC

The ~3100 bp pASK-IBA vector together with the ~4300 bp wild type *PfAdoMetDC/ODC* gene gives a total linear construct size of ~7400 bp (A/Owt). Deletion of the A1 and A2 inserts (A/OΔA1 and A/OΔA2) results in PCR products of roughly the same size as the wild type (Figure 3.5).

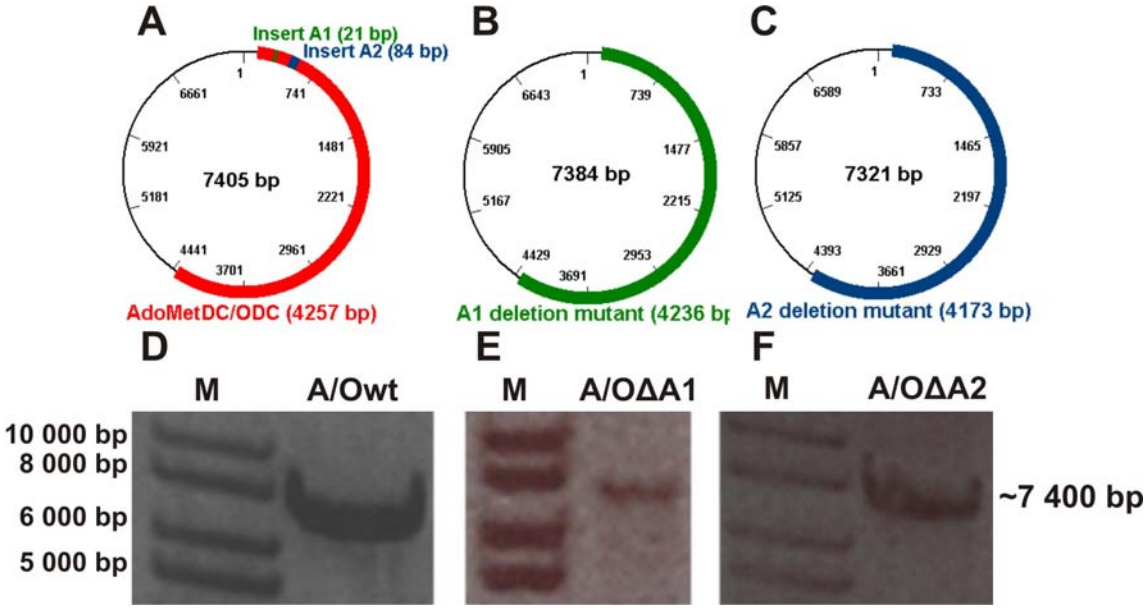

Figure 3.5: Agarose gel electrophoresis of the A/OΔA1 and A/OΔA2 PCR products.
Schematic vector diagrams of the wild type (A), the 21 bp deletion mutant A/OΔA1 (B) and the 84 bp deletion mutant A/OΔA2 (C) *PfAdoMetDC/ODC* genes inserted into pASK-IBA3 vectors (vector size ~3100 bp). The agarose electrophoresis gel of the deletion mutagenesis PCR products is given in the bottom panel showing the A/Owt (D), A/OΔA1 (E) and A/OΔA2 (F) PCR products of ~7400 bp. (M) 1 kb DNA marker.

The deletion of the A1 and A2 parasite-specific inserts removed 21 and 84 nt, respectively, and thus resulted in PCR products of approximately 7400 bp (Figure 3.5 E and F), which corresponds to the size of wild type template (Figure 3.5 D). The independent deletion mutagenesis results of each of the A1 and A2 inserts were verified with nucleotide sequencing (Figure 3.6). The deletion of the largest A3 parasite-specific was performed in Chapter 2 (Figure 2.3).

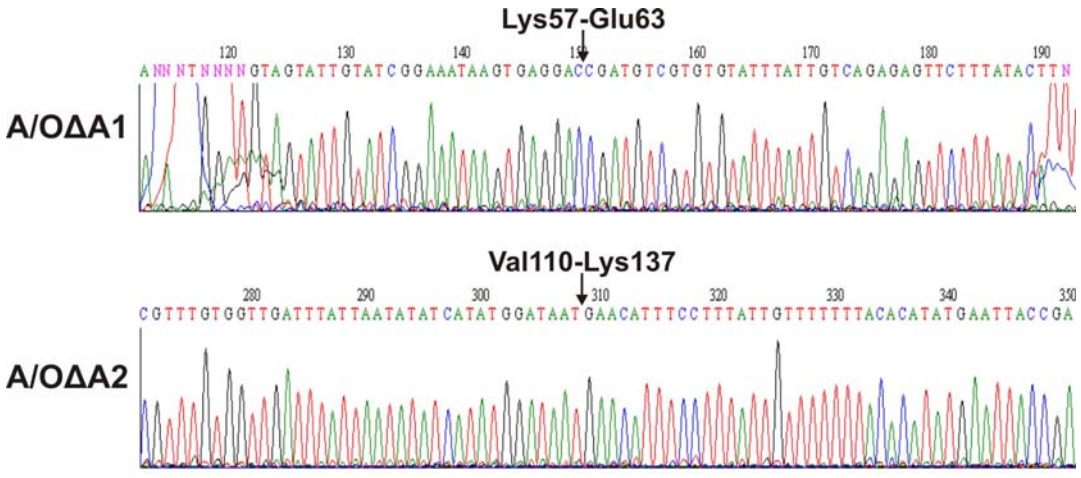

Figure 3.6: Nucleotide sequencing chromatograms of the PfAdoMetDC/ODC insert-deleted constructs.
The arrows indicate the positions where the A1 (top panel, A/OΔA1) and A2 (bottom panel, A/OΔA2) parasite-specific inserts were deleted.

Automated nucleotide sequencing of the A/OΔA1 clones resulted in two out of five mutant clones (40% mutagenesis efficiency) while the deletion of the A2 insert with the overlapping primer method was only 20% successful. All three of the parasite-specific inserts were thus successfully removed (Figure 2.3 for A/OΔA3 and Figure 3.6 for A/OΔA1 and A/OΔA2), which can be used to determine the individual effect of each insert on the activity of the corresponding as well as the neighbouring decarboxylase domain.

3.5.3 Mutagenesis of delineated areas within the PfAdoMetDC parasite-specific inserts

The PCR products obtained with the site-directed mutagenesis reactions were visualised with agarose gel electrophoresis. Once again a DNA band of ~7400 bp was expected for each of the mutagenesis products (Figure 3.5 A), which can be seen for both the A/OpA2a and A/OΔA3b products below (Figure 3.7 B and C, respectively).

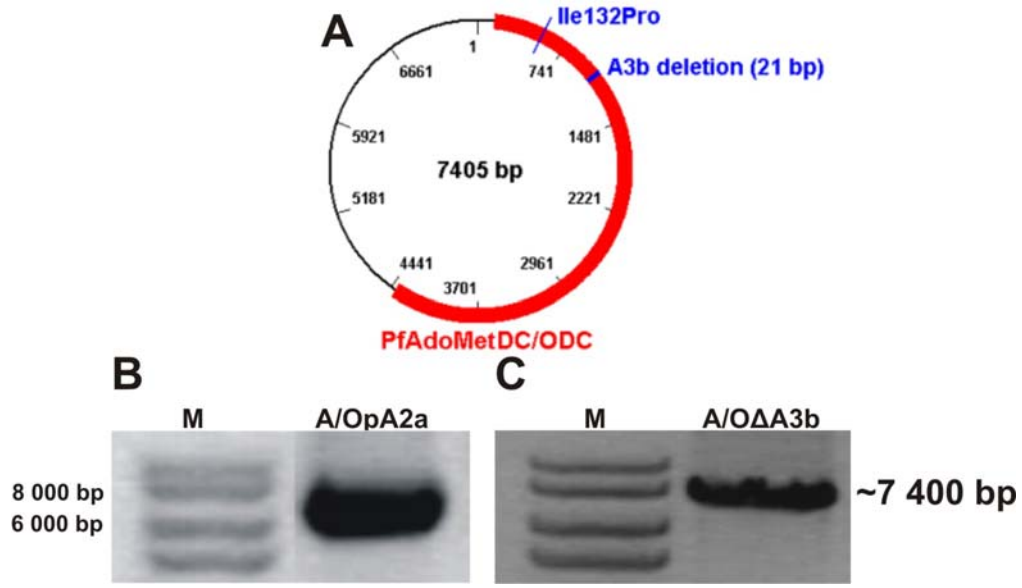

Figure 3.7: Agarose gel electrophoresis of the A/OpA2a and A/OΔA3b PCR products.
(A) A schematic diagram of *PfAdoMetDC/ODC* (~4300 bp) cloned into pASK-IBA3 (~3100 bp). The location of the Ile132Pro point mutation and A3b deletion is indicated in blue. (B) 1% Agarose gels were used to visualise the A/OpA2a (B) and A/OΔA3b (C) PCR products with the expected sizes of ~7400 bp. (M) 1 kb DNA ladder.

Nucleotide sequencing of the mutant clones was subsequently performed to determine whether the point mutation at amino acid position 132 was successfully incorporated and if the β-sheet in insert A3 was deleted. The K215A2 reverse primer was used to detect the presence of the Ile132Pro point mutations in the five clones. The reverse complement of the nucleotide sequences shows the CCA mutation as TGG, which was seen in three out of the five clones analysed giving a 60% mutagenesis efficiency with the overlapping primer

method (Figure 3.8). The K215A1 sequencing primer was used for the verification of the β-sheet deletion within insert A3. The sequencing results obtained indicated that the sheet was once again absent in three out of the five clones analysed also resulting in a 60% mutagenesis efficiency (Figure 3.8).

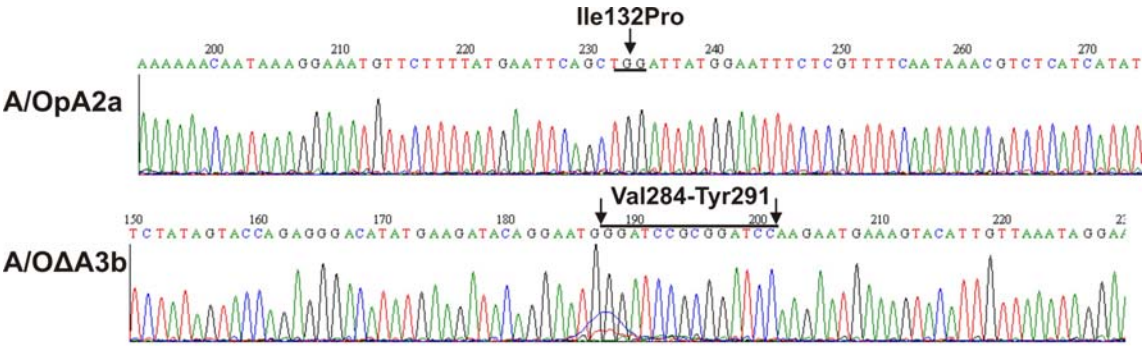

Figure 3.8: Nucleotide sequencing chromatograms of the A/OpA2a and A/OΔA3b constructs. The black bar indicates the position of the Ile132Pro point mutation within pA/OpA2a (top panel). The longer black bar in the bottom panel indicates the position of the *Bam*HI restriction enzyme sites that were inserted in place of the A3 parasite-specific insert in pA/OΔA3b with the RE-mediated inverse PCR method.

3.5.4 Influence of the PfAdoMetDC inserts on bifunctional activity

3.5.4.1 Isolation of the mutant PfAdoMetDC/ODC proteins

The wild type and insert-deleted *PfAdoMetDC/ODC* sequences cloned into the pASK-IBA3 vectors were transformed into heat shock competent *E. coli* EWH cells. The recombinant proteins were subsequently isolated via cell disruption, ultracentrifugation and *Strep*-tag affinity chromatography. There was no significant difference between the amount of isolated protein of the wild type and the mutant samples ($p > 0.05$) indicating that the inserts may not have had an influence on the overall expression levels of the recombinant proteins in the soluble fractions (Figure 3.9). The average total amount of protein obtained from 1L culture per sample was 200 µg.

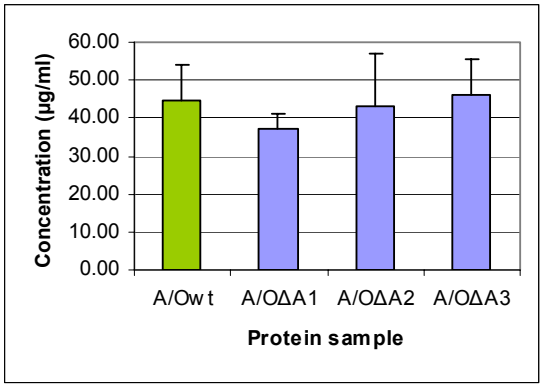

Figure 3.9: Protein expression levels of the wild type PfAdoMetDC/ODC and the PfAdoMetDC insert-deleted proteins.
The wild type protein (A/Owt) is shown in green and the mutant ones in blue (A/OΔA1, A/OΔA2 and A/OΔA3). The concentrations were determined from three independent experiments. The standard deviations of the mean are indicated as error bars on each graph.

The recombinantly expressed proteins were analysed with SDS-PAGE. Protein bands of ~160 kDa (heterodimer: ~150 kDa consisting of covalently linked PfAdoMetDC/ODC and the 9 kDa β-subunit of PfAdoMetDC) were obtained after recombinant protein expression and isolation of the wild type PfAdoMetDC/ODC as well as the PfAdoMetDC insert-deleted proteins (Figure 3.10). The amount of each protein loaded onto the SDS polyacrylamide gel averaged at 2.5 µg per lane, but this did not reflect the amount of the desired ~160 kDa protein. Inspection of the PAGE result showed that the amount of ~160 kDa protein decreased from the A/Owt to the A/OΔA3 protein sample while the intensities of contaminating proteins were the highest for the insert-deleted mutated protein samples (Appendix A, Table 1A). Lower amounts of *Strep*-tagged purified ~160 kDa protein in the mutant samples could not be attributed to the presence of misfolded proteins in inclusion bodies as this would have resulted in the absence of these proteins in the soluble protein fractions and a significant decrease in the total amount of protein isolated. In a previous study the crude *E. coli* lysates were also visualised with SDS-PAGE and the results showed that these proteins are absent in the *Strep*-tag purified proteins samples [results not shown, (Niemand, 2007)].

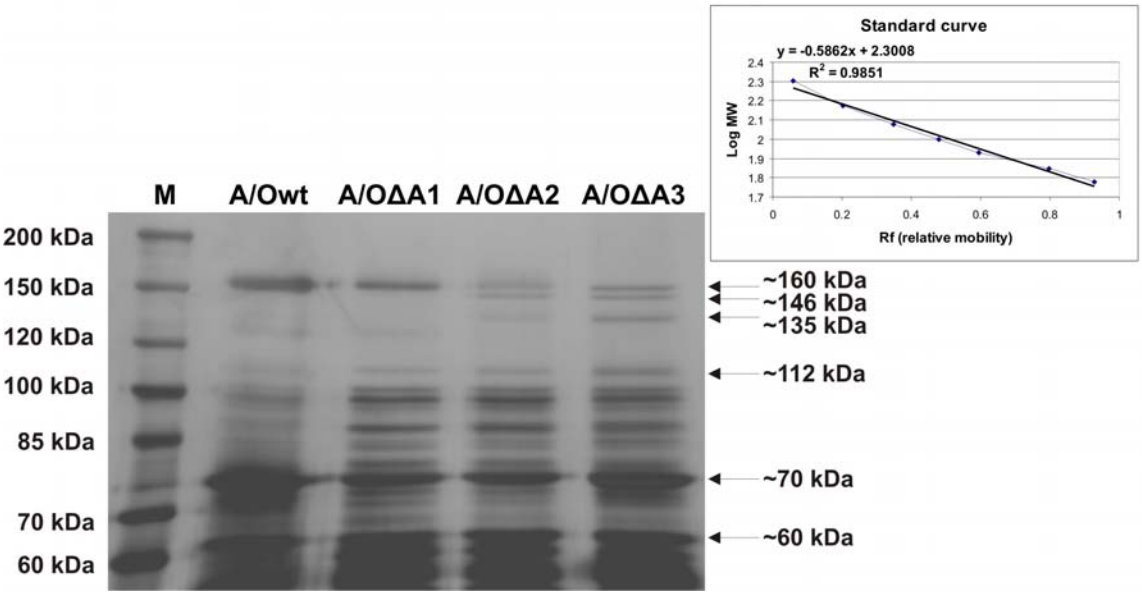

Figure 3.10: SDS-PAGE analysis of the expressed wild type and the bifunctional PfAdoMetDC insert-deleted recombinant proteins.
The protein size-determining marker is shown in lane M. The denatured bifunctional heterodimeric protein is seen as a ~160 kDa protein band. Calibration curve: distance moved against logMW for each of the standard proteins in lane M.

The expression and purification of *P. falciparum* proteins is a common obstacle for many researchers in the field and may be attributed to various factors such as the high A+T content of the malarial genome, the increased sizes of the proteins due to the high occurrence of LCRs and parasite-specific inserts and extensive RNA secondary structures (Pizzi and Frontali, 2001; Gardner *et al.*, 2002; Birkholtz *et al.*, 2003; Mehlin *et al.*, 2006). It is thus not surprising that these proteins are difficult to express in adequate and pure quantities in heterologous protein expression systems. Mehlin *et al*. recently expressed 1000 *P. falciparum* proteins in *E. coli* but managed to obtain soluble quantities of only 63 proteins that were sufficient for subsequent purification. The size, degree of disorder and pI of these proteins negatively influenced their soluble expression in the heterologous system (Mehlin *et al.*, 2006). Furthermore, the stretches of A and T bases in the genes often result in frame shift mutations and false internal start codons leading to truncated protein products of smaller sizes.

In a previous study, apart from the correctly sized ~160 kDa PfAdoMetDC/ODC protein band, three major proteins sized ~112 kDa, ~70 kDa and ~60 kDa were obtained with denaturing PAGE, which can also be seen in the figure above. Various experiments were subsequently performed in this laboratory in order to identity these contaminating proteins (Niemand, 2007). Size-fractionation studies suggested that contaminating proteins associate with the full-length PfAdoMetDC/ODC protein to form high molecular weight complexes of ~600 and ~400 kDa, which is in-line with previous studies that showed that the PfODC domain

mediates the dimerisation of the bifunctional protein via an aromatic amino acid zipper, several hydrophobic interactions and a salt bridge (Birkholtz *et al.*, 2003; Birkholtz *et al.*, 2004). Any additional proteins containing PfODC would thus form tight interactions with PfODC in the main protein and result in the co-elution of these proteins during *Strep*-tag affinity chromatography. The ~60 kDa protein was not detected with *Strep*-tag Western immunodetection and was thus regarded as either a C-terminal truncated protein or a host-derived protein.

Explanations for the presence of the ~112 and ~70 kDa *Strep*-tagged proteins include post-translational degradation, in frame ribosomal slippage due to the high abundance of mRNA secondary structures and false initiation codons. Ribosomal slippage on mRNA secondary structures as the cause of the differently expressed proteins was excluded as these expressed contaminating proteins was found to only possess C-terminal *Strep*-tags and no N-terminal tags. Subsequent analysis of the *PfAdoMetDC/ODC* gene revealed the presence of two possible prokaryotic Shine-Dalgarno-like sequences downstream of start codons, which may lead to the translation of the ~112 and ~70 kDa proteins from internal mRNA initiation sites to produce the N-terminally truncated proteins. These internal sequences have no effect on the *in vivo* translation of the proteins within the eukaryotic host but it can cause the expression of these truncated proteins from these sites when using the prokaryotic *E. coli* expression system. MS analysis of the major contaminating bands revealed some interesting results: the ~112 kDa protein is an N-terminal truncation of the full-length protein and the ~70 kDa and 60 kDa bands were identified as *E. coli* 70 kDa (with some traces of N-terminally truncated PfAdoMetDC/ODC) and 60 kDa heat shock proteins (HSP), respectively. The purification of these two proteins with the full-length protein implies that these chaperones are tightly bound to PfAdoMetDC/ODC, possibly in an effort to cope with the expression and folding of the recombinant protein. Overall, these studies revealed that the presence of internal translation initiation sites within the gene sequence results in the production of a multi-component protein complex and thus prevents the homogenous purification of a recombinant protein (Niemand, 2007).

A possible explanation for the higher intensity of contaminating proteins in the soluble fraction of the mutated protein samples in Figure 3.10 above, may be that the deletion of regions that are possibly necessary for their correct folding can place further stress on the expression of the recombinant proteins leading to the co-elution of chaperone proteins and possible degradation products. The presence of the contaminating proteins in the purified protein samples may interfere with downstream experiments and needs to be taken into consideration especially in the determination of the effects that the inserts have on the activities of the full-length bifunctional protein. However, the activities obtained after the

deletion of each of the parasite-specific inserts in the PfAdoMetDC domain will be normalised to the activity of the wild type PfAdoMetDC/ODC protein sample, which will even out the effects of the contaminating proteins in all the samples. At present, the only route around this problem of heterogeneous protein isolates is to re-synthesise the *PfAdoMetDC/ODC* gene to remove internal Shine-Dalgarno-like sequences together with codon harmonisation to ease the burden on the heterologous expression system thus achieving better protein expression and isolation.

The electrophoresis gel also shows the presence of additional smaller sized protein bands that appeared upon the removal of the larger parasite-specific inserts (Figure 3.10, lanes A/OΔA2 and A/OΔA3). The approximate MW of these unknown proteins in lanes A/OΔA2 and A/OΔA3 were determined with the use of a calibration curve drawn up from the Rf (relative mobility) values *versus* the logMW of the standard proteins (Figure 3.10, inserted graph). Substitution of these unknown proteins' Rf values into the linear regression equation determined these to be ~146 kDa and ~135 kDa in size. The determination of protein sizes with SDS-PAGE is, however, not a reliable method as the conformation of the proteins can interfere with their mobility through the gel matrix. The formation of these smaller proteins with correspondingly smaller sizes were subsequently analysed with MS.

3.5.4.2 MS analysis of the PfAdoMetDC insert-deleted proteins

The recombinant A/OΔA2 and A/OΔA3 proteins were separated with SDS-PAGE and visualised with an MS compatible colloidal Coomassie staining protocol. The gel was dried and the ~146 kDa shadow bands directly beneath the ~160 kDa bands in the last two lanes in Figure 3.10 were cut out and analysed with MS after trypsin digestion. Table 3.4 lists the different peptides identified with MS.

Table 3.4: Peptides identified with MS

2. Plasmodium_falciparum_3D7|MAL10|PF10_0322|Pf

Mass: 168063 **Score:** 48 **Queries matched:** 7

Annotation|Plasmodium_falciparum_TIGR|(protein coding)

S-adenosylmethionine decarboxylase-ornithine decarboxylase

Query	Observed	Mr(expt)	Mr(calc)	Delta	Score	Expect	Rank	Peptide
498	593.74	1185.47	1183.67	1.80	8	18	1	K.NNNVLLTLQR.N
616	629.24	1256.47	1255.65	0.82	3	57	10	R.YMVAASSTLAVK.I
629	635.16	1268.30	1267.58	0.72	16	4.3	1	K.NIGNNFSSSNSK.L
929	779.31	1556.60	1554.79	1.81	48	0.0012	1	K.IVVVDTNTFFDASK.R
382	545.26	1632.76	1631.87	0.89	15	5.9	1	K.IHYCTLSLQEIKK.D
828	734.93	2201.77	2202.11	-0.34	13	8	1	K.VLIKMIDTNLYECINY NK.E

All the peptides that were identified were complementary to the PfAdoMetDC/ODC sequence (Figure 3.11), indicating that the smaller protein bands seen in Figure 3.10 (lanes A/OΔA2 and A/OΔA3, sized ~146 kDa) isolated together with the A2- and A3-deleted proteins are PfAdoMetDC/ODC albeit with a very low Mascot score of only 48. The Mascot score gives the probability that the observed protein match between experimental data and a protein sequence is a random event and is regarded insignificant when it scores below 74. In this case, the low score may be attributed to the low intensity of the protein band that was tested, which was thus insufficient for effective MS analysis.

```
   1 MNGIFEGIEK RVVIKLKESF FKGNRNVNSF LDIPKELWEE KLKYIGCSIV SEISEDKNER
  61 RGERCRVYLL SESSLYIFDD SLFIKTCGKT RVLFFIPFVV DLLIYHMDNV GIIEKNCVYD
 121 ETFIENEKFH NIAEFIKEHF LYCFFTHMNY RNKTKDGYFE QEYPHKSLED EKKFFEFFFK
 181 NVQMYNTHLP MEKMHYIFFY SSDDVHMTDI ASTFKFCSEI HLFGINKYNE KNQFHDAYLN
 241 NKSLNLFTRV HEDNLKLYDS SDADKEVTTH IYSTRGTYED TGMVNCVDVI YKNESTLLNR
 301 NNIENIPSIE NKESNNNSRC CHNNNYSGSC HNIVSVVPSE RNNDHVHHRH YEDTLNRSNI
 361 SAEDNNRNAQ PEKEKDEDVR RDDEENKVLI KMIDTNLYEC INYNKESFLY NEFYFTPCGY
 421 SCNVSEKNNY FCVHYSPEDS VSYVSVEVSS NLSCDRFLDF IHKQLNFYNG KYMFMINYVF
 481 CEESNNMSKM VPDDDNNNYS SGKSCVYYQD LNKKEKEEYY RLNKKLRNDL FINSKQFYEL
 541 HTFTERTVGF MRVQYFVYKL RDVVKCVEKE TLLARSSSCL FMFNNIKRND VHDDYVTKSS
 601 NGGVIKQLTE RDVDDMYEYA LNFCKQNKIV VVDTNTFFFD ASKRKENLIK LEKVQTNEKD
 661 EYEEKDEVYR RGNNELSSLD HLDSKNNLIH MYYEKNKCDI INKDDENSTI ATNNNDNNND
 721 SSSYDKSITI SRSSSCNNSH LSYSSFDNNH GNEKMKDYIS VDENNNNNNN NKNNNVLLTL
 781 QRNSDDENGK DKDNEKNDVS LENNMEKNYK EEIWNYYTKN KVEVKTLEKV LNENIDTSVV
 841 CINLQKILAQ YVRFKKNLPH VTPFYSVKSN NDEVVIKFLY GLNCNFDCAS IGEISKVIKL
 901 LPNLSRDRII FANTIKSINS LIYARKENIN LCTFDNLDEL KKIYKYHPKC SLILRINVDF
 961 KNYKSYMSSK YGANEYEWEE MLLYAKKHNL NIVGVSFHVG SNTKNLFDFC LAIKLCRDVF
1021 DMSSNMGFNF YIINLGGGYP EELEYDNAKK HDKIHYCTLS LQEIKKDIQK FLNEETFLKT
1081 KYGYYSFEKI SLAINMSIDH YFSHMKDNLR VICEPGRYMV AASSTLAVKI IGKRRPTFQG
1141 IMLKELKDHY DPLNFAQQEN KKQDETKINH NNDNNDNNDN NDNNINNNNN NQKGGQGNIM
1201 NDLIITSTND STSKKNDHSS SQVIQNVSCT IRDKEGDNIK INTHTINNPN INGKENTVDG
1261 DNINIAHKNI GNNFSSSNSK LGNITNIKKK VVNINDNRYN YFSYYVSDSI YGCFSGIIFD
1321 EYNRCPIYVI KNKNNPNQNF MNFNLYLANV FGQSCDGLDM INSITYLPEC YINDWLLYEY
1381 AGAYTFVSSS NFNGFKKCKK VYIFPESKPS LKGQPNKHW
```

Figure 3.11: Peptides identified with MS aligned with the PfAdoMetDC/ODC sequence.
The positions of the three PfAdoMetDC parasite-specific inserts are shown in green while the peptides that were identified with MS analysis are shown in red. The methionine residues at the beginning of the protein sequences as possible translation initiation sites are highlighted in red.

The smaller contaminating proteins could be formed as a result of post-translational degradation of the expressed protein or the presence of false translation initiation sites downstream of the start codon that occur in-frame to the particular open reading frame and are exposed as a result of conformational changes upon the deletion of the inserts (Niemand, 2007). Unfortunately, these bands could not be detected with anti-*Strep* antibodies due to their close proximity to the mutated PfAdoMetDC/ODC protein (results not shown). Western analysis would indicate whether the deletions resulted in N-terminal truncations of the full-length protein, as these would still contain their C-terminal *Strep*-tags. It is also possible that the deletions result in conformational changes leading to proteolysis sites becoming accessible to proteolytic enzymes or start codons becoming accessible to the protein translation initiation complex, which are usually buried, resulting in the formation of smaller protein products. The latter is a possibility due to the high abundance of secondary structures present on mRNA strands. If Shine-Dalgarno-like sequences are situated

downstream and in close proximity to exposed Met start codons, the formation of the ~146 kDa protein could be as a result of translation initiation taking place from Met107 situated between inserts A2 and A3 while the ~135 kDa protein could be formed if translation takes place from Met184, 191 or Met194. The exact identities of these protein bands and the manner in which they are produced thus require further investigation.

3.5.4.3 Activity assays of the PfAdoMetDC insert-deleted proteins

The isolated recombinant proteins were subjected to radioactivity assays during which ^{14}C-labelled substrates were co-incubated with the isolated enzymes to generate $^{14}CO_2$. The labelled product was captured and counted with a liquid scintillation counter. The results obtained were normalised against the specific activity (nmol/min/mg) of the wild type protein and expressed as a percentage of its activity (Figure 3.12). The altered sizes of the mutated proteins (A/Owt = 156 090 Da, A/OΔA1 = 155 430 Da, A/OΔA2 = 153 120 Da and A/OΔA3 = 141 020 Da) were taken into consideration. In addition, densitometric analyses of the band intensities were performed and the percentage contribution of the bifunctional protein was used to determine the amount compared to the total protein concentration (Appendix A, Table 1A). The percentage contributions of the truncated versions of the bifunctional proteins to the total protein concentrations were not taken into consideration for the activity determinations since monofunctional PfODC has negligible activity (Krause *et al.*, 2000).

The small A1 insert occurs in all *Plasmodium* species of known sequences and has a high similarity with the other *Plasmodium* sequences (*P. yoelii*, *P. berghei*, *P. chaubaudi* and *P. knowlesi*). The second insert in the PfAdoMetDC domain is also highly conserved while insert A3 is the most divergent one (Wells *et al.*, 2006). Previous mutagenesis studies on a region encompassing insert A3 severely effected PfAdoMetDC activity but had no impact on the formation of the bifunctional complex (Birkholtz *et al.*, 2004), which is in agreement with the PfAdoMetDC homology model where this insert is positioned on the edge opposite to the dimerisation boundary of the domain. This insert, however, was identified before the PfAdoMetDC model was solved, which means that the deletion removed part of the core structure (residues 214 to 410) of the protein possibly resulting in the observed activity loss (Wells *et al.*, 2006). Multiple alignments and the homology model of the PfAdoMetDC domain resulted in the identification of three parasite-specific inserts, which forms the focus of this study.

Deletion of insert A1 within the PfAdoMetDC domain of the bifunctional protein significantly decreased this domain's activity by 47%. The results also show 98% inhibition of PfAdoMetDC activity upon the deletion of the A2 and A3 inserts (Figure 3.12).

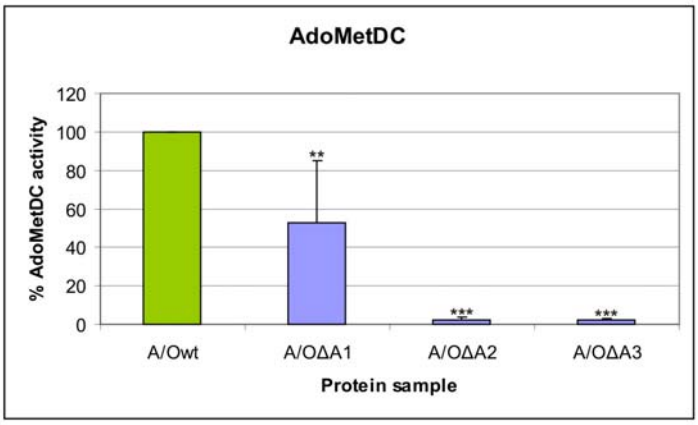

Figure 3.12: AdoMetDC activity assays of the wild type PfAdoMetDC/ODC and bifunctional PfAdoMetDC insert-deleted proteins.
Wild type A/Owt activity is shown in green at 100% while the various mutant proteins activities normalised to the A/Owt activity are shown in blue. The values were determined from three independent experiments carried out in duplicate. The standard deviations of the mean are indicated as error bars on each graph. Significant differences at a confidence level of 95% are represented as follows: ** for $p < 0.01$and *** for $p < 0.001$.

The effects of the deletion of these inserts in the bifunctional protein on the neighbouring PfODC domain were also investigated. Figure 3.13 shows the normalised PfODC activities upon the deletion of the PfAdoMetDC inserts in the PfAdoMetDC/ODC protein. From this figure, it is clear that the deletion of these inserts also resulted in significant losses in activity of the neighbouring PfODC domain where each deletion decreased PfODC activity by 95, 82 and 90%, respectively.

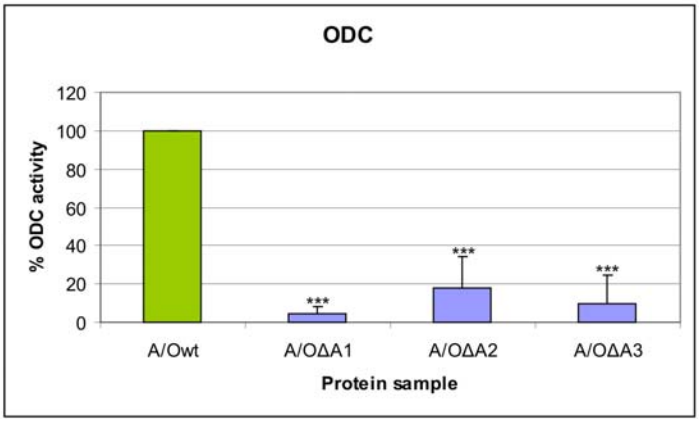

Figure 3.13: ODC activity assays of the wild type PfAdoMetDC/ODC and bifunctional PfAdoMetDC insert-deleted proteins.
Wild type A/Owt activity is shown in green at 100% while the various mutant proteins activities normalised to the A/Owt activity are shown in blue. The values were determined from three independent experiments carried out in duplicate. The standard deviations of the mean are indicated as error bars on each graph. Significant differences at a confidence level of 95% are represented as follows: *** for $p < 0.001$.

While the deletion of the seven amino acid A1 insert halved PfAdoMetDC activity, it had a greater effect on the adjacent PfODC domain with a 95% decrease in activity. This supports previous studies where the PfODC domain was shown to be effected to a greater extent than that of the PfAdoMetDC domain (Birkholtz *et al.*, 2004; Roux, 2006). The A1 insert is similar

to O1 in the sense that it is short and highly conserved amongst the *Plasmodium* species. Previous studies on the O1 insert showed that this highly conserved area, positioned close in linear amino acid sequence to the neighbouring domain and hinge region, plays essential roles in the activities of both domains in the bifunctional protein and also mediates the association of the monofunctional PfAdoMetDC and PfODC proteins into an active bifunctional heterotetrameric protein (Birkholtz *et al.*, 2004). It is thus interesting to note that, despite the linear location of the conserved A1 insert close to the N-terminus of the bifunctional protein (residues 57-63), its deletion resulted in only 47% active PfAdoMetDC protein and 5% active PfODC protein, which may be due to similar effects as seen for O1. The reason for such a severe loss in activity might be due to conformational changes communicated to the PfODC domain with direct consequences on the function of the active site or the dimerisation of this domain via protein-protein interactions. Studies by Wrenger *et al*. showed that the active sites of the two domains function independently (Wrenger *et al.*, 2001). However, here the removal of a *Plasmodia* conserved parasite-specific insert in the PfAdoMetDC domain had, in terms of catalytic activity, a detrimental effect on the PfODC domain corroborating reports by Birkholtz *et al*. that interdomain interactions are essential for both activities in the bifunctional complex (Birkholtz *et al.*, 2004).

The two smallest, non-LCR containing inserts namely A1 and O1 are similar in their size, in their conservation across the *Plasmodium* species and their apparent functional roles in the domain activities of PfAdoMetDC/ODC. The content of positively charged Lys and Asn residues in inserts A1 and O1, which are often involved in protein-protein interactions via hydrogen bond formation, are also considerably high at 30 and 25%, respectively (Singh *et al.*, 2004). These regions therefore need to be investigated further as sites for possible inhibitor targeting, which could result in decreased levels of the polyamines within the parasites.

The deletion of the larger A2 and A3 inserts mostly depleted both PfAdoMetDC (98% activity inhibition) and PfODC (82% and 90% inhibition, respectively) activities in the bifunctional protein. Previous deletion mutagenesis studies on the A1 (as identified before the homology model of PfAdoMetDC was solved), O1 and O2 inserts in the bifunctional protein effected not only the activity of the domain within which the insert resides but also the activity and/or conformation of the neighbouring domain. The surface localisations of these inserts imply that they may participate in intra- as well as interdomain interactions, which are brought about by long-range interactions propagated throughout the full-length protein between the surface localised inserts and the respective active sites (Myers *et al.*, 2001; Yuvaniyama *et al.*, 2003). A 3-dimensional structure of the PfAdoMetDC domain together with the parasite-specific inserts where the 3-dimensional location of the inserts are shown will shed more light

on the manner in which these unique areas interact with the remainder of the protein. These inserts might also be involved in the dimerisation of the PfODC monomers, which would explain the severe depletion of this domain's activity. The two active sites of the PfODC domain are formed as a result of its dimerisation and an interference with this conformation would thus lead to an inactive enzyme (Müller *et al.*, 2000).

The results therefore suggest that the parasite-specific inserts in the PfAdoMetDC domain play important roles in the catalytic activities of both domains, which is in agreement with studies performed on the hinge and the PfODC domain inserts where the latter domain was shown to be more dependent on interdomain interactions than PfAdoMetDC (refer to Figure 3.1) (Birkholtz *et al.*, 2004; Roux, 2006). Similar observations have been made in another *P. falciparum* bifunctional protein; monofunctional TS, which is located at the C-terminal of DHFR/TS, is only active within the hybrid complex with the N-terminal DHFR domain (Shallom *et al.*, 1999). It is therefore highly plausible that the bifunctional arrangement of PfAdoMetDC/ODC and DHFR/TS is to maintain optimal catalytic activities and/or stabilities of their C-terminal domains via interdomain interactions across the entire protein, including the inserts. This is supported by experimental evidence that the N-terminal domains of both these bifunctional proteins are functionally active in the absence of their respective C-terminal domains but not *vice versa* (Shallom *et al.*, 1999; Wrenger *et al.*, 2001).

The presence of a number of contaminating proteins following affinity chromatography may also be interfering with the bifunctional protein by forming complexes with it thereby reducing the amount of the desired active protein. These unwanted proteins might be interfering with the effectiveness of the radioactivity assays and need to be taken into consideration when analysing the results. The normalised activities of the mutant proteins are, however, a means of standardising the influence of contaminating proteins.

A possible explanation for the presence of parasite-specific inserts in PfAdoMetDC/ODC and the high abundance of charged residues therein might thus be their involvement in intramolecular protein-protein interactions and the stabilisation of the active, heterotetrameric bifunctional complex. Information on the involvement of the inserts in the PfAdoMetDC domain on complex formation are, however, still outstanding. The possibility exists that the extreme decreases in protein activities after large deletions of entire parasite-specific inserts are due to general conformational changes and cannot be excluded. The deletions could result in unstable proteins or multiple conformations thereof and it was thus hypothesised that the disruption of definite structures within the parasite-specific inserts would be a more sensible approach to study the roles of these areas.

Since a previous study focused on the predicted secondary structures in the hinge and PfODC parasite-specific inserts (Roux, 2006), the specific roles of the inserts in the PfAdoMetDC domain in the activity of both proteins, whether through multiple conformations interfering with discrete interdomain interactions or the removal of such large areas from the protein, needed to be investigated further. The following section will look at delineated areas within the parasite-specific inserts in this domain as possible sites for protein-protein interactions.

3.5.5 The roles of secondary structures within the PfAdoMetDC inserts on bifunctional activity

3.5.5.1 Recombinant protein expression of the newly created constructs

Due to unforeseen experimental complications, protein purification and subsequent activity analysis on the A/OΔA3b mutant protein is still in progress. The proteins encoded by the wild type pA/Owt and α-helix disrupted pA/OpA2a plasmids were recombinantly expressed and isolated with *Strep*-tag affinity chromatography. As can be seen in Figure 3.14, there was once again no significant difference between the expression levels of the wild type (A/Owt) and mutant (A/OpA2a) proteins ($p > 0.05$), which averaged at 70 µg/ml. The total amount of protein obtained from 1L culture was approximately 350 µg.

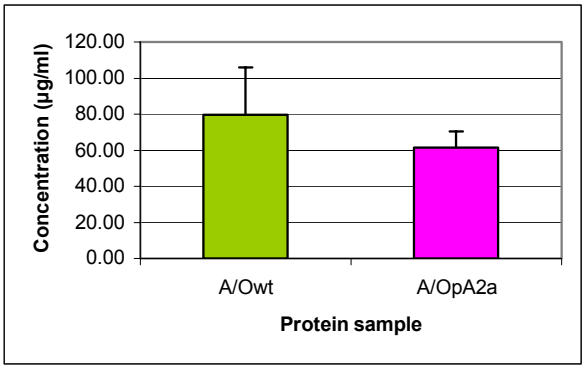

Figure 3.14: Protein expression levels of the wild type PfAdoMetDC/ODC and A/OpA2a proteins.
The wild type protein (A/Owt) is shown in green and the mutant (A/OpA2a) in pink. The concentrations were determined from three independent experiments. The standard deviations of the mean are indicated as error bars on each graph.

The correct size protein bands of ~160 kDa were obtained after recombinant protein expression and isolation of the wild type PfAdoMetDC/ODC as well as the helix-disrupted A/OpA2a protein. The amount of protein loaded onto the SDS-polyacrylamide gel averaged at 2.1 µg per lane (Figure 3.15). As can be seen from the figure below, even though similar

amounts of total protein were eluted and loaded onto the SDS-PAGE, the amount of the mutant ~160 kDa A/OpA2a protein was much lower than the A/Owt full-length protein. The intensity of the co-eluted contaminating proteins (especially at ~70 kDa) during A/OpA2a isolation is again much higher possibly as a result of recombinant protein degradation and the binding of host chaperone proteins to assist with the folding of the protein (discussed in section 3.5.3.1). The intensities of each band on the SDS-PAGE gel are given in Table 1B (Appendix B) as a percentage of the total protein amount loaded per gel lane.

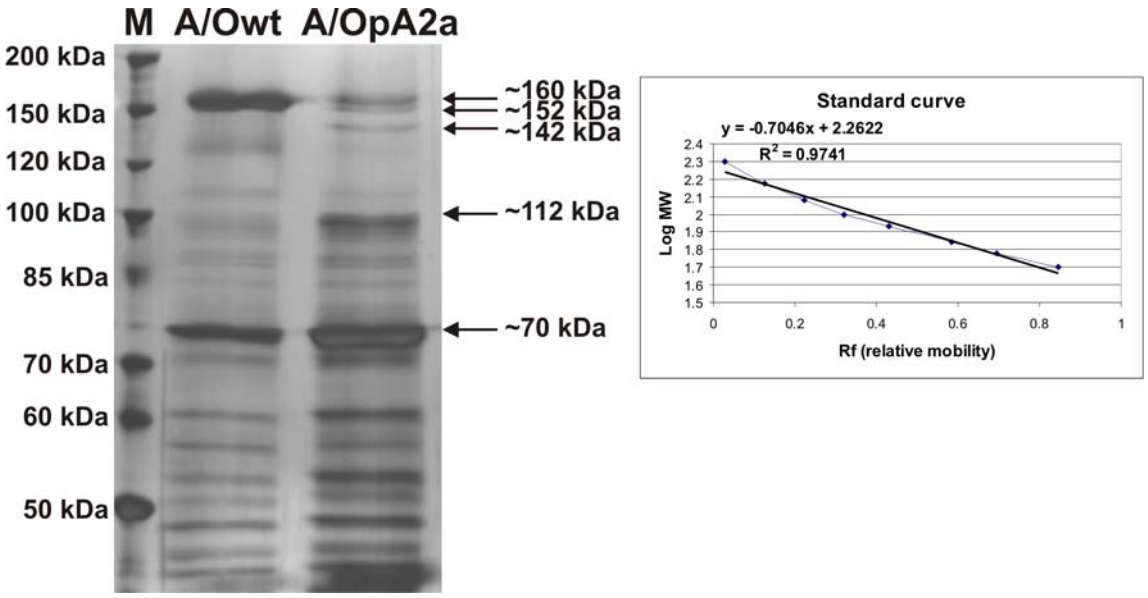

Figure 3.15: SDS-PAGE analysis of the wild type and A/OpA2a recombinant proteins.
(M) 10 to 200 kDa protein ladder. Calibration curve: distance moved against logMW for each of the standard proteins in lane M.

The disruption of the helix in insert A2 resulted in definitive increases in especially the amount of ~112 kDa truncated PfAdoMetDC/ODC and ~70 kDa HSP70/truncated PfODC proteins (Figure 3.15). It seems that, in comparison to the SDS-PAGE profile of the wild type protein, the mutated protein is placing severe stress on the heterologous system for its expression. The helix may be involved in protein-protein interactions throughout the full-length protein, which is abolished upon its disruption resulting in correlative increases in the amount of *E. coli* chaperone protein in an attempt to aid the correct folding of the recombinant protein. Once again unknown proteins of smaller sizes can be seen directly underneath the mutant protein (Figure 3.15 lane A/OpA2a sized ~152 and ~142 kDa), which slightly differs in size from those calculated in Figure 3.10, possibly due to the differences in resolution between the two gels and the mere estimation of sizes with a Rf calibration curve. These ~150 kDa PfAdoMetDC/ODC protein bands (identified with MS in section 3.5.3.2) could thus be produced as a result of any changes that are made within the region of the A2 and A3 inserts.

As mentioned previously, the *cis-trans* isomerisation of the Pro residue inserted to disrupt a helix could lead to a conformational change of the entire protein and not the exclusive disruption of the helix. It is thus possible that such a conformational change could result in the formation of misfolded versions of the protein, which would lead to the aggregation of insoluble proteins in inclusion bodies. The observation that there was no significant difference between the amount of isolated wild type and mutant protein possibly indicates that the introduction of the Pro residue did not enhance the formation of inclusion bodies as this would lead to large increases in the amount of protein in the insoluble fraction and decreases in the amount of protein in the soluble fraction as compared to that of the wild type sample. However, the possibility still remains that the Pro point mutation could have caused a general conformational change that led to the appearance of additional truncated versions of the protein in the mutant sample without resulting in insoluble misfolded proteins. Regarding the non-truncated, mutated bifunctional protein ~161 kDa in size, a general conformational change upon the introduction of the Pro residue should lead to an overall decrease in PfODC activity as this domain would be in the incorrect conformation for proper functioning. In other words, if the disruption of the helix resulted in a general conformational change then the protein downstream of the mutation would be more inactive compared to the when the entire insert was removed as in the previous study.

The isolated proteins were subsequently subjected to activity assays to determine whether the delineated area in insert A2, i.e. the conserved α-helix, contributes to the activities of the proteins in the bifunctional PfAdoMetDC/ODC complex.

3.5.5.2 Activity assays of the secondary structure-mutated proteins

Previous studies in which the conserved α-helix in the O1 insert was disrupted, resulted in PfODC activity depletion while the PfAdoMetDC enzyme retained a mere 6% activity. These effects were subsequently ascribed to the involvement of this delineated area in protein-protein interactions for the formation of the heterotetrameric complex (Birkholtz *et al.*, 2004; Roux, 2006). Similarly, the severe consequences on PfAdoMetDC and PfODC activities observed upon the deletion of the entire A2 insert above, led to the identification of a conserved α-helix within this region, which possibly serves as a protein interaction site for the subsequent formation of the active bifunctional PfAdoMetDC/ODC complex.

The isolated A/Owt and A/OpA2a recombinant proteins were subjected to radioactivity assays. Once again, the amount of ~161 kDa bifunctional protein in each of the total protein samples were taken into account during the determination of the specific activities of the proteins (Appendix B, Table 1B) and the percentage contributions of the truncated versions

of the bifunctional proteins were not taken into consideration since monofunctional PfODC has negligible activity (Krause *et al.*, 2000). Figure 3.16 shows the normalised activity of PfAdoMetDC in the mutant recombinant protein. The results show very little residual PfAdoMetDC domain activity of 15% when only the secondary structure within the A2 insert is disrupted compared to the 98% activity loss when the entire insert was removed.

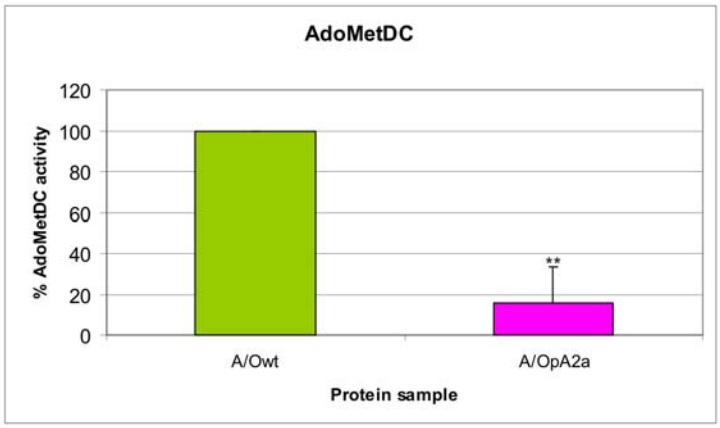

Figure 3.16: AdoMetDC activity assays of the of the wild type PfAdoMetDC/ODC and bifunctional A/OpA2a mutant proteins.
Wild type A/Owt activity is shown in green at 100% while the mutant proteins activity normalised to the A/Owt activity is shown in pink. The values were determined from three independent experiments carried out in duplicate. The standard deviations of the mean are indicated as error bars on each graph. Significant differences at a confidence level of 95% are represented as follows: ** for $p < 0.01$.

Figure 3.17 shows the normalised PfODC activity of the insert A2 helix-disrupted PfAdoMetDC/ODC protein against wild type protein activity. The disruption of only the α-helix in the A2 parasite-specific insert of PfAdoMetDC/ODC resulted in a significant decrease to 45% of wild type PfODC activity within the bifunctional PfAdoMetDC/ODC protein whereas the deletion of the entire A2 insert resulted in a decrease to only 18% of wild type PfODC activity (Figure 3.13).

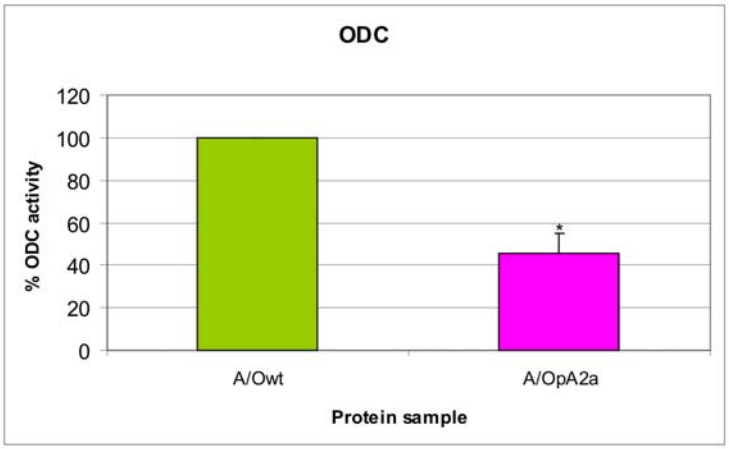

Figure 3.17: ODC activity assays of the wild type PfAdoMetDC/ODC and bifunctional A/OpA2a mutant proteins.

Wild type A/Owt activity is shown in green at 100% while the mutant proteins activity normalised to the A/Owt activity is shown in pink. The values were determined from three independent experiments carried out in duplicate. The standard deviations of the mean are indicated as error bars on each graph. Significant differences at a confidence level of 95% are represented as follows: * for $p < 0.05$.

The increase in PfODC activity observed here, indicates that the Pro hypothesis, which states that the use of a Pro residue in order to disrupt an α-helix could lead to undesired conformational changes within the protein, is not valid here as such a conformationally changed protein would not be active at all. These results thus indicate that the secondary structure within the A2 insert is indeed essential for the correct functioning of the PfAdoMetDC domain and that it also interacts with the adjacent domain via long-range interactions.

From the combined results of this study, Birkholtz *et al*. and Roux it thus seems that PfODC is more vulnerable to changes in the bifunctional protein, i.e. it is more dependent on the hinge and PfAdoMetDC domain for stabilisation and activity, and it is at the same time also the domain where initialisation of heterotetrameric complex formation was thought to take place (Birkholtz *et al.*, 2004; Roux, 2006). The deleterious influences of the insert mutations on the activities of both domains indicate possible allosteric-type effects that the two domains exert on one another for the maintenance of optimum intracellular polyamine levels. The reaction product of the PfODC enzyme does not stimulate the activity of PfAdoMetDC (Wrenger *et al.*, 2001) while PfODC is strongly feedback regulated by its own product putrescine (Krause *et al.*, 2000). PfODC is at the same time also dependent on the presence of the hinge region as well as PfAdoMetDC, which further controls the levels of putrescine and spermidine since the product of PfAdoMetDC is utilised by PfSpdSyn to synthesise spermidine from putrescine and dcAdoMet. Inactive PfAdoMetDC thus creates a bottleneck for subsequent reactions in the polyamine metabolism of *P. falciparum*, which is mediated by the presence of unique parasite-specific inserts. Targeting these inserts in the PfAdoMetDC domain with a specific compound would thus have severe effects on the activity of PfODC leading to a temporary halt in polyamine synthesis until these products are obtained extracellularly.

The analysis of the role of the β-sheet in the A3 insert on the activities of PfAdoMetDC/ODC is being investigated

In conclusion, this chapter discussed studies performed on the secondary structures in the PfAdoMetDC parasite-specific inserts of PfAdoMetDC/ODC to delineate possible interacting areas within the bifunctional heterotetrameric complex. From the results obtained it is clear that these secondary structures, particularly an α-helix in insert A2, are important for the activity of the PfAdoMetDC/ODC protein. The results obtained here are important for the

design and synthesis of possible non-active site based antimalarial drugs targeting these unique areas within the bifunctional PfAdoMetDC/ODC protein. The next chapter will focus on the conserved α-helix in the O1 parasite-specific insert to prove the involvement of secondary structures within the parasite-specific inserts in mediating interdomain protein-protein interactions.

Chapter 4: Investigations of the conserved O1 parasite-specific insert

4.1 Introduction

As mentioned previously, the *P. falciparum* bifunctional AdoMetDC/ODC protein contains six parasite-specific inserts when compared to other homologous proteins. These inserts are species-specific, hydrophilic and non-globular ranging from 21 to 438 bp in length (Müller *et al.*, 2000; Birkholtz *et al.*, 2004; Wells *et al.*, 2006). Some of these inserts mediate physical interactions between the two domains of the bifunctional protein, and are involved in the decarboxylase activities as well as the dimerisation of the PfODC domain (Birkholtz *et al.*, 2004; Roux, 2006). These unique characteristics of this important bifunctional enzyme provide strong support for studies aimed at the evaluation and validation of the enzyme as an antimalarial drug target.

The insert that proved to be the most important for both decarboxylase activities is the 39 amino acid insert O1 in the PfODC domain (Birkholtz *et al.*, 2004). This insert as well as the hinge region linking the two domains has also been shown to be important for hybrid bifunctional complex formation (Birkholtz *et al.*, 2004). Finer demarcations of areas within this insert were subsequently performed to possibly explain the involvement of insert O1 in PfODC dimerisation and thus the formation of the active sites at the dimer interface. The presence of Gly residues on either side of the insert were predicted to provide mobility to the insert, which was confirmed with mutagenesis experiments as well as molecular dynamics studies. The mutation of these mobile Gly residues to Ala residues decreased the activities of both domains and molecular dynamics predicted that activity loss was due to insert immobility (Roux, 2006). S-adenosylmethionine synthetase also has a flexible polypeptide loop that allows the access of substrates into its active site and remains closed during the catalytic steps (Taylor and Markham, 2003). Similarly, molecular dynamics studies have shown the loop of *P. falciparum* SpdSyn to be mobile (Burger *et al.*, 2007). Subsequent crystallisation of PfSpdSyn showed that the substrate dcAdoMet stabilises the conformation of this active site gatekeeper loop (Dufe *et al.*, 2007). The disruption of the conserved α-helix in the same O1 insert of PfAdoMetDC/ODC via an Ile to Pro mutation severely depleted the activities of both domains, which suggests that this structure may be a site involved in protein-protein interactions and dimerisation of the PfODC monomers (Roux, 2006). The involvement of α-helices in protein-protein interactions is discussed in section 3.3.2.

It is thus currently hypothesised that the O1 insert may either serve as a gate-keeping loop that controls the access of substrate into the PfODC active site pocket or its immobilisation abolishes PfODC dimerisation by preventing the α-helix from partaking in protein-protein interactions. Monofunctional PfODC mutants with immobile and α-helix disrupted O1 inserts should thus be analysed for both activity and dimerisation. If it is found that the α-helix is essential in the formation of the active PfODC homodimer, then a specific synthetic interface peptide can be rationally designed that would bind to and thereby interfere with protein dimerisation (Singh *et al.*, 2001).

4.2 Peptides as therapeutic inhibitors of protein-protein interactions

Protein-protein interactions play important roles in most biological processes and therefore represent an important class of drug targets for therapeutic intervention. In this respect interface peptides as inhibitors of protein-protein interactions have greatly contributed towards the development of novel therapeutic agents as these only have to cover the high-affinity binding regions or the so-called “hotspots” (rich in Trp, Arg and Tyr) and not the entire protein binding surface (de Vega *et al.*, 2007). Synthetic peptides have been successfully applied as inhibitors of *P. falciparum* triosephosphate isomerase (PfTIM) (Singh *et al.*, 2001), HIV-1 protease (Babe *et al.*, 1992; Schramm *et al.*, 1996), *Lactobacillus casei* TS (Prasanna *et al.*, 1998) and *T. brucei* farnesyltransferase (Ohkanda *et al.*, 2004).

Even though biologically active peptides have a great potential for therapeutic applications, they often need to be modified to enhance their pharmacological properties, bioavailability, cellular penetration and resistance to enzymatic degradation (Baran *et al.*, 2007). Several disadvantages exist for specifically targeting oligomeric proteins with inhibitory peptides. Firstly, the large size of the protein interface makes several contacts between the subunits and is often non-contiguous, which cannot be mimicked with a simple synthetic peptide. Myers *et al*. showed that the stabilisation of the *T. brucei* ODC dimer is as a result of the sum of multiple, long-range interactions along the dimer interface (Myers *et al.*, 2001), which hinders the search for relatively small molecules that can disrupt oligomeric proteins (Pérez-Montfort *et al.*, 2002). Obtaining selectivity for a given protein is often difficult as many protein-protein interfaces are relatively featureless. Screening chemical libraries for small “drug-like” molecules as effective disruptors of protein-protein interactions is also not extremely helpful, and the natural ligands of the target protein do not provide valuable information during small molecule design as is the case in active site inhibitor development (Yin and Hamilton, 2005). Alternatively, scaffolds are often used that can be easily modified

in different ways by, for instance, varying the substituents present to probe the protein binding interactions for a good ligand fit (Hershberger *et al.*, 2007).

Targeting inhibitors to the active site of an enzyme is limited by the high structural conservation of active sites between the host and, for example, the disease-causing parasite. The greater structural variability of protein-protein interfaces suggests that these interface contact sites may provide important target sites that are sufficiently different between the host and the parasite. In this manner drug selectivity can be achieved. The large PfAdoMetDC/ODC complex possesses several protein-protein interaction regions that are absent in the host monofunctional counterparts and can thus be selectively targeted. Another advantage of targeting areas other than the active site is the reduced resistance pressure that is placed on the organism when a non-active site-based drug is used. Resistance to the drug via the introduction of mutations in the active site, as is seen for DHFR/TS (Yuvaniyama *et al.*, 2003), will develop at a slower rate, which is extremely valuable in drug development against the multi-drug resistant malaria-causing *P. falciparum* parasites (Singh *et al.*, 2001). Several other advantages of using peptides as therapeutic molecules include: 1) high activity and specificity; 2) unique 3-dimensional characteristics; 3) no accumulation in organs due to small size; 4) low toxicity; and 5) low immunogenicity (Sehgal, 2006).

As discussed in Chapter 3, secondary structures within interfaces of oligomeric proteins are often essential for specific binding recognition and protein-protein interactions and it has been concluded that protein interfaces are more closely related to the hydrophilic surfaces of proteins (Sheinerman *et al.*, 2000). Singh *et al*. tested synthetic peptides corresponding to two distinct regions of the subunit interface in the homodimeric *P. falciparum* TIM as possible inhibitors. They found that a 12 residue peptide corresponding to loop 3 of the protein decreased enzymatic activity by 55% at a 1000-fold excess of the peptide, which indicates that this region is possibly involved in the stabilisation of the dimer. These studies showed that interface peptides are useful towards the design of a lead sequence for the inhibition of protein-protein interactions (Singh *et al.*, 2001).

Mutations in the p53 transcription factor are important triggers for tumour development in approximately 50% of the human cancers. Overexpression of the normal p53 induces the expression of various downstream genes that ultimately lead to cell cycle arrest and apoptosis. p53 degradation is mediated through an ubiquitin-dependent proteasomal pathway and various small molecules have been identified that bind to and stabilise p53 against ubiquitin-dependent degradation leading to the death of cancer cells (Foster *et al.*, 1999; Takimoto *et al.*, 2002; Wang *et al.*, 2003). Another strategy for controlling the levels of p53 is by targeting its interaction with the oncoprotein mouse double minute 2 (MDM2).

MDM2 regulates p53 turnover by promoting its ubiquitination and MDM2 overexpression in cancer cells abolishes the ability of p53 to induce cell-cycle arrest (Chen *et al.*, 1996; Haupt *et al.*, 1997). García-Echeverría *et al*. have subsequently reported that a peptide consisting of residues 18 to 23 of p53 represents the minimum-binding epitope for HDM2 (the human analogue of MDM2) recognition and binding. This hexapeptide was shown to block the p53-HDM2 interaction with an IC_{50} in the micromolar range while a larger 13-residue peptide blocked the interaction to an even greater extent (García-Echeverría *et al.*, 2000). These studies provide an important proof-of-principle for the use of peptides in the activation of p53 by targeting its interaction with HDM2 in the treatment of cancer.

GpA forms an extremely stable dimer via specific side-by-side interactions between transmembrane α-helices (Lemmon *et al.*, 1992). As mentioned earlier, even in the presence of a detergent, such as SDS, GpA remains a stable dimeric protein. Bormann *et al*. developed and used a synthetic peptide (GPA-TM) that mimics the transmembrane domain, and which resulted in the separation of the dimeric protein into its monomeric components, and characterisation of the exact segments involved in dimerisation. A simplified model of GpA association with the peptide is shown in Figure 4.1 (Bormann *et al.*, 1989).

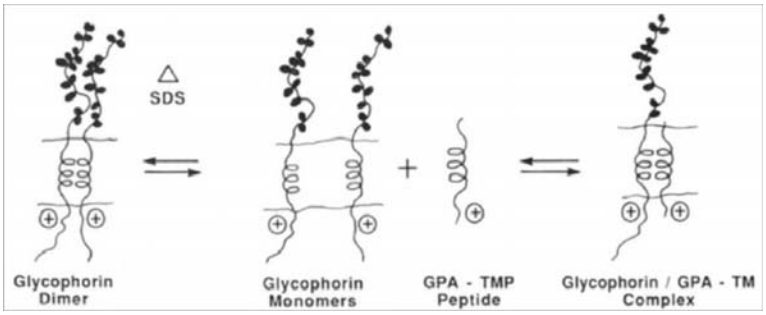

Figure 4.1: A model diagram depicting the association between Glycophorin A's α-helix and a synthetic peptide.
GpA exists in an equilibrium state of monomeric and dimeric forms. Heat and a detergent was used to dissociate the dimeric protein. In the presence of the monomeric GpA protein the GPA-TM synthetic protein, which corresponds to the transmembrane domain of GpA, was able to compete for the monomeric GpA to form a protein: peptide complex (Bormann *et al.*, 1989).

4.2.1 Important criteria for the design of interface peptides

Based on the crystal structure of PfTIM, two loops consisting of mostly polar residues were identified that are involved in extensive intersubunit interactions. The residues that are involved in the subunit interfaces were delineated using an interatomic cut-off distance of 4 Å, which showed that the dimeric interface is composed of three discontinuous peptide segments. Two of these segments consisted of at least five consecutive residues along the polypeptide chain and were thus chosen for inhibitor studies. Peptide I (10 amino acids)

corresponds to loop I of the protein and contains one of the active site residues and a Cys residue that is involved in extensive interactions across the interface with atoms of the other subunit. The region is also highly conserved among all the TIM sequences. Peptide II (12 amino acids) corresponds to loop 3, which protrudes from the core of the monomeric protein and docks into a narrow pocket close to the active site of the other monomer. This region is extensively involved in intersubunit interactions and is also involved in stabilising the dimerisation of the monomeric proteins. The region also contains a Tyr residue that makes several contacts at the subunit interface for the association of the monomeric proteins and forms part of an aromatic cluster, which is frequently associated with the stabilisation of folded protein structures [such as PfODC, (Birkholtz *et al.*, 2003)]. These characteristics of the peptides that were used in the study by Singh *et al*. thus provide important criteria for the design of peptides targeting the interfaces of other multimeric proteins (Singh *et al.*, 2001).

Similarly, the peptides selected for the interface interference of the dimeric TS enzyme from *L. casei*, were chosen based on the number of contacts made between the residues of the two subunits and were approximately 20 residues in length. The peptide that was found to be the most potent in the inhibition of the enzyme contained 11.1% charged, 77.7% polar and 11.1% hydrophobic residues, which indicates that polar interactions involving hydrogen bonds and salt bridge formations are reminiscent of dimer interfaces (Prasanna *et al.*, 1998). The peptide that disrupted the SDS-stable GpA dimer was complementary to the transmembrane domain portion of the protein and was able to compete for a complete molecule of GpA in dimer formation. The 34-residue helical peptide interacted with the corresponding helix of the transmembrane domain of a GpA monomer to form a GpA-peptide complex (Bormann *et al.*, 1989). Subsequent mutagenesis studies on a specific Val residue implicated its involvement in interhelical interactions and the dimerisation of GpA. Substitution of hydrophilic residues (Glu, Gln, Asp, Asn, Arg, Lys and His) at this Val disrupted dimer association while replacement with residues of a smaller size to or similar than Val (Met, Ala and Cys) was only slightly disruptive. However, at this position non-polar residues with larger side chains (Trp and Tyr) or Leu also disrupted dimer formation possibly as a result of steric hindrance, which suggested intimate packing of residues at the dimer helical interface (Lemmon *et al.*, 1992). These experiments thus show the critical involvement of specific residues within protein-protein interactions and the importance of hydrogen bond formations in these types of associations.

The structure of synthetic peptides targeting essential areas in solution should also be taken into account when they are used to bind to and prevent surfaces from forming protein-protein interactions. The correlation between structure and inhibitory potency has been determined. The dimer interface of TS from *L. casei* is mainly formed by the interaction of two six-

stranded β-sheets and only a peptide with considerable structure was shown to have good inhibitory activity (Prasanna *et al.*, 1998).

The presence of unique parasite-specific inserts in the bifunctional PfAdoMetDC/ODC protein allows for the rational design of drugs specifically targeting these non-homologous regions. The involvement of the O1 insert in the dimerisation of the PfODC subunits for the subsequent heterotetrameric complex formation in PfAdoMetDC/ODC (Birkholtz *et al.*, 2004) suggests that the design and application of an interface inhibitory peptide targeting this interacting area, and specifically the α-helix within this insert, might prevent dimer formation resulting in the depletion of catalytic activity of the two rate-limiting enzymes in the essential polyamine biosynthesis pathway of *P. falciparum*.

4.3 Methods

4.3.1 Mutagenesis of areas within the O1 insert of PfODC

4.3.1.1 Cloning of monofunctional *PfODC* into pASK-IBA3

PfODC together with 144 residues of the hinge region was previously cloned into the pASK-IBA7 vector [henceforth called pODCwt, (Institut für Bioanalytik, Germany)] (Krause *et al.*, 2000). This construct, ~5500 bp in size, was used as template for the mutagenesis of the α-helix and the mobile Gly residues within the O1 parasite-specific insert.

4.3.1.2 Site-directed mutagenesis

The primers were designed in a previous study to introduce point mutations in the O1 insert of the bifunctional PfAdoMetDC/ODC (Roux, 2006) and were used in this study to create monofunctional PfODC O1 insert point mutations (Table 4.1). These were designed according to the principles of the QuickChange® Site-directed Mutagenesis (QCM) method (Stratagene). The method involves the design of primers that are complementary to each other and anneal to the same sequence on opposite strands of the plasmid.

The O1aF and R primers were used for the Ile408Pro mutation in the α-helix of insert O1 (ODCpO1a). The introduction of the Pro residue disrupts the secondary structure by creating an unsatisfied main chain hydrogen bond acceptor, which allows the assessment of this structure's possible role in protein-protein interactions. This point mutation, however, may introduce an overall conformational change of the region and should be taken into consideration during analysis of the role that the helix plays in protein structure formation.

Table 4.1: The mutagenic primers for the introduction of specific mutations in the O1 insert of the monofunctional *PfODC* gene (Roux, 2006)

Primer	Length (nt)	Tm* (°C)	Primer Sequence (5' to 3')	Alteration
O1aF	56	67	gtcttcaagaaattaaaaaagatccac aaaaatttcttaatgaagaaacatttctc	Ile408Pro helix breaker
O1aR		67	gagaaatgtttcttcattaagaaattt ttgtggatctttttaatttcttgaagac	
G1F	52	69	ggatttaatttttatataataaatttag cagcagcatatccaggaggattag	Gly376-378Ala immobility mutation
G1R		69	ctaatcctcctggatatgctgctgct aaatttattatataaaaattaaatcc	
G2F	51	68	catttctcaagacgaaatatgcata ctatagttttgaaaaaataacattgg	Gly423Ala immobility mutation
G2R		68	ccaatgttatttttttcaaaactata gtatgcatatttcgtcttgagaaatg	

* The Tm's were calculated according to the Rychlik *et al*. formula:
69.3 + 0.41(%GC) – (650/N) where N is the number of nucleotides (Rychlik *et al.*, 1990). The positions of the point mutations in the primers are underlined.

The immobilisation of the insert was performed in two sequential steps: the G1F and R primers were firstly used to introduce the Gly376-378 to Ala376-378 mutation (ODCpG1), which was subsequently used as the new template for the Gly423Ala mutation with the G2F and R primers (ODCpG2). These mutations cause the insert to become rigid and immobile so that the role of the mobile insert as a possible active site gatekeeper can be investigated.

The PCR mutagenesis reaction for the ODCpO1a mutation was set up as follows: a 50 µl reaction contained 10 fmol template (of the ~5500 bp pODCwt construct), 10 pmol of each primer, 200 µM of each dNTP, 1 x *Pfu* reaction buffer and 2.5 U *Pfu* (Fermentas, Canada). The temperature cycles were performed in a GeneAmp 9700 thermocycler (PE Applied Biosystems, USA) as follows: an initial denaturation step for 3 min at 94°C, followed by 30 cycles of 94°C for 30 sec, 60°C for 1 min and an extension step at 62°C for 2 min/kb. The PCR conditions for the ODCpG1 and ODCpG2 mutagenesis reactions were identical except for the lower annealing temperature of 48°C that was used for both reactions.

4.3.1.3 Post-PCR analysis

The sizes of the PCR products were visualised with agarose gel electrophoresis as described in section 2.2.1.7. The construct containing the ODC-Hinge insert cloned into the pASK-IBA7 vector (pODCwt) has a size of approximately 5500 bp (vector size ~3200 bp, gene size ~2300 bp) and the PCR products should give identically sized bands.

The wild type, parental templates were subsequently removed with 10 U of *Dpn*I (Fermentas, USA) at 37°C for 3 hrs. The NucleoSpin® Extract II PCR cleanup kit (Macherey-Nagel,

Germany) was used to clean the digested samples before the linear DNA was linearised overnight with 3 U of T4 DNA Ligase (Promega, USA) at 22° (blunt-end ligation). The circular plasmids were now ready for their incorporation into competent cells.

The newly created circular plasmids and a wild type control (pODCwt) were electroporated into DH5α cells. The preparation of the cells as well as the electroporation protocol is discussed in section 2.2.1.8.

4.3.1.4 Plasmid isolation and restriction enzyme screening

Five colonies from each transformation reaction were inoculated overnight in 5 ml LB-amp medium (LB-medium with 50 µg/ml ampicillin) and allowed to grow at 37°C with moderate agitation. The plasmids (pODCpO1a, pODCpG1 and pODCpG2) were isolated from each overnight culture with the peqGOLD Plasmid Miniprep Kit I (Biotechnologie, Germany).

The isolated, possibly mutant, plasmids were subsequently digested with 10 U of *Hind*III (Promega, USA) at 37°C for 3 hrs followed by visualisation on agarose gels (section 2.2.1.7). In addition, the pODCpG1 plasmids were digested with 10 U of *Eco*RV (Promega, USA) as the successful incorporation of this point mutation results in the removal of an *Eco*RV recognition site and can thus be used to give an indication of the mutagenesis efficiency.

4.3.1.5 Nucleotide sequencing

The plasmids were analysed with automated nucleotide sequencing to verify the incorporation of the specific mutations. The sequencing primer ODCseq1 (5'-tatggagctaatgaatatgaatg-3') was used as it anneals 172 bp upstream from the start of the O1 insert. The nucleotide sequencing and DNA ethanol precipitation protocols are described in section 2.2.1.11.

4.3.1.6 Protein expression and isolation

The expressed wild type (ODCwt) and newly created mutant ODCpO1a and ODCpG2 monofunctional proteins were isolated as described in section 3.4.3 with the exception that the proteins were expressed at 37°C for 3 hrs before being harvested for subsequent *Strep*-tag affinity purification (Krause *et al.*, 2000). The bifunctional A/Owt and previously mutated A/O full-length O1 insert proteins (A/OpO1a and A/OpG2) were also isolated as previously (Roux, 2006).

4.3.2 Size-exclusion FPLC for the determination of protein sizes

Superdex 200 prep grade preparative gel filtration media (Amersham Biosciences, UK) was used as matrix for size-exclusion chromatography (SEC) which combines the gel filtration properties of dextran with the chemical and physical stability of cross-linked agarose resulting in a matrix that is capable of separating proteins in the range of 10 to 600 kDa.

The medium was resuspended with gentle swirling and poured into a 500 ml glass beaker, washed twice with $dddH_2O$, and allowed to settle to a volume of approximately 475 ml. Tween-20 (Merck, Germany) was added to reduce the surface tension and to create an even slurry. The slurry was carefully and continuously added to a C16/70 column (Amersham Biosciences), at a constant flow rate, down the sides of the column with the help of a sterile glass pipette. The slurry was allowed to settle and was continuously filled until the settled media reached ±10 cm from the top of the column. The AC 16 adaptor (Amersham Biosciences) was finally positioned at the top opening of the column and was inserted until it was directly above the settled media. The adaptor was then connected to the Äkta *prime* FPLC system (Amersham Biosciences). The system pump was used to compress the media with $dddH_2O$ at a flow rate of 1 ml/min and any changes in the height of the resin were noted.

4.3.2.1 Calibration of column with protein standards

The void volume of the packed media in the column was determined with the application of Dextran Blue, which, with a size of 2 000 kDa, is excluded from the media and simply passes through the column without entering the pores of the micro beads. A volume of 2 ml equilibration buffer (50 mM Tris-HCl, pH 7.5, 100 mM KCl) containing Dextran Blue (Sigma-Aldrich, UK) at a final concentration of 2 mg/ml was injected into the column previously equilibrated with the same buffer. Fractions of 1.5 ml each were collected at a flow rate of 0.5 ml/min for approximately one bed volume (~130 ml). Absorbencies at 280 nm were measured for all the fractions to identify the volume at which Dextran Blue elutes, which should give a peak at A280 of ~1 at this concentration and wavelength.

Once the void volume was determined, the column could be calibrated with protein standards with known MWs. The sizes of unknown proteins can subsequently be obtained from a standard curve drawn from the different elution volumes (Ve) and the logMW of the standard proteins.

The protein standards supplied in the Gel Filtration Molecular Weight Markers kit (Sigma-Aldrich) was used to generate a standard curve. The kit consists of the following proteins: carbonic anhydrase, albumin, alcohol dehydrogenase, β-amylase, apoferritin and thyroglobulin (Table 4.2). A volume of 2 ml protein mixture (with final concentrations shown in

Table 4.2) in equilibration buffer was loaded onto the column and fractions were collected at a flow rate of 0.5 ml/min.

Table 4.2: Protein standards for the calibration of the size-exclusion chromatography column

Protein standard	MW (Da)	Final concentration (mg/ml) in 2 ml mixture
Carbonic anhydrase	29 000	1.5
Albumin	66 000	5
Alcohol dehydrogenase	150 000	2.5
β-Amylase	200 000	2
Apoferritin	443 000	5
Thyroglobulin	669 000	4

Fractions of 1.5 ml each were collected and absorbencies were measured at 280 nm. A standard curve of logMW against Ve/Vo was plotted.

4.3.2.2 Separation of proteins by size-exclusion FPLC

The ability of the wild type and mutant O1 insert proteins to form either monofunctional PfODC dimeric (~170 kDa: a dimer consisting of two ~70 kDa monomeric polypeptides and 144 residues of the hinge region) or bifunctional PfAdoMetDC/ODC heterotetrameric (~330 kDa: a tetramer consisting of two ~150 kDa PfAdoMetDC/ODC subunits and two 9 kDa β-subunits of PfAdoMetDC) proteins via protein-protein interactions were determined by SEC. Separately expressed and purified bifunctional PfAdoMetDC/ODC (A/Owt, A/OpO1a, A/OpG2) and monofunctional PfODC (ODCwt, ODCpO1a, ODCpG2) proteins (~120 µg) were applied to the SEC column previously equilibrated with Wash Buffer (150 mM NaCl, 1mM EDTA, 100 mM Tris, pH 8) at a flow speed of 0.5 ml/min and collected in fractions of 1.5 ml each. The absorbency of each fraction was determined at 230 nm as this wavelength is very sensitive to the presence of peptide bonds within proteins. A wavelength of 280 nm (measurement of aromatic residues) was not used as before due to the decreased amount of recombinantly isolated proteins that elute per fraction compared to that of the standard proteins.

4.3.2.3 Western immunodetection of collected protein fractions

The oligomeric states of the eluted bifunctional PfAdoMetDC/ODC and monofunctional PfODC proteins were validated with dot blot Western immunodetection. Briefly, the fractions collected with FPLC were dot-blotted onto Immobilon-P PVDF transfer membranes (Millipore, USA) using a BioDot apparatus (BioRad, USA). The membranes were subsequently blocked overnight with blocking buffer [Phosphate buffered saline (PBS) containing 3% w/v BSA and 0.5% v/v Tween-20] at 4°C. For immunodetection of the *Strep*-tag II peptide, the membranes were incubated for 1 hr at 37°C in PBS containing 1% w/v BSA, 0.5% Tween-20 and 1/4000

or 1/2000 monoclonal *Strep*-tag II mouse antiserum (Acris antibodies, Germany) for the PfAdoMetDC/ODC and PfODC proteins, respectively. The antibody is coupled to keyhole limpet haemocyanin and is supplied as a liquid Protein G purified immunoglobin fraction, conjugated to horseradish peroxidase. The membranes were washed six times and incubated for 5 min in equal volumes of the Luminal/Enhancer and Stable Peroxidase solutions [SuperSignal® West Pico Chemiluminescent Substrate, (Pierce, USA)]. The horseradish peroxidase enzyme produces a hydroxide ion that results in the transition of luminol to 3'-aminophthalate with the concurrent emission of light. Hyperfilm High Performance chemiluminescence films (Amersham Biosciences, UK) were exposed for several minutes to the membranes and subsequently developed (3 min) and fixed (1 min) with ILFORD Universal Paper Developer and Rapid Fixer, respectively (ILFORD Imaging UK limited, UK).

4.3.3 Synthetic peptides targeting protein-protein interactions in the O1 insert

The importance of the O1 insert and secondary structures within it allows for opportunities aimed at targeting this site with specific peptides as a means to inhibit PfODC activity and/or dimerisation. In the absence of a crystal structure that would indicate precise residue contact points, specific peptides were designed to target either the entire 39 amino acid insert or only the α-helix. The peptides were also analysed to reveal their polarity, the presence of residues often involved in aromatic clusters and protein binding hotspots as well as their propensities to form hydrogen bonds.

4.3.3.1 Isolation of wild type PfAdoMetDC/ODC protein

The wild type PfAdoMetDC/ODC protein was isolated as described in section 3.4.3, SDS-PAGE analysis was also performed to ensure that the protein with the correct size was isolated (section 3.4.3.6).

4.3.3.2 Protein:peptide incubation

The peptides were dissolved in dddH_2O and stored at -70°C until further use. These stock solutions were prepared in 10x, 100x and 1000x molar excess peptide stocks to the 5 µg of the wild type bifunctional PfAdoMetDC/ODC protein (156 090 g/mol), which was used throughout the inhibitor studies. The wild type protein was pre-incubated with each of the three peptides at the three different molar excess quantities at 37°C for 1 hr. Results, however, showed that incubation at this temperature effected the positive control (wild type protein) activity and it was thus decided to perform the incubation steps for 30 min and 2 hrs, both at 22°C with gentle agitation.

4.3.3.3 Activity determination of the protein:peptide samples

The protein:peptide samples were subsequently subjected to large-scale AdoMetDC and ODC radioactivity assays mostly as described in section 3.4.3.8 but only 12.5 nCi of each radioactive substrate was used while a total of 100 µM substrate was maintained throughout. The activity of the wild type PfAdoMetDC/ODC protein (treated the same as the samples) was used as positive control and gave an indication of the extent to which the peptides affected the function of the bifunctional protein through their possible interference at the dimer interface of the PfODC domain.

The activities of the samples were normalised to the positive control's activity from three different experiments performed in duplicate and expressed as a percentage of the wild type activity.

4.3.3.4 Statistical analysis

The significance of the results was calculated with a directional one-tailed t-Test assuming unequal variances. Results with p values smaller than 0.05 meant that there was a significant difference between the untreated and the treated samples.

4.4 Results and Discussion

4.4.1 Creation of monofunctional PfODC insert O1 mutations

Figure 4.2 shows the location of the Gly point mutation sites and the α-helix breaker within the O1 parasite-specific insert. The mobile Gly residues are situated at the edges of the insert while the helix is situated more or less at the centre. The three Gly residues on the N-terminal side of the insert and the helix are conserved between *Plasmodia* species (Birkholtz *et al.*, 2004; Roux, 2006).

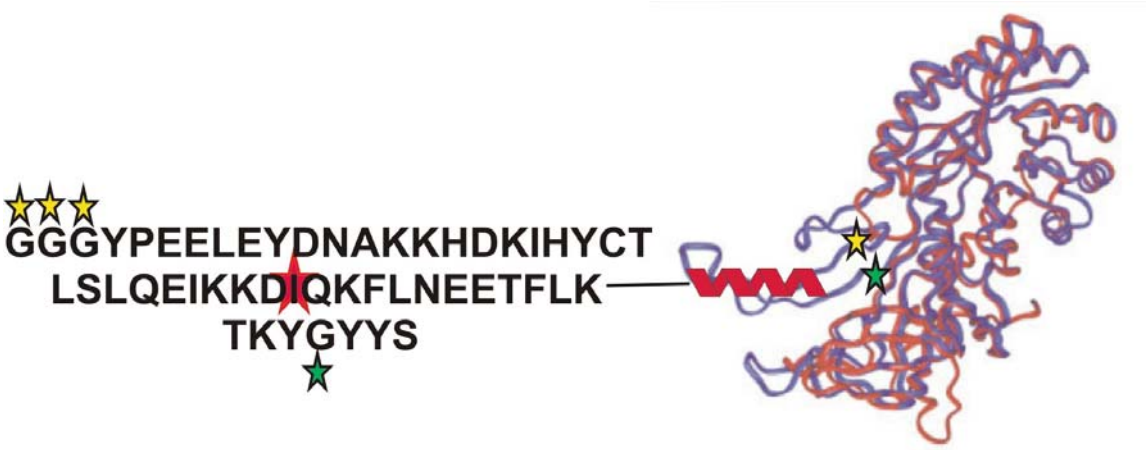

Figure 4.2: The sites of the mobile Gly residues and the α-helix in the O1 parasite-specific insert.
The yellow stars on the PfODC monomer homology model indicate the three conserved Gly residues that were mutated to Ala residues and termed ODCpG1. The green star indicates the single Gly to Ala residue point mutation at the C-terminal end of the O1 insert to produce the double mutant termed ODCpG2. The red star indicates the position of the Ile408Pro helix breaker. The α-helix is also shown in red on the PfODC model. The two superimposed models on the right are the human (red, without O1 insert) and the *P. falciparum* (blue, with the O1 insert) ODC monomers. Homology model obtained from (Birkholtz *et al.*, 2004).

The mutagenesis primers are listed in Table 4.1 (Birkholtz *et al.*, 2004; Roux, 2006). All the primers are approximately 50 nt in length and terminate in a G or a C residue. The O1a primers were designed to disrupt the conserved α-helix in the O1 parasite-specific insert by mutating a strong helix former Ile residue to a weak Pro one. The G1 and G2 primers are specific for the immobilisation of the same insert by introducing Gly to Ala point mutations on either side of the insert.

The sizes of the mutagenesis PCR products were visualised with agarose gel electrophoresis. All the products were ~5500 bp in size (Figure 4.3 B, C and D), which corresponds to the size of the wild type plasmid (Figure 4.3 A). The ODCpG1 product was used as template for the introduction of the ODCpG2 mutation (Figure 4.3 C).

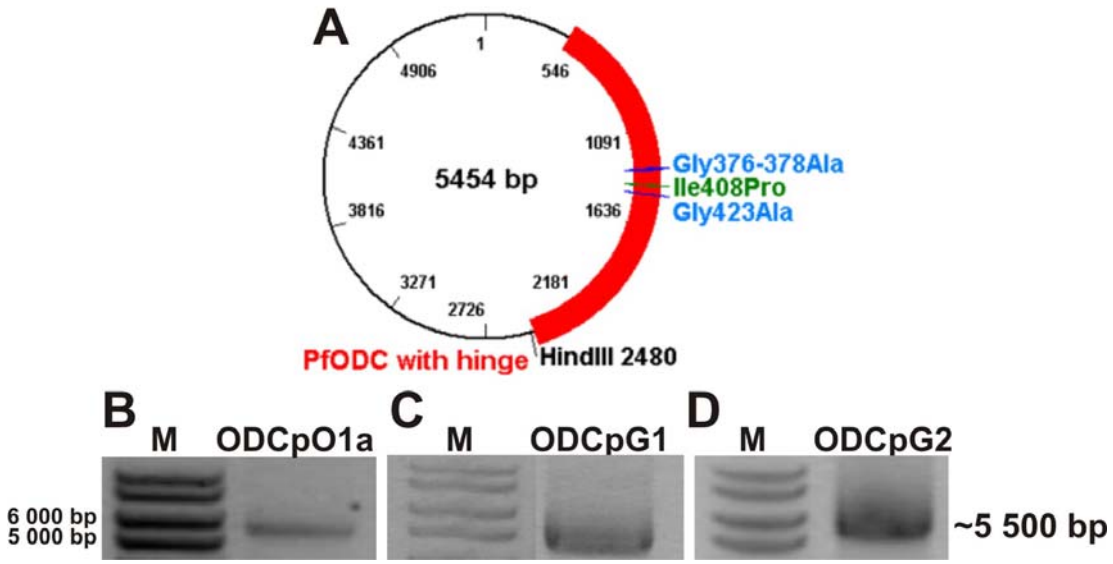

Figure 4.3: Agarose electrophoresis gels of the monofunctional PfODC O1 insert PCR mutagenesis products.
(A) Schematic diagram of the wild type vector (ODCwt, vector size ~3200 bp, gene size ~2300 bp) showing the positions of the Gly376-378Ala, Ile408Pro and Gly323Ala mutations within the O1 insert as well as the single *Hind*III restriction enzyme site. 1% Agarose gels were used to visualise the ~5500 bp ODCpO1a (B), ODCpG1 (C) and ODCpG2 (D) PCR products. (M) 1 kb DNA ladder.

The linear PCR products were ligated and electroporated into competent DH5α cells. Plasmids for each of the three different mutations were isolated from five separate colonies and checked for viability and size with *Hind*III restriction mapping and for mutagenesis efficiency via sequencing with the ODCseq1 primer. The wild type plasmid (pODCwt) was also digested with the same enzyme as a comparative control. *Hind*III cuts the plasmid at a single position creating a linear plasmid of ~5500 bp upon digestion (Figure 4.3 A). All five isolated pODCpO1a plasmids gave the correct sized DNA band after restriction enzyme digestion as compared to that of the ODCwt plasmid (Figure 4.4).

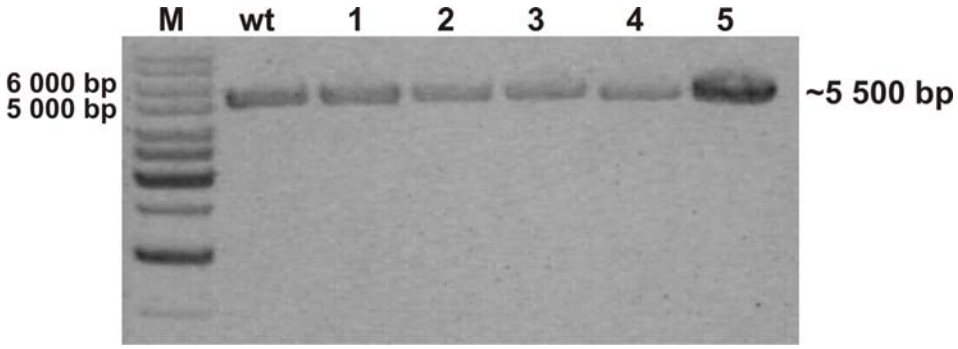

Figure 4.4: Agarose gel electrophoresis of the ODCpO1a *Hind*III digested plasmids.
A 1% agarose gel shows the linear plasmids (~5500 bp) for the five isolated plasmids (lanes 1 to 5) and the comparison of these to the band obtained when the wild type plasmid was treated with the same endonuclease (lane wt). (M) 1 kb DNA ladder.

The removal of an *Eco*RV digestion site as a result of the successful incorporation of the ODCpG1 point mutation was used to preliminary screen the plasmids. *Eco*RV cuts the wild type plasmid at three positions resulting in three DNA bands sized ~3300, ~1100 and ~1000 bp (Figure 4.5 A). The ODCpG1 mutation, on the other hand, results in only two digestion products sized ~3300 and ~2100 bp (Figure 4.5 B).

From the restriction enzyme screening results of the pODCpG1 plasmids it can be seen that three mutant plasmids were possibly created, namely plasmids 2, 3 and 4. The digestion of these plasmids resulted in two bands corresponding to the sizes given by the restriction enzyme map (Figure 4.5 B and C, lanes 2, 3 and 4). The restriction profile of plasmid 5 is identical to that of the wild type plasmid suggesting that the parental wild type template was not removed during the *Dpn*I digestion step (Figure 4.5 A and C, lanes wt and 5). Plasmid 1 gave unknown results.

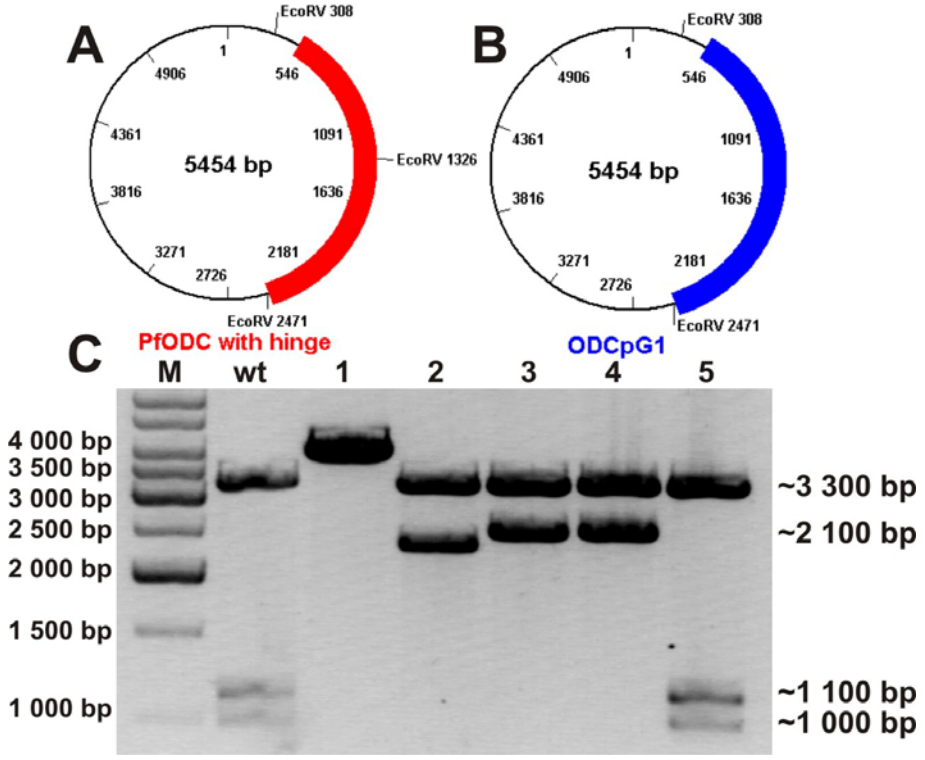

Figure 4.5: *Eco*RV restriction enzyme screening of the ODCpG1 plasmids.
In the top panel the positions of the *Eco*RV recognition sites on the wild type (A) and ODCpG1 mutant (B) constructs are indicated. In (C) the 1% agarose gel shows the different DNA bands obtained after restriction enzyme digestion. The digestion of the wild type plasmid results in three bands of ~3300, ~1100 and ~1000 bp (C, lanes wt and 5) while the ODCpG1 mutant plasmid only creates two bands sized ~3300 and ~2100 bp (C, lanes 2, 3 and 4). (M) 1 kb DNA ladder.

And finally, five pODCpG2 plasmids were once again isolated and digested with *Hind*III to check their sizes after they were ligated and transformed into competent *E. coli* cells. Digestion of the pODCwt plasmid results in its linearisation (Figure 4.3 A) and was used as a control to test the *Hind*III digestion profiles obtained from the five different isolated pODCpG2 plasmids (Figure 4.6).

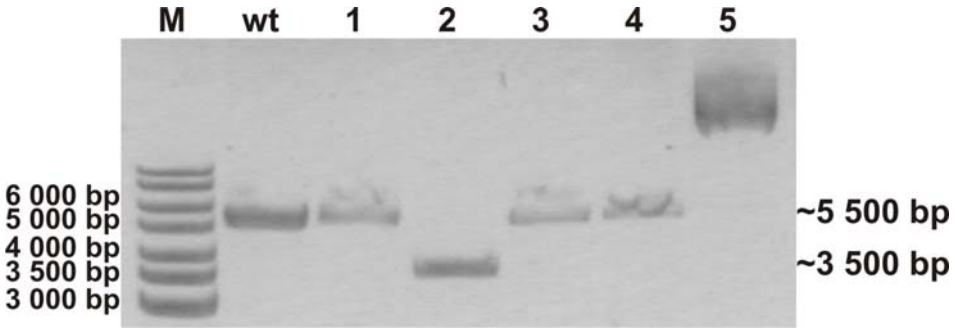

Figure 4.6: Agarose gel electrophoresis of the ODCpG2 *Hind*III digested plasmids.
The 1% agarose gel of the digested DNA from the five isolated plasmids (lanes 1 to 5) and the comparison of these to the band obtained when the wild type plasmid (size of ~5500 bp) was treated with the same endonuclease (lane wt). (M) 1 kb DNA ladder.

Digestion of plasmids 1, 3 and 4 gave the correct sized, linear DNA bands as compared with the wild type digestion product (Figure 4.6 lanes wt, 1, 3 and 4) and were subsequently sequenced. Plasmids 2 and 5 gave incorrect digestion products and were not analysed further.

Isolated plasmids from all three of the transformed reactions were subsequently sequenced to confirm the presence of the three different mutations. All five of the pODCpO1a plasmids were sequenced and all were found to be positively mutated containing the GGT to CCA point mutation (Figure 4.7 ODCpO1a). ODCpG1 plasmids 2, 3 and 4 were also sequenced to corroborate the restriction enzyme screening results in Figure 4.5. The sequencing results showed that only plasmid 2 was positively mutated and contained the CGTCGTCGT to GCAGCAGCA point mutations (Figure 4.7 ODCpG1). ODCpG1 plasmids 3 and 4 were possibly formed as a result of mispriming during the mutagenesis PCR reaction resulting in PCR products of different sizes. Sequencing results also confirmed that only plasmid 1 of the pODCpG2 plasmids contained the correct CGT to GCA point mutation (Figure 4.7 ODCpG2).

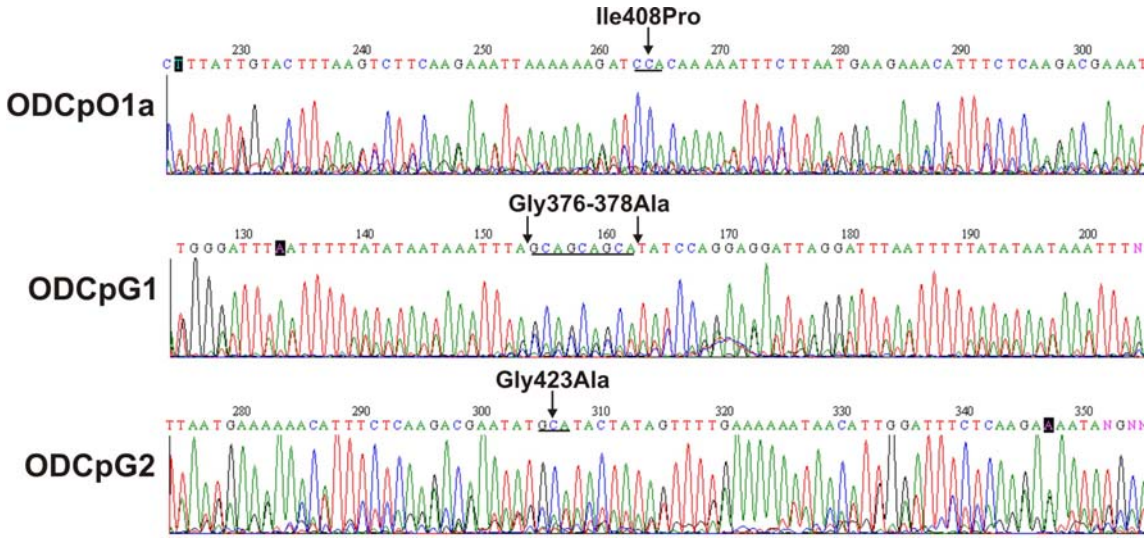

Figure 4.7: Nucleotide sequencing chromatograms of all three the monofunctional PfODC O1 insert mutations.
The black bars indicate the positions of the Ile408Pro (ODCpO1a), Gly376-378Ala (ODCpG1) and Gly423Ala (ODCpG2) point mutations.

The mutagenesis efficiencies of the ODCpG1 and ODCpG2 point mutations (20%) were significantly lower than that of the ODCpO1a mutation (100%) and could possibly be due to the different primers used for each reaction. All the monofunctional O1 insert mutations were, however, successfully created and could be used for further studies aimed at elucidating whether the specific structures within the O1 parasite-specific insert are involved in protein-protein interactions and the dimerisation of PfODC.

The mutant proteins were subsequently expressed and isolated with *Strep*-tag affinity chromatography. As expected, activity assays of these newly constructed mutant proteins normalised to the wild type PfAdoMetDC/ODC specific activity showed almost no activity (~0.021 nmol/min/mg).

4.4.2 Size-exclusion FPLC

4.4.2.1 Calibration of column with protein standards

Size-exclusion FPLC was performed on the *Strep*-tagged purified wild type and mutated monofunctional and bifunctional proteins to determine the ability of the various proteins to form dimers. The wild type heterotetrameric bifunctional PfAdoMetDC/ODC protein is ~330 kDa in size while an inability of the bifunctional protein to dimerise will result in a heterodimeric bifunctional protein of only ~160 kDa. The monofunctional PfODC dimeric protein together with half of the hinge will result in an eluted protein in a fraction corresponding to a size of ~170 kDa while its monomeric form will elute as an approximately ~85 kDa sized protein (Figure 4.8).

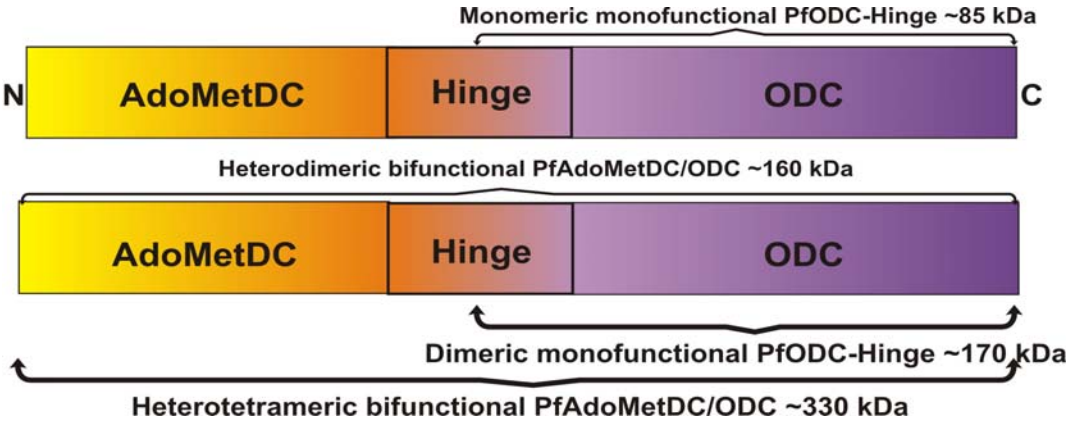

Figure 4.8: A schematic diagram showing the sizes of the bifunctional as well as the monofunctional multimeric proteins.
The sizes of the monomeric PfODC and heterodimeric PfAdoMetDC/ODC proteins are shown above the coloured domains while the dimeric PfODC and heterotetrameric PfAdoMetDC/ODC ones are indicated below the domains in bold.

During the determination of the void volume, Dextran Blue eluted as an almost symmetrical peak in fraction 33, which corresponds to a volume of 49.5 ml. This elution volume thus represents the void volume (Vo) of the SEC column, as this sugar complex is too large (>2000 kDa) to flow through the pores of the matrix (Figure 4.9).

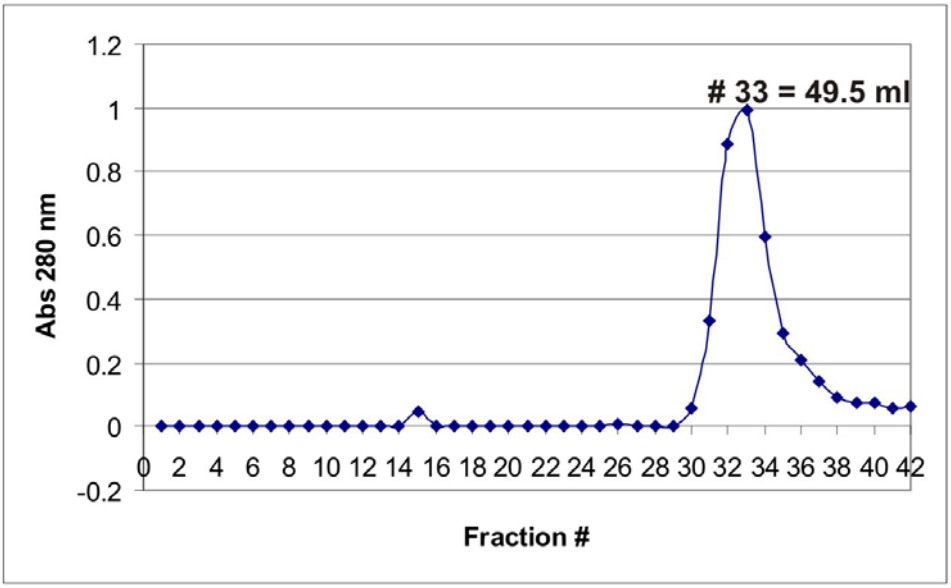

Figure 4.9: SEC elution profile of Dextran Blue for the determination of the void volume of the size-exclusion column.
Dextran eluted in fraction 33, which is indicated on the graph and corresponds to a void volume of 49.5 ml (Vo).

The column was subsequently calibrated with six protein standards with known molecular weight sizes (Table 4.2). The elution volumes of these standards were used to set up a calibration curve from which an unknown protein's size can be determined. The

chromatogram in Figure 4.10 below shows the absorbency peaks obtained when all six the protein standards were eluted together with the calibration curve corresponding to the elution volumes of the protein standards.

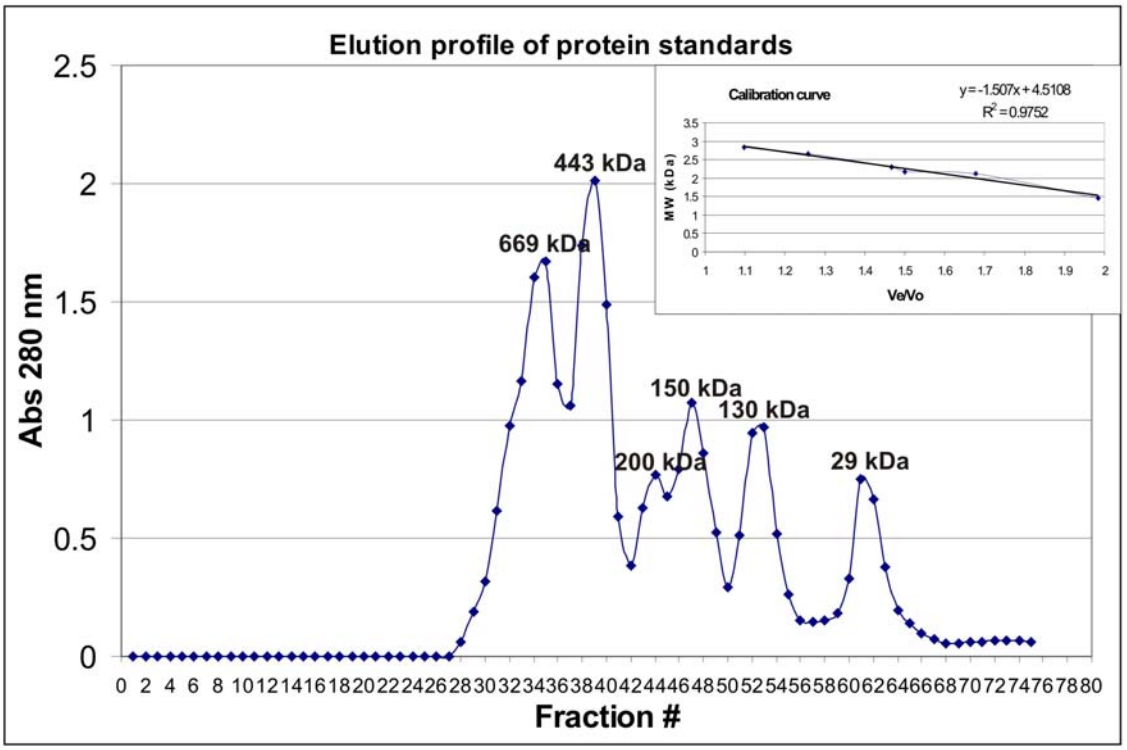

Figure 4.10: Elution profile of protein standards by size-exclusion FPLC.
The peaks are shown from left to right and correspond to the following protein standards: thyroglobulin (669 kDa), apoferritin (443 kDa), β-amylase (200 kDa), alcohol dehydrogenase (150 kDa), dimeric albumin (130 kDa) and carbonic anhydrase (29 kDa). The inserted calibration curve shows the linear regression equation and the R^2 value of the trend line.

Based on the results obtained in the elution profile above, four proteins were selected and once again loaded onto the column to observe whether individual, symmetrical peaks could be obtained. This would give an indication of the capability of the gel media to separate proteins into individual fractions. The following proteins were selected and loaded as above: thyroglobulin, alcohol dehydrogenase, albumin and carbonic anhydrase (Figure 4.11).

The correlation coefficient (R^2) obtained from the standard curve below is reliable since it has a confidence level of ~98% which means that there exists a strong negative linear association between the x and y values, therefore, the earlier the protein elutes from the column, the larger its size. The sizes of sample proteins could thus be determined with the use of the calibration curve that has been set up. Based on the elution volumes of the sample proteins, their sizes could be read from the graph and these should correspond to the location of the Western blot-detected protein dots on the membrane (results to follow).

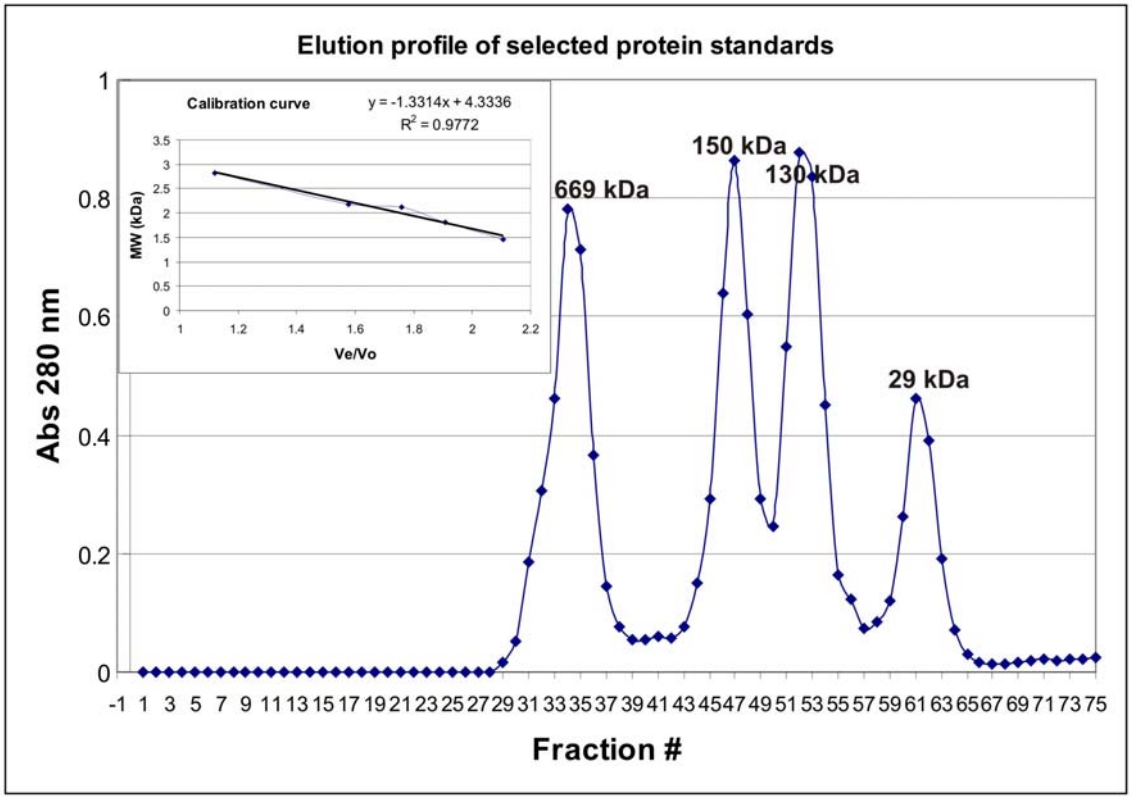

Figure 4.11: Elution profile of four selected protein standards by size-exclusion FPLC.
The peaks from left to right: thyroglobulin (669 kDa), alcohol dehydrogenase (150 kDa), dimeric albumin (130 kDa) and carbonic anhydrase (29 kDa). The inserted calibration curve gives the linear regression equation and the correlation coefficient (R^2) obtained from the trend line.

4.4.2.2 Separation of the isolated recombinant proteins by SEC

The bifunctional wild type A/Owt, helix-disrupted A/OpO1a and immobile A/OpG2 constructs were recombinantly expressed and isolated with *Strep*-tag affinity chromatography and subsequently analysed with SEC. Fractions of 1.5 ml each were collected. The fractions where the proteins were expected to elute were determined with the linear regression equation obtained from the calibration curve in Figure 4.11. These experiments were also repeated with the monofunctional PfODC proteins.

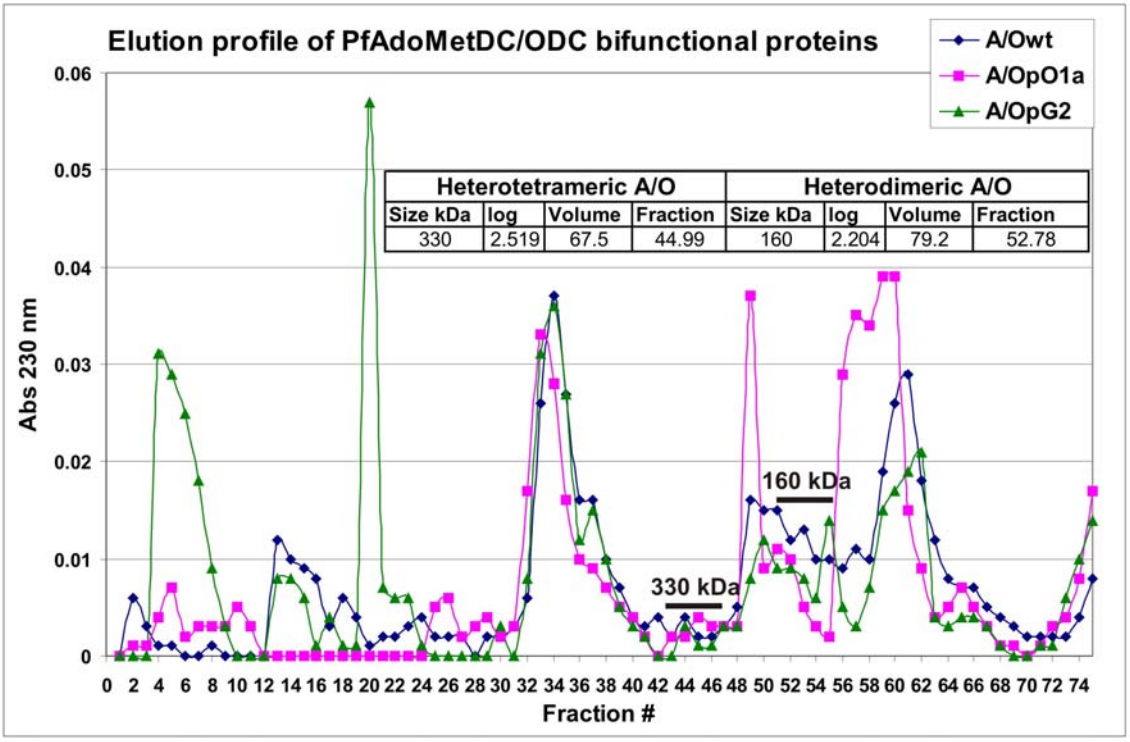

Figure 4.12: Elution profile of the bifunctional PfAdoMetDC/ODC proteins separated with size-exclusion FPLC.
The chromatograms of the different proteins at 230 nm are given. The expected fractions for elution of the heterotetrameric bifunctional PfAdoMetDC/ODC protein (~330 kDa) and the heterodimeric protein of ~160 kDa were calculated as shown in the inserted table and indicated on the graph as black bars.

The bifunctional PfAdoMetDC/ODC protein should exist in two oligomeric forms: the heterotetrameric ~330 kDa protein and the heterodimeric protein sized ~160 kDa (Müller *et al.*, 2000). The wild type protein (Figure 4.12, blue) eluted at the fractions corresponding to both these forms i.e. fractions ~45 and ~53 for the tetrameric and dimeric proteins, respectively. Similar results could be seen for the helix-disrupted (pink) and immobile (green) proteins. In addition, contaminating proteins were eluted in basically every fraction resulting in unwanted peaks corresponding to proteins of all sizes. The sizes of these proteins corresponding to all the protein peaks that were detected at 230 nm are listed in Table 4.3. In a previous study, size-exclusion HPLC as well as native-PAGE of recombinant PfAdoMetDC/ODC purified with *Strep*-tag affinity chromatography showed the presence of large protein complexes of ~600 and ~400 kDa. It was concluded that the contaminating proteins (~112, ~70 and ~60 kDa, as discussed in section 3.5.3.1) could associate with the full-length protein resulting in the formation of these large complexes (Niemand, 2007). In this study, the ~600, ~400, ~112, ~70 and ~60 kDa proteins would elute in fractions corresponding to 39, 43, 57, 62 and 63, respectively. As can be seen from Figure 4.12 and Table 4.3 all these proteins were detected, which is in good agreement with previous studies (protein complexes ~600 and ~400 kDa are absent in A/OpO1a). Other protein peaks could

be due to the presence of various contaminating proteins detected at the very sensitive protein wavelength of 230 nm.

Table 4.3: Calculated MW of the peaks detected with SEC for the bifunctional proteins

A/Owt		A/OpO1a		A/OpG2	
Fraction	**kDa**	**Fraction**	**kDa**	**Fraction**	**kDa**
13	6443	10	8514	4	14867
34	916	26	1926	13	6443
37	**693**	33	1005	20	3363
42	**436**	41	478	34	916
49	227	45	330	**37**	**693**
51	189	49	227	**44**	**362**
53	157	51	189	48	249
56	**119**	**57**	**108**	51	189
61	**75**	**59**	**90**	**55**	**130**
65	**51**	**65**	**51**	**62**	**68**

Fractions corresponding to the approximate proteins sizes that were expected are highlighted in grey. These include the following complexes and contaminating proteins with sizes: ~600, ~400, ~112, ~70 and ~60 kDa.

These results also corroborate the contaminating proteins observed with SDS-PAGE results in section 3.5.3.1 when A/Owt was isolated. The oligomeric states of the recombinant proteins could thus not be successfully determined based only on their elution profiles as only a small percentage of the protein peaks in the desired region would be attributable to the respective recombinant protein. Another method to validate the presence of the functional, multimeric proteins in the required fractions would be to perform activity assay analysis on the protein fractions (Birkholtz *et al.*, 2004). If activity is detected it would mean that the bifunctional protein is present and protein-protein interactions were not disrupted with the incorporation of the insert O1 mutations. However, the protein concentrations were determined with a Bradford assay, which showed the presence of less than 4 µg/ml eluted protein in fraction 45 of each protein sample (results not shown).. Activity assays were therefore not performed as a result of the low protein yields obtained after SEC.

Following the FPLC results with the bifunctional proteins, the monofunctional PfODC template was also used to introduce the same mutations. These expressed proteins (ODCwt, ODCpO1a and ODCpG2) were once again analysed with SEC to see whether the mutated delineated areas within the O1 parasite-specific insert disrupt PfODC dimerisation resulting in only the monomeric protein of ~85 kDa. It must be noted that the wild type ODC protein is capable of rapidly exchanging its subunits to form either the dimeric complex of ~170 kDa or a monomeric complex of ~85 kDa (Coleman *et al.*, 1994; Osterman *et al.*, 1994).

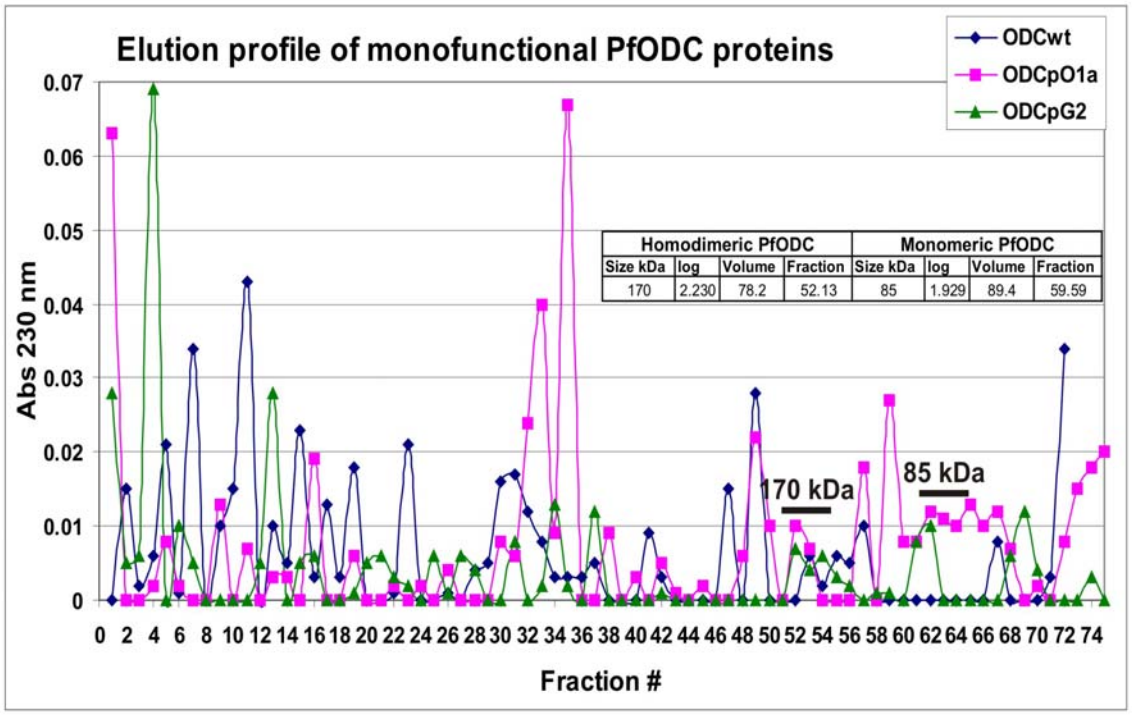

Figure 4.13: Elution profile of monofunctional proteins separated with size-exclusion FPLC. The chromatograms of the different proteins at 230 nm are given. The expected fractions for elution of the dimeric monofunctional PfODC protein (~170 kDa) and the monomeric protein of ~85 kDa were calculated as shown in the inserted table and indicated on the graph as black bars.

The wild type monofunctional protein (Figure 4.13 blue) eluted, it seems, only in fraction 52 corresponding to the dimeric protein. The mutated proteins produced elution peaks in the ~52 and ~60 fractions corresponding to the dimeric and monomeric proteins, respectively. Once again, however, contaminating proteins were eluted together with the recombinant proteins, which produced various unwanted peaks. The sizes of all the peaks that were detected at the 230 nm for each of the monofunctional proteins are listed in Table 4.4.

Table 4.4: Calculated MW of the peaks detected with SEC for the monofunctional proteins

ODCwt		ODCpO1a		ODCpG2	
Fraction	**kDa**	**Fraction**	**kDa**	**Fraction**	**kDa**
19	3690	26	1926	25	2113
23	2545	30	1328	27	1755
31	1210	35	835	31	1210
37	**693**	**38**	**632**	34	916
41	**478**	**42**	**436**	**37**	**693**
47	274	49	227	52	172
49	227	52	172	54	143
53	157	**57**	**108**	**62**	**68**
57	**108**	59	90	69	35
		65	**51**		

Fractions corresponding to the approximate proteins sizes that were expected are highlighted in grey. These include the following complexes and contaminating proteins with sizes: ~600, ~400, ~112, ~70 and ~60 kDa.

The oligomeric states of the recombinant monofunctional proteins could thus not be conclusively determined based only on FPLC analysis as a result of the large amount of contaminating proteins detected at 230 nm. The eluted fractions from all the proteins were thus subsequently identified with Western Immunodetection.

4.4.2.3 Western dot blots

In an effort to validate the SEC results and identity the various forms of the proteins, the SEC eluted fractions of the different proteins were subsequently dot-blotted for Western immunodetection. Based on the calibration curve in Figure 4.11, the expected fractions in which the proteins would elute could be determined. The bifunctional heterotetrameric wild type PfAdoMetDC/ODC protein has a size of ~330 kDa and would therefore elute in fraction ~45, while the bifunctional heterodimeric protein (~160 kDa) would elute in fraction ~53. Due to the constant fluctuation between the bound and unbound states of PfODC (Coleman *et al.*, 1994; Osterman *et al.*, 1994), the wild type protein will be present as both heterotetrameric and dimeric proteins. According to the hypothesis, the mobile Gly residues flanking the O1 parasite-specific insert positions the helix in such a way that it can interact with other areas for the essential dimerisation of the PfODC domain. It is thus expected that the α-helix disrupted mutated protein (A/OpO1a) will be unable to form the ~330 kDa heterotetrameric protein complex and will hence elute only in the fraction corresponding to a size of ~160 kDa, the size of the heterodimeric bifunctional protein.

As expected, the wild type A/Owt protein eluted as both heterotetrameric (~330 kDa, fractions 44-46) and dimeric (~160 kDa, fractions 53-55) proteins (Figure 4.14 top panel). The A/OpO1a mutant protein eluted only as a bifunctional heterodimeric protein of ~160 kDa (middle panel, fractions 53-55), which means that the protein-protein interactions necessary for the dimerisation of the PfODC domains were disrupted. This is an important result; the α-helix thus represents the delineated area that forms direct contacts within the dimer interface of the bifunctional protein. The conserved helix in the O1 parasite-specific insert is therefore not only involved in the decarboxylase activities of both domains (Roux, 2006), but also in protein-protein interactions that are required for the proper dimerisation of the PfODC subunits into a functional dimeric complex. The possibility that the disruption of the helical structure with the introduction of a Pro residue caused a local conformational change that resulted in activity depletion and dimer instability still remains a concern with these type of mutagenesis experiments and needs to be investigated further. On the other hand, the A/OpG2 protein was still capable of forming the heterotetrameric protein (~330 kDa, fractions 44-46), which suggests that the mobility of the O1 insert provided by the flexible Gly residues were possibly more important for the active site gate-keeping activity of the insert rather than the positioning of the α-helix. This protein also exists as the dimeric protein (~160 kDa,

fractions 54-55), which is similar to that obtained for the A/Owt protein. Once again, it is possible that dimerisation could be maintained as the mutagenesis of the flexible Gly residues to rigid Ala residues did not introduce any conformational changes that prevented the α-helix from taking part in subunit interactions. It is thus highly plausible that the Gly residues do allow the O1 insert to act as an active site loop, which explains the severe activity loss once the insert is made immobile.

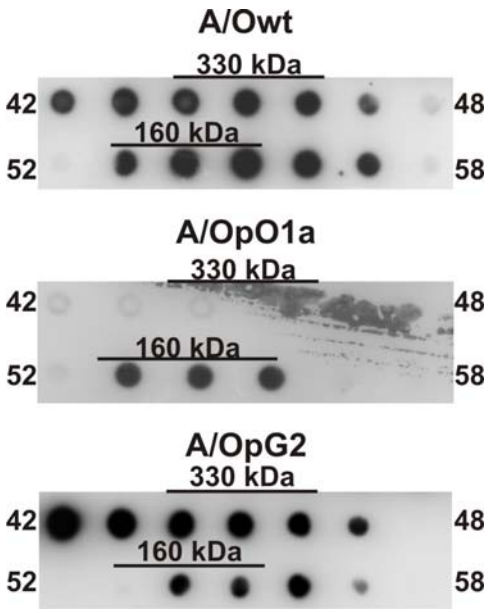

Figure 4.14: Western immunodetection of the fractions obtained from size-exclusion FPLC of the different bifunctional PfAdoMetDC/ODC proteins.
From the top panel to the bottom the blots are shown for the bifunctional A/Owt, the α-helix disrupted A/OpO1a and the immobile A/OpG2 proteins. The number of the fraction on the left and right of each row is given. The sizes of the proteins in the detected dots where the different proteins are found are indicated with black bars.

These results were repeated with the use of monofunctional PfODC proteins (Figure 4.15). The wild type PfODC protein exists as both dimeric (~170 kDa) and monomeric (~85 kDa) proteins and will thus elute in fractions ~52 and ~60, respectively. Based on the results above, the ODCpG2 protein should give similar results as ODCwt, while the ODCpO1a protein will only elute as a single monomeric protein due to the disruption of the α-helix within the O1 insert effecting essential protein-protein interactions needed for the dimerisation of the PfODC domain.

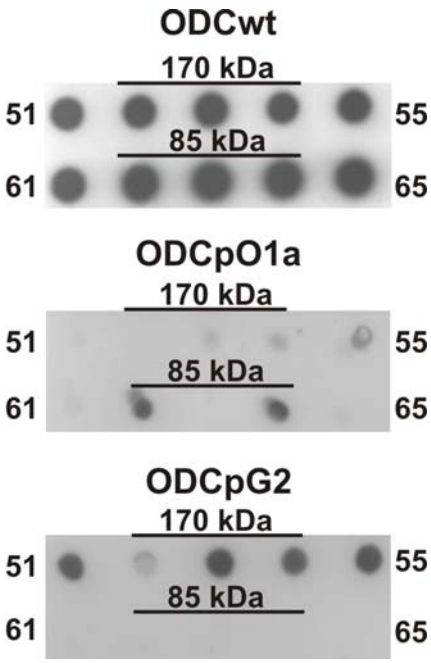

Figure 4.15: Western immunodetection of the fractions obtained from size-exclusion FPLC of the different monofunctional PfODC proteins.
From the top panel to the bottom the blots are shown for the monofunctional ODCwt, the α-helix disrupted ODCpO1a and the immobile ODCpG2 proteins. The number of the fraction on the left and right of each row is shown. The sizes of the proteins in the detected dots where the different proteins are found are indicated with black bars.

The results above confirm those obtained when the bifunctional proteins were used (Figure 4.14). The wild type PfODC protein eluted as both dimeric (~170 kDa, fractions 52-54) and monomeric (~85 kDa, fractions 62-64) proteins (Figure 4.15 top panel). As expected, the ODCpO1a mutant protein eluted only as a monomeric protein of ~85 kDa (middle panel, fractions 62, 64), which means, once again, that the protein-protein interactions necessary for the dimerisation of the PfODC domains were disrupted. The ODCpG2 protein eluted as a dimeric protein (~170 kDa, fractions 52-54), but the monomeric protein was not identified, possibly because the concentration of the eluted protein was too low for immunodetection. However, it cannot be specifically concluded that the helix within the O1 insert causes dimerisation as the disruption of this structure could have introduced a local conformational change instead of an exclusive helical change that resulted in the inability of the monomeric proteins to dimerise.

Since some experimental evidence now exists for the involvement of the O1 parasite-specific insert and the α-helix within this insert in the functioning and dimerisation of the bifunctional PfAdoMetDC/ODC protein, mechanistically novel non-active site-based peptides were designed to inhibit the activity of this essential protein by disrupting protein-protein interactions involved in the dimerisation of its domains. If it is found that the synthetic peptides severely affect the functioning of the protein, steps can be taken towards the

development of an inhibitor against the unique bifunctional protein as a possible antimalarial drug.

4.4.3 Synthetic peptides as inactivators of multimeric enzymes

It is hypothesised that the flexible Gly residues flanking the most structured and conserved O1 parasite-specific insert positions the conserved α-helix, present within the same insert, in such a way that it is capable of forming protein-protein interactions for the subsequent dimerisation of the PfODC subunits and complex formation of PfAdoMetDC/ODC. This area is positioned close to the entry of the active site pocket, which either allows it to act as a gate-keeping loop or to interact with the other subunit across the dimeric interface. The three peptides that were specifically designed to target and interfere with the PfODC dimer interface are listed in Table 4.5. The first peptide is identical to the entire O1 parasite-specific insert sequence (NY-39), including the mobile Gly residues, and carries an overall charge of +3. The second peptide is identical to the 21 amino acids of the α-helix (LK-21) within this insert, carries no charge and is expected to bind to this helix via hydrogen bond interactions or to the corresponding interacting binding partner of this helix. While the third peptide is an anti-helix peptide where the positively charged residues in the helix are replaced with negatively charged ones and *vice versa* resulting in an overall charge of -2 (LE-21). This peptide can therefore form strong electrostatic interactions with the helix in insert O1. The peptides were synthesised and purified (>98%) by GL Biochem (Shanghai) Ltd. (China).

Table 4.5: Possible peptides as interface inhibitors of PfODC dimerisation

Peptide	Target	Sequence (N- to C- terminal)	%Polarity	Size
NY-39	O1 insert	**NAKKHDKIHYCTLSLQEIKKDIQKFLNEETFLKTKYGYY**	74	39
LK-21	α-helix	**LSLQEIKKDIQKFLNEETFLK**	62	21
LE-21	Anti-α-helix	**LSLQKIEEDIQEFLNKKTFLE**	62	21

Residues involved in protein binding hotspots and aromatic clusters are highlighted with yellow and Cys residues involved in disulfide bonds are highlighted with green.

High-affinity binding regions within proteins or so-called “hotspots” are often characterised by the presence of Trp, Arg and Tyr residues while the latter one is also involved in aromatic clusters and protein-protein interactions. The NY-39 peptide contains four such residues, which may implicate this area in the formation of a subunit interface while the helix peptides are devoid of Tyr residues. Cys residues form disulfide bonds that connect proteins. Only one Cys residue, however, is present in the full-length NY-39 peptide. All three the chosen peptides are rich in hydrophilic polar residues, which are abundant at the interfaces of protein

subunits and readily form hydrogen bonds (Table 4.3). The peptides used for the inhibition of PfTIM and *L. casei* TS were also 70 to 80% polar (Prasanna *et al.*, 1998; Singh *et al.*, 2001). A possible strategy involving the helix peptides can be deduced from that of the transmembrane GpA peptide that prevented the dimerisation of the protein (Bormann *et al.*, 1989). LK-21, which is complementary to the helix in insert O1, can interact with this site or its natural binding helix and thereby prevent the dimerisation of PfODC. The interaction between the anti-α-helix peptide and the helix in O1 is expected to be stronger and cause a more severe disruptive effect on dimerisation.

4.4.3.1 Protein:peptide incubation

The wild type PfAdoMetDC/ODC proteins were isolated and analysed with SDS-PAGE (results not shown). Prior to radioactivity assay studies, the proteins were incubated with the different peptides at three molar excess quantities of peptide (1000x, 100x and 10x) at 22°C for 30 min and 2 hrs. This incubation temperature was chosen because previous experiments showed that incubation of the protein at 37°C, which is already an unstable protein, affects the activity of the protein and will thus give false inhibition results. After 30 min of incubation at 37°C, only 36% PfODC activity remained compared to the activity obtained after incubation at 22°C. The rationale for choosing a longer incubation period of 2 hrs was that at this lower temperature the kinetic energy of the molecules is lowered and longer time periods would thus be required for the peptides to reach and effectively bind to their target sites on the protein.

4.4.3.2 Activity assays of protein:peptide samples

The AdoMetDC and ODC activity assays of the wild type control (incubated with $ddd H_2O$) and the three protein:peptide samples at the three different molar concentrations were subsequently performed. Figure 4.16 shows the PfAdoMetDC and PfODC results obtained when the samples were incubated for 30 min.

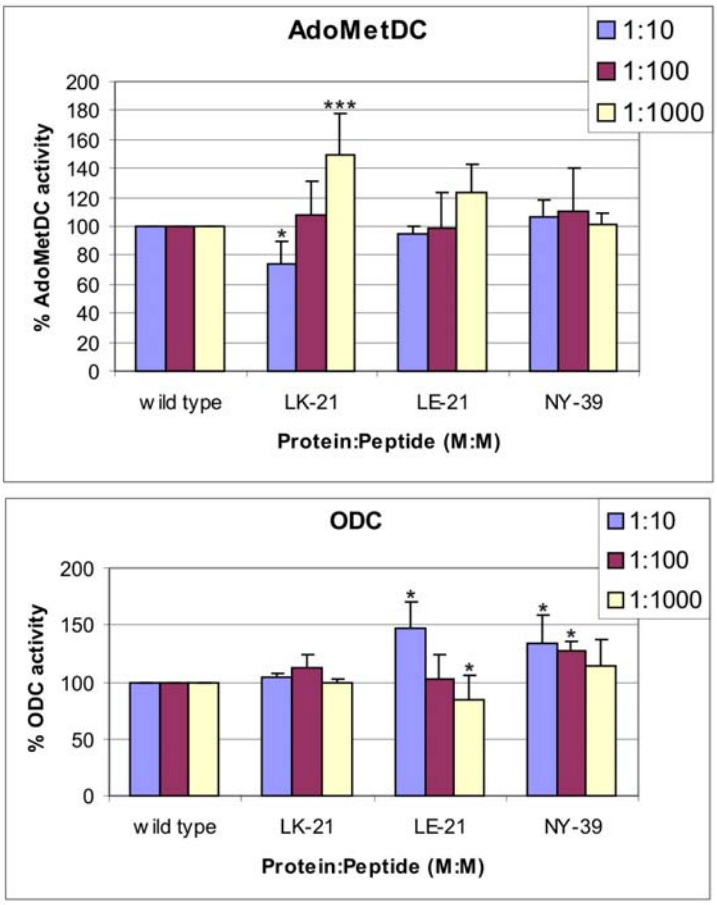

Figure 4.16: AdoMetDC and ODC activity assays after a 30 min incubation of three different peptides with PfAdoMetDC/ODC at three different molar quantities of the peptides.
The AdoMetDC results are shown in the top graph and the ODC results in the bottom. The values were determined from three independent experiments carried out in duplicate. The standard deviations of the mean are indicated as error bars on each graph. Significant differences at a confidence level of 95% are represented as follows: * for $p < 0.05$ and *** for $p < 0.001$.

The peptides were designed to target the O1 parasite-specific insert of the PfODC domain. The effects of the peptides were thus expected to have more severe consequences on the PfODC activity than on the PfAdoMetDC activity. The results, however, indicated that after only 30 min of incubation and at 1000x molar excess quantities of the LK-21 and LE-21 peptides, PfAdoMetDC activity increased (significant only for LK-21) indicating that this protein became stabilised and that the O1 helix may form interactions with the adjacent domain. It is thus possible that the peptides are binding to an interacting site of the O1 helix on the PfAdoMetDC domain thereby replacing the O1 helix from this interaction and stabilising the protein from its control through allosteric domain-domain interactions. This type of ease in the control of the bifunctional protein can also be seen when the PfAdoMetDC domain is independently expressed as a monofunctional protein (Wrenger *et al.*, 2001). Another possibility is that the replacement of the helical interaction within PfODC causes a conformational change, which is communicated to the PfAdoMetDC domain, leading to an increase in its activity in preparation for the pending release of putrescine. A 100x molar

excess of both the helix peptides did not significantly affect the PfAdoMetDC or PfODC activities and was similar to that of the wild type's activity.

No significant change was observed in the PfODC activity when LK-21 was used at all three concentrations. However, a 1000x molar excess of the LE-21 peptide resulted in a significant inhibition of approximately 20% in PfODC activity, which was expected since this peptide is opposite in charge to that of the helix in O1 and would therefore interact with this target site rather than the corresponding interaction site. At the same time, 1000x of this LE-21 peptide increased PfAdoMetDC activity by ~20%, which means that the allosteric restraint was possibly eliminated and the PfAdoMetDC domain could function independently. The NY-39 peptide, which is complementary to the entire O1 insert, slightly increased the PfAdoMetDC and PfODC activities. This could possibly be due to the increased size of this peptide compared to that of the helix peptides (39 *versus* 21 amino acids).

The incubation periods were subsequently increased to 2 hrs to investigate whether the peptides would have more profound effects as opposed to the results obtained when the samples were incubated for a much shorter period (Figure 4.16). The results indicated that after a 2 hr incubation period, 1000x molar excess quantities of all three peptides significantly increased the PfAdoMetDC activities by ~60% resulting in the protein becoming more stabilised. The stabilisation of the polyamine biosynthesis proteins by the peptides is not necessarily a negative result as unbalanced levels of putrescine and dcAdoMet disrupt polyamine homeostasis within the cell that can possibly lead to cell death (Xie *et al.*, 1997). A 100x molar excess of the helix peptides did not significantly affect the PfAdoMetDC or PfODC activities and was similar to that of the wild type's activity. A 10x molar excess of these two peptides slightly decreased the activities of both PfAdoMetDC and PfODC (not significant). The peptide that was most effective in inhibiting PfODC activity was a 1000x molar excess quantity of the anti-α-helix peptide, LE-21, which resulted in a significant decrease of 40% in PfODC activity with a concurrent significant increase of 66% in PfAdoMetDC activity. The NY-39 peptide stabilised both the PfAdoMetDC and PfODC activities at all concentrations (Figure 1.17).

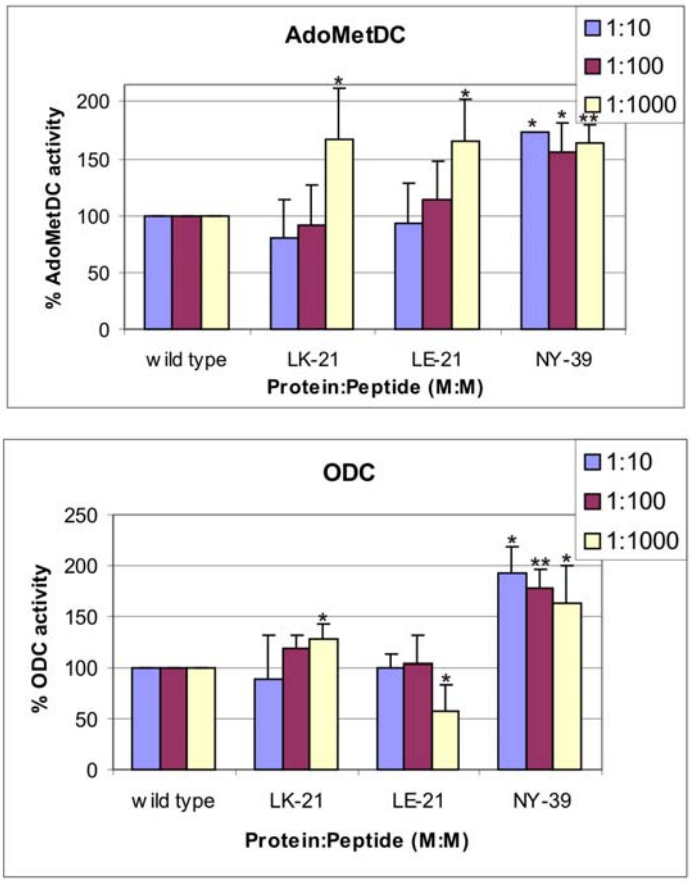

Figure 4.17: AdoMetDC and ODC activity assays after a 2 hr incubation of three different peptides with PfAdoMetDC/ODC at three different molar quantities of the peptides.
The AdoMetDC results are shown in the top graph and the ODC results in the bottom. The values were determined from three independent experiments carried out in duplicate. The standard deviations of the mean are indicated as error bars on each graph. Significant differences at a confidence level of 95% are represented as follows: * for $p < 0.05$ and ** for $p < 0.01$.

The success of the LE-21 peptide in decreasing PfODC activity could be ascribed to the charged residues residing on this peptide that is capable of forming stable salt bridges with the oppositely charged residues on the target site of the protein, resulting in PfODC-peptide complexes. This interaction therefore prevents dimerisation of the PfODC monomers, which allosterically affects the adjacent domain while maintaining the structure of the overall heterotetrameric PfAdoMetDC complex even though PfODC no longer exists as a dimer. Alternatively, the observed effects upon the treatment of the LE-21 peptide may be as a result of metabolite accumulation. Previous studies have shown that the PfODC product putrescine does not stimulate PfAdoMetDC activity as in the mammalian enzyme (Wrenger *et al.*, 2001). The inhibition of PfODC with the peptide could thus lead to the accumulation of ornithine, which can interact with the bifunctional protein, leading to a conformational change that allows PfODC and PfAdoMetDC to become active for the pending release of putrescine and dcAdoMet respectively, which can then be utilised by PfSpdSyn for the synthesis of spermidine.

The presence of the mobile Gly residues in the NY-39 peptide may allow it to act as a gate-keeping loop allowing the entrance of the substrate ornithine. As is the case in PfSpdSyn (Dufe *et al.*, 2007), binding of the substrate may stabilise the gate-keeping loop resulting in conformational changes at the active site of the protein, which increases its activity. These conformational changes may then be communicated to the adjacent domain in the bifunctional complex in order to increase the activity of this enzyme for the production of dcAdoMet. These interdomain interactions may well explain the unique arrangement of these two proteins in a bifunctional complex as such a structure allows for the optimum maintenance of the essential polyamines.

Dose-dependent effects were observed for several of the peptides where increased peptide concentrations resulted in increased (i.e. PfAdoMetDC activities with LK, LE-21 and PfODC activity with LK-21) or decreased (i.e. PfODC activity with LE-21) protein activity. Whether any of these peptides target and bind to their complementary sites on the target protein is unknown and it is possible that the NY-39 and LK-21 peptides are binding to the interacting sites of the O1 helix rather than the helix itself. Such an interaction would relieve the allosteric regulation on the PfAdoMetDC domain and have no effect on PfODC. These interacting sites may be determined with circular dichroism or chemical cross-linking experiments. FPLC analyses of the protein:peptide samples were not performed, as this would require large amounts of peptide, which renders FPLC impractical. This type of experiment would, however, be useful, as it would show whether the synthetic peptides are capable of preventing dimerisation of the proteins and would indicate the potency in using such peptides as inactivators of multimeric enzymes.

The conformation of the peptides will greatly contribute to the ability of these peptides to inhibit protein activity within a solution (Prasanna *et al.*, 1998), which may be influenced by the salt concentration as well as the pH of the reaction conditions. These may be varied in such a way that the peptides remain charged and structurally intact. The activity assays were performed at pH 7.5 since PfAdoMetDC and PfODC activities are optimum at pH 8.0 and 7.5, respectively. Altering the salt concentration may, however, have unwanted effects on the conformation of the PfAdoMetDC/ODC protein. Additional peptides that are not expected to bind to PfAdoMetDC/ODC should also be tested as negative controls to make sure that not just any peptide is capable of binding to the target and that they must be specifically complementary to the protein. Specific residues within the target site may also be altered in such a way that the conformation of the insert would be maintained but the interactions between the mutant protein and peptide would be disrupted leading to the restoration of wild type PfAdoMetDC and PfODC activities. Such mutagenesis studies were performed on GpA

to delineate the critical residues necessary for the helical interactions and dimerisation of the protein and would, in this case, serve as good negative controls (Lemmon *et al.*, 1992).

Once again, the presence of various contaminating proteins after *Strep*-Tactin affinity chromatography may influence the ability of these peptides to bind to their target sites. Pure protein is thus needed for the accurate determination of the effects that these synthetic peptides have on the activity of the PfAdoMetDC/ODC protein.

An alternative strategy that can be employed for the disruption of protein-protein interfaces in PfAdoMetDC/ODC is the “credit-card” library approach recently developed by Xu *et al*. The approach involves the design and synthesis of a small parallel library consisting of “credit-card” compounds, which are derived from a planar, aromatic scaffold and functionalised with chemical diversity. The authors viewed the hotspots at protein interfaces as aromatic, slot-like regions or “card readers” and that the insertion of a “credit-card” into the “reader” could trigger a disruptive event at the interface. The effectiveness of this approach was tested by disrupting the Myc-Max dimer interaction where Myc belongs to the basic helix-loop-helix leucine zipper (bHLH-ZIP) family of proteins and is often deregulated in human cancer cells (Xu *et al.*, 2006).

In this study, the importance of the O1 insert and the α-helix in the activity and dimerisation of the bifunctional protein was exploited in the design and application of parasite-specific, mechanistically novel, inhibitory peptides that are specific for this non-homologous insert. Synthetic peptides have been successfully applied as protein interface inhibitors of *P. falciparum* TIM. One specific peptide resulted in a 55% decrease in protein activity at a 1000x molar excess of the peptide, which indicated that this region is possibly involved in the stabilisation of the dimer (Singh *et al.*, 2001). The investigation of various peptides complementary to regions of the O1 parasite-specific insert identified LE-21, which is the oppositely charged partner of the O1 insert helix, as being a potential peptide for the successful inhibition of PfODC activity. This peptide decreased PfODC activity by ~40% and increased PfAdoMetDC activity by 66% at the same molar excess of peptide as was used for the inhibition of PfTIM. These studies are thus comparative to published work and at the same time shows that interface peptides are useful in the design of lead compounds for the inhibition of protein-protein interactions.

Chapter 5: Concluding discussion

The malaria burden falls heavily on sub-Saharan Africa, where more than 90% of the recorded deaths occur due to this parasitic infection and 5% of children die from severe malaria before the age of five (Phillips, 2001). Globally, malaria presents a threat to 40% of the world's population and is responsible for 2.7 million deaths per year, the majority of which are as a result of cerebral malaria caused by *P. falciparum* (Korenromp *et al.*, 2005). The burden is continuously intensified by the development of parasite resistance to all classes of currently used antimalarials including chloroquine, mefloquine, sulfadoxine-pyrimethamine and the most recent compound, artemisinin (Jambou *et al.*, 2005; Bathurst and Hentschel, 2006). New drug targets are thus urgently needed as a means for possible chemotherapeutic intervention, which are more effectively identified once the parasite physiology and host-parasite relationships are better understood. The presence or absence of specific essential pathway enzymes and differences in the structures between host and parasite enzymes can subsequently be identified and investigated in possible malaria disease prevention strategies (Assaraf *et al.*, 1984).

Urgent advances in vaccine development and drug discovery to curb the malaria burden can be assisted with the production of pure recombinant malarial proteins. The isolation of *P. falciparum* proteins using *E. coli* as an expression system is complicated by the parasite's codon bias and the presence of unique inserts and LCRs (Gardner *et al.*, 2002). Vedadi *et al*. performed a large-scale protein expression study in an attempt to obtain as many as possible crystal structures from seven different Apicomplexan genomes. The group managed to purify 304 proteins for which 97 crystal structures could be successfully determined. They showed that a codon-enhanced commercial *E. coli* strain can be used as an effective expression system for the recombinant protein purification and crystallisation of Apicomplexan proteins (Vedadi *et al.*, 2006). Their results supported the conclusions made by Mehlin *et al*. in which a weak association exists between A+T content and protein expression (Mehlin *et al.*, 2006). Once the proteins are isolated to homogeneity, structural biology studies can be performed when protein crystallisation seems dismal. These studies are important in the identification of novel drugs that specifically inhibit parasite enzymes without having to experimentally test thousands of chemicals. The chemical library can also be narrowed down by applying "Lipinski's rule of 5" as a general guideline. These rules estimate the solubility and permeability of chemical compounds, which deem them viable or not as potential drug candidates (Lipinski *et al.*, 2001).

Protein structural knowledge together with bioinformatic tools enhance drug discovery on several levels. The structure firstly gives an indication of the druggability of the protein with special focus on binding regions and molecular functions that may be exploited during inhibitor design (Hopkins and Groom, 2002). Secondly, it contributes to the design of a chemical molecule with optimised binding interactions to the target. And finally, the 3-dimensional structure of a proposed target can be used to virtually screen thousands of ligands for an ideal candidate that will exert the most direct effect while being the least toxic and cheapest to synthesise (Blundell *et al.*, 2005). Another important use of protein crystal structures are the insights they provide into antimalarial drug resistance; for example, the crystal structures of the wild type and mutant *P. falciparum* DHFR/TS proteins revealed molecular mechanisms used by the enzyme to lower the drug binding capacity of pyrimethamine and proguanil and at the same time provided templates for the design of new drugs to overcome drug resistance (Yuvaniyama *et al.*, 2003).

Homology models of all the polyamine pathway enzymes in *P. falciparum* have been determined while only PfSpdSyn has been crystallised (Dufe *et al.*, 2007). These structures provide important information on the active site residues involved in substrate, cofactor and inhibitor binding as well as regions involved in the dimerisation of the proteins (Birkholtz *et al.*, 2003; Wells *et al.*, 2006; Burger *et al.*, 2007).

The widespread prevalence of polyamines goes hand in hand with their roles in a multitude of functions in diverse processes ranging from cell proliferation and differentiation to cell death (Wallace *et al.*, 2003). DFMO in combination with bis(benzyl)polyamine analogues cures *P. berghei*-infected mice (Bitonti *et al.*, 1989), which provides strong support for combination chemotherapy targeting the polyamine pathway in rapidly proliferating parasites to control malaria infections. The levels of the polyamines are most pronounced during trophozoite and schizont stages when macromolecular synthesis is taking place (Assaraf *et al.*, 1984; Das Gupta *et al.*, 2005), which signify the importance of polyamines in rapid growth and parasite survival. ODC and AdoMetDC are the rate limiting enzymes in the polyamine pathway and are usually individually regulated on transcriptional, translational and post-translational levels. In *P. falciparum,* both these enzymes are uniquely encoded within a single open reading frame (PfAdoMetDC/ODC) (Müller *et al.*, 2000). The two decarboxylase activities of the bifunctional protein function independently (Wrenger *et al.*, 2001) but inter- and intradomain interactions occur, which are necessary for the stabilisation of the active bifunctional protein (Birkholtz *et al.*, 2004). The arrangement of both these proteins in a single complex provides an important difference between the host and parasite polyamine biosynthesis pathway enzymes that can be exploited during drug design to simultaneously inhibit both these enzymes.

In addition to the bifunctional arrangement of PfAdoMetDC/ODC, the ability of PfSpdSyn to synthesise both spermidine and spermine due to the absence of a gene encoding SpmSyn, (Haider *et al.*, 2005) provides further support in targeting the polyamine biosynthesis pathway of *P. falciparum*. Combination drugs targeting the bifunctional complex as well as PfSpdSyn would severely affect the intracellular polyamine pools. Polyamine-specific transporters in *P. falciparum* have not been identified and are also an important aspect to consider when designing novel inhibitors against polyamine biosynthesis enzymes. Inhibitor and product replenishment studies, however, suggested the presence of a putrescine transporter (Assaraf *et al.*, 1984; Das Gupta *et al.*, 2005) but the existence of a spermidine-specific transporter remains uncertain (Haider *et al.*, 2005). An ideal inhibitor must deplete intracellular polyamines by its combined action on the target enzyme/s and polyamine transporter/s. The treatment of polyamine biosynthesis enzymes with different inhibitors showed that these enzymes are essential for the growth of the parasites (Assaraf *et al.*, 1987; Das Gupta *et al.*, 2005; Haider *et al.*, 2005). In addition, the inability to successfully create null mutants of the polyamine biosynthesis pathway enzymes (Dr I.B. Müller, personal communication) reinforces the essentiality of polyamines in the survival of the parasites and suggests their value as potential drug targets.

In order for a parasite protein to be effective as a drug target, significant differences should exist between the parasite and host proteins for the exclusive inhibition of the parasite enzyme. The *P. falciparum* polyamine biosynthesis enzymes have been characterised on genetic, molecular and structural levels. Exceptional parasite-specific properties have been identified that may be exploited during lead drug development. Previous studies have shown that unique parasite-specific inserts in PfAdoMetDC and PfODC are involved in the activities of the respective and adjacent domains (Birkholtz *et al.*, 2004). These areas present innovative opportunities for designing drugs that target regions distant from the active sites.

The roles of the parasite-specific inserts in the PfAdoMetDC domain were investigated as previous studies showed that the presence of these seemingly unstructured areas are important in the complex formation and activities of the PfAdoMetDC/ODC protein (Birkholtz *et al.*, 2004). A logical way to determine the roles of these inserts is to simply remove them from the parental template and to subsequently assess the effects of the mutated proteins on protein activity. A decrease in activity would indicate that the inserts are important in the functioning of the proteins, may it be via direct involvement with the active site, protein-protein interactions forming the complex or by interacting with regulatory proteins. A literature study identified several PCR-based methods that can be employed for the deletion of large areas from genes. A comparative study was thus performed in order to determine which method is the most effective in deleting the largest A3 parasite-specific insert (>400 bp) in

the PfAdoMetDC domain from a large construct (~7400 bp). Application of the QCM and ExSite™ methods in deleting the insert did not produce PCR products while the inverse PCR and overlapping primer methods produced PCR products of the required size. A fifth method based on the inverse PCR method was additionally tested. The primers of the RE-mediated inverse PCR method contain unique RE sites at the 5'-ends of both the forward and reverse inverted tail-to-tail primers. PCR with these primers amplify the entire construct except for the desired region (insert) between the 5'-ends of the two primers. Subsequent PCR product digestion with the unique RE increases the number of deletion products by eliminating any primary parental product still containing the insert. But most importantly, RE digestion creates products with sticky-ends that improve the ligation efficiency during the circularisation of the mutant products into plasmids. The application of this deletion mutagenesis method also resulted in a PCR product of the correct size indicating that the A3 insert was possibly removed. RE mapping and nucleotide sequencing showed that the overlapping primer method was 40% efficient while the RE-mediated inverse PCR method resulted in 80% mutagenesis efficiency.

The RE-mediated inverse PCR method was also tested on a second *P. falciparum* protein; the method successfully removed a parasite-specific insert (>600 bp) form *PfPdxK* (~4600 bp) from all the clones tested, which indicates that the efficacy of the method is better on smaller templates. However, this is not dependent on the particular gene sequence. A highly efficient method was therefore created and tested which can be used to successfully remove large DNA regions (>100 bp) from abnormally large A+T rich *P. falciparum* genes (Williams *et al.*, 2007). The method proved to be invaluable in deciphering the involvement of the parasite-specific inserts in the structure and activity of PfAdoMetDC/ODC.

The smaller A1 and A2 inserts were removed with the overlapping primer method and were, together with the previously created A3 insert-deleted mutant, investigated in a structure-activity relationship study. The newly created deletion mutants were recombinantly expressed with C-terminal *Strep*-tags and isolated with *Strep*-Tactin affinity chromatography. Similar levels of recombinant proteins were isolated and subsequently visualised with SDS-PAGE. Gel electrophoresis showed that various contaminating proteins co-eluted with the desired ~160 kDa protein. The presence of three contaminating proteins (~60 kDa, ~70 kDa and 112 kDa) were identified in a previous study as being *E. coli* chaperones (HSP60 and HSP70), produced to aid the poor expression of the recombinant protein, and heterologously derived N-terminal PfAdoMetDC/ODC truncations sized ~70 kDa and ~112 kDa formed due to the presence of false internal translation initiation sites (Niemand, 2007). In addition to these three bands, the recombinant expression of the A2 and A3 insert-deleted proteins produced smaller proteins, which were located directly underneath the ~160 kDa bands. MS

analysis identified these as being PfAdoMetDC/ODC but the manner in which they were produced remains uncertain.

The affects that the inserts have on the activities of both the enzymes in the bifunctional complex were subsequently determined in an attempt to show that these inserts are evolutionary preserved as a result of the specific roles that they play in the bifunctional protein complex. The deletion of the sequence and structurally conserved A1 insert halved the PfAdoMetDC activity while the PfODC activity was depleted by 95%. This insert was predicted to have a similar role to that of the O1 insert due to their high Plasmodial conservation and lack of LCRs. The similarity and combined functional roles of these two inserts in the activities of both the domains in the bifunctional complex can therefore be exploited in the design of a single inhibitory compound capable of binding to both these areas. Such a compound would result in the reduction of PfODC activity by the inhibition of PfAdoMetDC activity (to ~50% of wild type activity) and, in turn, result in the reduction of PfAdoMetDC activity (to ~23% of the wild type activity) by the inhibition of PfODC activity.

The A2 and A3 deletion mutants severely affected both PfAdoMetDC and PfODC domain activities, which could possibly be due to the disruption of protein-protein interactions between these inserts and the remainder of the complex upon their removal. Based on these deletion mutagenesis studies, it thus seems that the two domains of the bifunctional protein are allosterically regulated via the presence of parasite-specific inserts to maintain optimum levels of polyamines. Large conformational changes upon deletion of these latter inserts could also be responsible for the depletion of the bifunctional activity. However, the roles of the various contaminant proteins are unknown and cannot be discounted at the current time.

Following the severe consequences of insert deletion on protein activity, the A2 and A3 inserts were analysed for the presence of secondary structures as these are often involved in protein-protein interactions across homodimeric interfaces (Guharoy and Chakrabarti, 2007). Popular secondary structure prediction programmes as well as HCA plots were used to analyse the inserts. It is expected that the large bifunctional PfAdoMetDC/ODC protein complex would contain a number of protein-protein interaction sites to stabilise the entire heterotetrameric protein complex and it was thus predicted that these inserts might be involved in additional interactions that are absent in the mammalian counterparts. Secondary structures are also involved in the formation of super-secondary structures that often characterise the function of a particular fold such as leucine zippers and β-barrels (Sansom and Kerr, 1995; Gromiha and Parry, 2004). Super-secondary structures of PfAdoMetDC/ODC include the PfAdoMetDC domain αββα-fold, the N-terminal α/β TIM and C-terminal modified Greek-key β-barrels of PfODC (Birkholtz *et al.*, 2003; Wells *et al.*, 2006).

Predicting secondary structures from amino acid sequences are also useful in the absence of a PfAdoMetDC/ODC crystal structure in which the location and structure of the parasite-specific inserts would be shown. Application of the prediction programmes and HCA identified two *Plasmodia* conserved structures that were further investigated, namely an α-helix in insert A2 and a β-sheet in insert A3. The helix was disrupted with an Ile to Pro point mutation while the sheet in insert A3 was deleted with the RE-mediated inverse PCR method. Once again, similar recombinant expression levels of the α-helix disrupted and wild type proteins were obtained while SDS-PAGE analysis showed the presence of several co-eluting contaminating proteins, which were higher with the mutated protein sample. These were attributed to possible degradation products formed as a result of the recombinant expression of the mutant sample and an increase in chaperone proteins rather than the formation of misfolded protein upon the introduction of the Pro helix-breaker residue.

Subsequent activity assays revealed some interesting results; only 15% PfAdoMetDC activity and 45% of the wild type PfODC remained upon the disruption of the conserved helix within insert A2. The effects of the mutation were thus communicated to the neighbouring PfODC domain, which indicates that this structure might be involved in interactions across the entire protein complex. These results are analogous to those when the conserved α-helix in insert O1 was disrupted in a similar manner. It thus seems plausible that secondary structures within the unique parasite-specific inserts are involved in the conformation of the bifunctional complex and the possibility that they are involved in protein-protein interactions for the dimerisation of the multimeric complex needs to be investigated.

Previous studies have also shown that the PfODC domain is more refractory to change and is thus largely affected once mutations are introduced within this domain and in the hinge region (Birkholtz *et al.*, 2004; Roux, 2006). Most importantly, the C-terminal PfODC domain is highly dependent on the presence of the N-terminal PfAdoMetDC domain and the hinge region connecting these two domains while PfAdoMetDC can function independently (Krause *et al.*, 2000; Wrenger *et al.*, 2001). These properties are mirrored in the malarial DHFR/TS bifunctional protein where the C-terminal TS domain is highly dependent on its interactions with the neighbouring N-terminal DHFR domain (Shallom *et al.*, 1999). It was previously thought that initialisation of the heterotetrameric complex takes place from the PfODC domain, but the results of these studies indicate that the parasite-specific inserts within the PfAdoMetDC domain are also responsible for the activities and/or stability of both the domains. These unique inserts can thus be investigated as possible drug targets for the disruption of the entire PfAdoMetDC/ODC complex activity.

Based on the results obtained, which showed an apparent functional role of the structurally conserved A1 insert and the importance of the conserved α-helix in insert A2 in the activities of both domains possibly via protein-protein interactions, the structurally distinct and conserved helix-containing O1 insert was further investigated. Previous studies showed that this insert is very important for both decarboxylase activities and that its deletion prevents dimerisation of the PfODC monomers and influences the association of PfODC with the adjacent PfAdoMetDC domain to form the bifunctional complex (Birkholtz *et al.*, 2004). The respective point mutations disrupting the helix (identified with secondary structure prediction programmes) and immobilisation of the insert resulted in severe activity depletions of both the decarboxylase domains, which demonstrated the essential roles of these delineated areas within O1 (Roux, 2006). The flexible Gly residues were shown with molecular dynamics to impart mobility on the insert, implying that this insert might be acting as an active site gatekeeper due to its close proximity to the active site as revealed with homology modelling (Birkholtz *et al.*, 2003; Roux, 2006). Alternatively, the mobile loop was thought to position the helix in such a way that it can interact with protein areas to establish the active dimeric proteins. If this is true then the O1 insert represents a valuable drug target, as dimerisation will be prevented leading to the inactivation of the entire protein and a subsequent loss in the biosynthesis of polyamines.

The O1 helix-disrupted and immobile mutations with the bifunctional gene as template were created in a previous study (Roux, 2006). The same mutations were also introduced in the monofunctional PfODC template. These two different monofunctional and bifunctional constructs were subsequently used in a study to determine whether these delineated areas are responsible for protein-protein interactions and dimerisation of the proteins. The different constructs were recombinantly expressed and purified with *Strep*-Tactin affinity chromatography. The recombinant proteins were applied to a size-exclusion column, which was calibrated with four standard proteins and the protein sizes were determined with FPLC. The ability of the respective mutated proteins to dimerise could thus be determined based on the elution volumes of the proteins and a linear regression equation. The sizes were confirmed with Western dot blot immunodetection with a *Strep*-tag II antibody. The wild type bifunctional and monofunctional proteins eluted in fractions corresponding to the sizes of the bifunctional heterodimeric and tetrameric proteins while the monofunctional proteins eluted as both monomeric and dimeric proteins. Both oligomeric states were eluted due to the rapid exchange of the ODC subunits between its monomeric and dimeric forms (Coleman *et al.*, 1994; Osterman *et al.*, 1994). The elution profiles of the immobile Gly mutant proteins were identical to that of the wild type protein, which means that even though the O1 insert loop is no longer mobile it is still takes part in protein-protein interactions for the dimerisation of the PfODC domain. The Gly mutant protein is therefore still capable of forming the bifunctional

complex but the ability of the substrate to stabilise the active site loop and induce an active site conformation may be affected (Dufe *et al.*, 2007), which explains the depletion in activity upon the creation of this immobile loop.

The abilities of the helix-disrupted proteins to form heterotetrameric PfAdoMetDC/ODC and dimeric PfODC proteins were lastly tested. The monofunctional PfODC protein only eluted as a monomeric protein while the bifunctional PfAdoMetDC/ODC protein exclusively eluted in a fraction corresponding to the size of the heterodimeric protein. This means that the O1 helix could no longer partake in protein-protein interactions and thus represents the exact delineated interacting area necessary for the dimerisation of the domains. Western blots confirmed these results. These studies once again reinforce the potential in targeting this insert with an inhibitory compound, which would prevent the complex formation of PfAdoMetDC/ODC leading to the simultaneous inactivation of both the enzymatic domains. Next, a proof-of-principle study was performed to test whether synthetic peptides targeting the O1 insert could affect bifunctional activity.

Experimental evidence proving the involvement of the O1 insert in the dimerisation of the PfODC and PfAdoMetDC/ODC proteins and activity of both the domains prompted the design of mechanistically novel, non-active site based peptides that could target and bind to this area to disrupt protein activity. Similar studies have been performed on another malarial protein, which showed that a peptide targeting the protein dimerisation interface resulted in a 50% loss in enzyme activity (Singh *et al.*, 2001). Three different peptides were designed: 1) NY-39 which is complementary to the entire 39 amino acid O1 insert; 2) LK-21 which is identical to only the α-helix within this insert; and 3) LE-21 which is similar to LK-21 but opposite in charge. The full-length PfAdoMetDC/ODC proteins were incubated at three different molar quantities with these different peptides and subsequently subjected to activity assays to determine the effects of the peptides on protein activity.

A 2 hr incubation at 22°C of the LE-21 peptide at a 1000x molar peptide excess depleted 40% of the PfODC activity while PfAdoMetDC activity increased by 66%. This peptide possibly forms salt bridges with the O1 helix in the target protein, thereby preventing it from interacting with its natural binding partner resulting in the inhibition of PfODC activity. The increase in PfAdoMetDC activity could be due to the alleviation of interdomain regulation or stabilisation in the absence of the adjacent domain. The exact interacting areas of the peptides on the full-length protein are, however, unknown and might explain why some activity still remained. The structures of the peptides in solution are also important and might mediate their ability to bind to the target site. A control peptide, which is not complementary to the target protein, should be tested to see if not just any peptide is capable of interacting

with PfAdoMetDC/ODC. The NY-39 peptide, which is identical to the O1 insert, would also compete with PfODC binding to its complementary site and caused an increase in both the PfAdoMetDC and PfODC activities. Finally, these inhibitory experiments should also be performed at physiological temperature, which was initially avoided due to the inhibitory effect the temperature had on the positive wild type control. The true effect of these ~2.3 kDa peptides on the polyamine levels can in future be tested *in vitro*. However, even if the peptides were to be taken up by the parasites via endocytosis, they would most probably end up in endosomes or the food vacuole, and not in the cytoplasm where PfAdoMetDC/ODC is located. These peptides, however, merely serve as a starting point for future studies aimed at using these peptides as scaffolds for the synthesis of chemical compounds that can be more effectively employed as therapeutic inhibitors.

In the last four years, studies performed on the bifunctional PfAdoMetDC/ODC complex by the introduction of various mutations and the use of synthetic peptides targeting the unique parasite-specific inserts have brought us closer to understanding the exact functions of these areas. Possible mechanisms have also been revealed that explain how polyamines levels are maintained by the tight regulation of the PfAdoMetDC and PfODC protein activities, which is possibly made more efficient as a result of their arrangement in a single bifunctional complex.

Table 5.1 summarises all the studies that have been performed involving the PfODC domain and how these affected protein activity and/or dimerisation. Several obvious trends can be seen in Table 5.1. Any alterations involving the conserved O1 insert prevented the dimerisation of the PfODC domain and therefore severely affected bifunctional activity. Bifunctional heterotetrameric complex formation only requires the presence of the two domains while dimerisation of PfODC depends on the hinge region. The flexible Gly residues of the O1 insert are important for the activities of both of the domains while a mobile insert is not required for the dimerisation of the PfODC domain or the complex formation of the heterotetrameric PfAdoMetDC/ODC complex. The effects of the insert O1 synthetic peptides on complex formation are still outstanding and would reveal their possible involvement in the disruption of protein-protein complexes.

An allosteric-type regulation of the domains in the bifunctional PfAdoMetDC/ODC domain is thus suggested since the activity of PfAdoMetDC becomes stabilised in the absence of the PfODC domain while the latter is inactive in the absence of the PfAdoMetDC domain (Krause *et al.*, 2000; Wrenger *et al.*, 2001). It is also possible that the opening and closure of the active site gate-keeping loop upon the binding and release of ornithine and putrescine,

respectively, is communicated to the PfAdoMetDC domain made possible by the interdomain interactions in the bifunctional complex

Table 5.1: Summary of the effects of O1 insert mutations on protein activity and dimerisation as well as its targeting with peptide inhibitors

Mutation/treatment	%AdoMetDC activity	%ODC activity	Dimerisation	Reference
PfODC - hinge	NA	3	✗	Birkholtz *et al*., 2004
PfODC + hinge	NA	6	✓	Birkholtz *et al*., 2004
PfODCΔO1	NA	9	✗	Birkholtz *et al*., 2004
PfODCpO1a	NA	-	✗	Current study
PfODCpG2	NA	-	✓	Current study
A/O - hinge	67	50	✓	Birkholtz *et al*., 2004
A/OΔO1	23	6	✗	Birkholtz *et al*., 2004
A/OpO1a	6	0	✗	Roux, 2006 and current study
A/OpG2	33	3	✓	Roux, 2006 and current study
O1 peptide + A/O	↑	↑	?	Current study
Helix peptide + A/O	↑	No change	?	Current study
Anti-helix peptide + A/O	↑	↓	?	Current study

Mutations that were performed: PfODC + hinge, monofunctional PfODC including 144 residues of the hinge region; PfODC - hinge, monofunctional PfODC without the hinge region; A/O - hinge, removal of residues 573-752 in the hinge region; ΔO1, deletion of the entire 39-residue O1 insert; pO1a, disruption of the α-helix within the O1 insert; pG2, mutagenesis of the flanking Gly residues in the O1 insert. The overall effects of the peptides after 2 hr incubation periods with the wild type bifunctional A/O protein at 22°C on protein activity are shown as either increasing (green) or decreasing (red) arrows. The abilities of the mutant monofunctional and bifunctional proteins to dimerise into dimeric PfODC or heterotetrameric PfAdoMetDC/ODC protein complexes are indicated with ticks or crosses. The activities were normalised as a percentage of the wild type PfAdoMetDC/ODC activity. "?" Shows that the results are outstanding. NA: non-applicable when the activity assays were performed with monofunctional PfODC as template. "-": When the activity was negligently low.

In conclusion, this study focussed on the parasite-specific inserts in the PfAdoMetDC domain and showed that these as well as the secondary structures within them are essential for the activities of both domains. The involvement of a PfODC parasite-specific insert in protein-protein interactions and dimerisation of the protein was subsequently evaluated. A conserved α-helix within this insert was shown to mediate the dimerisation of the PfODC domain and was targeted with a synthetic peptide, which depleted almost half of this protein's activity. This study has thus proven the importance of these inserts in the activity and structure formation of PfAdoMetDC/ODC. Finally, the design and application of a single inhibitory peptide that can recognize and bind to all the A1- and O1-type of parasite-specific inserts in *P. falciparum* proteins would lead to a global inhibition of proteins and would represent the ultimate drug to cure malarial infections.

References

Anders, R. F. and A. Saul (2000). "Malaria vaccines." Molecular Approaches to Malaria **16**: 444-447.

Aponte, J. J., P. Aide, M. Renom, I. Mandomando, Q. Bassat, J. Sacarlal, M. N. Manaca, S. Lafuente, A. Barbosa, A. Leach, M. Lievens, J. Vekemans, B. Sigauque, M. Dubois, M. Demoitié, M. Sillman, B. Savarese, J. G. McNeil, E. Macete, W. R. Ballou, J. Cohen and P. L. Alonso (2007). "Safety of the RTS,S/AS02D candidate malaria vaccine in infants living in a highly endemic area of Mozambique: a double blind randomised controlled phase I/IIb trial." The Lancet **370**: 1543-1551.

Argos, P. (1987). "Analysis of sequence-similar pentapeptides in unrelated protein tertiary structures. Strategies for protein folding and a guide for site-directed mutagenesis." Journal of Molecular Biology **197**: 331-348.

Assaraf, Y. G., L. Abu-Elheiga, D. T. Spira and H. Desser (1987). "Effect of polyamine depletion on macromolecular synthesis of the malarial parasite, *Plasmodium falciparum*, cultured in human erythrocytes." Biochemical Journal **242**: 221-226.

Assaraf, Y. G., J. Golenser, D. T. Spira and U. Bachrach (1984). "Polyamine levels and the activity of their biosynthetic enzymes in human erythrocytes infected with the malarial parasite, *Plasmodium falciparum*." Biochemical Journal **222**: 815-819.

Assaraf, Y. G., C. Kahana, D. T. Spira and U. Bachrach (1988). "*Plasmodium falciparum*: purification, properties, and immunochemical study of ornithine decarboxylase, the key enzyme in polyamine biosynthesis." Experimental Parasitology **67**: 20-30.

Babe, L. M., J. Rose and C. S. Craik (1992). "Synthetic "interface" peptides alter the assembly of the HIV 1 and 2 proteases." Protein Science **1**: 1244-1253.

Bachrach, U. (1973). Function of naturally occurring polyamines. New York, Academic Press.

Baran, I., R. S. Varekova, L. Parthasarathi, S. Suchomel, F. Casey and D. C. Shields (2007). "Identification of potential small molecule peptidomimetics similar to motifs in proteins." Journal of Chemical Information and Modeling **47**: 464-474.

Bathurst, I. and C. Hentschel (2006). "Medicines for Malaria Venture: sustaining antimalarial drug development." Trends in Parasitology **22**: 301-307.

Bennett, E. M., J. L. Ekstrom, A. E. Pegg and S. E. Ealick (2002). "Monomeric S-adenosylmethionine decarboxylase from plants provides an alternative to putrescine stimulation." Biochemistry **49**: 14509-14517.

Birkholtz, L. (2002). Functional and structural characterization of the unique bifunctional enzyme complex involved in regulation of polyamine metabolism in *Plasmodium falciparum*. Department of Biochemistry. Pretoria, University of Pretoria. ***Philosphiae Doctor***.

Birkholtz, L., F. Joubert, A. W. H. Neitz and A. I. Louw (2003). "Comparative properties of a three-dimensional model of *Plasmodium falciparum* ornithine decarboxylase." Proteins: Structure, Function, and Genetics **50**: 464-473.

Birkholtz, L., C. Wrenger, F. Joubert, G. A. Wells, R. D. Walter and A. I. Louw (2004). "Parasite-specific inserts in the bifunctional S-adenosylmethionine decarboxylase/ornithine decarboxylase of *Plasmodium falciparum* modulate catalytic activities and domain interactions." Biochemical Journal **377**: 439-448.

Bitonti, A. J., J. A. Dumont, T. L. Bush, M. L. Edwards, D. M. Stemerick, P. P. McCann and A. Sjoerdsma (1989). "Bis(benzyl)polyamine analogs inhibit the growth of chloroquine-resistant human malaria parasites (*Plasmodium falciparum) in vitro* and in combination with alpha-difluoromethylornithine cure marine malaria." Proceedings of the National Academy of Science USA **86**: 651-655.

Bjorkman, A. and P. A. Phillips-Howard (1990). "The epidemiology of drug-rsistant malaria." Transactions of the Royal Society: Tropical Medicine and Hygiene **84**: 177-180.

Blundell, T. L., B. L. Sibanda, R. W. Montalvão, S. Brewerton, V. Chelliah, C. L. Worth, N. J. Harmer, O. Davies and D. Burke (2005). "Structural biology and bioinformatics in drug design: opportunities and challenges for target identification and lead discovery." Philosophical Transactions of the Royal Society: Biological Sciences **361**: 413-423.

Bodley, A. L., J. N. Cumming and T. A. Shapiro (1998). "Effects of camptothecin, a topoisomerase I inhibitor, on *Plasmodium falciparum*." Biochemical Pharmacology **55**: 709-711.

Bormann, B., W. J. Knowles and V. T. Marchesi (1989). "Synthetic peptides mimic the assembly of transmembrane glycoproteins." Journal of Biological Chemistry **264**: 4033-4037.

Bradford, M. M. (1976). "A rapid and sensitive method for the quantitation of microgram quantities of protein utilising the principle of protein-dye binding." Analytical Biochemistry **72**: 248-254.

Braman, J. (2002). *In vitro* mutagenesis protocols, 2nd edn. Totowa, NJ, Humana Press.

Bray, P. G., R. E. Martin, L. Tilley, S. A. Ward, K. Kirk and D. A. Fidock (2005). "Defining the role of PfCRT in *Plasmodium falciparum* chloroquine resistance." Molecular Microbiology **56**: 323-333.

Bray, R. S., R. W. Burgess, R. M. Fox and M. J. Miller (1959). "Effect of pyrimethamine upon sporogeny and pre-erythrocytic schizogony of *Laverinia falciparum*." Bulletin of the World Health Organization **21**: 233-238.

Bull, P. C. and K. Marsh (2002). "The role of antibodies to *Plasmodium falciparum*-infected-erythrocyte surface antigens in naturally acquired immunity to malaria." Trends in Microbiology **10**: 55-58.

Burger, P. B., L. Birkholtz, F. Joubert, N. Haider, R. D. Walter and A. I. Louw (2007). "Structural and mechanistic insights into the action of *Plasmodium falciparum* spermidine synthase." Bioorganic and Medicinal Chemistry **15**: 1628-1637.

Bzik, D. J. (1991). "The structure and role of RNA polymerase in *Plasmodium*." Parasitology Today **7**: 211-214.

Callebaut, I., G. Labesse, P. Durand, A. Poupon, L. Canard, J. Chomilier, B. Henrissat and J. P. Mornon (1997). "Deciphering protein sequence information through hydrophobic cluster analysis (HCA): current status and perspectives." Cellular and Molecular Life Sciences **53**: 621-645.

Carucci, D. J., A. A. Witney, D. K. Muhia, D. C. Warhurst, P. Schaap, M. Meima, J. Li, M. C. Taylor, J. K. Kelly and D. A. Baker (2000). "Guanylyl cyclase activity associated with putative bifunctional integral membrane proteins in *Plasmodium falciparum*." Journal of Biological Chemistry **275**: 22147-22156.

Chakraborty, K., P. Shivakumar, S. Raghothama and R. Varadarajan (2005). "NMR structural analysis of a peptide mimic of the bridging sheet of HIV-1 gp120 in methanol and water." Biochemical Journal **390**: 573-581.

Chan, H. S., S. Bromberg and K. A. Dill (1995). "Models of cooperativity in protein folding." Philosophical Transactions of the Royal Society: Biological Sciences **348**: 61-70.

Chauhan, P. M. S. and R. Srivastava (2001). "Present trends and future strategy in chemotherapy of malaria." Current Medicinal Chemistry **8**: 1535-1542.

Cheesman, S., S. McAleese, M. Goman, D. Johnson, P. Horrocks, R. G. Ridley and B. J. Kilbey (1994). "The gene encoding topoisomerase II from *Plasmodium falciparum*." Nucleic Acids Research **22**: 2547-2551.

Chen, J. D., X. W. Wu, J. Y. Lin and A. J. Levine (1996). "MDM2 inhibits the G1 arrest and apoptosis functions of the p53 tumor suppressor protein." Molecular and Cellular Biology **16**: 2445-2452.

Chiu, J., P. E. March, R. Lee and D. Tillett (2004). "Site-directed, Ligase-Independent Mutagenesis (SLIM): a single methodology approaching 100% efficiency in 4h." Nucleic Acids Research **32**: e174.

Chou, P. Y. and G. D. Fasman (1974). "Conformational parameters for amino acids in helical, beta-sheet, and random coil regions calculated from proteins." Biochemistry **13**: 211-222.

Clarke, J. L., D. A. Scopes, O. Sodeinde and P. J. Mason (2001). "Glucose-6-phosphate dehydrogenase-6-phosphogluconolactonase. A novel bifunctional enzyme in malaria parasites." European Journal of Biochemistry **268**: 2013-2019.

Cohen, S. S. (1971). Introduction to the polyamines. New York, Prentice hall.

Coleman, C. S., B. A. Stanley, R. Viswanath and A. E. Pegg (1994). "Rapid exchange of subunits of mammalian ornithine decarboxylase." Journal of Biological Chemistry **269**: 3155-3158.

Coleman, R. E., A. K. Nath, I. Schneider, G. H. Song, T. A. Klein and W. K. Milhous (1994). "Prevention of sporogeny of *Plasmodium falciparum* and *P. berghei* in *Anopheles stephensi* mosquitoes by transmission-blocking antimalarials." American Journal of Tropical Medicine and Hygiene **50**: 646-653.

Cooper, R. A., C. L. Hartwig and M. T. Ferdig (2005). "*Pfcrt* is more than the *Plasmodium falciparum* chloroquine resistance gene: a functional and evolutionary perspective." Acta Tropica **94**: 170-180.

Cooper, R. A., K. D. Lane, B. Deng, J. Mu, J. J. Patel, T. E. Wellems, X. Su and M. T. Ferdig (2007). "Mutations in transmembrane domains 1, 4 and 9 of the *Plasmodium falciparum* chloroquine resistance transporter alter susceptibility to chloroquine, quinine and quinidine." Molecular Microbiology **63**: 270-282.

Cowman, A. F. and B. S. Crabb (2006). "Invasion of red blood cells by malaria parasites." Cell **124**: 755-766.

Cowman, A. F. and A. M. Lew (1990). "Chromosomal rearrangements and point mutations in the DHFR/TS gene of *Plasmodium chabaudi* under antifolate selection." Molecular and Biochemical Parasitology **42**: 21-29.

Das Gupta, R., T. Krause-Ihle, B. Bergmann, I. B. Müller, A. R. Khomutov, S. Müller, R. D. Walter and K. Lüersen (2005). "3-Aminooxy-1-aminopropane and derivatives have an antiproliferative effect on cultured *Plasmodium falciparum* by decreasing intracellular polyamine concentrations." Antimicrobial agents and Chemotherapy **49**: 2857-2864.

Davis, J. M., L. K. Tsou and A. D. Hamilton (2007). "Synthetic non-peptide mimetics of α-helices." Chemical Society Reviews **36**: 326-334.

de Vega, M. J. P., M. Martín-Martínez and R. González-Muñoz (2007). "Modulation of protein-protein interactions by stabilising/mimicking protein secondary structure elements." Current Topics in Medicinal Chemistry **7**: 33-62.

Deitsch, K. W. and T. E. Wellems (1996). "Membrane modifications in erythrocytes parasitised by *Plasmodium falciparum*." Molecular and Biochemical Parasitology **76**: 1-10.

DePristo, M. A., M. M. Zilversmit and D. L. Hartl (2006). "On the abundance, amino acid composition, and evolutionary dynamics of low-complexity regions in proteins." Gene **378**: 19-30.

Dietmaier, W., S. Fabry and R. Schmitt (1993). "DISEC-TRISEC: di- and trinucleotide-sticky-end cloning of PCR-amplified DNA." Nucleic Acids Research **21**: 3603-3604.

Doolan, D. L. and S. L. Hoffman (1997). "Multi-gene vaccination against malaria: a multistage, multi-immune response approach." Parasitology Today **13**: 171-178.

Dufe, V. T., W. Qui, I. B. Müller, R. Hui, R. D. Walter and S. Al-Karadaghi (2007). "Crystal structure of *Plasmodium falciparum* spermidine synthase in complex with the substrate decarboxylated S-adenosylmethionine and the potent inhibitors 4MCHA and AdoDATO." Journal of Molecular Biology **373**: 167-177.

Dugger, C. W. (2006). WHO supports wider use of DDT vs. Malaria. New York Times. New York**:** p A.7.

Eckstein-Ludwig, U., R. J. Webb, I. D. Van Goethem, J. M. East, A. G. Lee, M. Kimura, P. M. O'Neill, P. G. Bray, S. A. Ward and S. Krishna (2003). "Artemisinins target the the SERCA of *Plasmodium falciparum*." Nature **424**: 957-961.

Edwards, G. and G. Biagini (2006). "Resisting resistance: dealing with the irrepressible problem of malaria." British Journal of Clinical Pharmacology **61**: 690-693.

Ekstrom, J. L., I. I. Mathews, B. A. Stanley, A. E. Pegg and S. E. Ealick (1999). "The crystal structure of human S-adenosylmethionine decarboxylase at 2.25 Å resolution reveals a novel fold." Structure **5**: 583-595.

Fairlamb, A. H., G. B. Henderson, C. J. Bacchi and A. Cerami (1987). "*In vivo* effects of difluoromethylornithine on trypanothione and polyamine levels in bloodstream forms of *Trypanosoma brucei*." Molecular and Biochemical Parasitology **24**: 185-191.

Feuerstein, B. G., N. Pattabiraman and L. J. Marton (1986). "Spermine-DNA interactions: A theoretical study." Proceedings of the National Academy of Science USA **83**: 5948-5952.

Feuerstein, B. G., N. Pattabiraman and L. J. Marton (1989). "Molecular dynamics of spermine-DNA interactions: sequence specificity and DNA bending for a simple ligand." Nucleic Acids Research **17**: 6883-6892.

Finkel, M. (2007). Bedlam in the blood: Malaria. National Geographic. **July 2007:** 32-67.

Foley, M. and L. Tilley (1998). "Quinoline antimalarials: mechanisms of action and resistance and prospects for new agents." Pharmacology Therapy **79**: 55-87.

Foster, B. A., H. A. Coffey, M. J. Morin and F. Rastinejad (1999). "Pharmacological rescue of mutant p53 conformation and function." Science **286**: 2507-2510.

Gaboriaud, C., V. Bissery, T. Benchetrit and J. P. Mornon (1987). "Hydrophobic cluster analysis: an efficient new way to compare and analyse amino acid sequences." FEBS Letters **224**: 149-155.

García-Echeverría, C., P. Chéne, M. J. J. Blommers and P. Furet (2000). "Discovery of potent antagonists of the interaction between human double minute 2 and tumor suppressor p53." Journal of Medicinal Chemistry **43**: 3205-3208.

Gardner, M. J., N. Hall, E. Fung, O. White, M. Berriman, R. W. Hyman, J. M. Carlton, A. Pain, K. E. Nelson, S. Bowman, I. T. Paulsen, K. James, J. A. Eisen, K. Rutherford, S. L. Salzberg, A. Craig, S. Kyes, M. Chan, V. Nene, S. J. Shallom, B. Suh, J. Peterson, S. Angiuoli, M. Pertea, J. Allen, J. Selengut, D. Haft, M. W. Mather, A. B. Vaidya, D. M. A. Martin, A. H. Fairlamb, M. J. Fraunholz, D. S. Roos, S. A. Ralph, G. I. McFadden, L. M. Cummings, G. M. Subramanian, C. Mungall, J. C. Venter, D. J. Carucci, S. L. Hoffman, C. Newbold, R. W. Davis, C. M. Fraser and B. Barrell (2002). "Genome sequence of the human malaria parasite *Plasmodium falciparum*." Nature **419**: 498-511.

Gelb, M. H. (2007). "Drug discovery for malaria: a very challenging and timely endeavor." Current Opinion in Chemical Biology **11**: 440-445.

Gilbert, S. C., V. S. Moorthy, L. Andrews, A. A. Pathan, S. J. McConkey, J. M. Vuola, S. M. Keating, T. Berthoud, D. Webster, H. McShane and A. V. S. Hill (2006). "Synergistic DNA-MVA prime-boost vaccination regimes for malaria and tuberculosis." Vaccine **24**: 4554-4561.

Gillet, J. M., J. Charlier, G. Boné and P. L. Mulamba (1983). "*Plasmodium berghei*: inhibition of the sporogonous cycle by α-difluoromethylornithine." Experimental Parasitology **56**: 190-193.

Ginsberg, H. (1990). "Alterations by the intra-erythrocytic malaria parasite in the permeability of its host cell membrane." Comparative Biochemistry and Physiology **95**: 31-39.

Golz, A., M. Focke and H. K. Lichtenthaler (1994). "Inhibitors of *de novo* fatty acid biosynthesis in higher plants." Journal of Plant Physiology **143**: 426-433.

Gornicki, P. (2003). "Apicoplast fatty acid biosynthesis as a target for medical intervention in apicomplexan parasites." International Journal of Parasitology **33**: 885-896.

Gromiha, M. M. and D. A. D. Parry (2004). "Characteristic features of amino acid residues in coiled-coil protein sructures." Biophysical Chemistry **111**: 95-103.

Guharoy, M. and P. Chakrabarti (2007). "Secondary structure based analysis and classification of biological interfaces: identification of binding motifs in protein-protein interactions." Structural Bioinformatics **23**: 1909-1918.

Hafner, E., C. Tabor and H. Tabor (1979). "Mutants of *Escherichia coli* that do not contain 1,4-diaminobutane (putrescine) or spermidine." Journal of Biological Chemistry **254**: 12419-12426.

Haider, N., M. Eschbach, S. de Souza Dias, T. W. Gilberger, R. D. Walter and K. Lüersen (2005). "The spermidine synthase of the malaria parasite *Plasmodium falciparum*: molecular and biochemical characterisation of the polyamine synthesis enzyme." Molecular and Biochemical Parasitology **142**: 224-236.

Hamana, K. and S. Matsuzaki (1992). "Polyamines as a chemotaxonomic marker in bacterial systematics." Critical Reviews in Microbiology **18**: 261-283.

Hanahan, D., J. Jessee and F. R. Bloom (1991). "Plasmid transformation of *Escherichia coli* and other bacteria." Methods in Enzymology **204**: 63-113.

Haupt, Y., R. Maya, A. Kazaz and M. Oren (1997). "MDM2 promotes the rapid degeneration of p53." Nature **387**: 296-299.

Hayashi, S. and Y. Murakami (1995). "Rapid and regulated degradation of ornithine decarboxylase." Biochemical Journal **306**: 1-10.

Heby, O. (1981). "Role of polyamines in the control of cell proliferation and differentiation." Differentiation **19**: 1-20.

Hershberger, S. J., S. Lee and J. Chmielewski (2007). "Scaffolds for blocking protein-protein interactions." Current Topics in Medicinal Chemistry **7**: 928-942.

Hobbs, C. A., B. A. Paul and S. K. Gilmour (2002). "Deregulation of polyamine biosynthesis alters intrinsic histone acetyltransferase and deacetylase activities in murine skin and tumors." Cancer Research **62**: 67-74.

Hoffman, S. L., G. M. Subramanian, F. H. Collins and J. C. Venter (2002). "*Plasmodium*, human and *Anopheles* genomics and malaria." Nature **415**: 702-709.

Hollingdale, M. R., P. P. McCann and A. Sjoerdsma (1985). "*Plasmodium berghei*: inhibitors of ornithine decarboxylase block exoerythrocytic schizogony." Experimental Parasitology **60**: 111-117.

Hopkins, A. L. and C. R. Groom (2002). "The druggable genome." Nature Reviews Drug Discovery **1**: 727-730.

Hughes, A. L. (2004). "The evolution of amino acid repeat arrays in *Plasmodium* and other organisms." Journal of Molecular Evolution **59**: 528-535.

Ishii, T. M., P. Zerr, X. M. Xia and C. T. Bond (1998). "Site-directed mutagenesis." Methods in Enzymology **293**: 53-71.

Ivanetich, K. M. and D. V. Santi (1990). "Thymidylate synthase-dihydrofolate reductase in potozoa." Experimental Parasitology **70**: 367-371.

Jambou, R., E. Legrand, M. Niang, N. Khim, P. Lim, B. Volney, M. T. Ekala, C. Bouchier, P. Esterre, T. Fandeur and O. Mercereau-Puijalon (2005). "Resistance of *Plasmodium falciparum* field isolates to *in vitro* artemether and point mutations of the SERCA-type PfATPase6." The Lancet **366**: 1960-1963.

Johnson, L. R. (1994). Physiology of the Gastrointestinal tract. New York, Raven Press.

Kaiser, A. E., A. M. Gottwald, C. S. Wiersch, B. Lindenthal, W. A. Maier and H. M. Seitz (2001). "Effect of drugs inhibiting spermidine biosynthesis and metabolism on the *in vitro* development of *Plasmodium falciparum*." Parasitology Research **87**: 963-972.

Kang, H. A. and J. W. Hershey (1994). "Effect of initiation factor eIF-5A depletion on protein synthesis and proliferation of *Saccharomyces cerevisiae*." Molecular and Cellular Biology **269**: 3934-3940.

Kanski, J., M. Aksenova, C. Schöneich and D. A. Butterfield (2002). "Substitution of Isoleucine-31 by helical-breaking Proline abolishes oxidative stress and neurotoxic properties of Alzheimer's amyloid β-peptide (1-42)." Free Radical Biology and Medicine **32**: 1205-1211.

Karlin, S., L. Brocchieri, A. Bergman, J. Mrazek and A. J. Gentles (2002). "Amino acid runs in eukaryotic proteomes and disease associations." Proceedings of the National Academy of Science USA **99**: 333-338.

Kerppola, T. K. (1998). "Transcriptional cooperativity: bending over backwards and doing the flip." Structure **6**: 549-554.

Knighton, D. R., C. C. Kan, E. Howland, C. A. Jason, Z. Hostomska, K. M. Welsh and D. A. Matthews (1994). "Structure of and kinetic channeling in bifunctional dihydrofolate reductase/thymidylate synthase." Nature Structural Biology **1**: 186-194.

Korenromp, E., J. Miller, B. Nahlen, T. Wardlaw and M. Young (2005). World Malaria Report 2005. World Health Organization (WHO) Roll Back Malaria (RBM) Department and the United Nations Children's Fund (UNICEF).

Krause, T., K. Lüersen, C. Wrenger and T. W. Gilberger (2000). "The ornithine decarboxylase domain of the bifunctional ornithine decarboxylase/S-adenosylmethionine decarboxylase of *Plasmodium falciparum*: recombinant expression and catalytic properties of two different constructs." Biochemical Journal **352**: 287-292.

Kremsner, P. G. and S. Krishna (2004). "Antimalarial combinations." The Lancet **364**: 285-294.

Krishna, S., A. Uhlemann and R. K. Haynes (2004). "Artemisinins: mechanisms of action and potential for resistance." Drug Resistance Updates **7**: 233-244.

Kroch, A. E. and K. G. Fleming (2006). "Alternate interfaces may mediate homodimeric and heterodimeric assembly in the transmembrane domains of SNARE proteins." Journal of Molecular Biology **357**: 184-194.

Kwok, S. C., C. T. Mant and R. S. Hodges (2002). "Importance of secondary structural specificity determinants in protein folding: insertion of a native β-sheet into an α-helical coiled-coil." Protein Science **11**: 1519-1531.

Laemmli, U. K. (1970). "Cleavage of structural proteins during the assembly of the head of bacteriophage T4." Nature **227**: 680-685.

Lang, K., F. X. Schmid and G. Fischer (1987). "Catalysis of protein folding by prolyl isomerase." Nature **329**: 268-270.

Lemmon, M. A., J. M. Flanagan, J. F. Hiunt, B. D. Adair, B. Bormann, C. E. Dempsey and D. M. Engelman (1992). "Glycophorin A dimerisation is driven by specific interactions between transmembrane α-helices." Journal of Biological Chemistry **267**: 7683-7689.

Lipinski, C. A., F. Lombardo, B. W. Dominy and P. J. Feeney (2001). "Experimental and computational approaches to estimate solubility and permeability in drug discovery and development settings." Advanced Drug Delivery Reviews **46**: 3-26.

Lüersen, K., R. D. Walter and S. Müller (1998). "The putative γ-glutamylcysteine synthetase from *P. falciparum* contains large insertions and a variable tandem repeat." Molecular and Biochemical Parasitology **98**: 131-142.

Maharaj, R., D. J. Mthembu and B. L. Sharp (2005). "Impact of DDT re-introduction on malaria transmission in KwaZulu-Natal." South African Medical Journal **95**: 871-874.

Makarova, O., E. Kamberov and B. Margolis (2000). "Generation of deletion and point mutations with one primer in a single cloning step." BioTechniques **29**: 970-972.

Marton, L. J. and A. E. Pegg (1995). "Polyamines as targets for therapeutic intervention." Annual Reviews of Pharmacology and Toxicology **35**: 55-91.

McFadden, G. I. and D. S. Roos (1999). "Apicomplexan plastids as drug targets." Trends in Microbiology **6**: 328-333.

Mehlin, C. (2005). "Structure-based drug discovery for *Plasmodium falciparum*." Combinatorial Chemistry and High Throughput Screening **8**: 5-14.

Mehlin, C., E. Boni, F. S. Buckner, L. Engel, T. Feist, M. H. Gelb, L. Haji, D. Kim, C. Liu, N. Mueller, P. J. Myler, J. T. Reddy, J. N. Sampson, E. Subramanian, W. C. Van Voorhis, E. Worthey, F. Zucker and W. G. J. Hol (2006). "Heterologous expression of proteins from *Plasmodium falciparum*: results from 1000 genes." Molecular and Biochemical Parasitology **148**: 144-160.

Merril, C. R., D. Goldman, S. A. Sedman and M. H. Ebert (1981). "Ultrasensitive stain for proteins in polyacrylamide gels shows regional variation in cerebrospinal fluid proteins." Analytical Biochemistry **72**: 248-254.

Meshnick, S. R. (2002). "Artemisinin: mechanisms of action, resistance and toxicity." International Journal of Parasitology **32**: 1655-1660.

Meshnick, S. R., A. Thomas, A. Ranz, C. M. Xu and H. Z. Pan (1991). "Artemisinin (qinghaosu): the role of intracellular hemin in its mechanism of antimalarial action." Molecular and Biochemical Parasitology **49**: 181-189.

Michelitsch, M. D. and J. S. Weissman (2000). "A census of glutamine/asparagine-rich regions: implications for their conserved function and prediction of novel prions." Proceedings of the National Academy of Science USA **97**: 11910-11915.

Miller, L. H. and S. L. Hoffman (1998). "Research toward vaccines against malaria." Nature Medicine **4**: 520-524.

Müller, S., G. H. Coombs and R. D. Walter (2001). "Targeting polyamines of parasitic protozoa in chemotherapy." Trends in Parasitology **17**: 242-249.

Müller, S., A. Da'dara, K. Lüersen and C. Wrenger (2000). "In the human parasite *Plasmodium falciparum*, polyamines are synthesised by a bifunctional ornithine decarboxylase, S-adenosylmethionine decarboxylase." Journal of Biological Chemistry **275**: 8097-8102.

Myers, D. P., L. K. Jackson, V. G. Ipe, G. E. Murphy and M. A. Phillips (2001). "Long-range interactions in the dimer interface of ornithine decarboxylase are important enzyme function." Biochemistry **40**: 13230-13236.

Nasizadeh, S., A. Jeppsson and L. Persson (2003). "Proteasomal degradation of a trypanosomal ornithine decarboxylase." Cellular Physiology and Biochemistry **13**: 321-328.

Neuhoff, V. N., D. Arold, D. Taube and W. Ehrhardt (1988). "Improved staining of proteins in polyacrylamide gels including isoelectric focussing gels with clear background at nanogram sensitivity using Coomassie Briliant Blue G-250 and R-250." Electrophoresis **9**: 255-262.

Niemand, J. (2007). A phage display study of interacting peptide binding partners of malarial S-adenosylmethionine decarboxylase/ornithine decarboxylase. Department of Biochemistry. Pretoria, University of Pretoria. ***Magister Scientiae***.

Nirmalan, N., P. Wang, P. F. G. Sims and J. E. Hyde (2002). "Transcriptional profiling of genes encoding enzymes of the folate pathway in the human malaria parasite *Plasmodium falciparum*." Molecular Microbiology **46**: 179-190.

Noonpakdee, W., J. Pothikasikorn, W. Nimitsantiwong and P. Wilairat (2003). "Inhibition of *Plasmodium falciparum* proliferation in vitro by antisense oligodeoxynucleotides against malarial topoisomerase II." Biochemical and Biophysical Research Communications **302**: 659-664.

Nwaka, S. and A. Hudson (2006). "Innovative lead discovery strategies for tropical diseases." Nature Reviews Drug Discovery **5**: 941-955.

Ohkanda, J., F. S. Buckner, J. W. Lockman, K. Yokoyama, D. Carrico, R. Eastman, K. Luca-Fradley de, W. Davies, S. L. Croft, W. C. van Voorhis, M. H. Gelb, S. M. Sebti and A. D. Hamilton (2004). "Design and synthesis of peptidomimetic protein Farnesyltransferase inhibitors as anti-*Trypanosoma brucei* agents." Journal of Medicinal Chemistry **47**: 432-445.

Olliaro, P. (2001). "Mode of action and mechanisms of resistance for antimalarial drugs." Pharmacology and Therapeutics **89**: 207-219.

Orzáez, M., J. Salgado, A. Giménez-Giner, E. Pérez-Payá and I. Mingarro (2004). "Influence of proline residues in transmembrane helix packing." Journal of Molecular Biology **335**: 631-640.

Osterman, A., N. V. Grishin, L. N. Kinch and M. A. Phillips (1994). "Formation of functional cross-species heterodimers of ornithine decarboxylase." Biochemistry **33**: 13662-13667.

Ovadi, J. (1991). "Physiological significance of metabolite channeling." Journal of Theoretical Biology **152**: 1-22.

Papworth, C., J. Bauer and J. Braman (1996). "Site-directed mutagenesis in one day with >80% efficiency." Strategies **9**: 3-4.

Pérez-Montfort, R., M. T. Gómez-Puyou and A. Gómez-Puyou (2002). "The interfaces of oligomeric proteins as targes for drug design against enzymes from parasites." Current Topics in Medicinal Chemistry **2**: 457-470.

Persson, L., A. Jeppsson and S. Nasizadeh (2003). "Turnover of trypanosomal ornithine decarboxylases." Biochemical Society Transactions **31**: 411-414.

Perutz, M. F., T. Johnson, M. Suzuki and J. T. Finch (1994). "Glutamine repeats as polar zippers: their possible role in inherited neurodegenerative diseases." Proceedings of the National Academy of Science USA **91**: 5255-5358.

Phillips, M. A., P. Coffino and C. C. Wang (1987). "Cloning and sequencing of the ornithine decarboxylase gene from *Trypanosoma brucei*. Implications for enzyme turnover and selective difluoromethylornithine inhibition." Journal of Biological Chemistry **262**: 8721-8727.

Phillips, R. S. (2001). "Current status of malaria and potential for control." Clinical Microbiology Reviews **14**: 208-226.

Pizzi, E. and C. Frontali (2000). "Divergence of noncoding sequences and of insertions encoding non-globular domains at a genomic region well conserved in *Plasmodia*." Journal of Molecular Evolution **50**: 474-480.

Pizzi, E. and C. Frontali (2001). "Low-complexity regions in *Plasmodium falciparum* proteins." Genome Research **11**: 218-229.

Plowe, C. V., J. F. Cortese, A. Djimde, C. Okey, P. A. Winstanley and C. K. Doumbo (1997). "Mutations in *Plasmodium falciparum* dihydrofolate reductase and dihydropteroate synthase and epidemiological patterns of pyrimethamine-salfadoxine use and resistance." Journal of Infectious Diseases **176**: 1590-1596.

Polhemus, M. E., A. J. Magill, J. F. Cummings, K. E. Kester, C. F. Ockenhouse, D. E. Lanar, S. Dutta, A. Barbosa, L. Soisson, C. L. Diggs, S. A. Robinson, J. D. Haynes, V. A. Stewart, L. A. Ware, C. Brando, U. Krzych, R. A. Bowden, J. D. Cohen, M. Dubois, O. Ofori-Anyinam, E. De-Kock, W. R. Ballou and D. G. Heppner (2007). "Phase I dose escalation safety and immunogenicity trial of *Plasmodium falciparum* apical membrane protein (AMA-1) FMP2.1, adjuvanted with AS02A, in malaria-naive adults at the Walter Reed Army Institute of Research." Vaccine **25**: 4203-4212.

Poulin, R., G. Pelletier and A. E. Pegg (1995). "Induction of apoptosis by excessive polyamine accumulation in ornithine decarboxylase-overproducing L1210 cells." Biochemical Journal **311**: 723-727.

Prasanna, V., S. Bhattacharjya and P. Balaram (1998). "Synthetic interface peptides as inactivators of multimeric enzymes: inhibitory and conformationl properties of three fragments from *Lactobacillus casei* thymidylate synthase." Biochemistry **37**: 6883-6893.

Ralph, S. A., M. C. D'Ombrain and G. I. McFadden (2001). "The apicoplast as an antimalarial drug target." Drug Resistance Updates **4**: 145-151.

Reed, M. B., K. J. Saliba, S. R. Caruana, K. Kirk and A. F. Cowman (2000). "*Pgh1* modulates sensitivity and resistance to multiple antimalarials in *Plasmodium falciparum*." Nature **403**: 906-909.

Richardson, J. S. (1981). "The anatomy and taxonomy of protein structure." Advanced Protein Chemistry **34**: 168-340.

Rogan, W. J. and A. Chen (2005). "Health risks and benefits of bis (4-chlorophenyl)-1,1,1-trichloroethane (DDT)." The Lancet **366**.

Roux, S. (2006). Modulation of functional properties of bifunctional S-adenosylmethionine decarboxylase/ornithine decarboxylase of *Plasmodium falciparum* by structural motifs in parasite-specific inserts. Department of Biochemistry. Pretoria, University of Pretoria. ***Magister Scientiae***.

Russell, D. H. (1985). "Ornithine decarboxylase: a key regulatory enzyme in normal and neoplastic growth." Drug Metabolism Reviews **16**: 1-88.

Rychlik, W., W. J. Spencer and R. E. Rhoads (1990). "Optimisation of the annealing temperature for DNA amplification *in vitro*." Nucleic Acids Research **18**: 6409-6412.

Sambrook, J., E. J. Fritsch and T. Maniatis (1989). Molecular cloning: a laboratory manual (2nd edition). New York, Cold Spring Harbor Laboratory Press.

Sansom, M. S. P. and I. D. Kerr (1995). "Transbilayer pores formed by β-barrels: molecular modeling of pore structures and properties." Biophysical Journal **69**: 1334-1343.

Schneider, D., C. Finger, A. Prodöhl and T. Volkmer (2007). "From interactions of single transmembrane helices to folding of α-helical membrane proteins: analysing transmembrane helix-helix interactions in bacteria." Current Protein and Peptide Science **8**: 45-61.

Schramm, H. J., J. Boetzel, J. Büttner, E. Fritsche, W. Göhring, E. Jaeger, S. König, O. Thumfart, T. Wenger, N. E. Nagel and W. Schramm (1996). "The inhibition of human immunodeficiency virus proteases by "interface peptides"." Antiviral Research **30**: 155-170.

Sehgal, A. (2006). Looking forward, the market for peptide drugs will begin to show increased market growth as drug candidates in Phase III and Phase II Clinical trials gain approval and enter the market. Business Wire. **June 12**.

Seiler, N. (2003). "Thirty years of polyamine-related approaches to cancer therapy. Retrospect and Prospect." Current Drug Targets **4**: 537-585.

Seiler, N., J. G. Delcros and J. P. Moulinoux (1996). "Polyamine transport in mammalian cells. An update." International Journal of Biochemistry and Cell Biology **28**: 843-861.

Shallom, S., K. Zhang, L. Jiang and P. K. Rathod (1999). "Essential protein-protein interactions between *Plasmodium falciparum* thymidylate synthase and dihydrofolate reductase domains." Journal of Biological Chemistry **274**: 37781-37786.

Sheinerman, F. B., R. Norel and B. Honig (2000). "Electrostatic aspects of protein-protein interactions." Current Opinion in Structural Biology **10**: 153-159.

Singh, G. P., B. R. Chandra, A. Bhattacharya, R. R. Akhouri, S. K. Singh and A. Sharma (2004). "Hyper-expansion of asparagines correlates with an abundance of proteins with prion-like domains in *Plasmodium falciparum*." Molecular and Biochemical Parasitology **137**: 307-319.

Singh, S., S. K. Puri, S. K. Singh, R. Srivastava, R. C. Gupta and V. C. Pandey (1997). "Characterization of simian malaria parasite (*Plasmodium knowlesi*)-induced putrescine transport in Rhesus monkey erythrocytes." Journal of Biological Chemistry **272**: 13506-13511.

Singh, S. K., K. Maithal, H. Balaram and P. Balaram (2001). "Synthetic peptides as inactivators of multimeric enzymes: inhibition of *Plasmodium falciparum* triosephosphate isomerase by interface peptides." FEBS Letters **501**: 19-23.

Spiller, D. G., P. G. Bray, R. H. Hughes, S. A. Ward and R. H. White (2002). "The pH of the *Plasmodium falciparum* digestive vacuole: holy grial or dead-end trail?" Trends in Parasitology **18**: 441-444.

Sternberg, M. J. E. (1996). Protein structure prediction (Rickwood, D. and Hames, B.D. edition). New York, Oxford University Press.

Stoute, J. A. (2007). "Phase I randomized double-blind safety and immunogenicity trial of *Plasmodium falciparum* malaria merozoite surface protein FMP 1 vaccine, adjuvanted with AS02A, in adults in western Kenya." Vaccine **25**: 176-184.

Surolia, N. and A. Surolia (2001). "Triclosan offers protection against blood stages of malaria by inhibiting enoyl-ACP reductase of *Plasmodium falciparum*." Nature Medicine **7**: 167-173.

Tabor, C. W. and H. Tabor (1976). "1,4-Diaminobutane (putrescine), spermidine, and spermine." Annual Reviews of Biochemistry **45**: 285-306.

Tabor, H. (1962). "The protective effect of spermidine and other polyamines against heat denaturation of deoxyribonucleic acid." Biochemistry **1**: 496-501.

Takimoto, F., W. G. Wang, D. T. Dicker, F. Rastinejad, J. Lyssikatos and W. S. El-Deiry (2002). "The mutant p53-conformation modifying drug, CP-31398, can induce apoptosis of human cancer cells and can stabilise wild-type p53 protein." Cancer Biology Therapy **1**: 47-55.

Taylor, J. C. and G. D. Markham (2003). "Conformational dynamics of the active site loop of S-adenosylmethionine synthetase illuminated by site-directed spin labelling." Archives of Biochemistry and Biophysics **415**: 164-171.

Thiel, L. (2005). Gathering of data on the global epidemiology of the malaria threat, applied interventions and socio-economic impact, MIA.

Thomas, T. and T. J. Thomas (2001). "Polyamines in cell growth and cell death: molecular mechanisms and therapeutic applications." Cellular and Molecular Life Sciences **58**: 244-258.

Tobias, K. E. and C. Kahana (1995). "Exposure to ornithine results in excessive accumulation of putrescine and apoptic cell death in ornithine decarboxylase-overproducing mouse myeloma cells." Cell Growth and Differentiation **6**: 1279-1285.

Todryk, S. M. and A. V. S. Hill (2007). "Malaria vaccines: the stage we are at." Nature Reviews Microbiology **5**: 487-489.

Tome, M. E., S. M. Fiser, C. M. Payne and E. W. Gerner (1997). "Excess putrescine accumulation inhibits the formation of modified eukaryotic initiation factor 5A (eIF-5A) and induces apoptosis." Biochemical Journal **328**: 847-854.

Tran, T. T., J. McKie, W. D. F. Meutermans, G. T. Bourne, P. R. Andrews and M. L. Smythe (2005). "Topological side-chain classification of β-turns: ideal motifs for peptidomimetic development." Journal of Computer-Aided Molecular Design **19**: 551-566.

Ungar, D. and F. M. Hughson (2003). "SNARE protein structure and function." Annual Reviews of Cell and Developmental Biology **19**: 493-517.

Vedadi, M., J. Lew, J. Artz, M. Amani, Y. Zhao, A. Dong, G. A. Wasney, M. Gao, T. Hills, S. Brokx, W. Qiu, S. Sharma, A. Diassiti, Z. Alam, M. Melone, A. Mulichak, A. Wernimont, J. Bray, P. Loppnau, O. Plotnikova, K. Newberry, E. Sundararajan, S. Houstan, J. Walker, W. Tempel, A. Bochkarev, I. Kozieradski, A. Edwards, C. Arrowsmith, D. S. Roos, K. Kain and R. Hui (2006). "Genome-scale protein expression and structural biology of *Plasmodium falciparum* and related Apicomplexan organisms." Molecular and Biochemical Parasitology **151**: 100-110.

Wallace, H. M., A. V. Fraser and A. L. Hughes (2003). "A perspective of polyamine metabolism." Biochemical Journal **376**: 1-14.

Wang, C. C. (1995). "Molecular mechanisms and therapeutic approaches to treatment of African trypanosomiasis." Annual Reviews of Pharmacology and Toxicology **35**: 93-127.

Wang, J. and M. F. Wilkinson (2001). "Deletion mutagenesis of large (12-kb) plasmids by a one-step PCR protocol." BioTechniques **31**: 722-724.

Wang, P., Q. Wang, P. F. G. Sims and J. E. Hyde (2007). "Characterisation of exogenous folate transport in *Plasmodium falciparum*." Molecular and Biochemical Parasitology **154**: 40-51.

Wang, W. G., F. Takimoto, F. Rastinejad and W. S. El-Deiry (2003). "Stabilization of p53 by CP-31398 inhibits ubiquitination without altering phosphorylation at serine 15 or 20 or MDM2 binding." Molecular and Cellular Biology **23**: 2171-2181.

Weissmann, G. (2006). "DDT is back: let us spray!" The FASEB Journal Editorial **20**: 2427-2429.

Wells, G. A., L. Birkholtz, J. F, W. R.D. and A. I. Louw (2006). "Novel properties of malarial S-adenosylmethionine decarboxylase as revealed by structural modelling." Journal of Molecular Graphics and Modelling **24**: 307-318.

Wendt, H., L. Leder, H. Härmä, I. Jelesarov, A. Baici and H. R. Bosshard (1997). "Very rapid, ionic-strength-dependent association and folding of a heterodimeric leucine zipper." Biochemistry **36**: 204-213.

Whaun, J. M. and N. D. Brown (1983). "Ornithine decarboxylase inhibition and the malaria-infected red cell: a model for polyamine metabolism and growth." Journal of Pharmacology and Experimental Therapeutics **233**: 507-511.

White, S. H. and W. C. Wimley (1999). "Membrane protein folding and stability: physical principles." Annual Reviews of Biophysics and Biomolecular Structure **28**: 319-365.

Williams, M., A. I. Louw and L. Birkholtz (2007). "Deletion mutagenesis of large areas in *Plasmodium falciparum* genes: a comparative study." Malaria Journal **64**: 1-9.

Wilson, R. J., P. W. Denny, P. R. Preiser, K. Rangachari, K. Roberts, A. Roy, A. Whyte, M. Strath, D. J. Moore and D. H. Williamson (1996). "Complete map of the plastid-like DNA of the malaria parasite *Plasmodium falciparum*." Journal of Molecular Biology **261**: 155-172.

Wirth, D. F. (2002). "The parasite genome: biological revelations." Nature **419**: 495-496.

Wootton, J. C. (1994). "Non-globular domains in protein sequences: automated segmentation using complexity measures." Computational Chemistry **18**: 269-285.

Wrenger, C., M. Eschbach, I. B. Müller, D. Warnecke and R. D. Walter (2005). "Analysis of the vitamin B6 biosynthesis pathway in the human malaria parasite *Plasmodium falciparum*." Journal of Biological Chemistry **280**: 5242-5248.

Wrenger, C., K. Lüersen, T. Krause, S. Müller and R. D. Walter (2001). "The *Plasmodium falciparum* bifunctional ornithine decarboxylase, S-adenosyl-L-methionine decarboxylase, enables a well balanced polyamine synthesis without domain-domain interaction." Journal of Biological Chemistry **276**: 29651-29656.

Wright, P. S., T. L. Byers, D. E. Cross-doersen, P. P. McCann and A. J. Bitonti (1990). "Irreversible inhibition of S-adenosylmethionine decarboxylase in *Plasmodium falciparum*-infected erythrocytes: growth inhibition *in vitro*." Biochemical Pharmacology **41**: 1713-1718.

Xie, X., M. E. Tome and E. W. Gerner (1997). "Loss of intracellular putrescine pool-size regulation induces apoptosis." Experimental Cell Research **230**: 386-392.

Xu, Y., J. Shi, N. Yamamoto, J. A. Moss, P. K. Vogt and K. D. Janda (2006). "A credit-card library approach for disrupting protein-protein interactions." Bioorganic and Medicinal Chemistry **14**: 2660-2673.

Xue, H. Y. and D. R. Forsdyke (2003). "Low-complexity segments in *Plasmodium falciparum* proteins are primarily nucleic acid level adaptations." Molecular and Biochemical Parasitology **128**: 21-32.

Yeh, I. and R. B. Altman (2006). "Drug targets for *Plasmodium falciparum*: a post-genomic review/survey." Mini-Reviews in Medicinal Chemistry **6**: 177-202.

Yin, H. and A. D. Hamilton (2005). "Strategies for targeting protein-protein interactions with synthetic agents." Angewandte Chemie International Ed **44**: 4130-4163.

Yuvaniyama, J., P. Chitnumsub, S. Kamchonwongpaisan, J. Vanichtanankul, W. Sirawaraporn, P. Taylor, M. D. Walkinshaw and Y. Yuthavong (2003). "Insights into antifolate resistance from malarial DHFR/TS structures." Nature Structural Biology.

Zhang, K. and P. K. Rathod (2002). "Divergent regulation of dihydrofolate reductase between malaria parasite and human host." Science **296**: 545-547.

Zheng, L., U. Baumann and J. Reymond (2004). "An efficient one-step-directed and site-saturation mutagenesis protocol." Nucleic Acids Research **32**: e115.

Appendices

Appendix A

The figure below shows the SDS-PAGE densitometric analyses of the wild type PfAdoMetDC/ODC (A/Owt) and AdoMetDC insert-deleted (A/OΔA1, A/OΔA2 and A/OΔA3) protein samples.

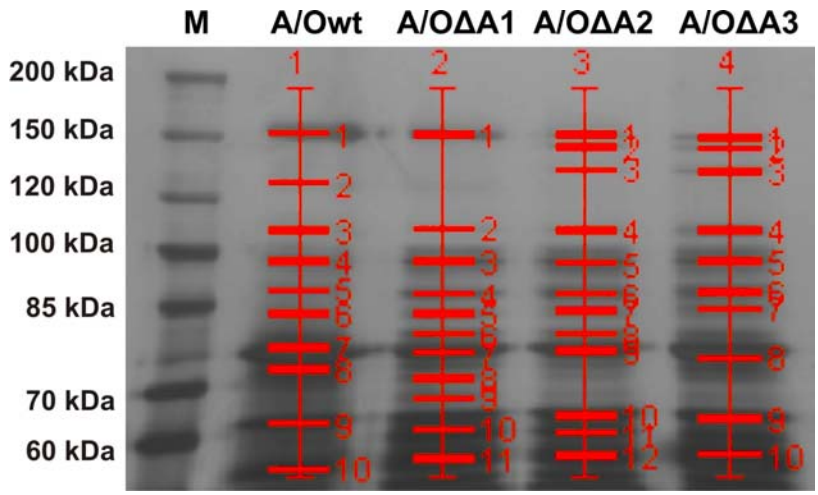

Figure 1A: Relative quantity band analyses of the expressed bifunctional wild type and PfAdoMetDC insert-deleted recombinant proteins.
The red lines indicate the specific bands analysed for each protein sample. The protein size-determining marker is shown in lane M.

The relative quantities of each band in each protein sample (refer to Figure 1A, red bands) were subsequently determined and given as a percentage of the total protein (i.e. the sum of all the band intensities determined) in the table below.

Table 1A: Relative quantities obtained after band analyses of the bifunctional wild type and PfAdoMetDC insert-deleted protein samples

	Relative quantities (%) Lane number				
Band number	**1**	**2**	**3**	**4**	**Protein**
1	**9.229**	**7.753**	**5.176**	**2.859**	**Bifunctional PfA/O**
2	7.113	**3.129**	2.462	2.833	**~112 kDa truncated PfA/O protein**
3	**4.784**	10.486	4.288	4.228	
4	8.397	5.327	**3.624**	**4.97**	
5	4.361	4.602	10.843	9.962	
6	4.138	4.088	5.644	5.898	
7	**11.283**	**10.658**	3.692	4.241	**~70 kDa HSP + truncated PfODC protein**
8	12.902	4.197	3.91	**20.037**	
9	9.326	4.171	**14.261**	7.176	
10	**9.623**	13.533	10.608	**18.333**	**~60 kDa HSP**
11		**8.156**	5.402		
12			**9.544**		

The relative quantities of the bifunctional wild type (1) and insert-deleted (2 to 4) proteins that were used in the determination of their specific activities are shown in yellow. The quantities of the bands corresponding to the ~112 kDa contaminant protein is shown in green. And the quantities of the ~70 and ~60 kDa HSP proteins in the different protein samples are shown in blue and pink, respectively.

Appendix B

The figure below shows the SDS-PAGE densitometric analyses of the wild type PfAdoMetDC/ODC (A/Owt) and insert A2 α-helix disrupted (A/OpA2a) protein samples.

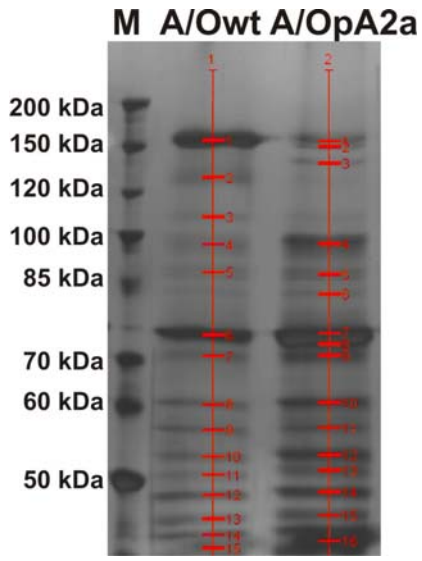

Figure 1B: Relative quantity band analyses of the expressed bifunctional wild type and insert A2 α-helix disrupted recombinant proteins.
The red lines indicate the specific bands analysed for each protein sample. The protein size-determining marker is shown in lane M.

The relative quantities of each band in each protein sample (refer to Figure 1B, red bands) were subsequently determined and given as a percentage of the total protein (i.e. the sum of all the band intensities determined) in the table below.

Table 1B: Relative quantities obtained after band analyses of the bifunctional wild type and insert A2 α-helix disrupted protein samples

	Relative quantities (%)		
	Lane number		
Band number	**1**	**2**	**Protein**
1	**8.728**	**3.251**	**Bifunctional PfA/O**
2	6.052	1.297	
3	2.321	2.015	
4	**5.308**	**6.816**	**~112 kDa truncated PfA/O protein**
5	3.658	3.317	
6	**6.701**	1.882	**~70 kDa HSP + truncated PfODC protein**
7	3.532	**6.863**	
8	3.387	2.527	**~60 kDa HSP**
9	3.106	4.297	
10	3.296	4.977	
11	2.92	3.356	
12	3.561	4.816	
13	3.062	3.136	
14	2.466	4.57	
15	6.176	3.549	
16		11.855	

The relative quantities of the bifunctional wild type (1) and insert A2 α-helix disrupted (2) proteins that were used in the determination of their specific activities are shown in yellow. The quantities of the bands corresponding to the ~112 kDa contaminant protein is shown in green. And the quantities of the ~70 and ~60 kDa HSP proteins in the different protein samples are shown in blue and pink, respectively.